Impacts du changement climatique sur l'activité des avalanches dans les Alpes : apports de la dendrogéomorphologie pour la reconstitution spatiotemporelle de l'activité des avalanches dans un contexte de changements environnementaux dans les hautes vallées du Guil et du Rhône

Adrien Favillier

Université Clermont Auvergne – Clermont-Ferrand

Ecole doctorale Lettres, Sciences Humaines et Sociales
UFR Lettres, Cultures et Sciences Humaines
UCA GEOLAB UMR 6042 CNRS
Laboratoire de Géographie Physique et Environnementale

Thèse présentée en vue de l'obtention du grade de
Docteur de l'Université Clermont-Auvergne

Impacts du changement climatique sur l'activité des avalanches dans les Alpes

Apports de la dendrogéomorphologie pour la reconstitution spatio-temporelle de l'activité des avalanches dans un contexte de changements environnementaux dans les hautes vallées du Guil et du Rhône

Adrien FAVILLIER
Géographie
sous la direction de Jean-Luc PEIRY et de Christophe CORONA

Soutenance publique le 15 octobre 2019

Etienne COSSART	Professeur, Université Jean Moulin Lyon 3, EVS UMR 5600, Lyon (rapporteur)
Vincent JOMELLI	Directeur de Recherche CNRS, LGP UMR 8591, Meudon (rapporteur)
Magali DELMAS	Maître de Conférence, Université de Perpignan Via-Domitia, HNHP UMR 7194, Perpignan (examinateur)
Nicolas ECKERT	Ingénieur en Chef des Ponts, des Eaux et des Forêts, UR ETNA, IRSTEA, Grenoble (examinateur)
Markus STOFFEL	Professeur, Université de Genève, Institute for Environmental Sciences, Genève, Suisse (examinateur)
Christophe CORONA	Chargé de Recherche CNRS, GEOLAB UMR 6042, Clermont-Ferrand (co-directeur)
Jean-Luc PEIRY	Professeur, Université Clermont-Auvergne, UMI 3189, Dakar (directeur)

“Orion”

C. Burton, J. Hetfield, L. Ulrich
Master of Puppets –Metallica, 1986

Résumé

Au 20ème siècle, les massifs montagneux, dont les Alpes, ont connu un réchauffement significatif avec une augmentation des températures deux fois plus importante que la moyenne mondiale. Un tel réchauffement altère les composantes de la cryosphère. Elle induit, par exemple, un passage des précipitations solides aux précipitations liquides, des phases de fonte des neiges plus fréquentes et plus intenses, ainsi qu'une forte diminution de la quantité de neige et une réduction de la durée de la couverture neigeuse. Aux horizons 2050–2100, les modèles climatiques prévoient que l'épaisseur du manteau neigeux sera considérablement réduite et que les propriétés de la neige, et notamment la stabilité du manteau neigeux, seront modifiées. Ces changements devraient entraîner des modifications importantes dans l'activité des avalanches. Parallèlement, l'afforestation induite par la déprise agro-sylvo-pastorale, la démocratisation des sports d'hiver et l'urbanisation des versants ont profondément modifié les paysages de montagne depuis le milieu du 18ème siècle, de même que l'exposition des individus.

Dans ce contexte, une documentation précise de l'activité passée des avalanches est cruciale pour mettre en évidence et comprendre les impacts du réchauffement climatique sur l'activité avalancheuse. Jusqu'à présent, cette documentation s'appuyait sur des chroniques historiques ou des observations systématiques. Cependant, les premières sont souvent discontinues et axées sur des événements catastrophiques, tandis que les secondes se limitent à la seconde moitié du 20ème siècle, excluant toute comparaison avec des périodes climatiques distinctes – tel que les phases froides du Petit Âge Glaciaire, par exemple. Sur les versants forestiers, l'approche dendrogéomorphique apparaît être un complément fiable aux archives historiques et aux séries d'observations systématiques, car elle permet de reconstruire l'activité passée des avalanches, en continu, à l'échelle des plusieurs siècles, avec une résolution annuelle. Pourtant, jusqu'à présent, même si de nombreuses reconstructions locales ont été proposées, la fiabilité de l'approche a été peu souvent analysée et aucune chronologie régionale – cruciale pour distinguer les interférences potentielles entre l'activité des avalanches, les fluctuations climatiques et les changements socio-économiques – n'a été développée dans les Alpes.

Dans cette thèse de doctorat, des avancées méthodologiques significatives ont été réalisées afin (1) d'améliorer la détection des avalanches dans les cernes de croissance, (2) d'éliminer les non-stationnarités liées à la diminution du nombre d'arbres au cours du temps dans les reconstructions et (3) d'agréger les reconstructions locales en chronologies régionales. Sur la base de ces développements, des chronologies régionales pluriséculaires homogénéisées ont été développées (4) pour 10 couloirs d'avalanche de la vallée de Goms (Valais, Alpes suisses, 1880-2014) et (5) 11 couloirs du massif du Queyras (Alpes françaises, 1560-2016). Ces dernières ont été confrontées aux fluctuations climatiques et aux changements d'occupation du sol. À Goms, l'absence de signal climatique clair dans la chronologie régionale souligne les interférences induites par les non-stationnarités locales et démontre qu'une stratégie d'échantillonnage à l'échelle régionale devra nécessairement constituer un préalable au développement d'une chronologie robuste. Dans le massif du Queyras, la forte diminution de l'activité avalancheuse observée au cours du 20ème siècle est attribuée au réchauffement climatique et au processus d'afforestation des versants.

Mots-clefs : dendrogéomorphologie ; avalanches ; changement climatique ; Alpes suisses ; Alpes françaises.

Abstract

For the 20th century, high mountain areas, such as the Alps, have undergone a significant warming with temperature increase twice as much as the global average. Such warming strongly alters the cryosphere components. It induces, for example, a shift from solid to liquid precipitation, more frequent and more intense snowmelt phases or a strong decrease in the amount and duration of snow cover, especially at the elevation of the snow-rain transition. In the future, climate models forecast that snow depth will be significantly reduced and that snow properties such as snow stability will be modified. These changes in snow cover characteristics and amounts are expected to induce significant changes in snow avalanches activity. At the same time, afforestation induced by the abandonment of agriculture and grazing, the democratization of winter recreation activities and the urban sprawl on the slopes have strongly modified the mountain landscapes since the mid-18th century as well as the exposition of individuals to snow avalanches.

In this context, a precise documentation of past snow avalanche activity is crucial to decipher and to understand the impacts of the undergoing climate warming on the snow avalanche activity. To date, this documentation usually relies on historical chronicles or systematic observations. However, the firsts are often discontinuous and focused on catastrophic events. The seconds are limited to the second half of the 20th century thus precluding a comparison from climatically distinct period. On forested paths, the dendrogeomorphic approach is theoretically a reliable approach complement to historical archives and series of systematic observation to infer past snow avalanche activity. Yet, so far, the robustness of this approach has been poorly questioned and no regional chronology, crucial to disentangle potential interferences between snow avalanche activity, climate fluctuations and socio-economic changes, has been developed in the Alps.

In this PhD thesis proposes new methodological frameworks to (1) detect avalanche events from tree-ring series, (2) remove non-stationarities related to the decreasing number of trees over time in the reconstruction and (3) aggregate locals reconstructions in regional chronologies. Based on these development, homogenized multicentennial regional chronologies developed (4) for 10 paths of the Goms Valley (Valais canton, Swiss Alps, 1880-2014) and (5) 11 paths from the Queyras Massif (French Alps, 1560-2016) are confronted to climatic fluctuations and land use changes. At Goms, the absence of clear climatic signal in the regional chronology evidence the interference with local non-stationarities and question the need for a sampling strategy at the regional scale to create a robust chronology. In the Queyras massif, the strong decrease of avalanche activity observed over the 20th century is attributed to global warming and to the afforestation process.

Keywords: Tree-ring; Snow avalanches; Climate changes; French Alps; Swiss Alps; Dendrogeomorphology.

Remerciements

Ce manuscrit est le résultat de quatre années de thèse passées au sein du laboratoire GEOLAB. Je tiens à remercier, ici, tous ceux qui ont pu rendre ce travail de thèse possible et qui ont participé à son excellent déroulement.

Tout d'abord, je remercie mon directeur de thèse **Jean-Luc Peiry**, Professeur à l'Université Clermont-Auvergne, pour m'avoir permis de candidater aux bourses de thèse de l'École Doctorale Lettres, Sciences Humaines et Sociales. Je tiens aussi à le remercier pour son suivi et ses conseils avisés malgré la distance entre Clermont-Ferrand et Dakar.

De même, je tiens à remercier très chaleureusement **Christophe Corona**, Chargé de Recherches au CNRS et co-directeur de ma thèse. Sa patience, son dynamisme, sa confiance et sa disponibilité ont été des atouts essentiels et décisifs à la réussite de cette thèse. Il a joué un rôle crucial dans l'ensemble de mes recherches, sans lui rien n'aurait été possible.

Ensuite, je remercie **Markus Stoffel**, Professeur à l'Université de Genève et directeur de Dendrolab, pour m'avoir confié et fait confiance pour traiter et explorer les données récoltées par ses équipes dans la vallée de Goms et à Täsch, dans la vallée de Zermatt, Valais, Suisse. Ces données m'ont permis de plonger dans ma thèse *in medias res*. De même, ses conseils ont été précieux et bénéfiques à la réalisation du travail de thèse et des articles scientifiques qui y sont attachés.

Je souhaite aussi remercier **Nicolas Eckert**, directeur de l'équipe Montagne, Décision, Risques Naturels, de l'UR ETNA d'IRSTEA, pour son rôle dans toutes les étapes de ce travail de thèse. En plus de ses précieux conseils et de ses inestimables connaissances, il a fourni, au travers du programme RARETE, un soutien humain et financier essentiel aux campagnes d'échantillonnages dans le Queyras et, en conséquence, à la portée de cette thèse.

Toute ma reconnaissance et mes remerciements vont aussi à **Jérôme Lopez-Saez** et **Mélanie Saulnier** qui, eux aussi, m'ont apporté un soutien scientifique et technique inestimable, tout au long de mes recherches.

Je souhaite aussi remercier **Vincent Jomelli** et **Etienne Cossart** qui ont accepté d'évaluer ce travail en qualité de rapporteur, ainsi que **Magali Delmas, Markus Stoffel et Nicolas Eckert** pour avoir intégré le jury en qualité d'examinateur.

Ce travail de thèse ne mobilise pas seulement des connaissances scientifiques, mais demande aussi un soutien administratif et technique important. C'est pourquoi je tiens à

remercier **Chantal Menaut, Oliver Voldoire et Estelle Theveniaud**, sans qui tout aurait été beaucoup plus compliqué ! Dans le même sens, je tiens tout particulièrement à remercier **Michel Gomeaux**, menuisier de l'Université Clermont Auvergne, pour son investissement et son travail dans la réalisation des indispensables supports de carottes et pour son accueil chaleureux au sein de la menuiserie quand j'ai eu besoin de poncer mes très nombreux prélèvements.

Je n'oublie pas non-plus toutes les personnes qui ont participé de près ou de loin aux campagnes de terrains suisses et queyrassiennes, puis aux traitements et à la digitalisation des carottes. En conséquence, je souhaite très grandement remercier **Juan** et **Daniel**, ainsi que l'ensemble de **l'équipe de terrain de Dendrolab** pour les campagnes de terrains et le traitement des échantillons du Valais. De même, un grand merci à **Michaël, Louis, Ana C. et Géraud** pour leurs participations aux campagnes de terrains et aux traitements des échantillons. Plus particulièrement, un grand merci à **Pauline Morel**, qui a participé à toutes les campagnes de terrains (!) et qui a analysé une très grande portion des échantillons suisses. Elle a été une des chevilles ouvrières qui a permis de construire une telle base de données.

Je souhaite aussi remercier particulièrement **Sébastien, Robin et Loïc**, comparses dendros, toujours présents pour prêter une oreille ou filer un coup de main technique ou scientifique. Ces remerciements s'adressent aussi à tous mes collègues doctorants et post-doctorants Geolabiens : **Audrey, Borí, Alfredo, Paul-Edgar, Lucas, Magali et Arthur**, mais aussi permanents et semi-permanents Irstéens : **Fred, Franck, Sylvain, David et Manon**, qui m'ont accueilli dans leurs bureaux et supportés durant mes séjours à Grenoble. Je n'oublie pas **tous les autres membres de GEOLAB**, sans qui journées, soirées et vannes auraient été beaucoup plus difficiles. Vous être trop nombreux pour vous citer, mais en tous cas, ces quelques années de recherches n'auraient pas été les mêmes sans vous.

Je tiens particulièrement à remercier **Georges Rovéra** qui a ouvert les portes de la recherche en géomorphologie et en bio-géographie avec passion à de très nombreux étudiants. Merci Georges !

Je remercie aussi mes parents et **ma famille** qui m'ont toujours soutenu dans mes études ou dans mes projets de vie. Un grand merci aussi à la famille **Guadagnini** pour leurs innombrables soutiens.

Enfin, merci à **Céline** qui m'a toujours soutenu et poussé vers le haut sans hésitation et qui a aussi su prêter l'oreille et conseils à toutes mes humeurs. Je ne serais pas arrivé jusque-là sans toi !

Liste des acronymes

CLPA Cartographie de Localisation des Phénomènes Avalancheux – *Snow avalanche localisation mapping*

DABD Destructive Avalanche Database – Base de données sur les avalanches destructrices

DEM *Digital Elevation Model* – Modèle numérique d'élévation

DTM *Digital Terrain Model* – Modèle numérique de terrain (MNT)

EPA Enquête Permanente sur les Avalanches – *Permanent survey about snow avalanche events*

FGA *Institut zur Erforschung der Geschichte des Alpenraums* – Institut pour l'étude de l'histoire de l'espace alpin

GD *Growth Disturbance* – Perturbation de croissance

- CT *Callus Tissue* – Tissu calleux, tissu cicatriciel
- CW *Compression wood* – Bois de compression
- GS *Growth suppression* – Réduction abrupte de croissance
- TRD *Tangential rows of Traumatic Resin Ducts* – Lignes tangentielles de canaux résinifères traumatiques

HBM *Hierarchical Bayesian Modelling* – Modélisation bayésienne hiérarchique

IGN Institut Géographique National

LBM *Larch Budmoth* – Tordeuse grise du mélèze (*Zeiraphera diniana* Gn.)

Level of Confidence – Niveau de confiance

- LLC *Low level of confidence* – Niveau de confiance faible
- MLC *Medium level of confidence* – Niveau de confiance moyen
- HLC *High Level of Confidence* – Niveau de confiance fort
- vHLC *very High Level of Confidence* – Niveau de confiance très fort

ME *Minimal Sliding Extent* – Emprise minimale de glissement

MNT voir DEM

MSE voir ME

Rims *Recurrence interval maps* – Carte d'intervalle de récurrence

SLF *Eidgenössisches Institut für Schnee- und Lawinenforschung* – Institut fédéral pour l'étude de la neige et des avalanches

Swisstopo *Federal Office of Topography* – Office fédérale de la topographie

SOMMAIRE

SOMMAIRE **13**

INTRODUCTION GENERALE **15**

CHAPITRE 1 **37**
Disentangling the impacts of exogenous disturbances on forest stands to assess multi-centennial tree-ring reconstructions of avalanche activity

CHAPITRE 2 **65**
Spatio-temporal maps of past avalanche events derived from tree-ring analysis

CHAPITRE 3 **95**
Tree-ring reconstruction of snow avalanche activity: Does avalanche path selection matter?

CHAPITRE 4 **121**
Non-stationarities induced by land-cover changes in dendrogeomorphic reconstructions of snow avalanche activity

CHAPITRE 5 **147**
Complex signals in regional tree-ring reconstructions of snow avalanches

CHAPITRE 6 **147**
Impacts des fluctuations climatiques sur l'activité des avalanches dans le Queyras

SYNTHESE GENERALE **201**

BIBLIOGRAPHIE **217**

TABLE DES ILLUSTRATIONS **247**

TABLES ET TABLEAUX **253**

TABLE DES MATIERES **255**

INTRODUCTION GÉNÉRALE

1. Contexte

1.1. Les avalanches, un aléa majeur en région de montagne

Les avalanches sont définies comme des écoulements gravitaires rapides de masses neigeuses, de volumes généralement supérieurs à 100 m^3, le long de versants de montagne (Ancey et Charlier, 1996 ; Rudolf-Miklau et al., 2015a; Schweizer, 2003). Le qualificatif d'écoulement rappelle que la distance parcourue est supérieure aux dimensions de la masse mobilisée. Le caractère gravitaire rapide permet de distinguer l'avalanche de mouvement plus lent de type fluage ou reptation. Schématiquement, Ancey et Charlier (1996) décomposent le processus en trois phases :

- **La phase de déclenchement** correspond à la mise en mouvement de la neige dans la zone supérieure, dite d'accumulation (bassin, cirque), des sites avalancheux et dont la pente est comprise entre 28° et 55°. Le déclenchement, spontané ou provoqué, et le type d'avalanche (dense ou en aérosol, sèche ou humide) sont contrôlés par un ensemble d'interactions complexes entre le sol (topographie, occupation, rugosité), le manteau neigeux (épaisseur, structure), les facteurs météorologiques (précipitations, températures, vent), et l'éventuel facteur déclenchant externe (Laute et Beylich, 2018; Schweizer, 2003) ;
- **La phase d'écoulement** se produit dans la zone médiane – entre 10° et 30° d'inclinaison – par laquelle transitent toutes les avalanches majeures du site. On distingue en général les zones confinées (couloir) et ouvertes (versant) ;
- **La phase de dépôt** se produit lorsque la masse de neige en mouvement décélère puis s'arrête. La surface sur laquelle s'est immobilisée la neige est appelée zone de dépôt. L'extension de cette dernière est le plus souvent liée à des critères d'inclinaison (>10°) et de rugosité du sol.

Dans les massifs de montagne, **les avalanches constituent un aléa majeur** (Fuchs et al., 2007, 2004 ; Schneebeli et al., 1997). **Elles font partie de la vie quotidienne des populations** (Granet-Abisset, 2006) qui ont cherché à s'en protéger en construisant à l'écart des zones exposées ou, plus rarement, en construisant des ouvrages de défense, comme à Vallorcine, où une étrave fut érigée pour protéger l'église et le presbytère en 1722 et renforcée en 1843 (Ancey, 1998). À partir du milieu du 19^e siècle, les techniques de génie paravalanche, en plein essor sous l'impulsion du service de Restauration des Terrains en Montagne (RTM), se focalisent sur la mise en place d'ouvrages de défense active. Ceux-ci

prennent essentiellement la forme de banquettes de reboisements destinées à fixer le manteau neigeux dans les zones d'accumulation (Ancey, 1998 ; Rudolf-Miklau et al., 2015a). Dans les années 1970, après une série d'événements catastrophiques dont celui de Val d'Isère, les techniques de prévention passive se développent : elles prennent la forme de structures de déviation (galerie, tremplin, tourne, digue, étrave) ou de freinage (tas, dent, obstacle).

Malgré la multiplication des stratégies de défense, les avalanches mettent chaque année en danger les infrastructures, les voies de communication et les personnes (Badoux et al., 2016 ; Bründl et al., 2004 ; Nöthiger et Elsasser, 2004; Techel et al., 2016). En dépit des efforts constants et des investissements publics importants réalisés pour réduire les risques, **les coûts humains et monétaires, directs et indirects** (Giacona et al., 2017), **ont augmenté de manière significative au cours des dernières décennies** (Einhorn et al., 2015). Cette tendance est attribuable à (1) l'augmentation de la fréquentation hivernale liée à la démocratisation et au développement de nouvelles activités récréatives dans les territoires de montagne, (2) l'intensification du trafic, la multiplication des infrastructures routières et (3) l'extension du tissu urbain sur les versants (Alpine Convention, 2015 ; Astrade et al., 2007 ; Fuchs et al., 2017) du fait de l'espace limité des surfaces potentiellement constructibles (Briquel, 2001). Dans ces conditions, **la connaissance de l'aléa avalancheux constitue une préoccupation croissante dans les communautés alpines** (Laternser et Pfister, 1997a) afin d'assurer une protection des populations et activités humaines mais également la libre circulation quotidienne (Ancey, 1998).

La meilleure stratégie de protection contre les avalanches consiste à installer le bâti et les infrastructures hors de la zone dangereuse, ce qui a été traditionnellement réalisé par le montagnard dans le choix de son habitat (Ancey, 1998). Cette stratégie de défense passive a conditionné, par le biais du zonage règlementaire (plan de prévention des risques, plan des zones exposées aux avalanches) établi sous l'hypothèse de stationnarité spatial et temporel de l'aléa, l'aménagement des territoires exposés en influant, par exemple, sur l'emplacement et les formes des bâtiments (Raška et al., 2014). **Cependant, depuis la fin du 19ème siècle, le réchauffement climatique récent tend à modifier la dynamique (fréquence, extension, nature) avalancheuse.** La déprise agro-sylvo-pastorale atténue les mosaïques paysagères caractéristiques (zonations longitudinales et latérales) crées par le passage répété des avalanches (Bebi et al., 2009 ; Giacona et al., 2018). **Ces changements**

environnementaux, modifient la pseudo-stationnarité de la dynamique avalancheuse et rendent le zonage complexe.

1.2. Réchauffement climatique et réduction du manteau neigeux dans les Alpes

Le réchauffement climatique récent (Beniston et al., 2018 ; IPCC, 2013) **impacte profondément et durablement la mise en place, la structure et la persistance du manteau neigeux** (Beniston, 1997 ; Uhlmann et al., 2009). La hausse des températures hivernales et printanières (+1,7°C depuis le début du siècle dans les Alpes, Auer et al., 2007; Böhm et al., 2009), sans évolution significative des totaux pluviométriques (Gobiet et al., 2014 ; Rajczak et al., 2013), ont conduit (1) à une modification importante des coefficients de nivosité (Nikolova et al., 2013; Serquet et al., 2011), (2) à la réduction de la quantité des précipitations neigeuses (Gobiet et al., 2014; Haeberli et al., 2007) et (3) à une accélération des phases de fonte du manteau neigeux (Klein et al., 2016).

Ces changements nivo-météorologiques ont induit une réduction de l'épaisseur de la couverture neigeuse depuis le milieu du 20ème siècle (Beniston et al., 2018 ; Durand et al., 2009b ; Reid et al., 2016). Cette évolution varie en fonction de l'altitude (Morán-Tejeda et al., 2013). Elle est particulièrement marquée entre 1500 et 2500 mètres d'altitude où la variation des températures autour de l'isotherme 0°C conditionne fortement la transition précipitations liquides / précipitations solides (Jomelli et al., 2004).

1.3. Réchauffement climatique et évolution de l'activité avalancheuse

Les avalanches résultent d'un processus physique complexe dont le déclenchement et la rhéologie sont liés à la nature changeante du manteau neigeux (Ancey, 2006). Des modifications de la structure et des caractéristiques de ce dernier, par le réchauffement climatique, sont susceptibles d'impacter durablement l'activité des avalanches.

1.3.1. Évolutions pluriséculaires de la dynamique avalancheuse : l'apport des études paléo-environnementales et des archives historiques

L'analyse lichénométrique (Jomelli et Pech, 2004 ; McCarroll, 1993), **l'analyse des sédiments lacustres** (Fouinat et al., 2018 ; Nesje et al., 2007; Vasskog et al., 2011) et **l'analyse palynologique** (Blikra et Selvik, 1998) **suggèrent une augmentation de la fréquence des avalanches dans le Nord et l'Ouest de l'Europe durant le Petit Age Glaciaire**. **Les paléo-indicateurs**, susceptibles de fournir des informations concernant

l'évolution de l'activité des avalanches à l'échelle du dernier millénaire, **sont cependant (1) rares, (2) spatialement limitées et ont (3) une résolution temporelle faible (décennale à centennale)**. Ces lacunes limitent la portée des études paléo-environnementales **et ne permettent pas de tirer des conclusions robustes concernant l'impact des fluctuations climatiques sur la dynamique avalancheuse** (Castebrunet et al., 2012 ; Laternser et Schneebeli, 2002).

À l'échelle pluriséculaire, Laternser et Pfister, (1997) et Schneebeli et al. (1997) ont reconstruit, l'activité des avalanches de forte intensité, entre 1500 et 1990, dans les Alpes suisses, à partir des archives historiques. **L'absence de relations significatives entre les séries d'avalanches, de résolution annuelle, et différents paramètres nivo-météorologiques est expliquée par le caractère discontinu des archives historiques**. Celles-ci ne représentent qu'un enregistrement partiel de l'activité passée des avalanches (Casteller et al., 2011 ; Corona et al., 2012a) et ne relatent, le plus souvent, que des événements ayant eu un impact sur les biens ou les personnes (Ibsen et Brunsden, 1996). De plus, le potentiel d'observation est susceptible de changer dans le temps, du fait de la présence ou non d'un observateur, mais également dans l'espace en raison de l'évolution des enjeux (Laternser et Pfister, 1997a).

1.3.2. Évolutions de la dynamique avalancheuse au cours des dernières décennies : l'apport des observations systématiques

Au cours des dernières années, plusieurs études se sont appuyées sur les séries d'observations systématiques disponibles dans les Alpes depuis les années 1950 afin de montrer les impacts du réchauffement climatique sur la dynamique des avalanches. Ces études utilisent les principales caractéristiques associées à chaque événement recensé (Bélanger et Cassayre, 2004 ; Jamard et al., 2002 ; SLF, 1989), telles que :

- Le mécanisme de déclenchement : spontané ou provoqué ;
- Le type de déclenchement et le type d'avalanche ;
- Les altitudes de départ et d'arrêt ;
- La longueur de l'avalanche et l'épaisseur du dépôt de neige ;
- Les dommages causés aux biens ou aux personnes ;
- Le contexte météorologique jusqu'à trois jours avant l'événement.

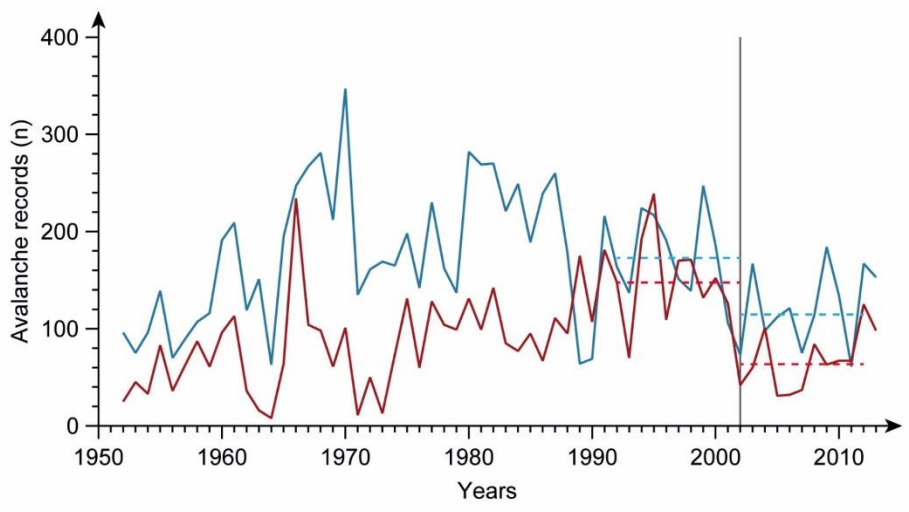

Figure I.1 – Nombre d'avalanches de neige sèche (bleu) et de neige humide (rouge) observées entre les hivers 1952 et 2013. La ligne verticale grise indique l'hiver 2002 où le nouveau système de codification des observations et de la base de données a été mis en place. Cette date coïncide avec une baisse systématique de la quantité de données. Les lignes pointillées correspondent à la moyenne décennale, avant et après l'hiver 2001-2002. Adapté de Pielmeier et al. (2013).

En Suisse, Laternser et Schneebeli (2002) ont ainsi utilisé les séries compilées dans la *Destructive Avalanche Database* (DADB) entre 1947 et 1999. Cette base de données est construite à partir des archives du *Eidgenössisches Institut für Schnee- und Lawinenforschung* [Institut fédéral pour l'étude de la neige et des avalanches] (SLF). Elle compile les informations relatives à plus de 10 000 avalanches ayant causé des dommages aux installations humaines et/ou aux personnes dans 84 stations d'observations (Laternser et Pfister, 1997a ; Laternser et Schneebeli, 2002). **La comparaison avec les séries climatiques n'a cependant pas permis de détecter une évolution significative de la fréquence des avalanches, ni de liens significatifs entre activité des avalanches et les précipitations hivernales.** Plus récemment, Pielmeier et al. (2013) ont étudié les caractéristiques des avalanches consignées par le SLF entre 1952 et 2013. Ils ont observé une augmentation de 13% de la part des avalanches entraînant de la neige humide par rapport aux avalanches entraînant de la neige sèche, entre 1952 et 2001 (Fig. I.1). Les auteurs ne montrent aucun lien statistique significatif entre cette part croissante des avalanches entraînant de la neige humide et les variations de hauteur du manteau neigeux. Ils expliquent, en revanche, cette tendance par l'augmentation des températures moyennes hivernales.

Dans les Alpes françaises, Eckert et al. (2010d) ont analysé les observations de 3900 couloirs d'avalanches, recensées dans l'Enquête Permanente sur les Avalanches (EPA ; Bourova et al., 2016 ; Mougin, 1922), à l'aide d'une approche bayésienne

hiérarchique. **Depuis les années 1960, ils ne mettent en évidence aucune tendance monotone de la fréquence des avalanches. Dans les Alpes françaises, malgré une forte variabilité interannuelle, un nombre maximal d'avalanches a été observé entre 1970 et 1990. Ce dernier a été associé à des séries d'hivers froids et humides** (Castebrunet et al., 2012). **Depuis la fin des années 1970, Eckert et al. (2013, 2010a) ont également observé une réduction de la distance d'arrêt des avalanches, en particulier pour les avalanches de forte magnitude** (Fig. I.2). Naaim et al. (2013) ont affiné ces observations en étudiant les caractéristiques de 730 avalanches recensées dans 26 couloirs de la Vallée de l'Arve. Les auteurs suggèrent que l'augmentation des températures affecte la dynamique d'écoulement de la neige (Köhler et al., 2018).

Ces évolutions doivent cependant être nuancées en fonction de l'altitude (Lavigne et al., 2015, 2012). En dessous de 2000 mètres, la diminution du coefficient de nivosité induite par le réchauffement climatique entraîne une diminution significative de l'activité des avalanches. Au contraire, au-dessus de 2000 mètres, l'intensification des précipitations neigeuses et l'augmentation de la fréquence des redoux hivernaux (Beniston, 2005) sont susceptibles d'entraîner une augmentation de l'activité des avalanches, tant que le manteau neigeux demeurera suffisant pour induire un déclenchement (Ballesteros-Cánovas et al., 2018 ; Lavigne et al., 2015). Ce régime transitoire pourrait s'accompagner de changements de la magnitude (volume, distance d'arrêt), du type (écoulement dense ou en aérosol) et de la répartition saisonnière des avalanches (Naaim et al., 2016).

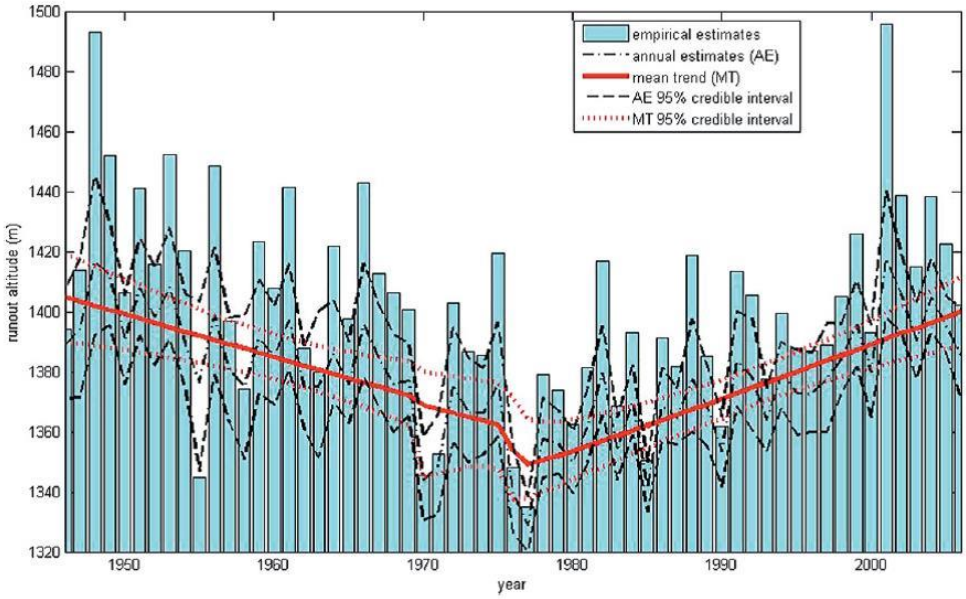

Figure I.2 – Variation interannuelle de l'altitude d'arrêt des avalanches dans les Alpes françaises, d'après l'EPA. Extrait de Eckert et al. (2010a).

Bien que particulièrement précieuses pour la compréhension des impacts du réchauffement climatique, ces études restent limitées par :

1. **La rareté des inventaires systématiques**, disponibles quasi-exclusivement dans les Alpes ;
2. **La qualité des observations**, dépendante de l'observateur et des conditions météorologiques d'observation. Par conséquent, ces observations s'avèrent souvent incomplètes, imprécises et sont parfois réalisées plusieurs mois après l'événement (Laternser et Schneebeli, 2002). De plus, les modifications des systèmes de codification (Laternser et Schneebeli, 2002) et les mises à jour des protocoles d'observation (Bélanger et Cassayre, 2004), puis la retranscription des observations sont aussi sources d'imprécisions ;
3. **La durée limitée des séries d'observations systématiques**, pour la plupart postérieures à la Seconde Guerre Mondiale et qui ne permettent d'étudier l'évolution des avalanches que sur quelques décennies caractérisées par une hausse importante des températures.

1.3.3. Évolutions de l'activité avalancheuse dans un climat futur

Aux horizons 2050 et 2100, les modèles climatiques prévoient une augmentation plus rapide des températures dans les Alpes que pour l'Europe occidentale (Gobiet et al., 2014). Selon les scénarii considérés, **la hausse des températures devrait être comprise entre +2,5°C à +5°C** à l'horizon 2100. **Cette augmentation impactera significativement le régime et la nature des précipitations**, et entraînera un décalage des saisons (Gobiet et al., 2014). **Ces évolutions nivo-météorologiques devraient induire une diminution significative et généralisée de la couverture neigeuse** (Jylhä et al., 2008) **et altérer significativement sa stabilité** (López-Moreno et al., 2009) en modifiant les propriétés mécaniques de la neige (Castebrunet et al., 2012).

Dans ce contexte, les rares études portant sur l'évolution de l'activité avalancheuse, souvent qualitatives, suggèrent une augmentation de la proportion d'avalanches mobilisant de la neige humide durant l'hiver (Lazar et Williams, 2008 ; Martin et al., 2001 ; Mitterer et al., 2011). Dans les Alpes françaises, sur la base d'un scénario moyen d'évolution de la concentration des gaz à effet de serre de l'IPCC AR4, Castebrunet et al. (2014) simulent une réduction de 20 à 30% de l'activité totale des avalanches au cours du 21ème siècle dans les alpes Française. Cette tendance varie en fonction de la latitude. Elle s'amenuise dans les Alpes françaises du sud, où l'altitude

supérieure, permet un maintien du manteau neigeux et de l'activité avalancheuse moyenne malgré une forte variabilité interannuelle de la fréquence d'événements.

Il faut **cependant** garder à l'esprit que **ces résultats reposent sur la combinaison de simulations nivo-météorologiques et de modélisations statistiques des relations avalanche–climat sur une période courte de quelques décennies.** De même, aucune de ces études ne prend explicitement en compte les changements d'occupation du sol induits par la déprise agro-sylvo-pastorale (Bebi et al., 2009).

1.4. Déprise agro-sylvo-pastorale et évolution de l'activité avalancheuse

Depuis le milieu du 19ème siècle, les espaces de montagne ont connu de profondes mutations socio-économiques à l'origine de transformations importantes des paysages en Europe (Ustaoglu et Collier, 2018). **Dans les Alpes, l'abandon des pratiques agro-sylvo-pastorales a été reconnu comme un des principaux facteurs à l'origine de la fermeture des paysages et de l'élévation de la limite supraforestière** (Cramer et al., 2008 ; Gellrich et al., 2007 ; Kulakowski et al., 2016; Levers et al., 2018). Kulakowski et al. (2011) ont par exemple observé une hausse de 13,4% de la surface forestière pour la période 1954–2000, dans les Alpes suisses. Celle-ci se concentre au niveau des anciennes zones agro-pastorales situées dans la tranche altitudinale 1600–2000 mètres.

Ces modifications dans le paysage se sont aussi traduites par une densification accrue et une fragmentation réduite des forêts (Jurasinski et Kreyling, 2007 ; Kulakowski et al., 2011 ; Moen et al., 2004; Walther et al., 2005). **Ces changements sont susceptibles d'entraîner des modifications dans l'accumulation du manteau neigeux, le déclenchement et la rhéologie des avalanches**. Dans les Alpes suisses, Bebi et al. (2009) ont montré que, **sous forêt, l'atténuation significative de la vitesse du vent de surface permet une distribution** plus **homogène de l'épaisseur de neige** et le comblement des accidents topographiques souvent à l'origine des discontinuités dans le manteau (Bebi et al., 2009 ; Miller, 1964). Ensuite, **les troncs des arbres, les débris et les souches contribuent directement à la stabilisation du manteau neigeux** (Salm, 1978 ; Schönenberger et al., 2005 ; Smith et McClung, 1997). Collectivement, ces processus **limitent l'écoulement de la neige** en avalanche aux pentes supérieures à 30° (Schneebeli et Bebi, 2004).

Les études prenant en compte l'impact de ces changements paysagers sur la dynamique avalancheuse sont très rares. Cependant, dans le massif des Asturies

(Pyrénées espagnoles), García-Hernández et al. (2017) ont attribué la réduction des dommages liés aux avalanches aux mutations économiques et sociétales ayant entraîné une réduction de la pression sur les ressources sylvicoles et une recolonisation forestière des versants. À ce jour, aucune étude comparable n'existe **dans les Alpes** où **les impacts de la déprise agro-sylvo-pastorale sont susceptibles d'interférer fortement avec le réchauffement climatique pour expliquer l'évolution de l'activité avalancheuse.**

1.5. Dendrogéomorphologie et reconstruction pluriséculaire de l'activité des avalanches

Sur les versants boisés, la dendrogéomorphologie (Alestalo, 1971 ; Stoffel et al., 2010a) **permet de pallier certains biais inhérents aux archives historiques et de reconstruire l'activité et l'emprise des avalanches avec une résolution annuelle pour des périodes pluriséculaires** (Butler et Sawyer, 2008a). Dérivée de la dendrochronologie, cette discipline, formalisée par Alestalo (1971), repose sur la capacité des arbres à enregistrer les perturbations du milieu dans leur cerne de croissance annuel (Stoffel et Corona, 2014a). Schématiquement, trois types de perturbations sont utilisés pour reconstruire les avalanches (Fig. I.3) :

1. Les diminutions abruptes de la croissance radiale causées par la perte partielle ou totale de l'apex ou d'une des branches majeures de l'arbre impacté ;
2. Les blessures, les tissus calleux et les lignes tangentielles de canaux résinifères traumatiques formées à la suite d'un impact mécanique direct ayant endommagé le cambium ;
3. Le bois de réaction qui se forme à la suite du basculement du tronc.

Les premières reconstructions dendrogéomorphologiques des avalanches ont été réalisées dans les années 1970 dans les Rocheuses américaines (Potter, 1969 ; Schaerer, 1972a ; Smith, 1973). Dans le sillage de ces travaux pionniers, **une recherche bibliographique a permis de dénombrer 66 études (203 couloirs d'avalanches) publiées dans des revues internationales entre 1978 et février2019.** La majorité de ces travaux (58/66) est cependant postérieure à 2001 (Fig. I.4).

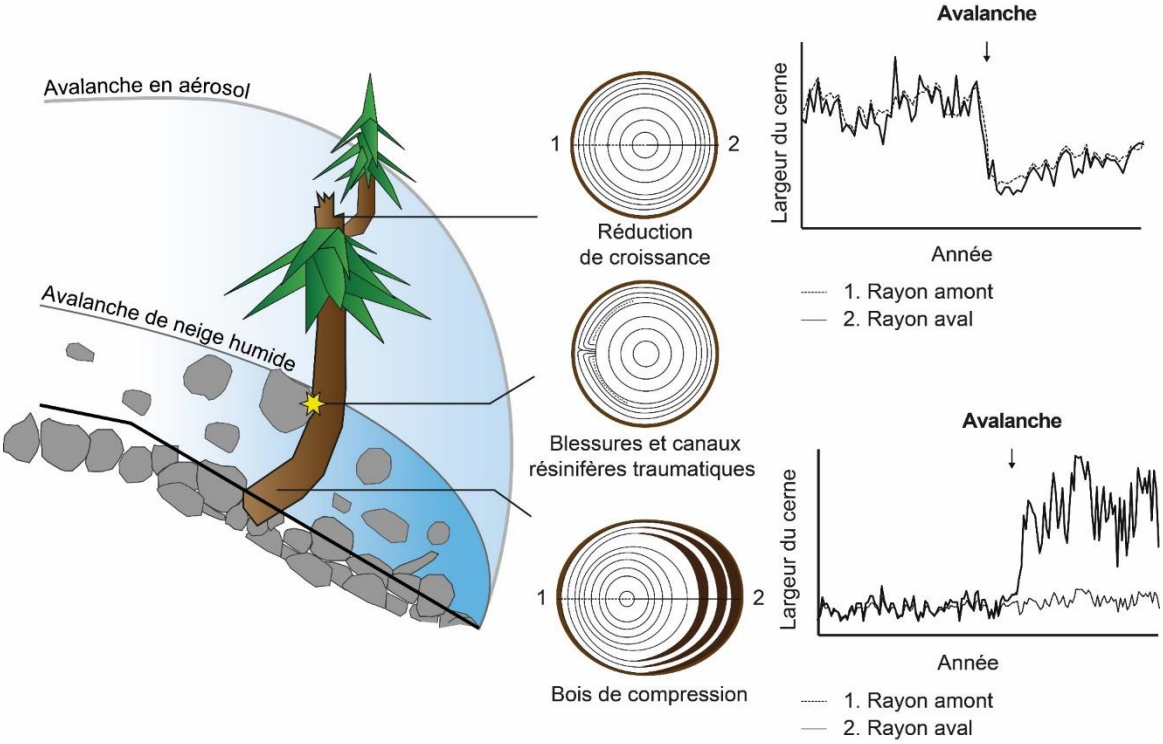

Figure I.3 – Types de blessures observés dans les cernes de croissance après une avalanche, adapté de Corona et al. (2013).

Ce nombre croissant d'études dendrogéomorphologiques a conduit à plusieurs développements méthodologiques. Ceux-ci concernent notamment :

1. L'utilisation de seuils (nombre d'arbres impactés, pondération des perturbations de croissance en fonction de leur intensité) permettant d'affiner la détection des événements passés (Butler et Sawyer, 2008a ; Chiroiu et al., 2015a ; Corona et al., 2012a; Germain et al., 2005; Pederson et al., 2006) ;
2. La discrimination des signaux induits par les avalanches et d'autres processus géomorphologiques (laves torrentielles, notamment) dans les séries de cernes de croissance annuel (Kogelnig-Mayer et al., 2011a ; Stoffel et al., 2006 ; Stoffel et Hitz, 2008; Szymczak et al., 2010; Voiculescu et Onaca, 2014) ;
3. La validation des chronologies obtenues par comparaison avec les données historiques (Corona et al., 2012a, 2010 ; Schläppy et al., 2013a) ;
4. L'utilisation de nouvelles perturbations de croissance (Larocque et al., 2001 ; Szymczak et al., 2010) ;
5. La diversification des espèces utilisées pour les reconstructions, et notamment l'utilisation des feuillus (Mundo et al., 2007 ; Šilhán et al., 2019) ;

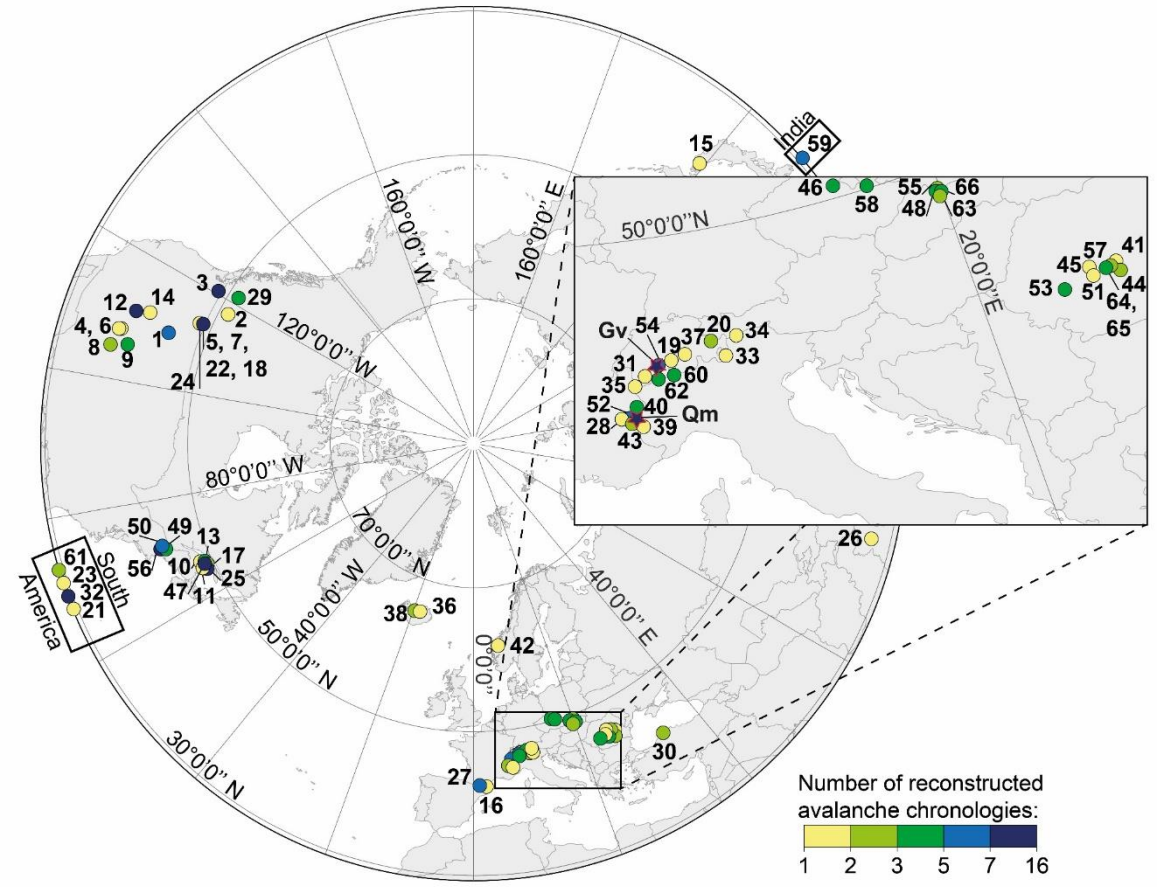

Figure I.4 – Synthèse des chroniques d'avalanche reconstruites à partir de séries de cernes de croissance. **1**. Potter (1969) ; **2**. Schaerer (1972) ; **3**. Smith (1973) ; **4**. Ives et al. (1976) ; **5**. Butler (1979) ; **6**. Carrara (1979) ; **7**. Butler et Malanson (1985a) ; **8**. Bryant et al. (1989) ; **9**. Rayback (1998) ; **10**. Larocque et al. (2001) ; **11**. Boucher et al. (2003) ; **12.** Hebertson et Jenkins (2003) ; **13**. Dubé et al. (2004) ; **14**. Jenkins et Hebertson (2004) ; **15**. Kajimoto et al. (2004) ; **16**. Muntán et al. (2004) ; **17**. Germain et al. (2005) ; **18.** Pederson et al. (2006) ; **19**. Stoffel et al. (2006) ; **20**. Casteller et al. (2007) ; **21**. Mundo et al. (2007) ; **22**. Butler et Sawyer (2008) ; **23**. Casteller et al. (2008) ; **24**. Reardon et al. (2008) ; **25**. Germain et al. (2009) ; **26**. Laxton et Smith (2009) ; **27**. Muntán et al. (2009) ; **28**. Corona et al. (2010) ; **29**. Johnson et Smith (2010) ; **30**. Köse et al. (2010) ; **31**. Szymczak et al. (2010) ; **32**. Casteller et al. (2011) ; **33**. Garavaglia et Pelfini (2011); **34**. Kogelnig-Mayer et al. (2011) ; **35**. Corona et al. (2012) ; **36**. Decaulne et al. (2012) ; **37**. Püntener et al. (2012) ; **38**. Arbellay et al. (2013) ; **39**. Corona et al. (2013) ; **40**. Schläppy et al. (2013) ; **41**. Voiculescu et Onaca (2013); **42**. Decaulne et al. (2014) ; **43**. Schläppy et al. (2014) ; **44**. Voiculescu et Onaca (2014); **45**. Chiroiu et al. (2015) ; **46**. Tumajer et Treml (2015); **47**. Germain (2016); **48**. Lempa et al. (2016) ; **49**. Martin et Germain (2016a); **50**. Martin et Germain (2016b); **51**. Pop et al. (2016) ; **52**. Schläppy et al. (2016) ; **53**. Voiculescu et al. (2016) ; **54**. Favillier et al. (2017) – Chapitre 1 ; **55**. Gądek et al. (2017) ; **56**. Martin et Germain (2017); **57**. Pop et al. (2017) ; **58**. Šilhán et Tichavský (2017); **59**. Ballesteros-Cánovas et al. (2018) ; **60**. Bollati et al. (2018) ; **61**. Casteller et al. (2018) ; **62**. Favillier et al. (2018) – Chapitre 2 ; **63**. Krause et Křížek (2018); **64**. Meseșan et al. (2018a) ; **65**. Meseșan et al. (2018b) ; **66**. Šilhán et al. (2019) ; **Gv** Goms valley (Valais, Switzerland) ; **Qm** Queyras massif (Hautes-Alpes, France).

Malgré ces avancées importantes, **trois lacunes majeures ont été identifiées dans les reconstructions proposées** :

1. Dans la plupart des cas, les reconstructions dendrogéomorphologiques permettent d'étendre et de densifier considérablement les archives historiques. En revanche, les taux de convergence avec les données de l'Enquête Permanente sur les Avalanches n'excèdent pas 50% quels que soient les seuils de détection utilisés (Corona et al., 2012a, 2010 ; Schläppy et al., 2013a). Les auteurs expliquent cette convergence limitée par la **difficulté à reconstruire les événements extrêmes**, destructeurs pour les peuplements forestiers, **ou les événements de magnitude insuffisante**, à partir des cernes de croissance. La **résolution limitée** de l'approche dendrogéomorphologique, **qui ne permet pas de reconstruire deux événements la même année** ou de distinguer deux événements rapprochés est également évoquée. Enfin, les avalanches limitées aux talwegs, souvent asylvatiques, ne sont, bien évidemment, pas reconstruites.

2. La majorité des études se limitent à la reconstruction de séries temporelles. **L'analyse spatiale est le plus souvent limitée** à une cartographie des avalanches ayant impacté le maximum d'arbres, considérées comme extrêmes (Butler et Sawyer, 2008 ; Decaulne et al., 2012 ; Pop et al., 2017, 2016 ; Voiculescu, 2017 ; Voiculescu et al., 2016 ; Voiculescu et Onaca, 2014, 2013). **La cartographie des périodes de retour, pourtant fondamentale pour le zonage de l'aléa, est rarement proposée** (Casteller et al., 2011 ; Corona et al., 2010 ; Martin et Germain, 2016a ; Pederson et al., 2006 ; Reardon et al., 2008 ; Voiculescu et Onaca, 2014). Le cas échéant, elle repose sur une interpolation des fréquences de perturbation calculées pour chaque arbre échantillonné. Ces cartographies ont été utilisées par Casteller et al. (2008) pour la calibration de simulations d'écoulement avalancheux dans les Andes et par Schläppy et al. (2014) ou de modèles statistique-dynamiques dans les Alpes.

3. Il faut également souligner que **parmi les 66 études dénombrées, seules 20 ont analysé le lien entre climat et activité avalancheuse**. Dix, réalisées à l'échelle d'un seul versant, ont permis d'identifier des relations statistiques significatives entre des covariables nivo-météorologiques et l'occurrence d'événements avalancheux (Dubé et al., 2004 ; Germain et al., 2009, 2005 ; Martin et Germain, 2016b; Voiculescu et al., 2016). **Dans les Alpes, l'un des massifs les plus étudiés en dendrogéomorphologie (13/66 études recensées), seuls Schläppy et al. (2016) ont réalisé une étude régionale.** Les reconstructions dendrogéomorphologiques obtenues sur cinq versants des Alpes françaises (de la Maurienne au Briançonnais) ont été comparées à la base de données EPA et aux ré-

analyses météorologiques SAFRAN-CROCUS (1959-2009). En utilisant un modèle linéaire généralisé couplé à une régression *stepwise*, **les auteurs ont pu isoler les co-variables nivo-météorologiques expliquant significativement les fluctuations de l'activité avalancheuse reconstruite. À l'échelle mensuelle, des relations statistiques très significatives sont observées entre l'activité des avalanches et les forts cumuls de précipitations liés à des tempêtes de neige.** D'autre part, les modèles statistiques proposés lient les avalanches documentées dans l'EPA à des anomalies de températures positives. **Les auteurs suggèrent que ce lien est dû à une coévolution des tendances dans les données comparées plutôt qu'à un lien de causalité entre température et avalanches.** Avec cet exemple, **ils soulignent la difficulté d'interprétation des liens entre l'activité des avalanches et le climat dans l'hypothèse où le nombre d'avalanches observées reste stationnaire.**

La problématique de l'impact du réchauffement climatique sur la fréquence des avalanches reste également très rarement abordée.

En Amérique du Nord, Martin et Germain (2017) ont comparé l'activité des avalanches du Massif Présidentiel (New Hampshire, États-Unis d'Amérique), depuis le début du 20ème siècle, avec plusieurs paramètres météorologiques. Ils suggèrent que **les variations de l'activité des avalanches sont en partie contrôlées par l'Oscillation Nord Atlantique dont l'influence affecte aussi la trajectoire des tempêtes de neige.**

En Himalaya, Ballesteros-Cánovas et al. (2018) ont mis en évidence une **augmentation du nombre d'avalanches** sur un versant himalayen **depuis le début des années 1970**. Ils expliquent cette tendance par l'**augmentation des températures hivernales moyennes, la hausse de la teneur en eau de la neige et une fréquence accrue des avalanches de fonte.**

Dans le massif des Tatras (Pologne), Gądek et al. (2017) ont reconstruit l'activité des avalanches extrêmes sur la base d'une approche multiproxy couplée à une rétro-simulation des événements détectés au cours des 100 dernières années. Malgré l'augmentation des températures moyennes, la réduction de l'épaisseur et de la durée du manteau neigeux, aucune tendance significative dans l'activité des avalanches n'est mise en évidence.

Dans les Alpes françaises du Sud, **dans le massif du Queyras, Corona et al. (2013)** ont reconstruit 38 avalanches ayant occasionné des dégâts sur un versant forestier, entre 1338 et 2010. Les auteurs **observent que les hausses de la fréquence des avalanches reconstruites coïncident avec des séries d'hivers anormalement froids** et avec des

périodes d'avancée des glaciers alpins. De même, ils observent une très nette diminution de l'activité des avalanches depuis le milieu du 19ème siècle. **Cependant, ils ne mettent pas en évidence de relation significative entre les variations de l'activité des avalanches et la variation des précipitations hivernales.**

Tous les auteurs soulignent cependant le caractère très préliminaire de leurs analyses, en grande majorité limitée au dernier siècle et sur le caractère local des études réalisées. Ils s'accordent notamment sur la nécessité de développer des chronologies régionales. Ces dernières permettront :

1. **De détecter des tendances robustes d'évolution de l'activité avalancheuse ;**
2. **De s'affranchir des signaux locaux ;**
3. **D'identifier le rôle respectif du réchauffement climatique et de la déprise agro-sylvo-pastorale dans les fluctuations de l'activité avalancheuse reconstruite.**

2. Objectifs et structure de la recherche

Les travaux réalisés durant cette thèse ont pour objectif de pallier les lacunes précédemment identifiées afin d'affiner les connaissances relatives à l'impact des changements environnementaux sur l'activité des avalanches dans les Alpes. Il s'agit, dans un premier temps, de mettre en évidence de potentielles tendances dans l'activité avalancheuse reconstruites, puis de discuter le rôle respectif de la déprise agro-sylvo-pastorale et du changement climatique dans les tendances détectées. **À cet effet, des chronologies d'avalanches, inédites par leur longueur (plusieurs siècles) et leur extension régionale ont été construites à partir de données dendrogéomorphologiques dans :**

- La **vallée de Goms** (Conches, en romand, dans le canton du Valais, Suisse) sur les versants de Münster, de Geschinen et d'Oberwald (11 couloirs, Figure I.5) ;
- Le **massif du Queyras** (Alpes françaises du sud, Hautes-Alpes, France) sur les versants des vallées de Souliers et du Ravin de la Salce (commune de Ristolas) (10 couloirs, Figure I.6).

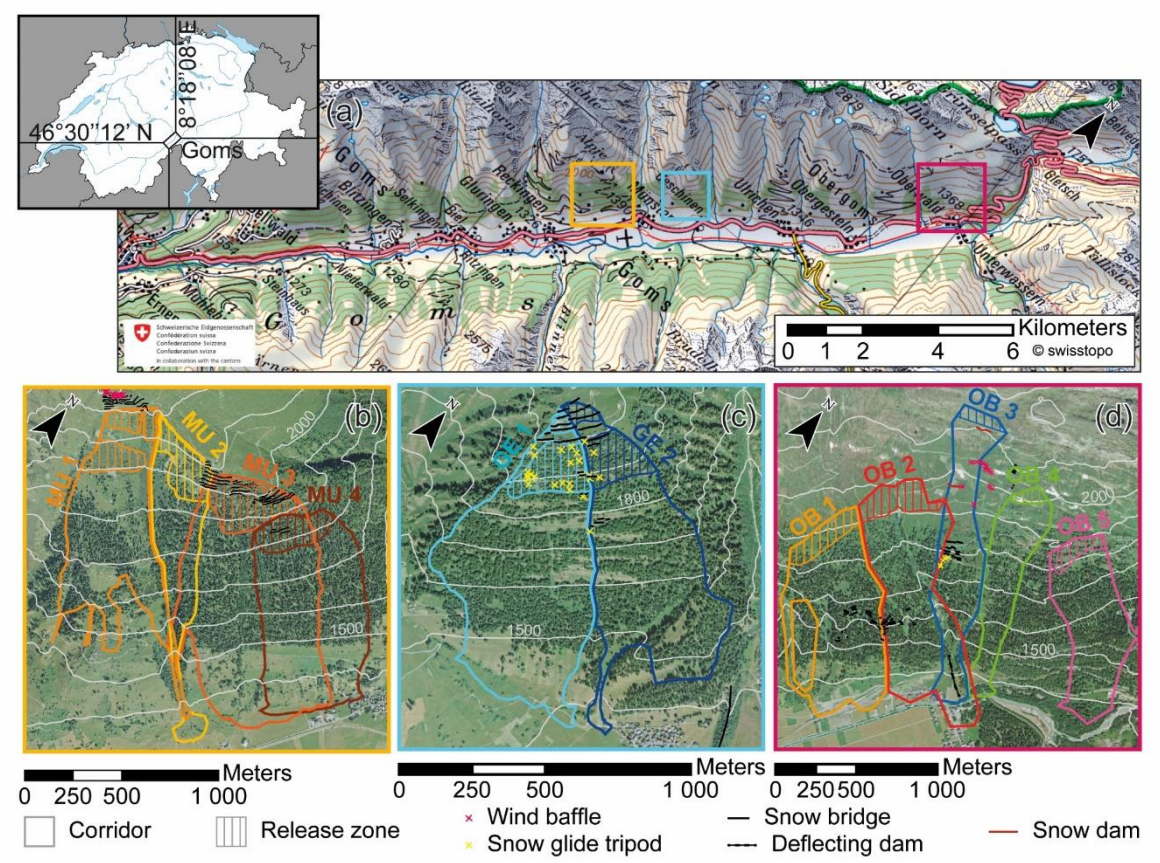

Figure I.5 – Localisation de (a) la haute vallée de Goms, Valais, Suisse, des versants étudiés de (b) Münster, (c) Geschinen et (d) d'Oberwald, et de leurs couloirs d'avalanches.

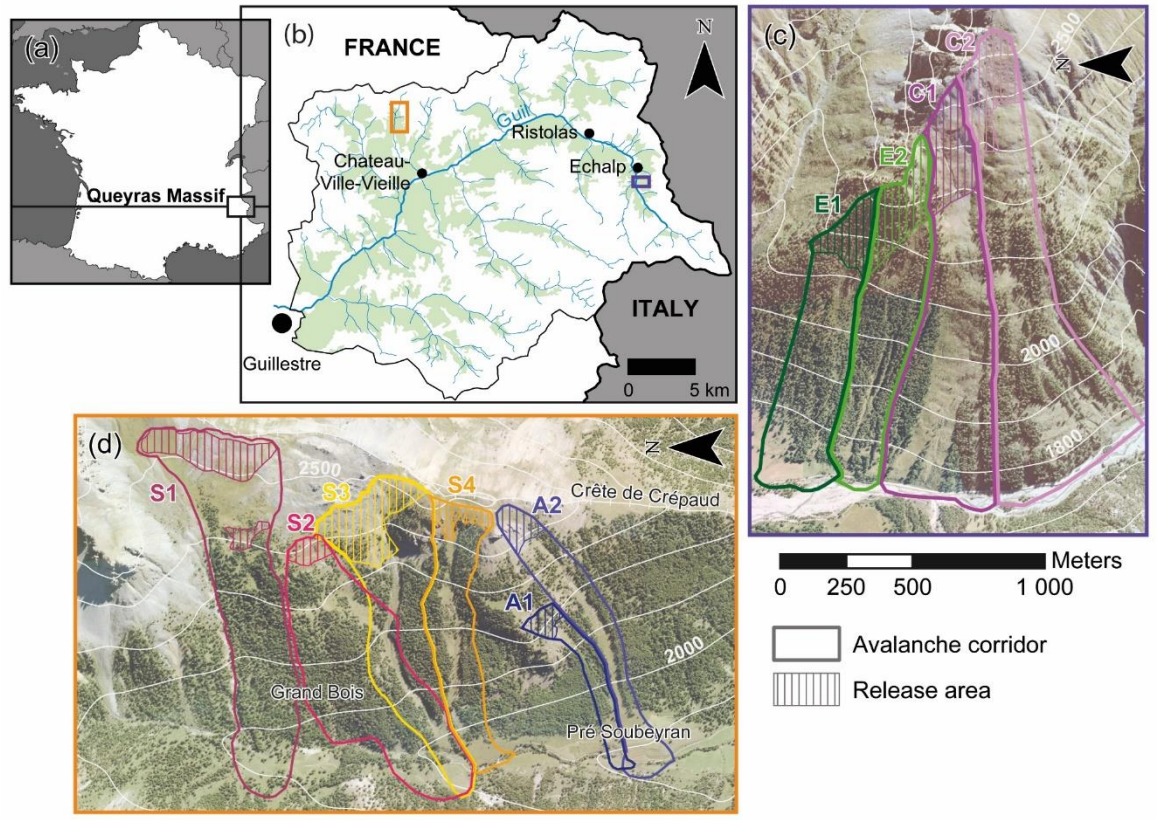

Figure I.6 – Localisation (a) du Massif du Queyras, des versants étudiés (b) du Ravin de la Salce, (c) de Souliers et de leurs couloirs d'avalanches.

La sélection de ces massifs est conditionnée par une quadruple contrainte :

1. Des climats contrastés, caractérisés par une continentalité importante dans la vallée de Goms, et des influences méditerranéennes dans le massif du Queyras, susceptibles d'impacter différemment la dynamique avalancheuse ;
2. L'existence de peuplements forestiers pluri-centenaires sur couloirs d'avalanches permettant potentiellement de reconstruire la dynamique avalancheuse durant le Petit Age Glaciaire ;
3. L'existence de travaux antérieurs dans les deux massifs (Corona et al., 2013 ; Stoffel et al., 2015, 2016) permettant de réduire les temps d'analyse et de les rendre compatibles avec la réalisation d'une thèse de doctorat ;
4. Une documentation historique importante permettant une comparaison des données reconstruites avec des événements observés.

Sur le plan méthodologique, notre objectif principal est centré sur une estimation de la qualité des chronologies produites. Pour cela, nous nous sommes attachés à :

1. Dissocier les perturbations de croissance liées aux avalanches de celles induites par d'autres signaux écologiques (épidémies de pathogènes) ou climatiques (sécheresse, froid) ;
2. Estimer systématiquement la robustesse de chaque événement détecté sur la base de l'intensité et du nombre de perturbations de croissance détectées mais également en tenant compte de potentielles interférences avec les autres signaux ;
3. Estimer la robustesse des chronologies par comparaison avec les données historiques.

Afin d'atteindre ces objectifs, ce manuscrit s'articule autour de cinq chapitres. Les trois premiers chapitres présentent les avancées d'ordre méthodologique réalisées dans ce travail. Ils représentent un préalable nécessaire à la mise en œuvre de chronologies régionales présentées dans les chapitres 4 et 5.

Le **Chapitre 1**, publié dans la revue *Quaternary Geochronology* (2017, volume 42, pages 89 à 104), développe une méthodologie en quatre étapes permettant d'affiner la détection des événements avalancheux passés et de quantifier la robustesse de chaque événement reconstruit. Cette dernière est basée sur (i) le nombre de perturbations annuelles, (ii) l'intensité des perturbations et (iii) de potentielles interférences entre le signal avalancheux et d'autres signaux écologiques et/ou climatiques susceptibles de perturber la croissance radiale.

Le **Chapitre 2**, publié dans la revue *Cold Regions Science and Technology* (2018, 154, pages 9 à 22), analyse le potentiel de l'approche dendrogéomorphologique pour la cartographie des périodes de retour de l'aléa. À la différence des publications existant dans la littérature – dans lesquelles les périodes de retour correspondent à l'interpolation de la fréquence de perturbations au niveau de chaque arbre – notre cartographie est basée sur (i) une estimation de l'enveloppe maximale atteinte par chaque événement puis (ii) du nombre d'avalanches ayant atteint chaque point du versant au cours de la période couverte par la reconstruction. Cette approche reproduit beaucoup mieux les patrons spatiaux attendus pour la période de retour (décroissance amont-aval et fréquence plus importante dans les talwegs) et permet de mettre en évidence l'intérêt de la dendrogéomorphologie pour le zonage de l'aléa.

Le **Chapitre 3**, publié dans la revue *Science of the Total Environment*, s'interroge sur le potentiel de différents versants pour une reconstruction continue et robuste des avalanches, cruciale avant d'analyser d'hypothétiques tendances liées aux changements environnementaux. Pour cela, les reconstructions obtenues sur quatre couloirs voisins mais de structure différentes (topographie, longueur, altitude des zones de départ, couvert forestier) sont analysées. Nos résultats démontrent que les fréquences reconstruites sont significativement supérieures sur des couloirs boisés, d'extension limitée où le taux de convergence avec les archives historiques dépasse 70%. Ces résultats ont des implications importantes sur la sélection des sites, en particulier pour les reconstructions dendrogéomorphologiques dans le contexte du réchauffement climatique.

Le **Chapitre 4**, proposé à la revue *Anthropocene*, montre l'impact des changements paysagers induits par la déprise sylvo-pastorale sur l'activité des avalanches. Dans cette optique, l'activité des avalanches a été reconstruite dans six couloirs adjacents de la vallée de Souliers (Queyras, Hautes-Alpes, France). L'analyse dendrogéomorphologique montre deux tendances distinctes : sur les trois couloirs d'avalanche situés en aval, une augmentation du nombre d'événements reconstruits est observée depuis les années 1970. À l'opposé, les trois couloirs, situés à l'amont, sont caractérisés par une diminution de l'activité des avalanches depuis les années 1930. L'analyse diachronique suggère que la dynamique de recolonisation forestière du versant depuis 1930 est à l'origine des changements observés : à l'amont, la colonisation des zones de départ et la densification du peuplement forestier, facilitées par l'abandon du pastoralisme depuis le milieu du 19^{e} siècle, ont induit une diminution de la fréquence des avalanches. À l'aval, la recolonisation de la portion distale des couloirs à la suite d'un événement de forte magnitude, à l'origine d'une augmentation du potentiel de reconstruction, explique l'évolution observée. Ces résultats soulignent l'importance des interrelations entre l'évolution du couvert forestier, les changements socio-économiques et le réchauffement climatique sur l'activité des avalanches.

Sur la base de ces avancées méthodologiques, le **Chapitre 5** (en préparation pour la revue *Progress in Physical Geography*) synthétise les résultats obtenus sur les 11 couloirs avalancheux de la vallée de Goms entre 1880 et 2014. Il propose une nouvelle méthode d'homogénéisation des chronologies régionales à l'aide d'une régression logistique bayésienne à double composante spatiale et temporelle. Cette approche statistique permet d'extraire des tendances spatio-temporelles robustes du régime annuel/régional moyen des avalanches en éliminant les non-stationnarités induites par la

diminution du potentiel dendrogéomorphologique dans le passé. Néanmoins, malgré la rigueur de l'approche utilisée, les comparaisons des fluctuations décennales de l'activité régionale des avalanches avec les données historiques pour la commune d'Obergoms, les Alpes suisses et françaises sont peu concluantes. De même, les relations entre fluctuations de l'activité avalancheuse et les facteurs climatiques (températures et précipitations) sont peu significatives. Les résultats de ce chapitre questionnent la pertinence des reconstructions dendrogéomorphologiques pour documenter les impacts des fluctuations climatiques sur l'activité avalancheuse. Elles soulèvent notamment des questions concernant le nombre et de la stratégie d'échantillonnage des couloirs à l'échelle régionale afin d'augmenter le ratio signal/bruit.

Le **Chapitre 6** synthétise les résultats obtenus sur les 11 couloirs avalancheux du massif du Queyras. La méthode en 4 étapes (chapitre 1) a permis la reconstruction de 156 événements d'avalanches sur les versants de Souliers et du Ravin de la Salce. Combiné au 26 événements identifiés par Corona et al. (2013), la chronologie régionale du Queyras compile 182 avalanches (93 années) entre 1560 et 2016. Cette dernière a été homogénéisée au moyen de la régression logistique bayésienne présentée dans le chapitre 5. Les résultats montrent la probabilité de déclenchement au cours de la première partie du 19ème siècle est significativement supérieure à celle calculée pour les dernières décennies. Cette la tendance centennale de l'activité régionale coïncide partiellement avec les phases de forte activité du processus identifiée par Jomelli et Pech (2004) durant les périodes 1780–1830, puis 1830–1950, dans le Massif des Écrins. Plusieurs décennies caractérisées par une fréquence avalancheuse forte coïncident avec des conditions climatiques anormalement humides et généralement plutôt froides. Inversement, l'activité avalancheuse plus faible coïncide avec des séries d'hivers plutôt chauds et secs. Ces résultats, encore très préliminaires, suggèrent un lien entre le réchauffement climatique et la diminution de la probabilité de déclenchement observée au cours des dernières décennies dans le Queyras.

Enfin, une **Synthèse Générale** des résultats (i) rappelle les apports méthodologiques de cette thèse, (ii) les principaux résultats obtenus concernant l'impact des changements environnementaux (déprise sylvo-pastorale, réchauffement climatique) sur l'activité des avalanches dans les deux régions étudiées puis (iii) propose des perspectives pour la poursuite des recherches.

Pour la réalisation de cette thèse, j'ai pu utiliser les prélèvements réalisés par le laboratoire Dendrolab (Chaire C-CIA, Institut des Sciences Environnementales, Université de Genève) dans le canton du Valais. Les données dendrogéomorphologiques des vallées

de Souliers et du Guil dans le Queyras (Hautes-Alpes, France) ont été récoltées pour partie, entre 2016 et 2018, par mes soins, avec l'appui financier et technique d'IRSTEA Grenoble, équipes ETNA et LESSEM, et du laboratoire GEOLAB (UCA UMR6042 CNRS). Enfin, ces travaux de thèse ont été en partie financés par la subvention du projet « RARETES » (the avalanche risk as revealer of long range interactions between environment and society) du programme AGIR-PEPS 2016 de l'Université Grenoble Alpes et par l'Agence Nationale de la Recherche à travers le Challenge 4 du programme « Investissement d'Avenir » (16-IDEX-0001 CAP 20-25) de l'Université Clermont Auvergne.

CHAPITRE 1

Disentangling the impacts of exogenous disturbances on forest stands to assess multi-centennial tree-ring reconstructions of avalanche activity

Disentangling the impacts of exogenous disturbances on forest stands to assess multi-centennial tree-ring reconstructions of avalanche activity in the upper Goms Valley (Canton of Valais, Switzerland)

Ce chapitre est en totalité constitué de l'article publié dans la revue :

***Quaternary Geochronology* 42, 2017, 89–104**

doi : 10.1016/j.quageo.2017.09.001

Co-auteurs et affiliations :

Adrien Favillier[1], Sébastien Guillet[2,3], Pauline Morel[2,3,4], Christophe Corona[1], Jérôme Lopez Saez[4], Nicolas Eckert[5], Juan Antonio Ballesteros Cánovas[2, 3], Jean-Luc Peiry[1,6], Markus Stoffel[2,3,7]

1. Université Clermont Auvergne, CNRS, GEOLAB, F-63000 Clermont-Ferrand, France.
2. University of Geneva - Institute for Environmental Sciences, Climatic Change and Climate Impacts, 66 Boulevard Carl-Vogt –CH-1205 Geneva, Switzerland.
3. Dendrolab.ch, Department of Earth Sciences, University of Geneva, rue des Maraîchers 13, CH-1205 Geneva, Switzerland.
4. UR EMGR, Irstea / Université Grenoble Alpes. 38402 St-Martin-d'Hères cedex – France.
5. UR ETNA, Irstea / Université Grenoble Alpes. 38402 St-Martin-d'Hères cedex – France.
6. CNRS, UMI3189, « Environnement, Santé, Sociétés », Faculté de Médecine, UCAD, BP 5005, DAKAR-FANN, Sénégal.
7. Department F.-A. Forel for Environmental and Aquatic Sciences, University of Geneva, 66 Boulevard Carl-Vogt, CH-1205 Geneva, Switzerland.

Remerciements et financements

This chapter and the following article were financially supported by the Forest and Landscape Department at the Canton of Valais and the Community of Obergoms. Dendrogeomorphic data were sampled, processed and analysed by Dendrolab.ch.

Abstract

The purpose of dendrogeomorphic analyses is to amplify the signal related to the geomorphic process under investigation, and to minimize the noise induced by other signals in the tree-ring series. Yet, to date, no study accounts specifically for interferences induced by climate conditions or exogenous disturbances and which can, potentially, affect the quality of tree-ring based process reconstructions. In this paper, we develop a specific procedure allowing evaluation of the quality of reconstructions in five avalanche paths at Oberwald (Swiss Alps). The study is based on possible interferences between snow avalanches, climatic conditions and ecological signals in the tree-ring series. Analysis of past events was based on tree-ring series from 564 heavily affected, multi-centennial European larch trees (*Larix decidua* Mill.) growing near or next to the avalanche paths. A total of 2,389 growth disturbances, such as scars, tangential rows of traumatic resin ducts, compression wood as well as abrupt growth suppressions or releases, were identified in the samples, indicating 43 destructive snow avalanches since AD 1780. At the same time, 31 potential events, which were detected with the conventional Shroder index value, were rejected from the final reconstruction due to potentially strong interferences between the different signals. This high rejection rate underlines the necessity to systematically–and carefully–discriminate ecological and climatic noise from avalanche-related disturbances. This discrimination is even more so crucial as a significant proportion of dendrogeomorphic studies in the Alps are based on L. decidua trees which are cyclically affected by larch budmoth outbreaks.

Keywords: Dendrogeomorphology; snow avalanches; spatio-temporal analysis; tree ring; Swiss Alps

Résumé

Les analyses dendrogéomorphologiques ont pour but d'amplifier le signal lié au processus géomorphologique étudié et de minimiser les bruits induits par les autres signaux dans les séries de cernes. Pourtant, à ce jour, aucune étude ne tient spécifiquement compte des interférences induites par les conditions climatiques ou les perturbations exogènes qui sont susceptibles d'affecter la qualité des reconstructions dendrogéomorphologiques du processus. Dans ce chapitre, nous développons une méthode spécifique permettant d'évaluer la qualité des reconstructions dans cinq couloirs d'avalanches à Oberwald (Valais, Suisse). L'étude est basée sur la discrimination des interférences possibles entre les avalanches, les conditions climatiques et les signaux écologiques dans les séries de cernes. La détection des avalanches passées est basée sur l'analyse des séries de cernes de croissance issues de 564 mélèzes d'Europe (*Larix decidua* Mill.) pluri-centenaires, fortement perturbés, poussant dans ou à proximité des couloirs d'avalanches. Au total, 2 389 perturbations de croissance, telles que des cicatrices, des rangées tangentielles de canaux résinifères traumatiques, du bois de compression ainsi que des réductions de croissance ont été dénombrées dans les échantillons, permettant la détection de 43 avalanches depuis 1780. Durant la même période, 31 événements potentiels, détectés avec l'indice I Shroder, ont été rejetés de la reconstruction finale en raison des fortes interférences potentielles entre les différents signaux. Ce taux de rejet élevé souligne la nécessité de faire une distinction systématique – et prudente – entre les bruits écologiques et climatiques et les perturbations de croissance liées aux avalanches. Cette discrimination est d'autant plus cruciale qu'une part importante des études en dendrogéomorphologie dans les Alpes est basée sur les mélèzes d'Europe, essence affectée de manière cyclique par des épidémies de tordeuse du mélèze.

Mots-clefs : dendrogéomorphologie, avalanches, analyses spatio-temporelles, cerne de croissance, Alpes suisses.

1. Introduction

Snow avalanches are a major natural hazard in the Alps. Every year, they affect transport infrastructure and may endanger settlements and threaten human life. Over the last century, urban sprawl in mountain areas in combination with a growing demand for mobility and recreational activities have increased avalanche risk significantly. Substantial efforts have therefore been deployed to build databases with past avalanche events so as to provide accurate information regarding their magnitude, spatial extent, and return period. However, historic documentation of past avalanche activity is most often biased toward events that caused damage to infrastructure or loss of life and remains largely nonexistent in sparsely or recently populated areas (Corona et al., 2012). On forested paths, dendrogeomorphology (Alestalo, 1971; Stoffel et al., 2010) has proven to compensate for the scarcity of written sources as it allows reconstruction of past, natural avalanche activity in time and space (Butler and Sawyer, 2008). The approach, first elucidated by (Alestalo, 1971), takes advantage of the fact that trees growing in temperate climates do not only form yearly increment rings, but that they will also record the occurrence of external disturbance events in their growth-ring series, thus allowing accurate dating and reconstruction of past process histories (Stoffel and Corona, 2014b). (Cook, 1987) described the tree growth as a linear aggregate of several unobserved subseries following:

$$R_t = A_t + C_t + \delta D1_t + \delta D2_t + E_t \quad \textbf{(Eq. 1.1)}$$

where Rt is the observed ring-width series; At is the age-size related trend in ring-width; Ct is the climatically related environmental signal; δD1t is the disturbance pulse caused by a local endogenous disturbance; δD2t is the disturbance pulse caused by a stand-wide exogenous disturbance; and Et is the largely unexplained year-to-year variability not related to the other signals.

The purpose of dendrogeomorphic approaches therefore is to amplify the parameter δD1t related to the process under investigation (i.e. snow avalanches) and to minimize the noise induced by other signals. The reconstruction of snow avalanching using tree rings has a fairly long history with increasing sophistication characterizing most recent applications (Butler and Sawyer, 2008). Since the seminal reconstructions of (Potter, 1969) and (Schaerer, 1972) in North America, new growth disturbances, such as tangential rows of traumatic resin ducts (referred hereafter as TRDs), have been added to more classical parameters (Stoffel et al., 2005; Schneuwly et al., 2008). In addition, different quantitative approaches have been proposed so as to enhance the detection of snow avalanche years (Corona et al., 2012; Schläppy et al., 2013; Chiroiu et al., 2015; Germain, 2016; Martin and

Germain, 2016). Paradoxically, no single study has so far accounted specifically for the interferences which can be induced potentially by climatic conditions (Ct) or by exogenous disturbances (e.g., insect and pathogen attacks, fire, windstorms or anthropogenic influences) on the dendrogeomorphic reconstructions.

The purpose of this study therefore is to maximize the tree-ring signal related to past snow avalanches. To this end, we focused on (i) the dendrogeomorphic reconstruction of past snow avalanches in the upper Goms Valley (Canton of Valais, Swiss Alps), where long chronologies of past snow avalanche activity are lacking, despite the fact that massive events in 1998/9 have damaged substantially century-old forest stand and infrastructure; (ii) the disentanglement of geomorphic signals in tree-ring series from climatic and ecological signals; (ii) a quantification of the reliability of each reconstructed event, based on the inclusion of information on historical events; and (iv) the qualitative magnitude of individual, past snow avalanche events.

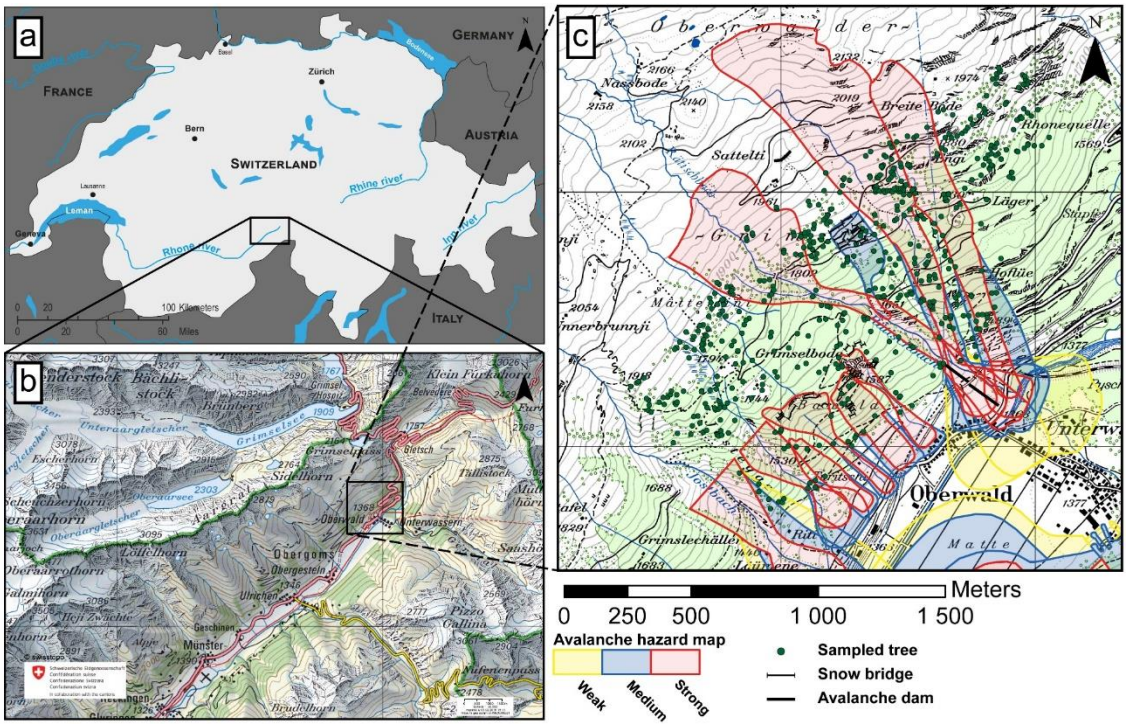

Figure 1.1 – Location of the study site in (a) Switzerland and (b) in the Goms Valley. (c) Spatial distribution of sampled trees. The colored areas represent the hazard map defined by the canton of Valais. Red indicates an area that is exposed to considerable danger with frequent avalanches (average return period of 30 years or less). In the blue colored area, avalanches are less frequent (30-100-year average return period) and have mean pressures of less than 30 kN/m². The yellow area is giving the extent of avalanches with return periods of 100–300 years, but also designates the runout zone of powder avalanches.

2. Study site

The Oberwald avalanche paths (46°32'N, 8°20'E, Fig. 1.1) are located on the south-facing slope of the upper Goms Valley in the Central Swiss Alps (Canton of Valais, Switzerland, Fig. 1.1a-b). These paths threaten the village of Oberwald and the Matterhorn-Gotthard Bahn (MGB) railway line connecting Brig (Canton of Valais) to Andermatt (Canton of Uri) (Fig. 1.1c). The site under investigation is 155 ha in size and has a difference in elevation of about 820 m (1360–2180 m asl) from the base of the slope to the highest release zones. Its geology is dominated by biotite gneisses interrupted by granitic cliffs-oriented E-W (Federal Office of Topography Swisstopo). Two main channels, i.e. the Rätischbach and one of its unnamed tributaries, have witnessed recent snow avalanche activity leaving a 260-m wide cone at the foot of the Rätischbach avalanche path.

According to data from the nearby meteorological station at Ulrichen (46°5'N, 8°31'E, 1346 m asl), annual temperature is 3.7°C for the period 1981-2010 and annual precipitation amounts to 1212 mm. During winter, mean air temperature (DJF) is -6.6°C and between November and April precipitation falls primarily as snow with average annual snowfall reaching 578 cm for the period 1999–2010 (the average snow cover period is 171 days). Snow avalanches release spontaneously at the site from a series of starting zones located between 1680 and 2200 m asl. Once released, they pass through a forested slope mainly composed of European larch (*Larix decidua* Mill.) and Norway spruce (*Picea abies* (L.) Karst.). Archival records report several avalanche events (section 3.1) since AD 1720 and the structure of the forest stand points to repeat and ongoing avalanche activity at the site to the current day. As a consequence, several rows of deflecting barriers have been put in place by the state authorities to stabilize snowpack in the source area of avalanches and to prevent the release of avalanches (Fig. 1.1).

3. Material and methods

3.1. Compilation of historical archives

First, we compiled a historical database of past snow avalanches at Oberwald based on different documentary sources available for the period 1900-2013 at the *Institut zur Erforschung der Geschichte des Alpenraums* (FGA) and from the local forest service. For this period, documentation was also extracted from technical reports established by the Swiss Federal Institute for Snow and Avalanche Research (SLF) and from local newspapers. Before the 20th century, local chronicles available at FGA and information contained in the Swiss database from (Laternser and Pfister, 1997) were reviewed in detail.

To complement the archival database, six aerial flight campaigns available from the Federal Office of Topography (swisstopo; in the scale of *ca.* 1:20,000) were used in addition so as to detect evidence of damaging avalanche events since 1946.

3.2. Delineation of avalanche path

Several factors render a precise delineation of the avalanche flow paths at Oberwald rather complex, namely (i) the multitude of release areas, (ii) the absence of preferential paths in the western part of the slope and (iii) the dense forest cover, which is effectively masking geomorphic evidence of past avalanche events. To overcome this limitation, we used the numerical avalanche dynamics model RAMMS (*Rapid Mass Movement System*; (Gruber and Bartelt, 2007; Christen et al., 2010), as it has proven to be useful for an accurate delineation of flow paths in complex terrain (Rudolf-Miklau et al., 2015). RAMMS predicts avalanche runout distances, flow velocities, impact pressures and a three-dimensional terrain model using a finite volume scheme to solve the shallow water equations. The required input parameters for RAMMS include (i) a digital elevation model (DEM), (ii) information about the size and location of the release area and snow height in the release area, as well as (iii) friction parameters. The simulations with RAMMS were based on a 1-m Digital Elevation Model (DEM) provided by the Canton of Valais. The spatial extent of avalanche release areas as well as the previously recognized hazard areas was determined based on expert knowledge (Fig. 1.1c). Paths were delineated based on return periods (30, 100 and 300 years) and the maximal extent of pressure output data given by the simulations.

3.3. Sampling strategy, identification, dating and classification of growth disturbances

To reconstruct past avalanche activity based on dendrogeomorphic techniques, a total of 1140 increment cores and 10 cross-sections were sampled from 564 of European larch (*Larix decidua* Mill.) and Norway spruce (*Picea abies* (L.) Karst.) trees using Pressler increment borers (diameter 5.15 mm, maximum length 40 cm) in summers 2013 and 2014. A minimum of two cores was extracted per tree, one perpendicular to the slope and one in the downslope direction. Additional data were collected for each tree including its diameter at breast height, description of the disturbance (i.e. number of scars, decapitation, tilting), exact position of the sampled tree using a 1-m precision GPS device and data about neighboring trees.

Trees presenting obvious evidence of snow avalanches, such as decapitation, tilting, and injury, were preferentially selected. Following recent recommendations by (Stoffel and Corona, 2014), old trees were selected to extend the reconstruction of past avalanche events as far as possible. Nevertheless, younger trees were also considered to account for the loss of sensitivity of older trees in recording mass-movement signals (Šilhán and Stoffel, 2015). Sampling height was chosen according to the morphology of the stem: (i) injured trees were sampled at the height of the disturbance from the overgrowing scar tissue; (ii) tilted tree samples were extracted at the maximum bending angle (Stoffel et al., 2013); (iii) cross-sections and cores from decapitated trees were taken at the lowest possible position on the tree to maximize the number of available rings (Stoffel and Bollschweiler, 2008). Samples were prepared and data processed following standard procedures described in (Stoffel et al., 2013a). Growth disturbances (GD) such as impact scars and callus tissues (CT) (Stoffel et al., 2010), tangential rows of traumatic resin ducts (TRD; Schneuwly et al., 2009a,b), compression wood (CW) and abrupt growth suppression (GS; Kogelnig-Mayer et al., 2013) were identified in the tree-ring series and cross-dated with two local reference chronologies (Büntgen et al., 2005), so as to correct our series for possibly missing rings.

Intensities were then assigned to each GD using criteria defined by Kogelnig-Mayer et al. (2011). This step was included to emphasize features which were clearly associated with avalanche activity. The intensities of growth suppression, compression wood, and TRDs were classified according to Schneuwly et al., (2008) and Frazer (1985) to distinguish between weak (intensity class 1), medium (intensity class 2), and strong (intensity class 3) reactions and clear evidence of injuries (intensity class 4).

3.4. Detection of past avalanche events in growth disturbance series

To detect past snow avalanches in the GD series and to disentangle potential effects of snow avalanches from disturbance pulses caused by climatic or exogenous factors, such as drought years or larch budmoth outbreaks, a four-step procedure was adopted in this study. The approach indeed combines the avalanche event detection methods developed by Shroder, (1978), Reardon et al., (2008), Kogelnig-Mayer et al., (2011) and Corona et al., (2012).

(i) In a first step, for each year t and for each path, an index I was calculated, according to Shroder (1978); this index is based on the percentage of trees showing responses in their growth ring record in relation to the number of sampled trees being alive

in year t:

$$I_t = \left(\left(\sum_{i=1}^{n} R_t \right) \Big/ \left(\sum_{i=1}^{n} A_t \right) \right) * 100 \qquad \textbf{(Eq. 1.2)}$$

where ΣR represents the number of trees responding to an event in year t, and ΣA is the number of trees alive in year t. Following recommendations from Butler and Sawyer (2008), a double threshold for sample sizes of 21−54 (GD > 4 and It >5%) and ≥55 trees (GD > 7 and It > 5%) has been used to discriminate potential avalanche and non-avalanche years in accordance with statistically determined thresholds as defined by Corona et al. (2012) for the Pèlerins avalanche path (France). These thresholds also aimed at limiting the inclusion of noise related to snow creeping (Stoffel and Corona, 2014b), snow loading (Martin and Germain, 2016a), or any other kind of ecological disturbances (Butler and Sawyer, 2008b; Corona et al., 2012b) in the process reconstruction (Fig. 1.2).

(ii) The grey larch budmoth (LBM, *Zeiraphera diniana* Gn.) is a foliage feeding Lepidopteran insect responsible for periodical outbreaks (8- to 10-year intervals), mainly in the interior valleys of the European Alps (Baltensweiler et al., 1977). The feeding of the LBM on larch needles causes massive defoliation resulting in growth suppression lasting over 3 to 4 years (Kress et al., 2009) which may, thus, interfere with the dendrogeomorphic

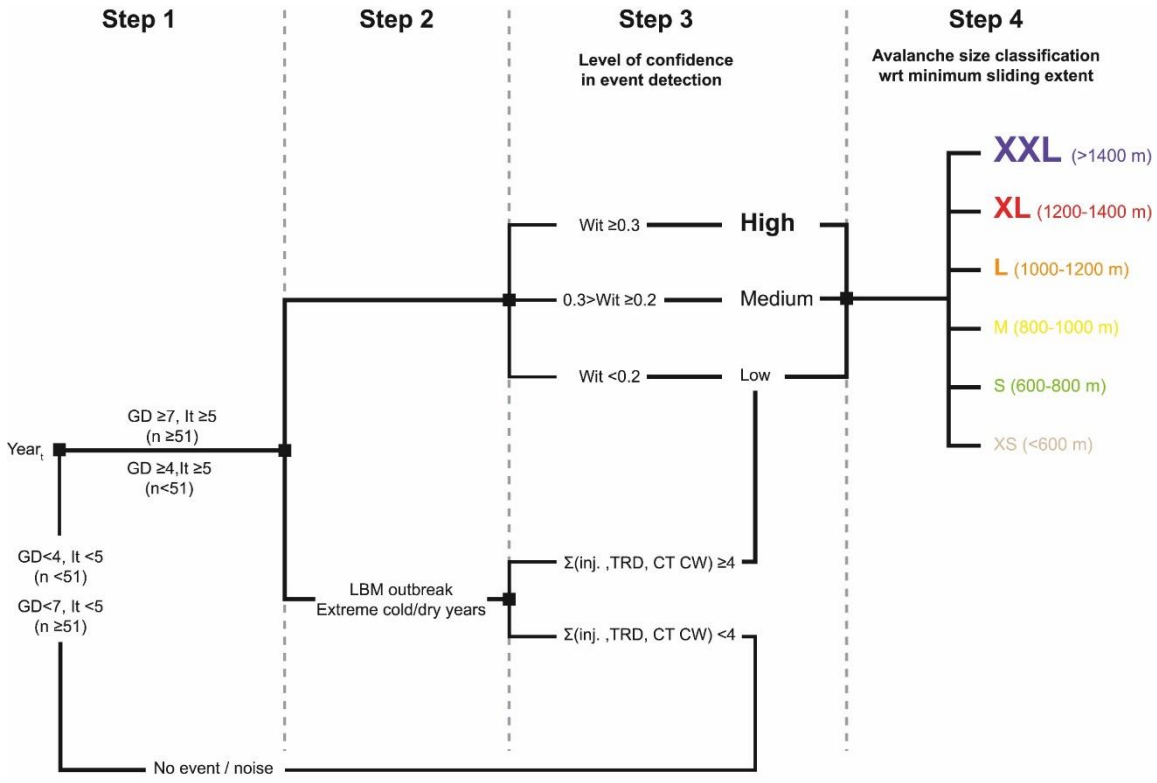

Figure 1.2 – Synoptic diagram of the 4-step approach used for the detection of avalanche events in tree-ring series.

signal contained in tree rings. In total, 21 triplets of LBM outbreak years (i.e. series of three consecutive years) have been reconstructed in the Swiss Alps since 1780 according to Esper et al. (2007) and Büntgen et al. (2009). Similarly, climate extremes such as cold summers and prolonged droughts are susceptible of durably affecting larch growth (Battipaglia et al., 2010; Lévesque et al., 2013; George et al., 2016) and to cause prolonged growth suppressions that may be assimilated to avalanche-related GDs. According to (Battipaglia et al., 2010), in the central Alps, extremely cold summers were recorded in tree-ring data and historical archives in 1814, 1816, 1829, 1833, 1851, 1860, 1896, 1912, 1924, 1964, 1972, 1984, and 1995. Based on the gridded HISTALP point temperature information (Efthymiadis et al., 2006) closest to the study site, 14 years with negative May-September anomalies of precipitation (with values exceeding–1.5 SD below the average) could be found for the period 1800-2003–and have thus been considered as dry years (Tab. 1.1).

Potential avalanche events detected in step 1 coinciding with LBM outbreak episodes or extremely cold/dry years were therefore examined in more detail. In order to limit possible interferences between geomorphic, climatic, and LBM signals, growth suppressions were systematically excluded from the account of GDs and a minimum threshold of 4 GDs was retained to discriminate avalanche from non-avalanche years (Fig. 1.2).

(iii) In a third step, the type and intensity of GDs were used to evaluate a qualitative level of confidence associated with the detection of each reconstructed event. To this end, a weighted index factor (Wit), adapted from (Kogelnig-Mayer et al., 2011), was computed for each avalanche event detected in step 1 as follows:

$$W_{it} = \frac{[(\sum_{i=1}^{n} T_i * 7) + (\sum_{i=1}^{n} T_s * 5) + (\sum_{i=1}^{n} T_m * 3) + (\sum_{i=1}^{n} T_w * 1)]}{\sum_{i=1}^{n} A_t} \quad \textbf{(Eq. 1.3)}$$

where, for each year t, T_i represents the sum of trees with injuries; T_S represents the sum of trees with strong GDs; T_m represents the sum of trees with medium-intensity GDs; T_w represents the sum of trees with weak-intensity GDs, and where A gives the total number of trees alive in year t. Based on the Wit, we then distinguish between low (LLC, Wit<0.2), medium (MLC, 0.3>Wit>0.2), and high (HLC, Wit>0.3) levels of confidence and attribute this evaluation to the avalanche event detection. In addition, and despite the precautions taken at each of the previous step, each event detected at step 2 was rated with a LLC (Fig. 1.2).

Table 1.1 – Larch budmoth events (according to Esper et al., 2007 and Büntgen et al., 2009), as well as extremely cold and dry summers (Efthymiadis et al., 2006) in the Swiss Alps. All these years have been carefully analyzed due to probable interferences between snow avalanche damage in trees, as well as LBM and climatic signals.

2003	*1965*	*1924*	**1888**	**1830**
1995	**1963**	**1923**	**1880**	*1829*
1989	1962	1919	1871	**1821**
1986	1959	**1915**	1870	*1816*
1984	**1954**	*1912*	**1864**	*1814*
1981	**1945**	**1908**	*1860*	**1811**
1976	**1937**	1906	**1856**	**1801**
1972	**1931**	**1896**	*1851*	**1792**
1972	1929	*1896*	**1838**	**1779**
1966	1928	1895	*1833*	**1771**

LBM-outbreak years, *Extreme cold summer*, Drought years

(iv) Finally, avalanche years and corresponding GDs were mapped using the ArcGis 10.2 Time Slider (Kennedy, 2013; ESRI, 2013) so as to estimate the minimum sliding extent (ME, w.r.t the barycenter of the avalanche release zones) of each avalanche event. On the basis of ME, avalanche events with ME<600, 600<ME<800, 800<ME<1000, 1000<ME<1200, 1200<ME<1400 and ME<1400 were classified as eXtra Small (XS), Small (S), Medium (M), Large (L), eXtra Large (XL), and eXtra eXtra Large (XXL) events, respectively.

The age structure of the stand was approximated by counting the number of tree rings in the selected trees and was visualized after interpolation. However, since trees were not sampled at their stem base and as piths as well as the innermost rings of some trees were rotten, the age structure does neither reflect inception nor germination dates. Nonetheless, this data may provide valuable insights into major disturbance events at the study site with reasonable precision, as *L. decidua* has been shown repeatedly to recolonize surfaces cleared by snow avalanches or other mass-movement processes in the years following an event (Stoffel et al., 2006; van der Burght et al., 2012).

For each path, the annual probability for an avalanche event was computed as:

$$AP_i = \left(\frac{A_i}{L_i}\right) \quad \textbf{(Eq. 1.4)}$$

where A represents the number of reconstructed events at path i and L is the period covered by the reconstruction at site i.

4. Results

4.1. Mapping of avalanche path at Oberwald

At Oberwald, precise geomorphic mapping–including field observations and a digital terrain model (DTM) generated from airborne Lidar data point clouds–as well as

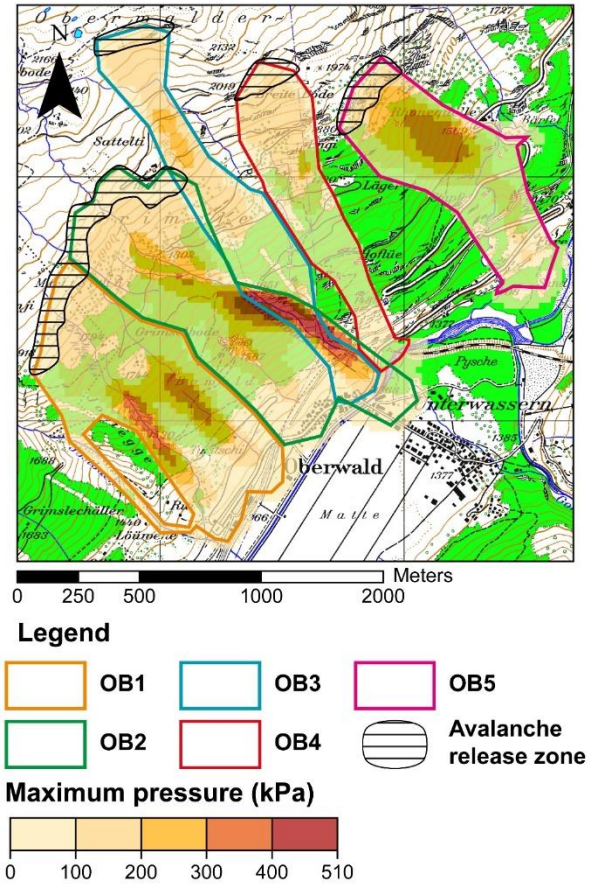

Figure 1.3 – Mapping of the avalanche paths (OB1-OB5) at Oberwald based on field observations and digital terrain model (DTM) data derived from airborne Lidar data point clouds, as well as maximal extension of avalanche flows as derived from maximal pressure data from RAMMS numerical snow avalanche simulations.

flow extensions with the RAMMS numerical snow avalanche simulations revealed a minimum of five distinct avalanche paths, namely form east to west: OB1 (57.8 ha, 1258 m long, 611 m wide), OB2 (66.6 ha, 1578 m long, 532 m wide), OB3 (39.15 ha, 1845 m long, 318 m wide), OB4 (29.63 ha, 1364 m long, 344 m wide), and OB5 (38.19 ha, 1141 m long, 377 m wide) (Fig. 1.3).

4.2. Snow avalanches recorded in historical archives

For the period AD 1780–2017, six events were found in local archives, namely in 1921, 1935, 1951, 1961, 1999, and 2003. During winter 1950–51, an extreme avalanche occurred at Rätischbach (OB3).

4.3. Age structure of the stand

In total, 564 European larch (*Larix decidua* Mill.) and Norway spruce (*Picea abies* (L.) Karst.) trees were sampled with 1140 increment cores and 10 cross-sections. The samples were distributed as follows between the five paths: OB1: 127 trees, OB2: 135 trees, OB3: 100 trees, OB4: 125 trees, and OB5: 77 trees. After cross-dating, data on the pith age at breast height indicates that European larch and Norway spruce trees growing at Oberwald were on average 206 yrs old (±115 yrs). The oldest tree selected for analysis attained sampling height in AD 1429 while the youngest tree only reaches breast height in AD 1991. As illustrated in Figure 1.4, the stand is dominated by 100-200-yr (37.1%) and 200-300-yr (27.8%) old trees. In total, 39 and 13 trees could be found with ages exceeding 400 years and 500 years, respectively. Young trees (≤100 yr, 16.8%) are scattered over the slope and do not show any significant pattern which would suggest forest recolonization after high-magnitude disturbance events. By contrast, the oldest trees are preferentially located in two patches

located above 1800 m a.s.l., on the interfluves of OB1/OB2 and OB2/OB3, thus suggesting that no event in the recent past would have had sufficient energy to completely destroy these forest stands over the last centuries.

4.4. Distribution of growth disturbances

Sampled cores and cross-sections permitted identification of 2,389 GD in the tree-ring series, 489 of which were considered strong avalanche indicators (Class 3 or 4). Table 1.2 summarizes the types of GD as well as their intensity. TRDs, CT and CW were the GDs most frequently (54.5%) identified in the samples, followed by growth suppressions (GS; 43.6%). By contrast, only 47 injuries were sampled, which represents 1.9% of the dated disturbances. In total, 51.2% of the GDs were rated as intensity 1 and 28.3% as intensity 2. Intensities 3 and 4 represent 18.5% and 1.9% of detected GDs, respectively. The oldest GD identified in the tree-ring series was dated to AD 1781. GDs are more frequent after AD 1900 and nearly every year exhibited GD in a small number of trees (Fig. 1.5).

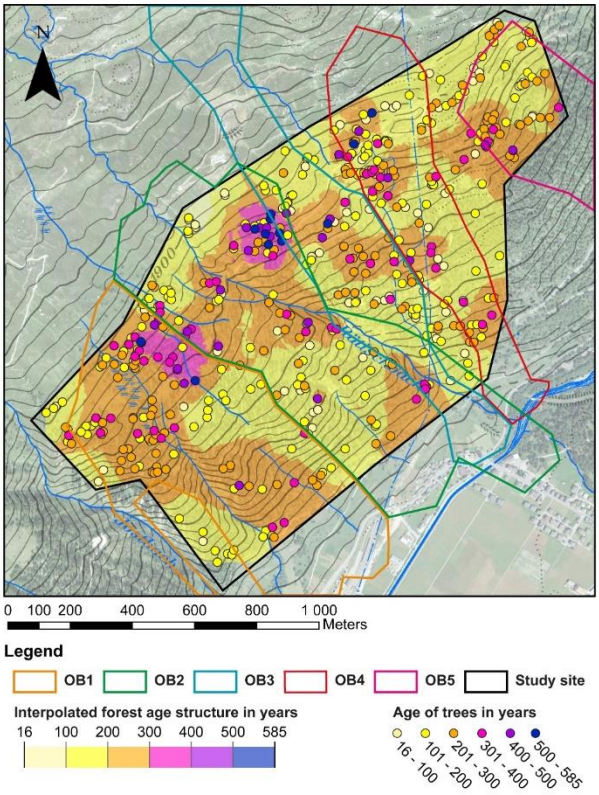

Figure 1.4 – Age structure of the forest stand growing in and next to the Oberwald avalanche paths.

Table 1.2 – Intensity of reactions and types of growth disturbances (GD) assessed in the 564 larch trees selected for analysis.

Intensity	1	2	3	4	Total
Injuries	-	-	-	47 (1.9%)	47 (1.9%)
CT, TRD	704 (29.5%)	313 (13.1%)	284 (11.9%)	-	1301 (54.5%)
GS	520 (21.8%)	363 (15.2%)	158 (6.6%)	-	1041 (43.6%)
Total	1224 (51.2%)	676 (28.3%)	442 (18.5%)	47 (1.9%)	2389 (100%)

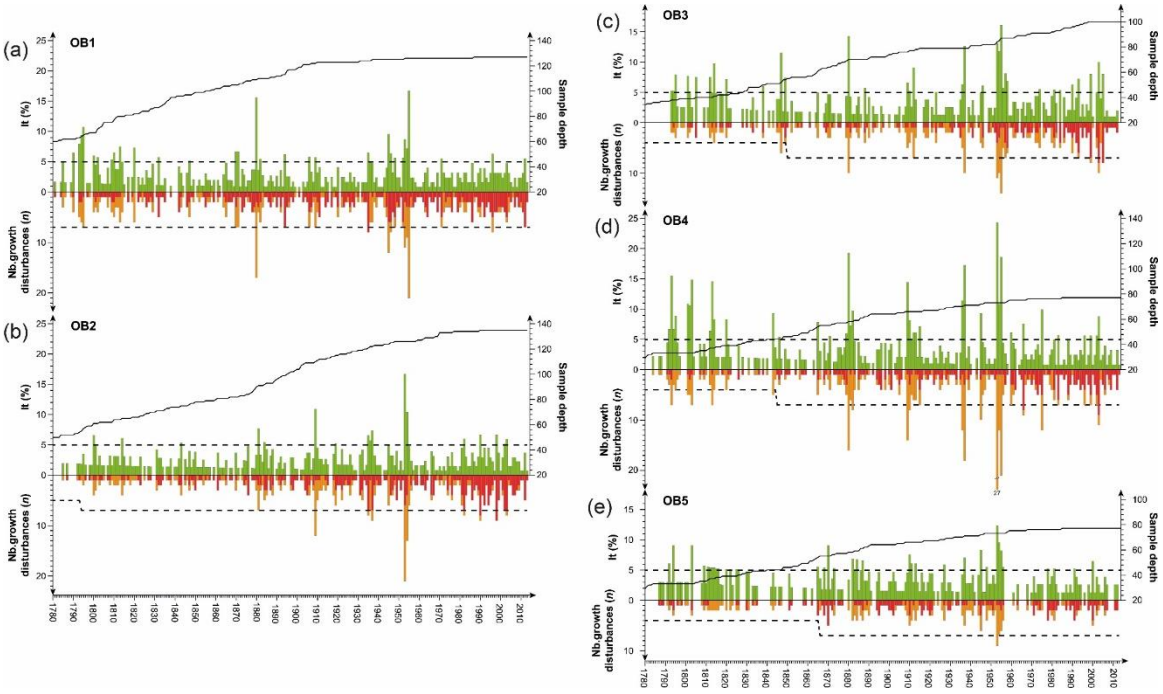

Figure 1.5 – Event-response histograms showing the total number of growth disturbances (GD, in red and orange) and the percentage of trees responding to an event (in green) at each of the five Oberwald paths (a-e). Orange bars show the total number of growth reductions which are possibly related to larch budmoth outbreaks or to climatic extremes. The dashed lines denote the GD and It thresholds used to reconstruct past avalanche events. The solid lines denote sample depth, i.e. the number of trees available for analysis for each year of the reconstruction.

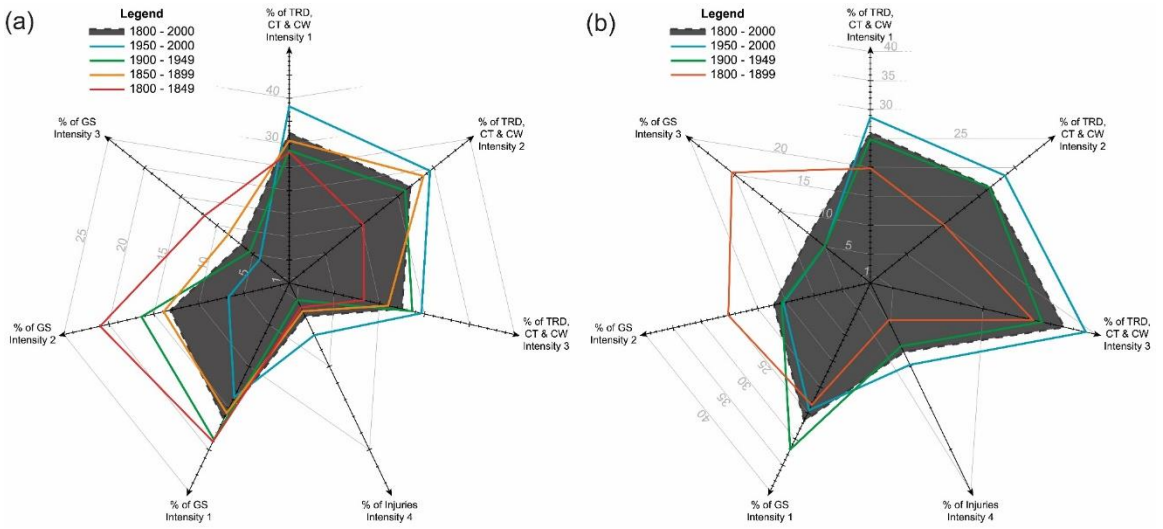

Figure 1.6 – Radar chart showing the distributions of GD types and intensities for 50-year periods between 1800 and 2000. Panel (a) includes all GD detected in trees, except during LBM outbreaks; panel (b) only shows GDs attributed to snow avalanche events.

GDs are almost evenly distributed between the five paths (OB1: 26.6%, 4 GD.tree^{-1}; OB2: 21.8%, 3.1 GD.tree^{-1}; OB3: 16.9%, 3.3 GD.tree^{-1}; OB4: 21.9%, 3.4 GD.tree^{-1}; OB5: 12.8%, 3.2 GD.tree^{-1}). A clear temporal trend is observed in the 50-yr distribution of GDs (Fig. 1.6), with an increasing frequency of TRD, CW, and CT since AD 1800 and an overrepresentation of injuries during the last 50 years. Conversely, the proportion of GS in the spectra of GDs continuously decreased from 46.7% for the period 1800-1850 to 17.5% after 1950.

4.5. Chronology of avalanche events

The event-response histogram depicted in Figure 1.5 shows all reactions recorded in the trees along the avalanche paths. On the basis of our 4-step-procedure (Fig. 1.7), tree-ring analyses allowed reconstruction of 43 avalanche events between 1780 and 2013 (Fig. 1.9), with the oldest event being recorded in 1795 (OB1-OB4), and the most recent one in 2012 (OB1). Despite the exclusion of GS which were obviously related to LBM outbreaks or climatic extremes (step 2), the spectra of GDs used to reconstruct these events show a clear overrepresentation of TRD, CW, CT, and injuries during the last 100 years (Fig. 1.6b).

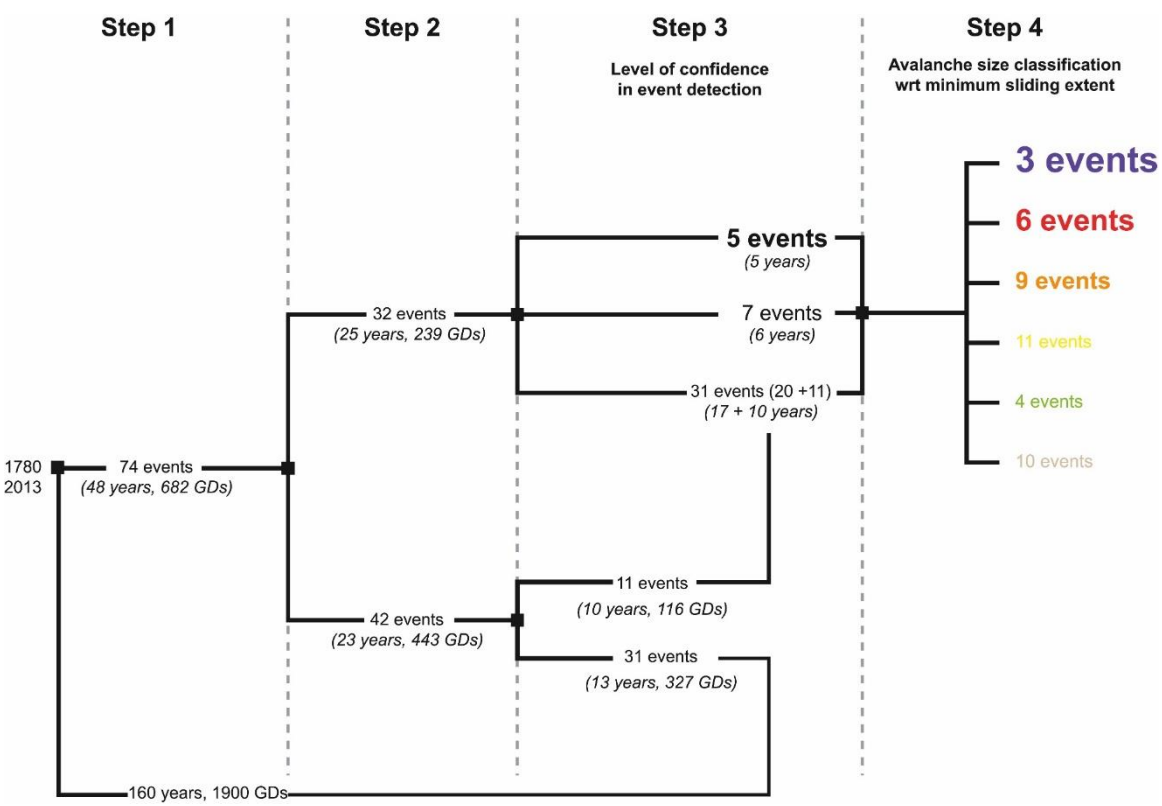

Figure 1.7 – Simplified synoptic diagram showing the characteristics (possible interference with climate or larch budmoth outbreaks, level of confidence, minimum slide extent) of the reconstructed events based on the 4-step procedure presented.

In total, 11 (1795-2012), 9 (1935-2003), 8 (1846-2005), and 15 (1795-2003) avalanche events were reconstructed at sites OB1-OB4, respectively. No event was reconstructed at site OB5. Based on possible interferences between the avalanche, climatic, and LBM signals in the tree-ring series (step 2), and on the basis of the Weighted Index Factor (Wit; step 3, Fig. 1.8) that accounts simultaneously for the type and intensities of GDs, we assigned high and medium levels of confidence to 5 and 7 events, respectively (see for example Fig. 1.10a, b). By comparison, 31 events with a Wit<0.2, and characterized by a majority of weak and medium GDs, were therefore reconstructed with a LLC (Fig. 1.9b, e). Amongst the 42 potential events that coincide with LBM outbreak episodes or extreme climatic years, 31 were excluded from the reconstruction, (Fig. 1.9f) and 11 were rated with a LLC (Tab. 1.3, Fig. 1.7, Fig. 1.10e).

Higher levels of confidence were assigned to events that occurred at OB3 (2 HLC and 4 MLC events) and OB4 (3 HLC and 2 MLC events). Tree-ring signatures related to past snow avalanche activity were, by contrast, less frequent and less intense at sites OB1 and OB2, and a large majority of events (95%) was considered to have a LLC. Tree-ring evidence for the historical events in 1935, 1999, and 2003 could be identified at tracks

Table 1.3 – Characteristics of reconstructed events coinciding with LBM outbreak episodes or extreme climatic events. The above events were retained in the final reconstruction due to their high proportion of strong GDs (i.e. callus tissue, injury, tangential rows and traumatic resin ducts, compression wood) which cannot be attributed to LBM outbreaks or climatic signatures. Nonetheless, events were rated with a low level of confidence due to probable interferences between the avalanche signals with growth suppressions induced by larch budmoth outbreaks and/or climatic extremes.

Years	External disturbance	Path	It (%)	GD	No. of Injuries CT, CW and TRD	W_{It}
1982	LBM outbreak	OB2	6.0	8	4	0.16
1971	LBM outbreak	OB1	5.6	7	5	0.13
1966	Drought	OB4	7.6	9	8	0.26
1954	LBM outbreak	OB2	10.4	13	4	0.23
1953	LBM outbreak	OB2	16.7	21	6	0.36
1953	LBM outbreak	OB3	13.1	11	4	0.25
1946	LBM outbreak	OB1	6.4	8	6	0.10
1945	LBM outbreak	OB1	9.6	12	6	0.16
1937	LBM outbreak	OB2	7.4	9	7	0.19
1915	LBM outbreak	OB4	7.1	7	4	0.19
1906	Drought	OB1	5.8	7	4	0.14

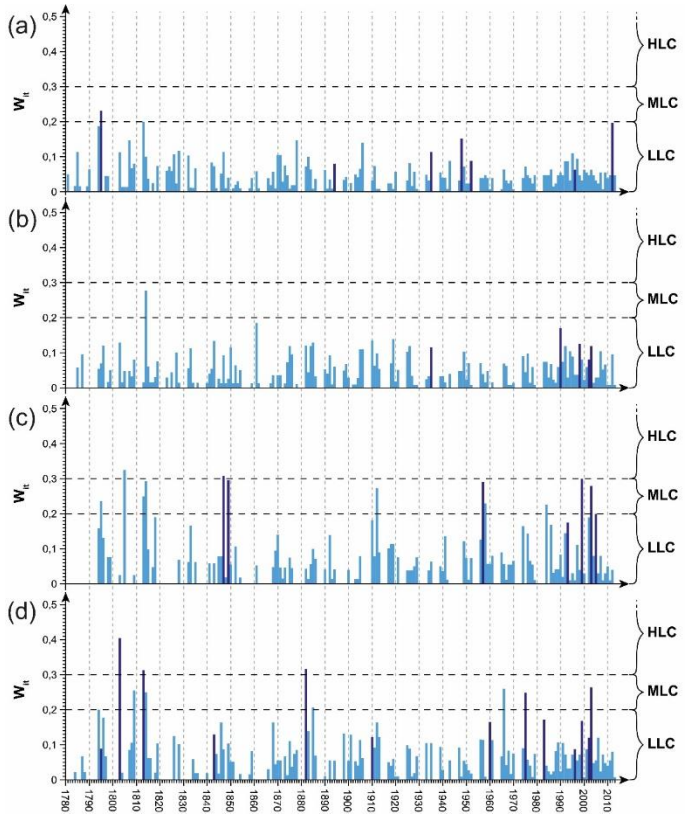

Figure 1.8 – Avalanche activity signals obtained with the weighted index factor (Wit) at (a) OB1, (b) OB2, (c) OB3 and (d) OB4. Light blue bars represent years rejected in step 1 and 2; dark blue bars denote avalanche years.

OB1/OB2, OB2/OB3, and OB2/OB3/OB4, respectively. By contrast, an insufficient number of GDs and/or possible interferences with LBM outbreaks and climatic extremes prevented reconstruction of the documented snow avalanches in winters 1920/21, 1950/51, and 1960/61.

With respect to the 1780-2013 period and at the level of the slope scale, the mean frequency of snow avalanches is 1.87 events decade^{-1}. The reconstruction is characterized by a clear increase in avalanche frequency from 0.75 (9 events) to 3.1 events decade^{-1} (34 events) for the periods 1780-1900 and 1901-2013, respectively. Maximum decadal frequencies are observed between 1951 and 1960 (5 events), 1991–2000 (6 events), and 2001–2013 (7 events). Conversely, no event was reconstructed for the periods 1780–1790, 1821–1834, 1831–1840, and 1851–1880. In more detail, the highest avalanche activity (16 events, amongst which 3 HLC and 4 MLC, 0.7 events decade^{-1} since 1780) was observed at OB4, especially since 1960 (8 events, 1.6 events decade^{-1}). By comparison, OB2 is characterized by a much lower snow avalanche frequency (9 LLC events, 0.4 events decade^{-1}) and an asymmetric distribution of reconstructed avalanche events, i.e. no event until 1934 and 9 events between 1935 and 2013.

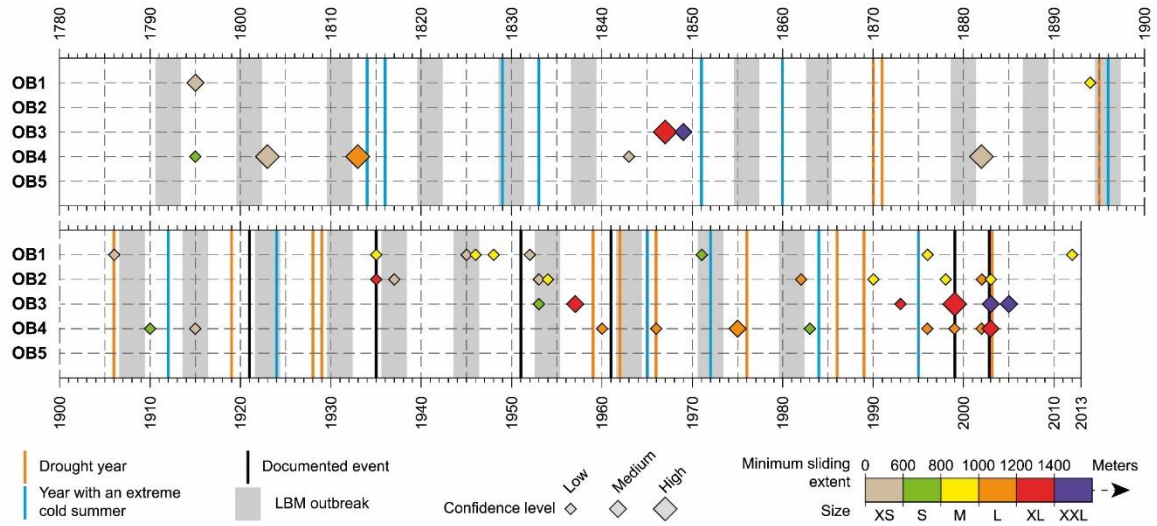

Figure 1.9 – Avalanche events reconstructed for the period 1780–2013 at the 5 avalanche paths. Symbol sizes are proportional to the level of confidence, whereas the color range denotes the minimum slide extent. Grey bands represent triplets of years associated to LBM outbreaks. Vertical lines show snow avalanche events documented in historical archives (black), as well as extremely dry (orange) and cold (blue) summers.

4.6. Spatial extent of avalanche events

In a final step, the spatial distribution of trees with GDs in a specific year has been used to estimate the minimum sliding extent (ME, w.r.t. to the barycenter of the release zones) for each reconstructed avalanche. In total, 18 out of the 43 (42%) reconstructed events exceed 1000 m in length and were thus classified as L (9), XL (6), or XXL (3) snow avalanches (Fig. 1.7a-d). Fourteen events, with a more limited slide extent (ME<800), were classified as S. Eight of these events (1906-OB1, 1915-OB4, 1937-OB2, 1945-OB1, 1953-OB2-OB3 and 1971-OB1) coincide with a LBM outbreak or a drought year. As the number of GDs was ≥4 during these years, they were reintroduced in the final reconstruction at step 3 of our detection procedure but considered events with a LLC. Paradoxically, no clear relation was observed between the size of the event and the level of confidence associated to the reconstruction of each event: by way of example, among the 15 L-XL events, 9 were considered with a LLC. Similarly, among the four events considered with a HLC, two were of limited extend (M, 1803-OB4 and 1882-OB4), two exceeded 1200 m in length (XL, 1847-OB3 and 1999-OB3), but not a single avalanche was reconstructed as an extreme (XXL) event. Only three extreme events were reconstructed (1849-OB3, 2003-OB3 and 2005-OB3) and were considered with a MLC.

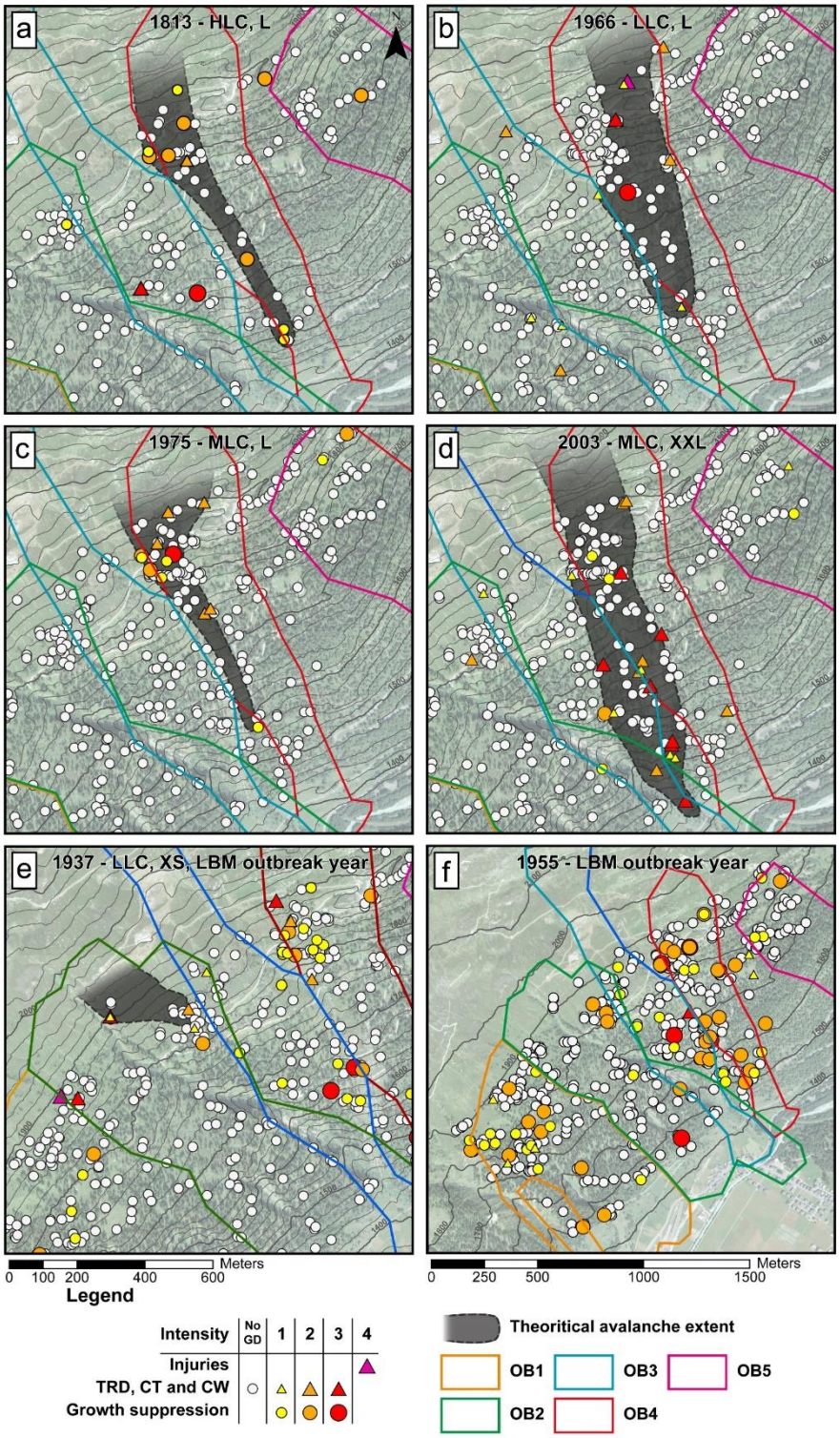

Figure 1.10 – Reconstructed minimum sliding extent for avalanches in (a) 1813, (b) 1966, (c) 1975, and (d) 2003; these events were reconstructed with high (HLC), medium (MLC) and low (LLC) level of confidence, respectively. Maps show all living trees and as well as those showing GDs related to the avalanche. Panels (e, f) are examples of events that were disregarded from the avalanche reconstruction due to the fact that geomorphic and LBM signals could not be disentangled in the tree-ring series.

5. Discussion

5.1. Isolation of the avalanche signal in tree-ring series

The study we report here employs dendrogeomorphic techniques for the analysis of snow avalanche activity on a complex forested slope located in the Valais Alps (Switzerland), with the aim of disentangling geomorphic signals in the tree-ring series (related to the occurrence of snow avalanches) from signals induced by other external disturbances. In addition, this study also aimed at estimating the robustness of tree-ring based snow avalanche reconstructions. To meet this objective, a detection procedure has been developed so as to include important methodological improvements achieved in the field of tree-ring based avalanche event detection over the last decade. This procedure therefore includes (i) a two-fold threshold with GDs and It that is varying according to the sample size (Corona et al., 2012; Stoffel et al., 2013) and which thus allows for a binary distinction between avalanche and non-avalanche years; (ii) local cyclic time series of insect outbreaks (Weber, 1997; Esper et al., 2007; Büntgen et al., 2009) and climatic extremes derived from existing reconstructions (Battipaglia et al., 2010; Efthymiadis et al., 2006) available for the Swiss Alps; and (iii) a weighted index that includes different response intensity classes (Germain et al., 2008; Kogelnig-Mayer et al., 2011) for the attribution of confidence levels to each of the detected snow avalanche events.

In a first step, 74 potential events were detected in the 1140 increment cores and 10 cross-sections sampled from *Larix decidua* and *Picea abies* trees. Interestingly, from these potential events, 31 were excluded from analysis in step 2, despite the fact that they exceeded the It and GD thresholds. This exclusion was motivated by the fact that these 31 years (i) coincided with known larch budmoth outbreaks detected in the tree-ring series (Weber, 1997; Esper et al., 2007; Büntgen et al., 2009) or extremely cold/dry summers (Battipaglia et al., 2010; Efthymiadis et al., 2006) in the Swiss Alps; (ii) did not present a sufficiently large number of GDs (i.e. scars, callus tissue and to a lesser extent compression wood) that would have attested of clear impacts of avalanche events on the forest stand; and (iii) showed a scattered distribution of impacted trees across the slope which is not compatible with observed snow avalanche patterns. Although the approach presented here does not explicitly account for ecological disturbances such as windstorms–yet very frequent in Switzerland (Stucki et al., 2014), considered as one of the main damage factor to Swiss forests (Usbeck et al., 2009), and susceptible to interfere with the geomorphic signal in tree-ring series (Martin and Germain, 2016) – the rejection rate (>40%) remains

very high. As such, the approach presented here also highlights the necessity to discriminate avalanche signals from other ecological disturbances, especially in larch stands which are prone to cyclic LBM outbreaks.

The necessity of having these elements included in dendrogeomorphic assessments is not new and was previously postulated in methodological papers (Stoffel and Bollschweiler, 2008; Stoffel et al., 2013), but has only rarely been applied in dendrogeomorphic studies so far. This lack of consideration is even more critical as a significant proportion of tree-ring based snow avalanche studies–but also, and in a much broader perspective, dendrogeomorphic studies in general–have been based on larch trees (Tab. 1.4) which are known of being cyclically affected by larch budmoth (LBM) outbreaks. It is therefore possible that some noise may potentially have been included in reconstructions considering GDs other than injuries, callus tissues, TRDs and compression wood.

5.2. Robustness of the reconstruction

Based on the recent statistical testing of optimum sample sizes and noise reduction thresholds, there is scope and reason to assume that the event reconstructions emerging from our four-step procedure will indeed best reflect real avalanche activity at the Oberwald paths. In total, 3 out of 6 events listed in the testimonies were retrieved with dendrogeomorphic techniques. This success rate is comparable to tree-ring reconstructions of avalanches performed in the Oisans (Corona et al., 2010), Maurienne (Schläppy et al., 2013) and Mont-Blanc massifs (Corona et al., 2012). The most recent avalanche that occurred in 2003 at OB4 destroyed about 500 m3 of the forest stand and was successfully identified in our reconstruction. Its spatial extent is also very well captured by the tree-ring series, as can be seen from visual comparison between the two aerial photographs taken in 1999 and 2003 (Fig. 1.11).

Yet and despite the stringency of our approach for noise reduction as well as the substantial proportion of strong avalanche indicators (class 3 or 4) in the GD spectra–values are comparable to those obtained by e.g., (Martin and Germain, 2016) – we realize that the robustness of our reconstruction remains quite low. Only 11 out of the 43 events detected in the tree-ring records (28%) were rated with a high or a medium level of confidence and a clear dichotomy exists in that regard between sites OB1/OB2 (5% of HLC/MLC events) and OB3/OB4 (45%).

Table 1.4 – Synthesis of dendrogeomorphic studies using growth disturbances in tree-ring series to reconstruct past snow avalanche activity. Almost one-fourth (22.9%) of the studies published after the year 2000 utilized European larch (Larix decidua Mill.).

Authors (year)	Location (country)	Paths (*n*)	Species	Sample size (*n*)	Period	Growth disturbances (*n*)	Minimal Index value	Avalanches events (*n*)
Potter (1969)	Wyoming (USA)	5	*Abies lasiocarpa, Pinus albicaulis*	50	1963	50	*n.c.*	1
Schaerer (1972)	British Columbia (Canada)	*n.p.*	*n.p.*	*n.p.*	*n.p.*	*n.p.*	*n.c.*	*ukn.*
Smith (1973)	Washington (USA)	13	*n.p.*	*n.p.*	*n.p.*	*n.p.*	*n.c.*	*ukn.*
Ives et al. (1976)	Colorado (USA)	*n.p.*	*Populus tremuloides, Picea engelmannii*	*n.p.*	1860-1974	56	*n.c.*	6
Butler (1979)	Montana (USA)	*n.p.*	*n.p.*	*n.p.*	*n.p.*	*n.p.*	*n.c.*	*n.p.*
Carrara (1979)	Colorado (USA)	*n.p.*	*Populus tremuloides, Picea engelmannii, Abies lasiocarpa*	50	1880-1796	*n.p.*	*n.c.*	4
Butler and Malanson (1985a)	Montana (USA)	2	*Picea engelmannii, Abies lasiocarpa, Pseudotsuga menziesii, Larix occidentalis, Pinus contorta*	30 + 48	1924-1979 1934-1981	*n.p.*	40%	10 + 15
Bryant et al. (1989)	Colorado (USA)	3	*Populus tremuloides, Picea engelmannii*	60 + 60 + 60	*n.p.*	*n.p.*	*n.p.*	*ukn.*
Rayback (1998)	Colorado (USA)	2	*Abies lasiocarpa, Picea engelmannii*	60	1838-1996	*n.p.*	*n.c.*	30
Larocque et al. (2001)	Québec (Canada)	1	*Picea glauca, Picea mariana, Abies balsamea, Larix laricina*	111	1885-2000	*n.p.*	10%	3
Boucher et al. (2003)	Québec (Canada)	1	*Abies balsamea, Picea mariana*	62	1895-1996	*n.p.*	10%	35
Hebertson and Jenkins (2003)	Utah (USA)	16	*Picea engelmannii, Abies lasiocarpa*	297 (8-26)	1928-1996	*n.p.*	*n.p.*	14
Dubé et al. (2004)	Québec (Canada)	3	*Thuya occidentalis, Abies balsamea, Betula papyrifera*	62 + 20 + 28	1871-1996	*n.p.*	10%	7
Jenkins and Hebertson (2004)	Utah (USA)	1	*Picea engelmannii, Abies concolor, Populus tremuloides*	78	1891-1995	*n.p.*	*n.p.*	13
Kajimoto et al. (2004)	*n.p.* (Japan)	1	*Abies mariesii*	34	*n.p.*	*n.p.*	*n.c.*	*n.c.*
Muntán et al. (2004)	Pyrenees (Spain)	1	*Pinus uncinata*	230	1750-2000	*n.p.*	*n.p.*	3
Germain et al. (2005)	Québec (Canada)	2	*n.p.*	78 + 52	1941-2004	420	*n.p.*	11
Pederson et al. (2006)	Montana (USA)	1	*Pseudotsuga menziesii*	109	1910-2003	*n.p.*	10%	27
Stoffel et al. (2006)	Alps (Switzerland)	1	*Larix decidua*	251	1750-2002	561	*n.c.*	9
Casteller et al. (2007)	Alps (Switzerland)	2	*Larix decidua, Picea abies*	66 + 79	*n.p.*	*n.p.*	*n.c.*	*n.c.*
Mundo et al. (2007)	Andes (Argentina)	1	*Nothofagus pumilio*	20	*n.p.*	*n.p.*	*n.c.*	*n.c.*
Butler et Sawyer (2008)	Colorado (USA)	2	*Abies lasiocarpa, Pseudotsuga menziesii, Pinus contorta*	10 + 12	1945-2008 1963-2008	*n.p.*	20%, 40%	15 + 9

n.p. – not provided; *n.c.* – not computed; *ukn.* – unknown

(continued on next page)

Table 1.4 – (continued)

Authors (year)	Location (country)	Paths (*n*)	Species	Sample size (n)	Period	Growth disturbances (*n*)	Minimal Index value	Avalanches events (*n*)
Casteller et al. (2008)	Andes (Argentina)	1	*Nothofagus pumilio*	50	*n.p.*	*n.p.*	*n.c.*	6
Reardon et al. (2008)	Montana (USA)	1	*Pseudotsuga menziesii*	109	1910-2003	*n.p.*	10%	27
Germain et al. (2009)	Québec (Canada)	12	*n.p.*	10-243	1895-1999	51-799	10%	19
Laxton and Smith (2009)	Himalaya (India)	1	*Cedrus deodara*	36	1972-2006	*n.p.*	*n.c.*	4
Muntán et al. (2009)	Pyrenees (Spain)	6	*Pinus uncinata*	26-131	1870-2000	*n.p.*	16-40%	3
Corona et al. (2010)	Alps (France)	1	*Larix decidua*	232	1611-1994	901	10%	20
Köse et al. (2010)	Kayaarka (Turkey)	2	*Abies bornmuelleriana*	61	*n.p.*	*n.p.*	*n.c.*	*n.c.*
Garavaglia and Pelfini (2011)	Alps (Italia)	1	*Picea abies*	71-17	1867-2007	854	*n.c.*	*n.c.*
Casteller et al. (2011)	Andes (Argentina)	9	*Nothofagus pumilio*	6-15	1820-2005	*n.p.*	*n.c.*	6
Kogelnig-Mayer et al. (2011)	Tyrol (Austria)	1	*Picea abies*	372	1869-2009	547	2 (Wit)	17
Corona et al. (2012)	Alps (France)	1	*Larix decidua, Picea abies*	209	1771-2010	645	Variable	34
Decaulne et al. (2012)	Fnjóskadalur valley (Iceland)	1	*Betula pubescens*	39	1900-2010	302	40%	5 + 47
Corona et al. (2013)	Queyras (France)	1	*Larix decidua*	163	1338-2010	514	5%	38
Voiculescu and Onaca (2013)	Bucegi mountains (Romania)	1	*Picea abies, Larix ecidua*	62	1954-2011	124	Variable	33
Decaulne et al. (2014)	Nordfjord (Norway)	1	*Betula pubescens, Alnus incana*	91	1900-2011	502	10%	26 + 5
Voiculescu and Onaca (2014)	Bucegi mountains (Romania)	2	*Picea abies, Larix ecidua*	108	1963-2011	171	Variable	32
Chiroiu et al. (2015)	Fagaras mountains (Romania)	1	*Picea abies*	105	1852-2013	534	Variable	15-20
Martin and Germain (2016a)	White Mountains (Canada)	6	*Abies balsamea, Populus tremuloides, Betula papyrifera, Tsuga canadensis*	450	1939-2012	2251	Variable	54
Martin and Germain (2016b)	White Mountains (Canada)	4	*Abies balsamea*	293	1865-2015	1233	10%	*ukn.*
Pop et al. (2016)	Southern Carpathians (Romania)	1	*Picea abies*	57	1900-2013	226	10%	12
Voiculescu et al. (2016)	Fagaras mountains (Romania)	4	*Picea abies*	293	1867-2012	853	10%	77
Favillier et al. (this study)	Valais, Goms (Switzerland)	5	*Larix decidua, Picea abies*	566	1780-2013	2389	Variable	48

n.p. – not provided; *n.c.* – not computed; *ukn.* – unknown

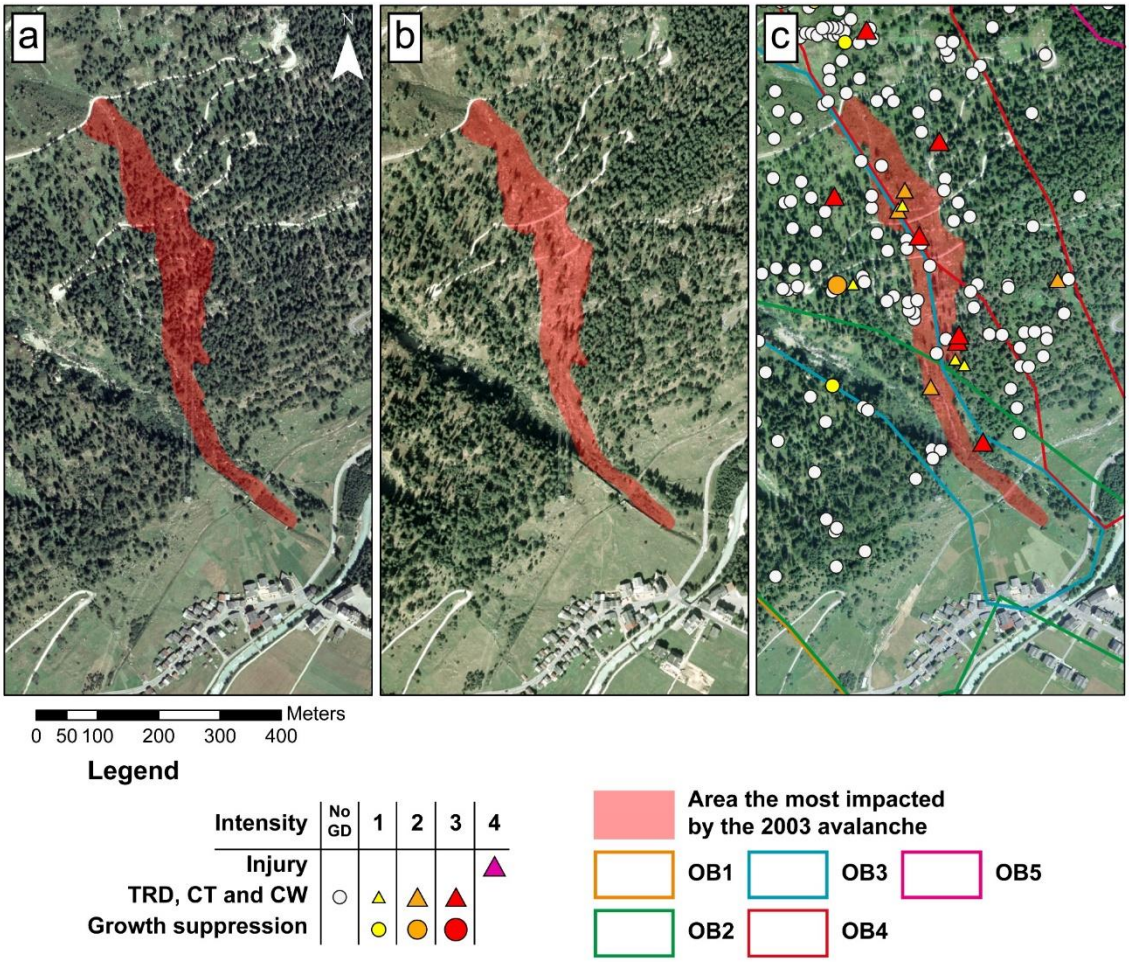

Figure 1.11 – (a, b) Diachronic evolution of the forest at Oberwald between 1999 and 2005. (c), tree-ring-based reconstruction of the 2003 avalanche event.

At OB1/OB2, the over-representation of LLC events (95% of the reconstructed events) probably results from the scarcity of high-magnitude snow avalanche events. This hypothesis is supported by (i) the presence of the oldest trees (>300 years, Fig. 1.4) in the upper part of both couloirs, which suggests that no catastrophic, high-energy event was able to destroy larger parts of the forest stand during at least the past three centuries, (ii) the smoother transversal profile of these paths which favors the occurrence of unconfined, rather than channelized, snow avalanches (Fig. 1.3) as well as the existence of several rows of protective deflecting barriers which effectively prevented the release of high-magnitude events over the last decades.

At OB3, we hypothesize that the under-representation of HLC and MLC events would result (i) from the channelization of snow avalanches in deeply incised paths (Stoffel et al., 2010; Corona et al., 2012) and (ii) from the limitations of dendrogeomorphic techniques in such environments. In the best case, snow avalanches in such settings can be reconstructed via impacted trees standing at the outer lateral margins of the couloirs where

impact energies are low and where trees are not necessarily affected during individual (smaller) events (Fig. 1.10a, b, c). Most often, avalanches located in or next to such couloirs will favor stem breakage – especially if (i) the bending stress exerted by the moving snow exceeds the bending strength of the tree stem (Johnson, 1987; Peltola et al., 1999) or if (ii) the applied torque overcomes the strength of the root-soil plate, leading to uprooting and overturning (Coutts, 1983). In this case, datable evidence of ancient events will be removed repeatedly and often almost systematically. This phenomenon is quite well exemplified by the snow avalanches which reportedly occurred at our site in the Jostbach and Rätischbach channels during the severe winter 1950-51 (Ancey, 2012). These events could not be retrieved from tree-ring records due to the lack of conifers growing in these channels and the widespread occurrence of young and flexible broadleaved trees (*Alnus viridis* or *Betula pendula* Roth), often in the form of large shrubs, unsuitable for the inference of information about past avalanche events.

5.3. Increase in avalanche frequency over the last decades

Despite the hypothetical limitations in reconstructing high-magnitude snow avalanches that would potentially have destroyed the forest stand in or at the vicinity of the main channels, we are rather confident that our reconstructions include a much smaller amount of noise than more conventional approaches. Interestingly, a clear temporal trend is observed in the reconstructions at each path, with 80% of the events being reconstructed during the 20th century and 25 out of 43 events since 1950.

This observation is in line with the clear increase in the total number of growth disturbances identified at each path since the mid-20th century as well as with a temporal shift in the 50-yr distribution of GDs, i.e. an increasing frequency of traumatic resin ducts, compression wood, callus tissues, and injuries (intensities 2, 3, 4) and a decreasing proportion of growth suppressions (Fig. 1.6b). This trend toward higher activity since the beginning of the 20th century at Oberwald can be explained reasonably by the fact that a large proportion of growth suppressions, very frequently observed in the GD spectra during the 19th century, were disregarded from analysis due to the possible confusions between snow avalanche, climatic, and LBM signals. In addition, the overrepresentation of CTs, TRDs and injuries–not attributable to external signals–has probably facilitated the detection of events over the last decades.

This bias is frequently observed in dendrogeomorphic reconstructions and mainly attributed to the effect of hidden scars. Because conifer trees mask scars of past events effectively, the existence and/or position of old scars can often not be detected on the stem surface (Stoffel and Perret, 2006), rendering the determination of suitable sample positions a difficult task (Trappmann and Stoffel, 2013). Older events can therefore be missed on increment cores of *L. decidua*, and older trees will tend to yield data on fewer impacts relative to their age which in turn affect return periods for the recent decades. On the other hand, the sampling of trees with visible scars will lead to a facilitated detection of the most recent events.

6. Conclusion

In this study, we used dendrogeomorphic techniques to document past avalanche activity in five avalanche paths at Oberwald (Swiss Alps) with the specific purpose to disentangle signals related to snow avalanche from other ecological disturbances. Based on a 4-step procedure including series of larch budmoth outbreaks and climatic extremes available for the Swiss Alps, 43 avalanche events were reconstructed at Oberwald, whereas 31 events were rejected from the final reconstruction due to potentially strong interferences between the different types of signals. This rejection rate demonstrates the importance of noise in classical, tree-ring based snow avalanche studies and the absolute necessity to discriminate, in future work, ecological from geomorphic disturbances. This is all the more so crucial in mountain environments where a high proportion of dendrogeomorphic studies has been based on larch trees, a species which is cyclically affected by larch budmoth outbreaks. The stringency of our procedure has resulted in the elimination of a large proportion of growth suppression signals which are very frequent in the spectra of growth disturbances, particularly during the 19th century. In this respect, the low level of confidence attributed to a majority of the detected events is interpreted the result of (i) unconfined low-magnitude events at OB1/OB2, and (ii) the limitations of dendrogeomorphic event detection in channelized paths (OB3/OB4) where ancient avalanches can only be reconstructed from surviving marginal trees. Similarly, the rather limited avalanche activity that we reconstruct for the coldest decades of the Little Ice Age and the clear increase in event frequencies since the mid-20th century should not be seen as climatically-driven variations, but more probably result from an overrepresentation of scars and tangential rows of traumatic resin ducts in the GD spectra for the last decades, representing a sampling bias.

CHAPITRE 2

Spatio-temporal maps of past avalanche events derived from tree-ring analysis

Spatio-temporal maps of past avalanche events derived from tree-ring analysis: a case study in the Zermatt valley (Valais, Switzerland)

Ce chapitre est en totalité constitué de l'article publié dans la revue :

***Cold Regions Science and Technology* 154, 2018, 9–22.**

doi: 10.1016/j.coldregions.2018.06.004

Co-auteurs et affliations :

Adrien Favillier[1] Sébastien Guillet[2,3], Daniel Trappmann[2,3], Pauline Morel[2,3,4], Jérôme Lopez-Saez[2], Nicolas Eckert[5], Gregor Zenhäusern[6], Jean-Luc Peiry[7], Markus Stoffel[2,3,8], Christophe Corona[1]

1. Université Clermont Auvergne, CNRS, GEOLAB, F-63000 Clermont-Ferrand, France.
2. University of Geneva - Institute for Environmental Sciences, Climate Change Impacts and Risks in the Anthropocene (C-CIA), 66 Boulevard Carl-Vogt – CH-1205 Geneva, Switzerland.
3. Dendrolab.ch, Department of Earth Sciences, University of Geneva, rue des Maraîchers 13, CH-1205 Geneva, Switzerland.
4. Univ. Grenoble Alpes, IRSTEA, UR EMGR, 38402 St-Martin-d'Hères cedex France.
5. Univ. Grenoble Alpes, IRSTEA, UR ETNA, 38402 St-Martin-d'Hères cedex France.
6. Forschungsinstitut zur Geschichte des Alpenraums, CH-3900 Brig, Switzerland.
7. CNRS, UMI3189, « Environnement, Santé, Sociétés », Faculté de Médecine, UCAD, BP 5005, DAKAR-FANN, Sénégal.
8. Department F.-A. Forel for Environmental and Aquatic Sciences, University of Geneva, 66 Boulevard Carl-Vogt, CH-1205 Geneva, Switzerland.

Remerciements et financements

The authors wish to address special thanks to Georges Tscherrig for his assistance in searching original newspaper articles. The authors acknowledge support from the Agence Nationale de la Recherche of the French government through the program ''Investissements d'Avenir'' (16-IDEX-0001 CAP 20-25). Finally, the authors acknowledge the two anonymous reviewers for their helpful and very positive comments on the manuscript and to Peter Gauer for the thorough editing.

Abstract

Expected runout distances and related return periods are the most important parameters needed for zoning in terrain prone to snow avalanching. Hazard mapping procedures usually allocate areas of land to zones with a different degree of danger based on return periods estimated for given snow volumes in the starting zone or with statistical/dynamical models. On forested avalanche paths, dendrogeomorphology has a great potential to add critical input data to these calculations in terms of recurrence intervals or return periods. However, quite paradoxically, recurrence interval maps of snow avalanches have only rarely been retrieved from tree-ring analysis and mostly represent the inverse of the mean frequency of avalanches that could be retrieved locally rather than the return period. The purpose of this study therefore was to propose a consistent approach for tree-ring based recurrence interval mapping of snow avalanche events. On the basis of 71 snow avalanches retrieved from 2570 GD growth disturbances identified in 307 larch trees from three avalanche paths located in the vicinity of Täsch (Canton of Valais, Swiss Alps), we first followed the classical approach used in dendrogeomorphology and derived recurrence interval maps through interpolation from recurrence intervals observed at the level of individual trees. We then applied an expert delineation of the spatial extent of past events based on the location of disturbed trees. Our results show that the second step improved representation of expected patterns of recurrence intervals that typically increase as one moves down the centerline of the avalanche path. Despite remaining limitations and uncertainties precluding from direct use of our maps for hazard mapping purpose, these results suggest that dendrogeomorphic time series of snow avalanches can yield valuable information for the assessment of recurrence intervals of avalanches on forested paths for which only very limited or no historical data exists, and that this data can be obtained independently from meteorological data or numerical modeling.

Keywords: Dendrogeomorphology; snow avalanches; recurrence interval maps; tree ring; Swiss Alps

Résumé

Les distances d'arrêts attendues et les périodes de retour associées sont les paramètres les plus importants pour le zonage de l'aléa dans les espaces exposés aux avalanches. Les procédures de cartographie de l'aléa attribuent une surface exposée à une zone avec un degré de danger. Celui-ci est déterminé sur la base de la période de retour estimée pour un volume de neige donné dans la zone de départ ou à l'aide de modèles statistiques/dynamiques. Dans les couloirs d'avalanche en milieu forestier, les techniques de dendrogéomorphologie sont susceptibles d'apporter un nombre important de données d'entrée, critiques aux calculs d'intervalle de récurrence et de période de retour. Cependant et paradoxalement, les cartes d'intervalle de récurrence d'avalanches sont rarement extraites des séries de cernes de croissance. Le cas échéant, elles représentent surtout l'inverse de la fréquence moyenne des avalanches, retrouvée localement, plutôt que la période de retour de l'aléa. L'objectif de cette étude est alors de proposer une approche cohérente pour la cartographie de l'intervalle de récurrence des avalanches sur la base de données dendrogéomorphologiques. Sur la base des 71 avalanches reconstruites à partir des 2570 perturbations de croissance – identifiée dans les cernes de croissance des 307 mélèzes d'Europe (*Larix decidua* Mill.) – dans les trois couloirs du versant de Täsch (Valais, Suisse), nous avons d'abord suivi l'approche classique utilisée en dendrogéomorphologie et dérivé des cartes d'intervalle de récurrence par interpolation de l'intervalle de récurrence observé à l'échelle de l'arbre. Nous avons ensuite effectué une délinéation à dire d'expert de l'emprise spatiale des événements sur la base de la disposition spatiale des perturbations de croissance. Nos résultats montrent que cette seconde solution améliore la représentation des patrons spatiaux attendus de l'intervalle de récurrence des avalanches, augmentant à mesure que l'on descend l'axe central du couloir. Malgré les limites et les incertitudes qui subsistent et qui empêchent l'utilisation directe de nos cartes à des fins de cartographie des risques, ces résultats suggèrent que (1) les chronologies dendrogéomorphologiques d'avalanches sont susceptibles de produire des informations précieuses pour l'évaluation de l'intervalle de récurrence des avalanches sur les couloirs forestiers d'avalanches pour lesquelles les données historiques sont rares, voire inexistantes, puis (2) que ces données peuvent être obtenues indépendamment des données météorologiques ou de modélisation numériques du processus.

Mots-clefs : Dendrogéomorphologie ; avalanches; cartes d'intervalle de récurrence; Alpes suisses.

1. Introduction

In mountainous regions, snow avalanches are substantial hazards that affect valley slopes, endanger infrastructure or transportation routes and may even cause fatalities (Bründl et al., 2004). In Switzerland, snow avalanches are considered the main natural hazard and have caused 378 fatalities between 1937 and 2015 (Badoux et al., 2016). Avalanche risk management usually involves predetermination of potentially damageable events (Eckert et al., 2008). To this end, it investigates the full set of past avalanche activity on a given path over a long-time period. The aim of this documentation is the realization of hazard maps to enforce building restrictions and to design defense structures. To achieve this goal, annual probabilities of occurrence with a given intensity need to be defined for each point of the runout zone (Maggioni et al., 2006; Schläppy et al., 2014).

Predetermination is complex as a result of the numerous sources of variability that constrain avalanche activity on a given path (i.e. release area, snow depth, snow quality, path roughness, Eckert et al., 2008). To limit these biases, avalanche specialists first used statistical–topographical or ‘‘Norwegian’’ methods (Lied and Bakkehøi, 1980). These “historical” models assume regional homogeneity in avalanche behavior for a given mountain range, and, to overcome data sparseness at the site-specific scale, pool data from various paths in a common database to derive a simple statistical regression explaining observed runout distances from topographic covariates. The approach was then further developed through the integration of the runout ratio method in which data transformation is applied to fit a probability distribution to standardized observed runout distances (McClung and Lied, 1987; Keylock, 2005). Yet, in alpine countries, where avalanche paths of the same mountain range only rarely exhibit similarity in shape, the fundamental assumption of avalanche homogeneity at the regional scale should be questioned. In addition, a major drawback of this approach is that it depends on the quantity and quality of available data. In many cases, the historical record of run-out distances is not long enough, and the resulting fitted probability distribution must be extrapolated to evaluate the run-out distance of avalanche events with long return periods (Ancey and Meunier, 2004).

The Swiss guidelines (Salm et al., 1990) are an alternative to the “Norwegian” method. Here, precipitation data is used to predetermine variations of snow depth for return periods of 30, 100, and 300 years (Salm et al., 1990). The corresponding amount of snow is propagated using the Voellmy (1955) model with tabulated friction coefficient values depending on path geometry and altitude, before the corresponding amount of snow is transformed into a runout distance and velocity profile using a propagation model (Bartelt

et al., 1999). One of the main weaknesses of this second family of methods is that the return period of the avalanche is the return period of the corresponding snow depth. The avalanche propagation thus remains a fully deterministic one-to-one link between snow input and runout distance (Eckert et al., 2007a). In addition, the number of basic physical processes (snow entrainment or release, turbulent suspension and transformation into an airborne avalanche) occurring in the avalanche course are either unknown or neglected in these models (Meunier and Ancey, 2004). Therefore, several studies highlighted weaknesses in the values proposed by these guidelines (see e.g. Barbolini et al., 2000), especially due to a significant mismatch in frictional parameter values fitted from field data (Ancey et al., 2004).

Finally, a third option consists in an explicit combination of a propagation model and statistical analysis using Monte Carlo simulations. These statistical-dynamical approaches (Bozhinsky et al., 2001; Barbolini and Keylock, 2002; Eckert et al., 2008, 2010) use probability distributions as input for the propagation model. Output variable replicates are then used to characterize the return period of snow avalanches. Calibration of statistical-dynamical models with site-specific archival records improves the reliability of the approach considerably (Ancey and Meunier, 2004). A major difficulty is the choice of input distributions that appropriately represent variability of the avalanche phenomenon at the studied site. Data available for calibration typically remains quite limited (Straub and Grêt-Regamey, 2006), non-explicit in nature, and difficult to be implemented in the friction law (Eckert et al., 2010b). Models are well capable to simulate contemporary events, corresponding to return period $\leq$30 yr on which they could be calibrated, but uncertainties increase as soon as longer return periods are investigated (Schläppy et al., 2014).

This shortcoming is mainly related to documentation that is only rarely available with satisfying spatial resolution over long timescales and as a continuous record. Historical records are most often biased towards events that caused damage to infrastructure or loss of life and remain largely unavailable for sites that are far away from existing towns (Corona et al., 2012). Any calibration of statistical-dynamical models with archival records has been shown to improve the reliability of the approach considerably (Ancey and Meunier, 2004).

In temperate climate zones, trees serve as silent witnesses of past geomorphic process activity and provide valuable information on event frequencies and spatial patterns of process occurrences (Stoffel and Bollschweiler, 2008). Consequently, they can theoretically yield valuable information for the assessment of recurrence intervals of

avalanches on forested paths with limited or no historical data, and this information can be obtained independently from meteorological data or numerical modeling.

The dating of geomorphic events using tree-ring series, known as dendrogeomorphology (Alestalo, 1971), has been applied repeatedly over the last decades in numerous mountainous regions worldwide to reconstruct multi-decadal to multi-centennial chronologies of snow avalanche events (Fig. 2.1) and to assess the spatial extent of individual events (see Favillier et al., 2017 – chapter 1 – for a recent review). With respect to this abundant literature, only twelve studies explore the mapping of return periods of snow avalanche with dendrogeomorphic methods (i.e. Casteller et al., 2011; Corona et al., 2010; Martin and Germain, 2016a; Reardon et al., 2008; Voiculescu and Onaca, 2014, see Fig. 2.1). In addition, most of the aforementioned studies estimate avalanche return period maps based on the interpolation of the disturbance frequency at the level of individual trees (F) as follows:

$$F_T = (nGDObs_T) \div (A_T) \quad \textbf{(Eq. 2.1)}$$

where nGDObs represents the number of growth disturbances related to snow avalanches observed in tree *T*, and A, the total number of years tree *T* was alive. Despite recent efforts to use anisotropic interpolation, that takes account of avalanche flow direction on the slope into account (e.g. Corona et al., 2010), these maps have so far failed to represent the expected patterns of recurrence intervals properly (in the sense that they did not show an increase in recurrence intervals as one moves down the centerline of an avalanche path; e.g. Meunier and Ancey, 2004; Eckert et al.., 2007a; Schläppy et al., 2014). Specifically, they do not represent the return period of avalanches, but the inverse of the mean frequency of avalanches that could be retrieved locally, which strongly depends on the local characteristics of the forest stand and on the chosen tree-ring methods (sampling strategy, event attribution procedure). As a sole exception, Schläppy et al. (2014, n°41 on Fig. 2.1), evaluated tree ring based return periods for avalanche runout distances focusing, for each event, on the tree of further reach only. This led a monotonically increasing one-to-one mapping between distance along the path profile and return period, which makes much more sense for potentially affected elements at risk. However, such an approach has never been applied in a 3D mapping frame, yet mandatory for hazard zoning purposes.

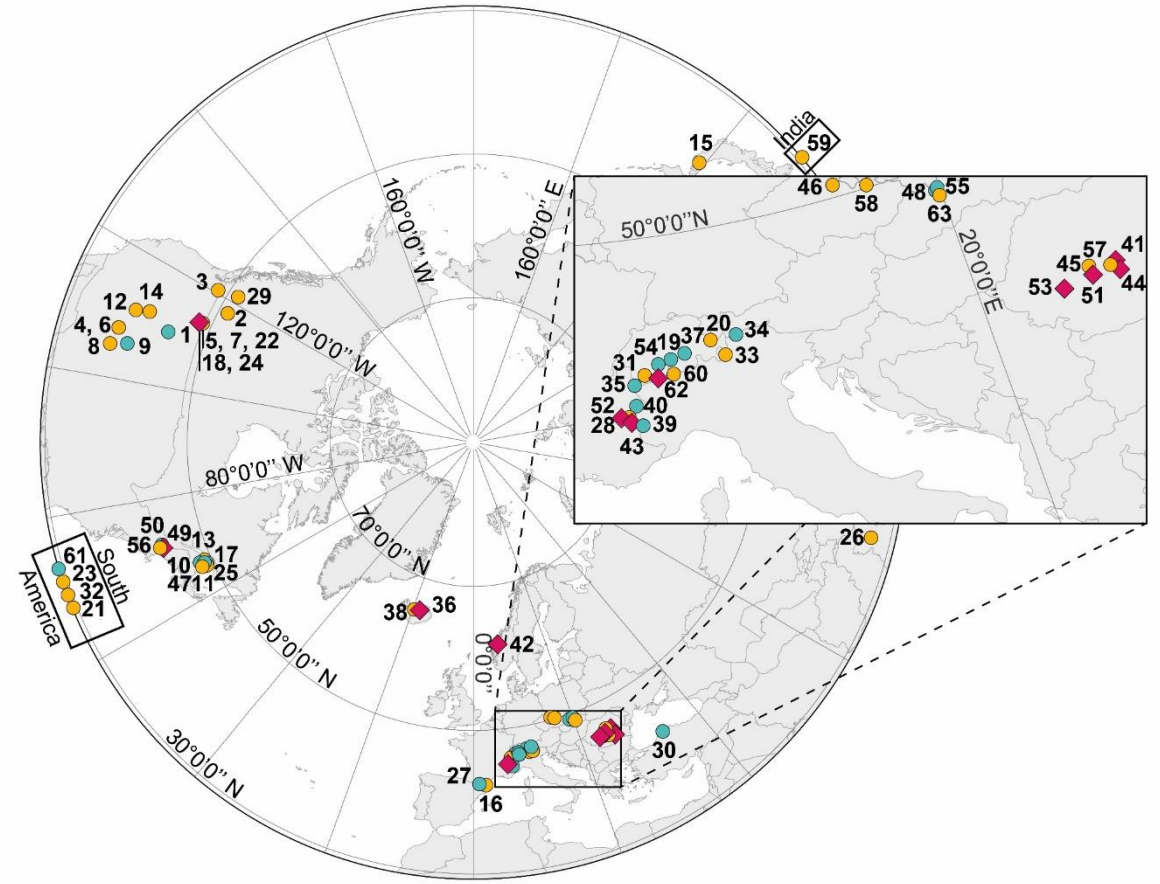

Figure 2.1 – Synthesis of tree-ring based avalanche reconstructions. Colored dots represent dendrogeomorphic snow avalanche studies with (green) and without (yellow) an estimation of the spatial extent of reconstructed snow avalanche events. Red lozenges represent studies for which avalanche recurrence interval maps have been computed. The red star corresponds to the location of this study. **1.** Potter (1969); **2.** Schaerer (1972); **3.** Smith (1973); **4.** Ives et al. (1976); **5.** Butler (1979); **6.** Carrara (1979); **7.** Butler and Malanson (1985a); **8.** Bryant et al. (1989); **9.** Rayback (1998); **10.** Larocque et al. (2001); **11.** Boucher et al. (2003); **12.** Hebertson and Jenkins (2003); **13.** Dubé et al. (2004); **14.** Jenkins and Hebertson (2004); **15.** Kajimoto et al. (2004); **16.** Muntán et al. (2004); **17.** Germain et al. (2005); **18.** Pederson et al. (2006); **19.** Stoffel et al. (2006); **20.** Casteller et al. (2007); **21.** Mundo et al. (2007); **22.** Butler and Sawyer (2008); **23.** Casteller et al. (2008); **24.** Reardon et al. (2008); **25.** Germain et al. (2009); **26.** Laxton and Smith (2009); **27.** Muntán et al. (2009); **28.** Corona et al. (2010); **29.** Köse et al. (2010); **30.** Szymczak et al. (2010); **31.** Casteller et al. (2011); **32.** Garavaglia and Pelfini (2011); **33.** Kogelnig-Mayer et al. (2011); **34.** Corona et al. (2012); **35.** Decaulne et al. (2012); **36.** Arbellay et al. (2013); **37.** Corona et al. (2013); **38.** Schläppy et al. (2013); **39.** Voiculescu and Onaca (2013); **40.** Decaulne et al. (2014); **41.** Schläppy et al. (2014); **42.** Voiculescu and Onaca (2014); **43.** Chiroiu et al. (2015); **44.** Tumajer and Treml (2015); **45.** Germain (2016); **46.** Lempa et al. (2016); **47.** Martin and Germain (2016a); **48.** Martin and Germain (2016b); **49.** Pop et al. (2016); **50.** Schläppy et al. (2016); **51.** Voiculescu et al. (2016); **52.** Favillier et al. (2017); **53.** Gądek et al. (2017); **54.** Krause and Krizek (2017); **55.** Pop et al. (2017); **56.** Šilhán and Tichavský (2017); **57.** Ballesteros-Cánovas et al. (2018); **58.** Casteller et al. (2018).

In this context, the purpose of this study is to provide a methodology to map tree-ring based recurrence intervals of snow avalanche events. To this end, and based on the procedure proposed by Favillier et al. (2017 – chapter 1) – where the noise induced by climate conditions or exogenous disturbances is minimized in tree-ring based process histories–we reconstruct snow avalanche event frequency (1740–2015) of an avalanche slope at Täsch (Canton of Valais, Swiss Alps). In a second step, the temporal accuracy of our reconstruction is checked through a comparison with the historical documentation available at our study sites. Finally, an expert delineation of the spatial extent of past events is used, and recurrence interval maps are derived from their distribution and confronted to the interpolations of the frequency of growth disturbances commonly used in the literature.

2. Study site

The site under investigation (46°3'N, 7°46'E, 307.6 ha, 1450–3247 m asl) is located on the west-facing slope of the upper Zermatt valley in the Swiss Alps (Canton of Valais, Switzerland, Fig. 2.2a). Its geology is dominated by gneisses with amphibolite zones oriented NE-SW (Federal Office of Topography Swisstopo). Snow avalanches are commonly naturally triggered from several non-forested release zones located between 2200 and 3500 m asl. Once released, they pass through a forested slope mainly composed of European larch (*Larix decidua* Mill.). At the bottom of the slope, the avalanche track crosses the road from Täsch to Zermatt during winter (Fig. 2.2b). Therefore, 10-m high deflecting dams and a tunnel were built in the 1990s to protect properties and infrastructures from snow avalanches.

In detail, three main paths have been identified at our study site (Fig. 2.2b):

(i) In the northernmost path T1 (60.6 ha), snow avalanches are released from a steep area (>35°) located between 2250 and 2700 m asl. The couloir, poorly incised, is characterized by steep slopes (25°–35°) between 1500 and 2300 m asl. The runout zone (<10°) is limited to the valley floor located below 1500 m asl.

(ii) The slope angle of T2 (87.8 ha) decreases progressively from >35° in the release area to 15-20° below 1700 m asl and <10° next to the Mattervispa (1500 m asl). In its upper part, this track has three steep incised rocky channels converging at ~1800 m asl with the Täschwang couloir. At this path, preliminary analysis of orthophotos highlights that the forest stand has repeatedly suffered from severe damage and deflecting barriers are installed along the left side of this channel (1750–2500 m

asl) to protect Zermettjen and the access road to Zermatt (Fig. 2.2) since at least 1941.

(iii) T3 (61 ha) is characterized by a complex release area divided into two units that are separated by a 150-m high rockwall at 2500 m asl. Below 2200 m asl, the forested slope is incised by several channels converging with the Täschwang couloir at 1650m asl.

According to the nearby weather station of Zermatt (46°3'N, 7°75'E, 1638 m asl), annual temperature in the Zermatt valley is 4.2 °C for the period 1981–2010 and average annual precipitation amounts to 639 mm. During winter, mean air temperature (DJF) is -3.7 ºC while precipitation amounts to 125 mm. From November to April, precipitation falls primarily as snow and average annual snowfall reaches 270.2 cm for the period 1982–2010 with an average of 39 days of snow per year. Finally, there are no indications in the

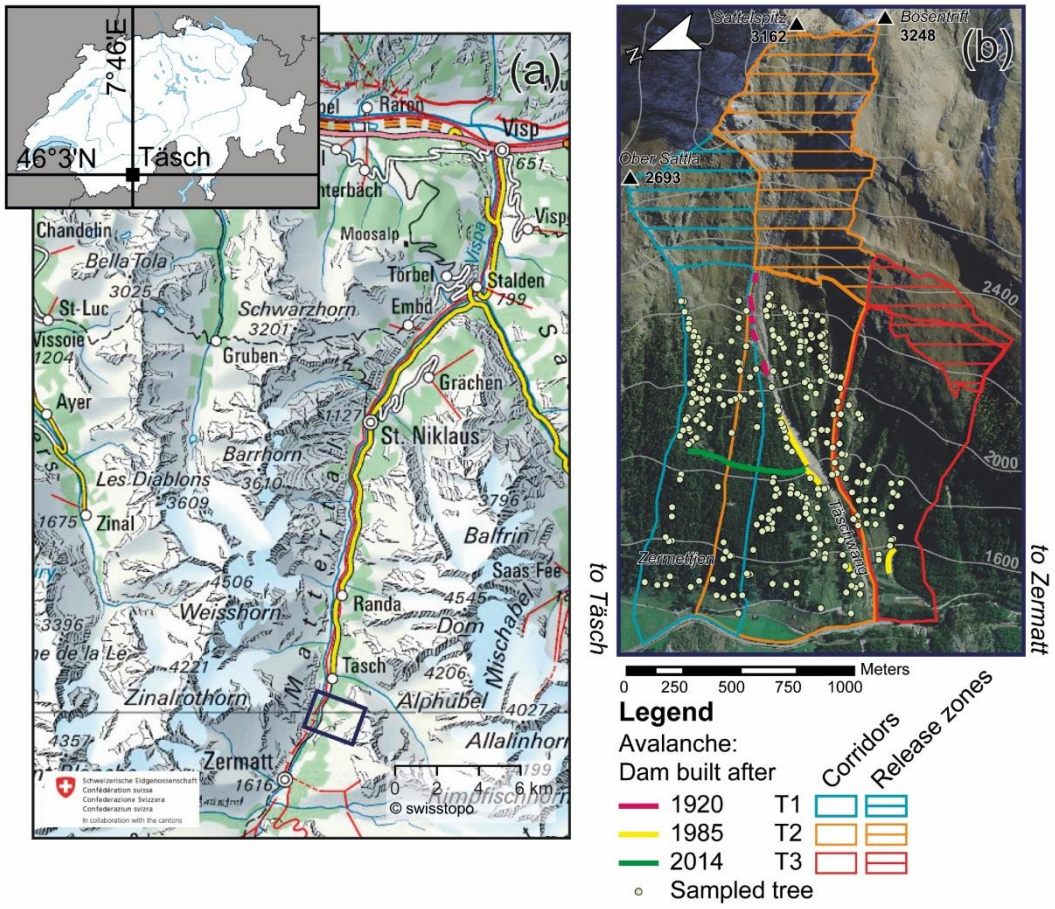

Figure 2.2 – Location of the study site: (a) the Zermatt valley in the canton of Valais, Switzerland, (b) Spatial distribution of the sampled trees within the three paths and their release areas. The green lines represent the avalanche dams built after major avalanche events. Map and aerial photography are reproduced by permission of swisstopo (BA18022).

historical archives nor in the local authority testimonies of any debris flow activity that could significantly affect the studied forested stand.

3. Material and methods

3.1. Compilation of historical archives

Several documentary sources were used in this study to compile a precise and as complete as possible historical chronology of snow avalanches in the Täschwang paths. Data were extracted from local newspapers, ecclesiastical archives and stakeholder chronicles. In total, 6 regional and local newspapers (i.e. Confédéré, Walliser Bote, Le Nouvelliste, Journal et Feuille d'avis du Valais, Le Rhône, La Sentinelle), published between September 1861 and June 2014, were examined via the Swiss virtual newspaper archives available online at http://newspaper.archives.rero.ch/Olive/ using keywords such as "Täschwang" corresponding to the toponymy of the main paths. In addition, "Täsch" and "Zermatt" were used as keywords, as they refer to the two closest localities as well as "avalanche" and "Lawine", the French and German words for snow avalanche. In addition, the annual winter reports published by the Institute for Snow and Avalanche Research (Institut für Schnee und Lawinenforschung–SLF) since 1935 and local chronicles available at the Institut zur Erforschung der Geschichte des Alpenraums (FGA) and from the Swiss-scale database from Laternser and Pfister (1997) were reviewed in detail. Finally, in order to complement this archival database, five aerial flight campaigns – available from the Federal Office of Topography (Swisstopo; 1:20,000) –and the Siegfried map (Mischabel, 533, edition 1909) were compared to detect potential damaging avalanches and to reconstruct forest dynamics since 1941.

3.2. Sampling strategy, identification, dating and classification of growth disturbances

To reconstruct past avalanche activity based on dendrogeomorphic techniques, a total of 620 increment cores and 60 cross-sections have been sampled from 307 European larch (*Larix decidua* Mill.) trees using a Pressler increment borer (diameter 5.15 mm, maximum length 40 cm) in autumn 2015. A minimum of two cores was extracted per tree, one upslope and one in the downslope direction (Stoffel and Bollschweiler, 2008). Additional data were collected for each tree including its diameter at breast height, description of the disturbance (i.e. number of scars, decapitation, tilting), and exact position of the sampled tree using a 1-m precision GPS device.

Trees presenting obvious evidence of snow avalanches, such as decapitation, tilting, and injury, were preferentially selected. Following recent recommendations by Stoffel and Corona (2014), old trees were selected to extend the reconstruction of past avalanche events as far as possible. Nevertheless, younger trees were also considered to account for the loss of sensitivity of older trees in recording mass-movement signals (Šilhán and Stoffel, 2015). Sampling height was chosen according to the morphology of the stem: (i) injured trees were sampled at the height of the disturbance from the overgrowing scar tissue; (ii) tilted trees were analyzed at the maximum bending angle (Stoffel et al., 2013); and (iii) cross-sections and cores from decapitated trees were taken at the lowest possible position on the tree to maximize the number of available rings (Stoffel and Bollschweiler, 2008). Samples were prepared and data processed following standard procedures described in Stoffel et al. (2013). Growth disturbances (GD) such as injuries – i.e. impact scars – and callus tissues (CT) (Stoffel et al., 2010), tangential rows of traumatic resin ducts (TRD) (Schneuwly et al., 2008, 2009), compression wood (CW) and abrupt growth suppression (GS; Kogelnig-Mayer et al., 2013) were identified in the tree-ring series and cross-dated against two local reference chronologies (Büntgen et al., 2005), so as to correct our series for possibly missing and false rings.

Intensities were then assigned to each GD using criteria defined by Kogelnig-Mayer et al. (2011). This step was included to emphasize features which were clearly associated with avalanche activity. Intensities of growth suppression, compression wood and TRDs were classified according to Schneuwly et al. (2008) and Frazer (1985) to distinguish between weak (intensity class 1), medium (intensity class 2), and strong (intensity class 3) reactions and clear evidence of injuries (intensity class 4).

3.3. Detection of past avalanche events in growth disturbance series

To detect past snow avalanche events – which correspond to the occurrence of one snow avalanche at least in the selected path at a yearly resolution – in the GD series, we adopted the four-step procedure described in Favillier et al. (2017 – chapter 1) that underlines the necessity to disentangle the potential effects of snow avalanches from disturbance pulses caused by climatic or exogenous factors, such as cold/dry years or larch budmoth outbreaks:

(i) In a first step, for each year *t* with a minimum of 15 trees available in each path, an index *I* was calculated, according to Shroder (1978) and based on the percentage of trees

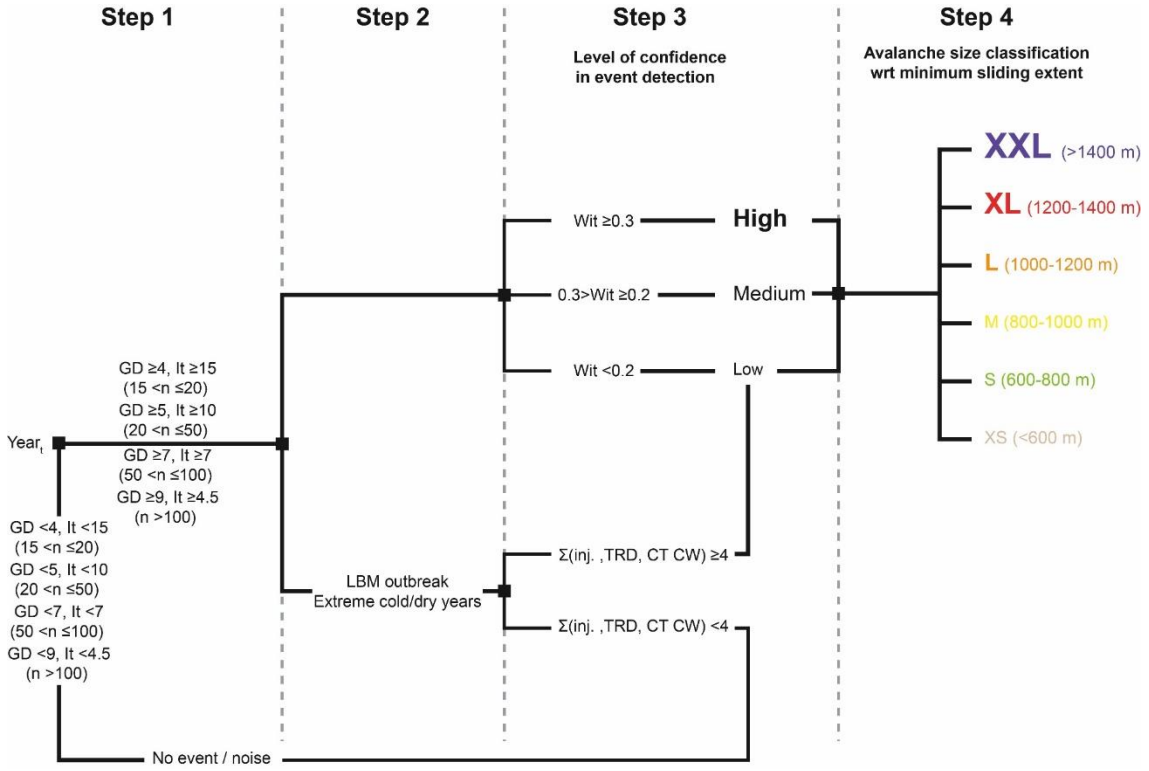

Figure 2.3 – Synoptic diagram of the 4-step approach used for the detection of avalanche events in tree-ring series, adapted from Favillier et al. (2017).

showing responses in their tree-ring record in relation to the number of sampled trees being alive in year t:

$$I_t = \left(\left(\sum_{i=1}^{n} R_t\right) \Big/ \left(\sum_{i=1}^{n} A_t\right)\right) * 100 \qquad \textbf{(Eq. 2.2)}$$

where ΣR represent the number of trees responding to an event in year *t*, and ΣA is the number of trees alive in year *t*. Following recommendations from Butler and Sawyer (2008), a double threshold for sample sizes of 15–20 (GD >4 and *It* > 15%), 21–50 (GD >5 and *It* > 10%), 51–100 (GD >7 and *It* > 7%), and ≥ 100 trees (GD >9 and *It* > 4.5%) has been used to discriminate potential avalanche and non-avalanche events in accordance with statistically determined threshold as defined by Corona et al. (2012). These thresholds also aimed at limiting the inclusion of noise related to snow creeping (Stoffel and Corona, 2014), snow loading (Martin and Germain, 2016a), or any other kind of ecological disturbances (Butler and Sawyer, 2008; Corona et al., 2012) in the process reconstruction (Fig. 2.3).

(ii) The grey larch budmoth (LBM, *Zeiraphera diniana* Gn.) is a foliage feeding Lepidopteran insect responsible for periodical outbreaks (8- to 10-year intervals), mainly in the interior valleys of the European Alps (Baltensweiler et al., 1977). The feeding of LBM on larch needles causes massive defoliation that results in growth suppression in trees

lasting for 3–4 years (Kress et al., 2009) which may, thus, interfere with the dendrogeomorphic signal contained in tree-ring series. In total, 26 triplets of LBM outbreak years (i.e. three consecutive years, see Table 1) have been reconstructed in the Swiss Alps since 1740 CE according to Esper et al. (2007) and Büntgen et al. (2009). Similarly, climate extremes such as cold summers and prolonged droughts are susceptible to lastingly affect larch growth (Battipaglia et al., 2010; Lévesque et al., 2013; George et al., 2017) and to cause prolonged growth suppressions that may be confound with avalanche-induced GDs. According to Battipaglia et al. (2010), extremely cold summers were reconstructed in the central Alps from tree-ring data and historical archives in 1740, 1742, 1767, 1769, 1814, 1816, 1829, 1833, 1851, 1860, 1896, 1912, 1924, 1964, 1972, 1984, and 1995. Based on the gridded HISTALP point temperature information (Efthymiadis et al., 2006) closest to the study site, 11 years with negative May-September anomalies of temperature – 1.5 SD below the average – could be found for the period 1780–2008 and have thus been considered as cold summers years (Tab. 2.1). In the same way, eight years with negative April–July precipitation anomalies (i.e. -1.5 SD) were identified in the HISTALP point precipitation database for the period 1800–2003 (Efthymiadis et al., 2006). These years have been considered as drought years.

Table 2.1 – Larch budmoth events (according to Esper et al., 2007 and Büntgen et al., 2009), as well as extremely cold and dry summers (Battipaglia et al., 2010; Efthymiadis et al., 2006) in the Swiss Alps. All these years have been carefully analyzed due to probable interferences between snow avalanche damage in trees, as well as LBM and climatic signals that may induce comparable growth reduction in tree-ring series.

2003	**1945**	*1903*	*1851*
1995	**1937**	**1896**	*1843*
1984	*1932*	*1896*	**1838**
1981	**1931**	1893	*1833*
1980	*1924*	1892	**1830**
1979	**1923**	**1888**	*1829*
1978	1921	**1880**	**1821**
1972	*1919*	*1879*	*1821*
1972	**1915**	1870	*1817*
1965	*1912*	1865	*1816*
1963	1911	**1864**	*1814*
1962	*1910*	*1860*	**1811**
1954	**1908**	**1856**	**1801**

LBM-outbreak years, *Extreme cold summer*, Drought years

Potential avalanche events detected in step 1 that coincided with LBM outbreak episodes or extremely cold/dry years were therefore examined in more detail. To limit possible interferences between geomorphic, climatic, and LBM signals, growth suppressions were systematically excluded from the account of GDs and a minimum threshold of 4 GDs was retained to discriminate avalanche from non-avalanche events (Fig. 2.3).

(iii) In a third step, the type and intensity of GDs were used to evaluate a qualitative level of confidence associated to the detection of each reconstructed event. To this end, a weighted index factor (W_{it}) adapted from Kogelnig-Mayer et al. (2011) was computed for each avalanche event detected in step 1 as follows:

$$W_{it} = \frac{[(\sum_{i=1}^{n} T_i * 7) + (\sum_{i=1}^{n} T_s * 5) + (\sum_{i=1}^{n} T_m * 3) + (\sum_{i=1}^{n} T_w * 1)]}{\sum_{i=1}^{n} A_t} \quad \textbf{(Eq. 2.3)}$$

where, for each year *t*, T_i represents the sum of trees with injuries; T_s represents the sum of trees with strong GDs; T_m represents the sum of trees with medium-intensity GDs; T_w represents the sum of trees with weak-intensity GDs, and where *A* gives the total number of trees alive in year *t*. Based on the W_{it}, we then distinguish between low (LLC, $W_{it} < 0.2$), medium (MLC, $0.3 > W_{it} > 0.2$), and high (HLC, $W_{it} > 0.3$) levels of confidence in the reconstruction and attributed this evaluation to the avalanche event detection. In addition, and despite the precautions taken at each of the previous step, each event detected at step 2 was only rated with a LLC (Fig. 2.3).

(iv) Finally, avalanche events and corresponding GDs were mapped using the ArcGis 10.2 Time Slider (Kennedy et al., 2013; ESRI, 2013) to estimate the minimum sliding extent (ME, w.r.t the barycenter of the avalanche release zones) of each avalanche event. On the basis of ME, avalanche events with ME<600 m, 600 m <ME<800 m, 800 m <ME<1000 m, 1000 m <ME<1200 m, 1200 m<ME<1400 m, and ME>1400 m were classified as eXtra Small (XS), Small (S), Medium (M), Large (L), eXtra-Large (XL) or eXtra-eXtra-Large (XXL) events, respectively.

The age structure of the stand was approximated by counting the number of tree rings of sampled trees and was visualized after interpolation. However, and because trees were not sampled at their stem base and the piths as well as the innermost rings of some trees were rotten, the age structure is biased and does not reflect inception or germination dates. Nonetheless, it may provide valuable insights into major disturbance events at the study site with reasonable precision, as *L. decidua* has been shown repeatedly to recolonize

surfaces cleared by snow avalanches or other mass-movement processes in the years following an event (Stoffel et al., 2006; van der Burght et al., 2012).

3.4. Computation of avalanche events recurrence interval maps

In total, three recurrence interval maps (Rims) were computed at our study site. In Rim1, the individual impact interval for each tree (F_T) was calculated according to Eq. 2.1, following the interpolation method previously used by Reardon et al. (2008), Corona et al. (2010), Decaulne et al. (2012), or Martin and Germain (2016a). Rim1 was then visualized in ArcGIS 10.2 (ESRI, 2013). To estimate realistic values for the impact interval of events in areas where it could not be determined with dendrogeomorphic methods (Dale and Fortin, 2014), we spatially interpolated individual recurrence intervals using an inverse distance weighted interpolation algorithm. To ensure spatial robustness, interpolations were performed with an ellipse-shaped search (major axis: 280-m; minor axis: 96-m) where the anisotropy was set using an angle of 280° due to the presence of a strong directional influence (i.e. points are strongly related to those upslope of their location). Between ten and twenty-five neighbors were included within the eight sectors.

Rim1 relies on trees considered as proxies for past avalanche events. Yet, it does not account for the nature nor the physic of snow avalanches, classified as fast-moving mass-movements (McClung and Schaerer, 2006) that may have a huge destructive power reinforced by transported debris (Bründl et al., 2010) and potentially affect every tree within their paths.

To limit this bias, Rims2–3 were computed with a three-step procedure. In a first step, we (i) delineated the minimum area affected by each reconstructed event based on the spatial pattern of impacted trees, the geomorphology of the slope and the flowing nature of the process under investigation. We (ii) calculated recurrence intervals at each point of the slope as the ratio between the total number of years included in the dendrogeomorphic reconstruction and the number of times the snow avalanches reached this point. Finally, we (iii) built Rims2–3 without applying an interpolation procedure. Rim2 differs from Rim3 by the total number of years (275 and 75 years, respectively) included in the dendrogeomorphic reconstruction. Provided a precise (i) estimation of the number of avalanche events and (ii) delineation of past events, this procedure enables an approximation of recurrence intervals of snow avalanches at each pixel of the paths, and independently from individual tree ages.

4. Results

4.1. Snow avalanches recorded in historical archives

Analysis of historical archives yielded data on 45 snow avalanches (32 avalanche years) in the vicinity of Täsch during the 20th century. In total, 24 (16 avalanche years) out of the 45 snow avalanches occurred at the Täschwang site. Within these avalanches, four were observed during the first half of the 20th century in 1907, 1914, 1919, and 1920. By contrast, 17 occurred during the period 1950–2000 in 1962, 1974, 1975 (4 events), 1977 (3 avalanches), 1978, 1979, 1980, 1981, 1983 (2 avalanches), and 1985 (2 avalanches). Finally, 3 avalanches were documented during the early 21st century in 2012, 2013, and 2014. According to the analysis of archival documents, avalanches occurred preferentially from January to April (75.5%) and at the beginning of June (4.4%).

(a)

Täſch. Der Neuſchnee erreichte hier die Höhe von über 2 Meter. Alle Lawinen ſind gebrochen und zu Tale geſtürzt und haben großen Schaden angerichtet, am meiſten die große Lawine im Täſchwang.

Dieſe nahm nicht ihren gewohnten Lauf, ſondern ergoß ſich oberhalb der ſog. „Metjen“ in den prachtvollen Tannenwald, den ſie von oben bis unten niederſchlug. Tauſende von Stämmen ſind zerſchlagen und liegen im Tal. Acht Scheunen und Ställe mit viel Heuvorräten wurden ebendaſelbſt untergemacht und 18 Schafe erſtickt. Der Schaden iſt auf 30,000 Fr. zu berechnen.

(b)

Figure 2.4 – (a) Description of the avalanche of January 1920 in the Walliser Bote published 17th of January, 1920. English translation: “*Täsch: The new snow at the locality exceeded 2 meters. All avalanche couloirs produced events to rush down to the valley where they caused large damage, especially in the case of the large Täschwang avalanche. The avalanche did not follow its usual* trajectory but *left its couloir above the so-called “Metjen” from where it descended into a wonderful conifer forest to destroy it all the way down to the valley floor. Thousands of stems have been broken and are now accumulated in the valley. Eight stables and barns with plenty of hay reserves have been devastated and 18 sheep have been killed. Damage has to be estimated in the order of 30,000 francs*”, (b) The snow avalanche (≈80,000 m^3) of March 4, 2014 buried the northern entrance of the avalanche protection tunnel and the road linking Täsch to Zermatt (Feistl et al., 2015), picture extracted from Techel et al. (2015).

Three high-magnitude avalanches are precisely described in historical documentation (1920, 1984 and 2014). According to the Walliser Bote newspaper, an extreme snow avalanche occurred on January 17, 1920. This avalanche did not follow the classical path; by contrast, it reached "Zermettjen" – a locality 780 m downslope of the usual avalanche deposit where it destroyed a huge part of the forest, burying a barn with a 9-m thick snow tongue and killing 18 cattle (Fig. 2.4a). In 1984, another avalanche reached the Mattervispa River and killed 11 persons in cars on the road linking Täsch to Zermatt. On March 4, 2014, several newspapers report a snow avalanche – with a volume of approximatively 80,000 m3, comparable to the 1984 event – that buried the road to Zermatt and filled the northern entrance of the avalanche protection tunnel built after the 1984 event (Fig. 2.4b).

4.2. Age structure of the stand

In total, 307 European larch (*Larix decidua* Mill.) trees were sampled with 620 increment cores and 60 cross-sections. In total, 108, 180, and 45 trees were sampled on tracks T1, T2 and T3, respectively. After cross-dating, data on the pith age at breast height indicates that European larch trees growing at Täschwang were on average 145 yrs old (σ ±98 yrs). The oldest tree selected for analysis reached breast height in 1617 CE while the youngest tree only attained sampling height in 2011. As illustrated in Figure 2.5, the stand is dominated by 10–100-yr (46.3%) and 200–300-yr (30.0%) old trees, whereas 100–200-yr old trees only represent 16.9%. In total, 14 trees could be found with ages exceeding 300 years.

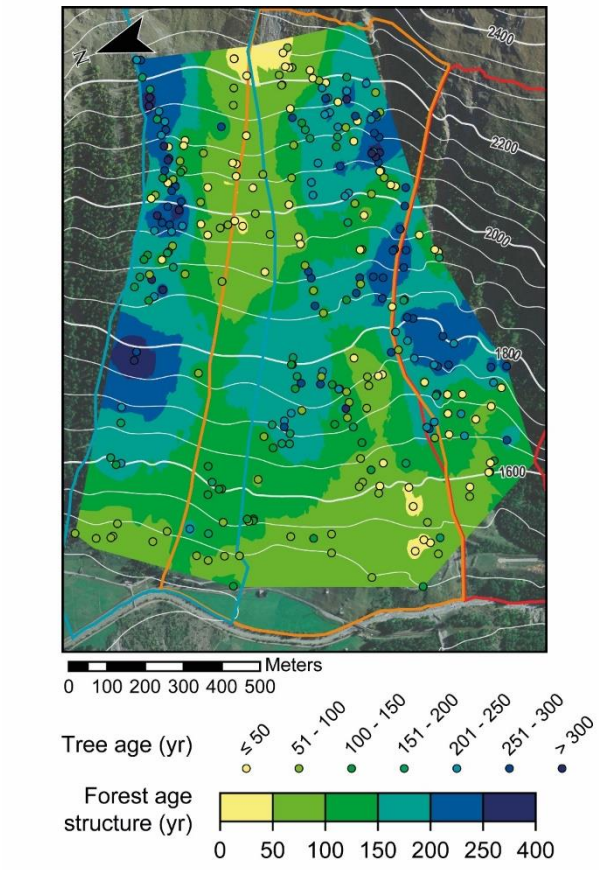

Figure 2.5 – Age structure of the forest stand growing at the Täschwang sites and its avalanche paths.

The comparison of aerial photographs and maps for the period 1909–2016 (Fig. 2.6) shows significant variations in the extent of the forest stand. In 1909, the uppermost trees were located at 2300–2400 m asl at T2 and reached

2000 m asl at T1. In 2016, this position has considerably evolved, and the current timberline is above 2300 m asl at both paths. At T1, the diachronic analysis reveals (i) the destruction of a 400 × 800 m strip of forest, located in the central parts of T1 and T2, between 1909 and 1941; (ii) a reforestation of this area between 1941 and 1977; and (iii) only a slight reshaping of the forest limits between 1977 and 2016. Coupling the diachronic analysis to both historical archives and the age structure of the stand lead us to hypothesize that approximately 32 ha of forest were destroyed by the high-magnitude snow avalanche of January 1920 and that this surface has been recolonized ever since.

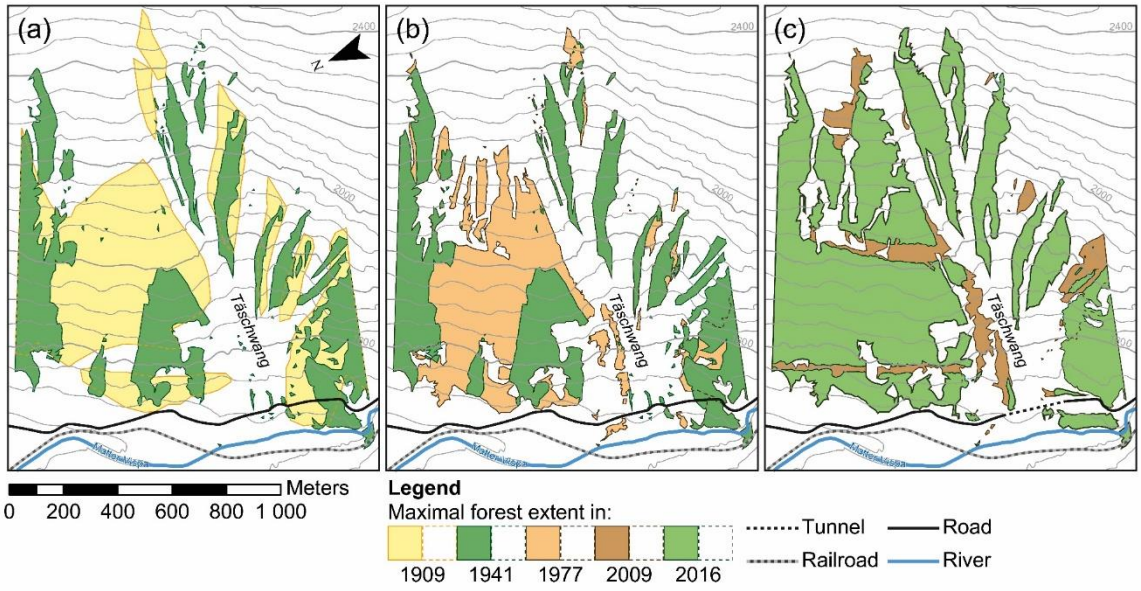

Figure 2.6 – Diachronic evolution of the forest stand at Täschwang for the period 1909–2016: (a) 1909–1941, (b) 1941–1977, and (c) 2009–2016.

Table 2.2 – Intensity of reactions and types of growth disturbances (GD) assessed in the 307 larch trees selected for analysis.

Type / Intensity	1	2	3	4	Total
Injuries	-	-	-	164 (6.4%)	164 (6.4%)
CT, TRD, CW	572 (22.3%)	403 (15.7%)	441 (17.2%)	-	1416 (55.1%)
GS	289 (11.2%)	507 (19.7%)	194 (7.5%)	-	990 (38.5%)
Total	**861 (33.5%)**	**910 (35.4%)**	**635 (24.7%)**	**164 (6.4%)**	**2570 (100%)**

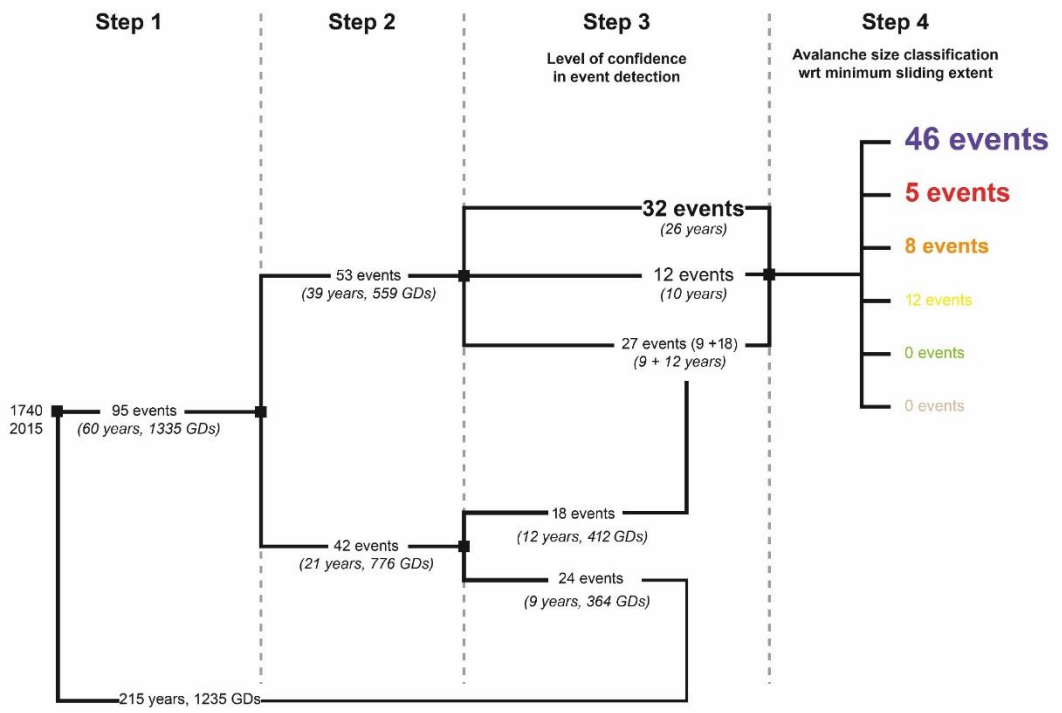

Figure 2.7 – Simplified synoptic diagram showing the characteristics (possible interference with climate or larch budmoth outbreaks, level of confidence, and minimum slide extent) of the reconstructed events.

4.3. Distribution of growth disturbances and chronology of avalanche events

Sampled cores and cross-sections allowed identification of 2,570 GD in the tree-ring series for the period 1740–2015, 799 of which were considered strong avalanche indicators (Classes 3 or 4). Table 2.2 summarizes the types of GD as well as their intensity. TRDs (49.4%), CT (3.1%), and CW (2.6%) were the GDs most frequently (55.1%) identified in the samples, followed by growth suppressions (GS; 38.7%). By contrast, only 164 injuries were sampled, which represents 6.4% of the dated disturbances. In total, 35.4% of the GDs were rated as intensity 2 and 33.5% as intensity 1. Intensities 3 and 4 represent 24.7% and 6.4% of all detected GDs, respectively. The oldest GD identified in the tree-ring series was dated to 1659 CE. GDs are more frequent after 1900 and nearly every year exhibited GD in a small number of trees.

On the basis of our 4-step-procedure (Figs. 2.3, 2.7), tree-ring analyses allowed identification of 51 years with evidences of snow avalanche in at least one path between 1740 and 2013 (Fig. 2.7). The oldest event was recorded in 1741 (T2), the most recent event in 2013 (T1-T2-T3).

In total, 31 (1740–2015), 35 (1740–2015), and 5 (1772–2015) avalanche events were reconstructed at sites T1, T2, and T3, respectively. Based on possible interferences between avalanche activity, climatic, and LBM signals in the tree-ring series (step 2), and

on the basis of the Weighted Index Factor (W_{it}; step 3, Figs. 2.7, 2.8) that accounts simultaneously for the type and intensities of GDs, we assigned high and medium levels of confidence to 32 and 12 events, respectively. By comparison, 27 events with a Wit<0.2, and characterized by a majority of weak and medium GDs, were therefore reconstructed with a LLC. Amongst the 42 potential events that coincide with LBM outbreak episodes or extreme climatic years, 24 were excluded from the reconstruction and 18 were rated with a LLC (Figs. 2.7, 2.8).

Higher levels of confidence were assigned to events that occurred in T1 (16 HLC and 4 MLC events) and T2 (11 HLC and 8 MLC events). Tree-ring signatures related to past snow avalanche activity were, by contrast, less frequent at T3 but all events were considered to have a HLC. For the period covered by historical archives, 9 (43.8%) out of the 16 avalanche years documented in historical archives were reconstructed with tree-ring records in T2 (1920, 1975, 1977, 1978, 1983, 2012 and 2013) and T1 (1962, 1975, 1977, 1978, 1981, 2013). By contrast, an insufficient number of GDs and/or possible interferences with LBM outbreaks and climatic extremes prevented us from retrieving the documented snow avalanches that occurred during winters 1907/08, 1918/19, 1961/62, 1973/74, 1978/79, 1979/80, 1980/81, 1984/85 and 2014/15.

Considering all reconstructed events within the study area, the mean event recurrence interval for the Täschwang avalanche paths is 3.8 years (or 2.6 events per decade) for the period 1740–2015. Avalanche event frequency is not, however, constant over time but shows a clear increase from one event per decade for the period 1740-1960 (22 events) to 8.9 events.decade^{-1} between 1961 and 2015 (49 events). Maximum decadal

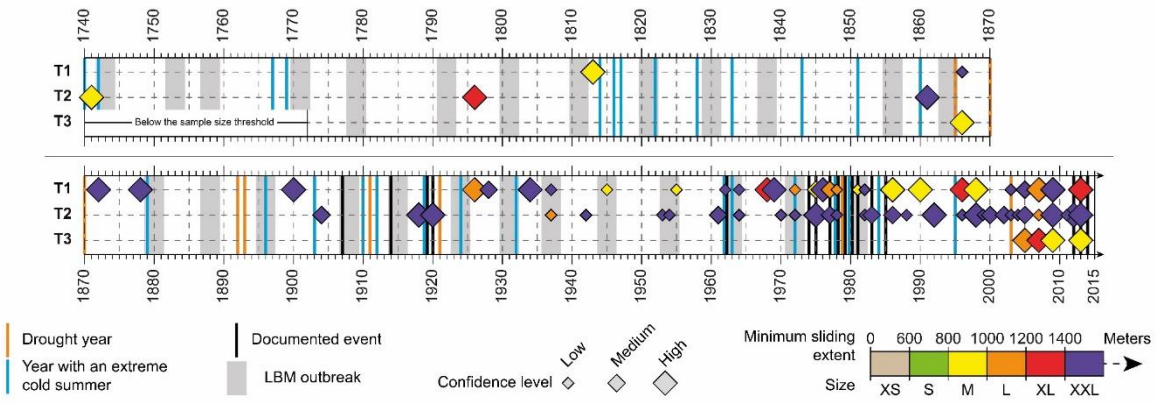

Figure 2.8 – Avalanche events reconstructed for the period 1740–2015 in avalanche paths T1, T2, and T3. Symbol sizes are proportional to the level of confidence, whereas the colour range denotes the minimum slide extent. Grey bands represent triplets of years associated to LBM outbreaks. Vertical lines show snow avalanche events documented in historical archives (black), as well as extremely dry (orange) and cold (blue) summers.

frequencies are systematically observed in the recent past, from 1971 to 1980 (9 events), 1981–1990 (8 events), and 2001–2010 (13 events). Conversely, no events could be reconstructed for the periods 1742–1795, 1804–1860, 1880–1899 and 1904–1918.

In details, at the level of individual paths, the highest avalanche activity was observed at T2 (35 events, 11 rated HLC, 8 MLC, mean recurrence interval 7.9 yr) and T1 (31 events, 16 rated HLC, 4 MLC, mean recurrence interval 8.9 yr). Conversely, T3 is characterized by lower activity (5 HLC events).

4.4. Spatial extent of avalanche events and recurrence interval maps

The spatial distribution of trees with GDs in a specific year has been used to estimate the minimum sliding extent (MSE) for each reconstructed avalanche. In total, 51 out of the 71 (71.8%) reconstructed events exceeded a length of 1200 m and were thus classified as XL (5) or XXL (46) snow avalanches (Fig. 2.9). The remaining 20 events were classified as L (8) or M (12) avalanches. There is no particular pattern between MSE and LBM outbreak or drought years. During these years, 11 out of 18 avalanche events were rated as XXL, 3 as M-sized and 2 as L-sized. Moreover, no clear relation was observed between the size of the event and the level of confidence associated to its reconstruction. By way of example, amongst the 46 XXL events, 20 were considered with a LLC. On the contrary, amongst the 32 events considered with a HLC, 16 events were reconstructed as extreme

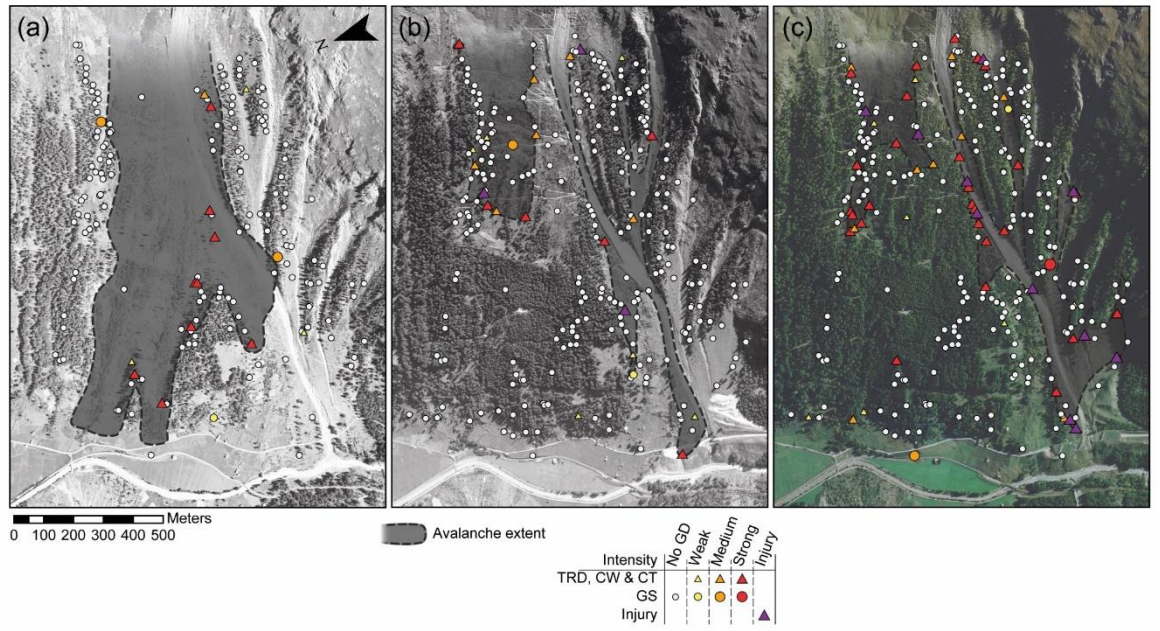

Figure 2.9 – Reconstructed Minimum Sliding Extent (MSE) of avalanches that occurred (a) on January 16, 1920, at T1 (b) in 1986, at T1 and T2, and (c) in 2009, at T1, T2 and T3, as derived from the location of disturbed trees and interpretation of the aerial pictures taken in 1941, 1988 and 2009 (in the background, aerial photographs are reproduced by permission of swisstopo, BA18022).

(XXL), five exceeded 1200 m in length (XL, 1796-T2, 1968-T1, 1996-T1, 2007-T3 and 2014-T1) and only eight were of limited extend.

The first recurrence interval map (Rim1, Fig. 2.10a) was computed from recurrence intervals as obtained for individual trees (Eq. 2.1) and by using an inverse distance weighted interpolation. Highest recurrence intervals (13–18 yr) are observed in the release areas of T1 and T2, above 2200 m asl and at the lowermost parts of the Täschwang channel whereas lower recurrence intervals (60-100 yr) are computed in the central part of the channel between 1650 and 2100 m asl. Conversely, highest recurrence intervals, derived from tree-ring analysis, exceed 150 years in the northern part of T1 and at the southern edge of T2. In addition, clear "bulls' eye" effects – related to the inverse distance weighting – can be observed e.g. at 1800 m asl on the northern part of T1 or at 1650 m asl in the southern margin of T3.

In Rim2 (Fig. 2.10b), our expert approach was used to delineate the spatial extent of each reconstructed event based on the position of disturbed trees, geomorphology of the slope and flow patterns of snow avalanches at the site. Rim2 results from the superimposition of all reconstructed extents and thus represents the average interval of time that elapses between events reaching a given location for the period 1740-2015. The spatial pattern of Rim2 obviously differs from Rim1: within T1 and T2, the recurrence intervals increased rapidly with distance downslope. Return periods range from 10 to 11 years at the release area of T1 (1900–2200-m asl) and T2 (2150–2400-m asl) and exceed 150–275 years on the interfluve between both paths (1500–1750-m asl). In addition, the Täschwang channel, characterized by < 10yr recurrence intervals is clearly delineated in Rim2 (whereas it remained invisible in Rim1). To account for the strong non-stationarity of the dendrogeomorphic reconstruction characterized by an obvious increase in avalanche recurrence intervals since the 1960s, Rim3 was also computed for the period 1961–2015 (Fig. 2.10c). Rim3 evidences recurrence intervals (i) <6 yr in the release areas of T1 and T2 and in the Täschwang channel and (ii) >18 yr in the lowermost part of both path below 1600 m asl. No information is available for the lowermost part of the forested strip, destroyed by the event of 1920, as no clear evidence of avalanche activity could be found in this sector since the 1960s.

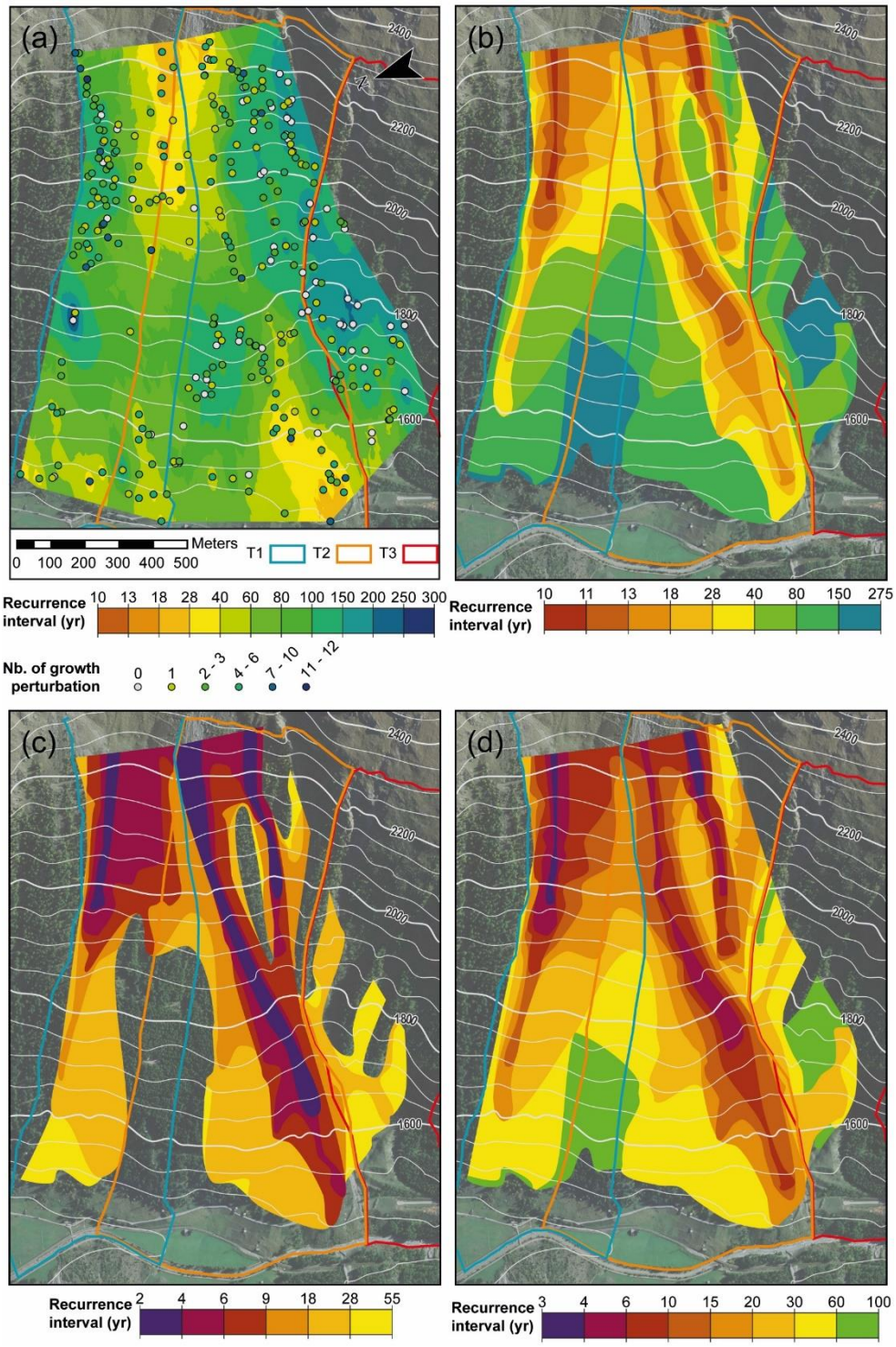

Figure 2.10 – (a) Interpolation of individual tree recurrence intervals (Rim1) often assimilated to avalanche return periods in the tree ring literature. Recurrence intervals computed according to the spatial delineation of past events based on growth disturbances in trees for the period 1740–2015 (Rim2, b) and 1960–2015 (Rim3, c). Map on panel (d) (Rim4) was transformed in order to adjust recurrence interval values from Rim2 and to estimate recurrence intervals in the missing portions of Rim3.

5. Discussion

5.1. Spatio-temporal accuracy of the reconstruction

The study we report here employs dendrogeomorphic techniques on three avalanche paths at Täschwang with the aim to assess recurrence interval maps of past avalanche activity. Specifically, we focus on events defined as the area affected a given winter by one or several snow avalanches in a given path. To meet this objective, the detection procedure developed by Favillier et al. (2017 – chapter 1) was used (i) to disentangle geomorphic signals in tree-ring series (related to the occurrence of snow avalanches) from signals induced by other external disturbances and (ii) to estimate the robustness of our tree-ring based snow avalanche reconstruction. Based on this procedure, 71 snow avalanche events were reconstructed in 51 different avalanche years. The reconstruction therefore complemented the historical chronology significantly as the first "only" yielded data on 24 snow avalanche events for 16 different winters between 1907 and 2014, and by extending the series back to 1740 CE. In total, 9 out of 16 (56.3%) avalanche years listed in historical documents were retrieved with the dendrogeomorphic approach, namely in 1920 (T2), 1962 (T1), 1975 (T1, T2), 1977 (T1, T2), 1978 (T1, T2), 1981 (T1), 1983 (T2), 2012 (T2), and 2013 (T1, T2, T3).

This success rate is comparable to previous tree-ring reconstructions performed both in the French (Corona et al., 2010, 2012; Schläppy et al., 2013) and the Swiss Alps (Favillier et al., 2017) but highlights, at the same time, some limitations in our approach in providing a complete picture of avalanche activity at a site. These limitations are related to (i) the energy of snow avalanches that have to be of sufficient magnitude to have impacts on trees; (ii) major avalanches that destroyed large parts of the forest stand and may remove evidence of past and subsequent events or disturb tree growth in such a way that younger events cannot be identified in the tree-ring record (e.g. Carrara, 1979; 1989; Kogelnig-Mayer et al., 2011). For example, we can reasonably attribute the clear temporal non-stationarity observed in the reconstructions (80% of the reconstructed events occurred during the 20th century and 36 out of 71 events even since 1960) to an increased potential to record past avalanche activity. This is related to the recolonization of the 400 × 800-m forest strip destroyed by the January 1920 event and in which trees reached maturity only in the 1950s. Similarly we found a large number of trees showing GD as a result of the avalanche activity of 2012 and 2013, but failed to identify the event of March 4, 2014 that severely damaged the forest stand in T2 by uprooting, breaking or bending 165, 259, and 696 trees, respectively (Feistl et al., 2015) ; (iii) potential biases towards larger avalanches, as smaller snow avalanches or events limited to the non-forested parts of the

avalanche system or strictly restricted to the incised Täschwang channel cannot be identified by means of tree-ring analysis; finally, (iv) our methodology is not normally able to provide a distinction between multiple events that occur at the same path during the same winter. As a consequence, and despite the stringency of the procedure employed in this paper, one has to keep in mind the number of reconstructed events has to be seen as a minimum frequency of natural avalanche activity.

On a spatial plan, past events were carefully delineated on the basis of growth disturbances observed in trees for a given year. Yet, limitations probably remain in the reconstruction of the boundaries of each event. In Chamonix, Corona et al. (2012) reported, by comparing archival records with tree-ring data, that runout distances tend to be underestimated with dendrogeomorphic techniques. Underestimations are attributed to (i) the modification of path geometry (steepness, curvature) by the geomorphic effect of the avalanches in the runout zone that may have induce rapid avalanche deceleration (McClung, 1990; McClung and Schaerer, 2006) and snow pressures that are insufficient to damage trees during some of the events; (ii) observation inaccuracies in historical archives, especially for old (Ancey, 2004) and extreme events involving very dry, non- cohesive snow and/or a powder cloud, for which the point of the farthest reach is sometimes very difficult to be located because of the absence of clearly visible deposits (Eckert et al., 2010b). Therefore, we must admit that the spatial patterns derived from our procedure contain some uncertainties that are not easily quantifiable and therefore have to be seen as the minimum yearly extent of avalanches that occurred in a given path.

5.2. From events to return period mapping

Dendrogeomorphology has a great potential to derive information on recurrence intervals of past avalanche events. Yet, only few studies (Fig. 2.1) really attempted to derive recurrence interval maps from tree-ring based reconstructions. In addition, by using an inaccurate definition of an avalanche return period, they usually failed to properly reproduce the expected patterns that typically increase as one moves down the avalanche path. In our study, Rim1 therefore is no exception to the rule. Classically based on the inverse distance weighting interpolation of individual tree recurrence intervals, the approach tends to homogenize recurrence intervals: a large part of the slope – with the exception of the release areas of T1 and at the outlet of the Täschwang channel (18–28 years) – are thus characterized by recurrence intervals that exceed 60 years with clear “bulls’ eye” effects. In addition, the map does not show a clear increase of recurrence intervals at the vicinity of the main channels. The

limited value and lack of realistic representation of avalanche activity in these maps is also limited by the high spatial variability of recurrence intervals in individual trees which can in turn be explained by (i) the heterogeneity of GDs observed in trees for a given event (i.e. not all trees located in the flowpath of an avalanche will show a GD, see e.g. Fig. 2.9), but also (ii) by the number and type of GDs recorded in each tree-ring series that directly depends on tree age (e.g. Šilhán and Stoffel, 2015) and tree species (Trappmann and Stoffel, 2013).

To overcome these biases, a new procedure was implemented in Rim2 and Rim3 that includes an expert delineation of past events based on disturbed trees. The resulting maps neither account for tree age nor do they involve interpolation processes. Instead, they represent a significant step towards a precise mapping of return period of avalanche events based on tree-ring analysis as they provide information on the time elapsing between two events for each location of the paths. Interestingly, they evidence similar patterns with highest recurrence intervals observed in the release areas of T1 and T2 and in the Täschwang channel. Owing to the non-stationarity of our reconstruction and to the increasing frequency of reconstructed snow avalanches for the last decades, the recurrence interval values of Rim2 (1740–2015) strongly exceed those computed for Rim3 (1961–2015). According to the limitations presented above for the early part of the reconstruction (see §5.2), we assume that Rim3 better estimates avalanche events recurrence intervals whereas Rim2 tends to strongly underestimate real avalanche activity as it only contains those snow avalanches that exceeded the boundaries of the 1920 extreme event, for example. Conversely, as no events could be retrieved in the lowermost part of the slope located between T1 and T2 since 1960, no recurrence interval could be computed at the interfluve between T1 and T2 on Rim3 which is more spatially limited. In order to (i) adjust recurrence interval values from Rim2 and to (ii) estimate the recurrence intervals in those parts not covered by Rim3, the distribution of the ratios Rim3/Rim2 was computed from those areas common to each map, and to then use the mean ratio (0.36) as a multiplier for Rim2. The composite recurrence interval map (Rim4, Fig. 2.10d) resulting from this transformation shows recurrence interval values >60 yr at the interfluve between T1 and T2 and <6 yr in the release areas of T2 and T3 and in the most active portions of the Täschwang channel. Interestingly, the latter values are in the same range as the recurrence intervals computed from historical documents for the period 1950–2000 (17 events, recurrence interval: 3 years) and 2000–2015 (3 events, recurrence interval 5 years).

Despite our efforts and encouraging results, we cannot consider at this stage that our recurrence interval maps can be readily used for hazard mapping purposes. Indeed, at a given location on the path, we compute the mean time separating two winters with at least one

avalanche instead of the mean time between two snow avalanches which is more relevant for elements at risk. Even more critically, the above-mentioned limitations in terms of spatio-temporal accuracy of the approach makes the reliability of our maps still hampered by some uncertainties related to: (i) the detection of past events and the difficulty to estimate real avalanche activity from both archival records and tree-ring data; (ii) inaccuracies in the delineation of the boundaries of past events which can, e.g., lead to significant underestimations of real runout distances difficult to quantify and (iii) the fact that we cannot be sure that each point of the avalanche path is reached by one and unique release area. Nonetheless, however, results presented here should be used with care in combination with archival records, expert judgement and modeling output to maximize knowledge and confidence in proposed mitigation strategies.

6. Conclusion

In this study, we used dendrogeomorphic technics and historical archives to document past avalanche activity for three paths of the Täschwang avalanche system (Canton of Valais, Swiss Alps) with the specific aim to improve tree-ring based recurrence interval mapping. To this end, a 4-step procedure was used to retrieve evidence on 71 avalanche events for the period 1740–2014. The comparison between our reconstruction and historical archives reveals that 9 out of 16 (56%) avalanche years listed in local records could be reconstructed with tree-ring analysis. In addition, tree-ring analysis and archival records enabled attribution of the apparent increase in the frequency of snow avalanches observed after the 1950s to the extreme avalanche that occurred at Täschwang in 1920. By contrast to those classically found in the tree ring literature, the different recurrence interval maps derived from our reconstruction for different sub-periods (1720–2015 and 1960–2015) clearly show a realistic upslope-downslope gradient as well as lateral variations in recurrence intervals, with the highest values being observed in the main Täschwang channel. Despite further potential for refinement to improve and test the accuracy of our maps, e.g. by comparison with numerical simulations or classical hazard mapping procedures, this study demonstrates that dendrogeomorphic data should be seen as an extremely valuable data pool for avalanche hazard zoning on forested paths with limited or no historical data.

CHAPITRE 3

Tree-ring reconstruction of snow avalanche activity: Does avalanche path selection matter?

Tree-ring reconstruction of snow avalanche activity: Does avalanche path selection matter?

Ce chapitre est en totalité constitué de l'article publié dans la revue :

***Science of the Total Environment* 284, 2019, 496–508**

doi : 10.1016/j.scitotenv.2019.05.194

Les résultats présentés dans ce chapitre sont issus du travail d'étude et de recherches réalisé par G. de Bouchard d'Aubeterre que j'ai encadré dans le cadre du stage exigé pour l'obtention du Master 1 Gestion de l'Environnement, mention Géoenvironnement. En plus de l'encadrement du stage, j'ai complété les calculs et les interprétations. Sur cette base, les résultats ont été réécrits, puis mis en forme pour la rédaction de l'article.

Co-auteurs et affliations :

de Bouchard d'Aubeterre G. [1], **Favillier A.** [1,*], Mainieri R. [2], Lopez Saez J. [3], Eckert N. [5], Saulnier M. [6], Peiry, J-L. [7], Stoffel M. [3,4,8], Corona C. [1]

1. Université Clermont Auvergne, CNRS, Université de Limoges, GEOLAB, F-63000 Clermont-Ferrand, France.
2. University Grenoble Alpes, Irstea, UR LESSEM, 2 rue de la Papeterie-BP 76, F-38402 St-Martin-d'Hères, France.
3. Institute for Environmental Sciences – University of Geneva, 66 Boulevard Carl Vogt, CH-1205 Genève, Switzerland.
4. Dendrolab.ch, Department of Earth Sciences, University of Geneva, rue des Maraîchers 13, CH-1205 Geneva, Switzerland.
5. Univ. Grenoble Alpes, IRSTEA, UR ETNA, 38402 St-Martin-d'Hères cedex France.
6. Faculty of Forestry and Wood Sciences, Czech University of Life Sciences, Kamýcká 129, 16521 Prague, Czech Republic.
7. CNRS, UMI3189, « Environnement, Santé, Sociétés », Faculté de Médecine, UCAD, BP 5005, DAKAR-FANN, Sénégal.
8. Department F.-A. Forel for Environmental and Aquatic Sciences, University of Geneva, 66 Boulevard Carl-Vogt, CH-1205 Geneva, Switzerland.

Remerciements et financement

The authors wish to address special thanks to Ana Casado, Loïc Francon, Pauline Morel, Louis Sembel and Taline Zgheib for their assistance on the field. This work was supported by Université Grenoble Alpes with the grant "RARETES" (avalanche risk as revealer of long-range interactions between environment and society, AGIR-PEPS 2016 program); and the French government IDEX-ISITE initiative 16-IDEX-0001 (CAP 20-25). Irstea is a member of Labex OSUG@2020. The authors acknowledge insightful feedback from the referees and the handling editor Elena Paoletti.

Abstract

In the current context of anthropogenic global warming, one of the purposes of dendrogeomorphic analyses is to provide long and continuous chronologies of mass movements, so as to detect potential trends or shift related to increasing temperatures. However, on documented slopes, the comparison between historical archives and tree-ring records suggests that dendrogeomorphic reconstructions systematically underestimate the natural activity of the process under investigation. In the specific case of snow avalanches, underestimation generally amounts to 50% and the main causes generally given for this difference are related to the magnitude of past events. In this study, we hypothesize that the morphometric characteristics of avalanche paths and their forest cover could have significant impacts on the length and reliability of tree-ring reconstructions. In order to test this hypothesis, we selected four adjacent, albeit differently structured, avalanche paths from the Queyras massif (French Alps), with the aim to compare their potential for a continuous reconstruction of past avalanche activity. On the most active avalanche paths characterized by high-altitude release areas (covered only by shrubby vegetation), tree-ring reconstructions do not exceed one century in length, with recurrence intervals of high magnitude events > 25 years. By contrast, on forested couloirs where lower slopes and forest coverage up to the release areas limits the intensity of events, the frequency of reconstructed snow avalanches is 2.5 times higher, the reconstructions span longer periods and the convergence rate with historical archives attest to the reliability of the dendrogeomorphic approach. These results suggest that a careful selection of couloirs is essential, and that priority should be given to forested sites as (i) they allow for exhaustive and (ii) reliable reconstructions over (iii) long periods of time.

Keywords: dendrogeomorphology; snow avalanche; forest cover; reliable reconstruction; French Alps; tree-rings.

Résumé

Dans le contexte du réchauffement climatique, un des objectifs des analyses dendrogéomorphologiques est de reconstruire des chronologies, longues et continues, de mouvement de masses dans le but de détecter des tendances ou des changements consécutifs à l'augmentation des températures. Cependant, sur les versants documentés, la comparaison entre les archives historiques et les chronologies reconstruites montre que l'approche dendrogéomorphologique sous-estime systématiquement l'activité naturelle du processus étudié. Dans le cas des avalanches, cette sous-estimation est de l'ordre de 50%. Elle est généralement expliquée par les différences de magnitude des événements passés. Dans cette étude, notre hypothèse est que les caractéristiques morphométriques et la couverture forestière sont susceptibles d'avoir un impact significatif sur la longueur et la fiabilité des reconstructions dendrogéomorphologiques. Pour tester cette hypothèse, quatre couloirs adjacents, avec une structure et une occupation forestière différentes, ont été sélectionnés dans le massif du Queyras (Alpes françaises), avec pour objectif de comparer leur potentiel respectif à reconstruire l'activité passé des avalanches. Sur les couloirs les plus actifs, caractérisés par des zones de départ localisé à haute altitude et recouvert seulement par de la végétation arbustive, la reconstruction dendrogéomorphologique ne dépasse pas un siècle de longueur, avec des événements de forte magnitude dont l'intervalle de récurrence est supérieur à 25 ans. A l'opposé, sur les couloirs sous-forêts, où les plus faibles pentes et la présence de forêt dans les zones de départ limitent la magnitude des événements, la fréquence des événements reconstruits est 2,5 fois supérieure et les reconstructions couvrent une période plus longue. Le niveau élevé de convergence avec les archives historiques atteste la fiabilité de l'approche dendrogéomorphologique dans ces couloirs. Ces résultats suggèrent qu'une sélection minutieuse des couloirs est cruciale et que les sites avec un peuplement forestier dense doivent être sélectionnés en priorité pour permettre (i) une reconstruction exhaustive et (ii) fiable de l'activité des avalanches pour (iii) de longues périodes.

Mots-clefs : dendrogéomorphologie ; avalanche ; couverture forestière ; fiabilité des reconstructions ; Alpes françaises.

1. Introduction

Avalanches are one of the major natural hazards in mountain regions. Every year, they damage urban infrastructures, transportation networks and endanger human lives (Bründl et al., 2004). During the 2017-2018 winter season, 64 avalanche-related accidents were recorded in France, including 26 fatal accidents (ANENA, 2018). In recent decades, the expansion of urbanization in mountainous massifs, increasing mobility, and the diversification of winter recreation have led to an increase in avalanche risk (Einhorn et al., 2015; Nöthiger and Elsasser, 2004; Techel et al., 2016). In France, observations of avalanche events are documented in the *Enquête Permanente sur les Avalanches* (EPA; or permanent avalanche survey), a database that contains ~100,000 avalanche events for ~4000 recognized paths in the French Alps and the Pyrenees since the beginning of the 20th century (Bourova et al., 2016; Mougin, 1922). Data on avalanches are gathered by forest rangers, who also record various quantitative (e.g., runout altitudes, deposit volumes) and qualitative (e.g., flow regime, snow quality) data (Jamard et al., 2002). Despite its uniqueness, the quality of EPA records locally depends to a large extent on the rangers' careful data recording, a fact that makes certain local series of limited use (Eckert et al., 2007b; 2010d). In addition, Teich et al. (2012) stated that in forested terrain, avalanches are sometimes poorly documented as they are not of key importance compared to large destructive events threatening settlements, infrastructure, and human lives in open terrain.

On wooded avalanche paths, forest stands act as protective barriers, or snow bridges in release areas (Bebi et al., 2009). Based on dendrogeomorphic approaches (Alestalo, 1971; Stoffel and Corona, 2014), focused on the identification and dating of growth disturbances in ring width series, trees can also be used to reconstruct past avalanche activity with annual resolution and for periods covering past decades to centuries (Butler and Sawyer, 2008) and to fill certain gaps in incomplete historical chronicles (Stoffel et al., 2010). Since the pioneer works in dendrogeomorphology (Burrows and Burrows, 1976; Butler, 1979; Carrara, 1979; Mears, 1975; Potter, 1969; Shroder, 1980, 1978), an increasing number of studies has focused on snow avalanches by using tree-ring analysis to reconstruct years of avalanche activity (Boucher et al., 2003; Casteller et al., 2007; Corona et al., 2013, 2012, 2010; Favillier et al., 2018, 2017; Garavaglia and Pelfini, 2011; Laxton and Smith, 2009; Muntán et al., 2004; Stoffel et al., 2006), to calibrate avalanche flow models (Casteller et al., 2008; Schläppy et al., 2014), to analyze the impact of ecological and anthropogenic disturbances on snow avalanche regimes (Germain et al., 2005) or to identify

the synoptic situations responsible for the triggering of regional snow avalanche activity (Casteller et al., 2011; Dubé et al., 2004; Germain et al., 2009; Muntán et al., 2009). In the current context of global warming (Gobiet et al., 2014), tree-ring reconstructions are also expected to provide insights into longer-term (multi-centennial) fluctuations of avalanche activity (Ballesteros-Cánovas et al., 2018; Corona et al., 2013; Heffernan, 2018; Schläppy et al., 2016; Stoffel and Corona, 2018).

However, on documented paths, comparison between observations listed in the EPA and tree-ring records suggests that the dendrogeomorphic reconstructions systematically underestimate years with natural avalanche activity (Corona et al., 2013, 2012, 2010; Schläppy et al., 2014). The main causes that are typically given for this difference are related to the magnitude of past events. Avalanches have to be of sufficient magnitude to create impacts on trees (Bartelt and Stöckli, 2001; Bebi et al., 2009). Conversely, major avalanches may remove or blur the evidence of previous or subsequent events in case large parts of the forest are destroyed (Bryant et al., 1989; Carrara, 1979), or disturb tree growth in such a way that younger events cannot be identified in the tree-ring record (Kogelnig-Mayer et al., 2011). In that regard, the morphometric characteristics of the avalanche path– through their influence on the frequency and/or magnitude of events and the long-term viability of the forest stand – are susceptible to have a significant impact on the completeness of the ensuing tree-ring reconstruction. We therefore hypothesize that, in the absence of anthropogenic interventions, the potential for a complete and continuous avalanche reconstruction could vary strongly amongst adjacent paths.

In order to test this hypothesis, (i) a dendrogeomorphic approach has been deployed on a slope of the upper Guil valley (Ristolas municipality, French Alps) in the Queyras massif. This slope was selected as it is composed of four avalanche paths characterized by comparably low anthropogenic interventions (i.e. very limited grazing or forest harvesting in the past) but marked differences in terms of morphology (starting zone altitudes and path lengths), avalanche dynamics (frequency and magnitude of events), and forest cover (i.e. forested paths and corridors characterized by a marked transverse zonation), thus enabling the comparison between reconstructions. In order to enhance the detection of snow avalanche years and to disentangle the potential effects of snow avalanches from disturbance pulses caused by climatic or exogenous factors, such as cold/dry years or larch budmoth outbreaks, the four-step procedure developed by Favillier et al. (2017 – chapter 1) has been used. (ii) The multi-centennial reconstructions are validated through comparison with historical chronicles, old maps, and aerial photographs. (iii) Their

comparison enables discussion of the dendrogeomorphic potential of each of the analyzed paths. This subsequently provides criteria that can, in the future, help to select the best sites for as complete as possible and continuous avalanche reconstructions, that are crucial for the detection of potential trends in avalanche activity related to climatic and other environmental changes.

2. Study site

The site under investigation is located on the western slope of the Upper Guil Valley, upstream from the Echalp hamlet, at the locality Ravin de la Salce (44°44'47" N, 6°59'42 E; Fig. 3.1). The talus slope covers an area of 1.47 km^2 and extends from the Guil thalweg (1740 m asl) to the Crête des Baysses (2700 m asl). The mean slopes in the upper part of the talus range between 35 and 40°, while the distal segment appears geometrically concave with mean slope angles comprised between 20 and 25°. The site is dominated by the Crête des Baysses, a 400-m schisto-calcareous rockwall cut by several subvertical faults oriented S-N and SW-NE (Lemoine and Tricart, 1986).

Climate is characterized by a mixed montane-Mediterranean to continental character (Touflan et al., 2010). According to to the data from the nearby meteorological station of Saint-Véran (2125 m asl), located 12 km south-west from the slope, annual temperature is -1.5 °C for the period 1981–2010 and average annual precipitation amounts to 710 mm. During winter, mean air temperature (DJF) is -5.3 °C while precipitation amounts to 127 mm. Precipitation falls primarily as snow from November to April. Average annual snowfall reached 320 cm (±183 cm) for the period 1928–2007. The forest cover is

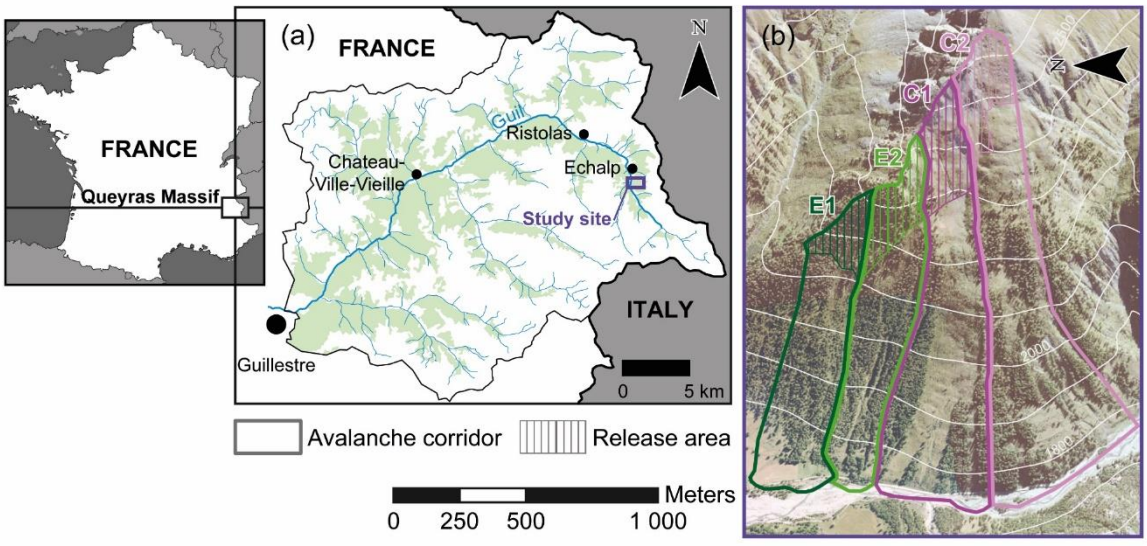

Figure 3.1 – Location of the study site in the Guil valley (Queyras massif, French Alps) (a) and delineation of the four avalanche paths on the Ravin de la Salce slope (b).

dominated by European larch (*Larix decidua* Mill.) between 1750 m and 2300 m asl. The understorey is dominated by herbaceous species and shrubs, namely *Rhododendron ferrugineum* L. (rhododendron), *Juniperus comunis* (common juniper) and *Vaccinium myrtillus* L. (bilberry).

3. Material and methods

3.1. Archival data on past events

First, we compiled a historical database of past snow avalanches at Ravin de la Salce using the EPA covering the period 1930-2013. Then, with the aim to complement the archival database, topographic maps and 19 aerial flight campaigns available from the French National Geographic Institute (IGN, at a scale of ca. 1:25,000) were used to detect evidence of damaging avalanche events since 1945.

3.2. Delineation of avalanche paths

The delineation of the avalanche paths at Ravin de la Salce is complex due to (i) multiple release areas and avalanche tracks in the eastern part of the slope, (ii) the absence of preferential flow paths, and (iii) the dense forest cover, which is effectively masking geomorphic evidence of past avalanche events in the western part of the study site. To precisely delineate the spatial extent of each path, we used the CLPA avalanche map (*Carte de Localisation des Phénomènes Avalancheux*) that complements the EPA and localizes the maximum lateral extent and runout elevations of avalanche paths as retrieved from historical testimonies and the analysis of aerial photographs (Bonnefoy et al., 2010). In addition, the numerical avalanche dynamics model RAMMS (Rapid Mass Movement System; Christen et al., 2010; Gruber and Bartelt, 2007; Rudolf-Miklau et al., 2015) – has been employed to estimate the spatial pattern of high magnitude avalanche events. RAMMS predicts avalanche runout distances, flow velocities and impact pressures on three-dimensional digital terrain models based on a Voellmy-fluid friction model.

RAMMS simulations were based on a 5-m Digital Elevation Model (DEM) extracted from the IGN RGE ALTI® database. Slopes with angles ranging from 30 and 45° were considered as potential release areas (Salm, 1982; Schweizer, 2003). In order to refine the detection, these thresholds were adjusted to account for the potential bias induced by the DEM resolution (ARPA and CEMAGREF, 2008) according to the following formula:

$$\alpha_r = \alpha \times RES^{-0.075} \quad \textbf{(Eq. 3.1)}$$

where α_r is the corrected angle value, α is the angle value (30-45) and RES is the resolution of the DEM (here RES=5 m).

For each delineated release area, one single simulation was performed with the objective of delineating the area exposed to extreme avalanche events. To this aim, typical friction parameter values were used following the recommendations of Gruber and Bartelt (2007). Snow depth in the release areas were set to 2 m, which, according to Gaume et al. (2013), corresponds to a return period of more than 100 years in terms of three-day snowfall events at the site.

3.3. Sampling strategy, identification, dating, and classification of growth disturbances

To reconstruct past avalanche activity based on dendrogeomorphic techniques, trees were sampled along three longitudinal transects. The upper transect (T1, 2200-m asl) is located in the release area of the two westernmost paths delineated according to the procedure detailed above, and at timberline for the easternmost paths. The intermediate transect (T2, 2000-2100 m asl) is located in the median part of each path. Finally, T3 (1880-1950-m asl) is situated in the distal and concave segment of the couloirs.

In summer 2017, 342 increment cores (52, 127, 77, 86 on E1, E2, C1, and C2, respectively) from 306 European larch (*Larix decidua* Mill.) trees were collected using a Pressler increment borer. The position of each tree was recorded with a 1-m precision GPS device and measurements were taken for the tree (diameter at breast height) and the disturbed feature (type, height). In this study, several kinds of growth disturbances (GD) to trees most commonly attributed to snow avalanches such as abrupt growth suppressions (Butler and Malanson, 1985b; Corona et al., 2012; Kogelnig-Mayer et al., 2013; Stoffel et al., 2013), impact scars (Corona et al., 2014; Stoffel and Perret, 2006; Trappmann et al., 2013), callus tissue (CT; Schneuwly et al., 2009b; Stoffel et al., 2010), tangential rows of traumatic resin ducts (TRD; Bollschweiler et al., 2008b; Schneuwly et al., 2009a; Stoffel and Hitz, 2008) as well as the initiation of compression wood (Butler et al., 2010; Timell, 1986) were retained in the analysis.

Following recent recommendations by Stoffel and Corona (2014), Tichavský and Šilhán (2016) and Šilhán and Stoffel (2015), old and young trees were considered in our sampling procedure in order to ensure the completeness of avalanche chronologies.

Sampling positions were optimized based on recommendations given by Stoffel et al. (2013). Sample preparation and analysis followed the procedures described in Stoffel

and Bollschweiler (2008) and Stoffel et al. (2013). GD were visually identified in the tree-ring series and cross-dated against the Echalp (1338-2010) and Souliers (1448-2009) local reference chronologies computed from undisturbed trees (Corona et al., 2013; Saulnier et al., 2017). In a subsequent step, intensities were assigned to GDs in order to emphasize features that are clearly associated with avalanche activity and to discriminate these from disturbances possibly induced by other factors (Corona et al., 2012; Stoffel et al., 2013). GDs were classified based on the visual quality of the evidence of reactions within each sample according to the intensity scale presented in Kogelnig-Mayer et al. (2011): weak (intensity class 1), medium (intensity class 2), and strong (intensity class 3) reactions and clear evidence of injuries (intensity class 4) were thus distinguished.

The age structure of the stand was approximated by counting the number of tree rings of sampled trees. However, since the innermost rings of some trees were rotten and trees were not sampled at their stem base, the age structure might be strongly underestimated (Bollschweiler et al., 2008a). Nonetheless, as *L. decidua* has been shown repeatedly to recolonize surfaces cleared by snow avalanches or other mass-movement processes and established dominance within a few decades, we believe that our age distribution could help the documentation of destructive events at our study site (Stoffel et al., 2006; Van der Burght et al., 2012). As a consequence, in order to detect potential forest recolonization dynamics, individual tree ages were spatially interpolated using an inverse distance weighted interpolation algorithm using ArcGIS (IDW; ESRI, 2013; Kennedy, 2013).

3.4. Detection of past avalanche events in growth disturbance series

To detect past snow avalanche years – during which at least one snow avalanche is reconstructed in the selected paths – in the GD series, we adopted the four-step procedure (Fig. 2) developed by Favillier et al. (2017) (Please refer to it for more details). This approach addresses the necessity to disentangle the potential effects of snow avalanches from disturbance pulses caused by climatic or exogenous factors, such as cold/dry years or larch budmoth outbreaks. Based on this procedure, the minimum population threshold was set to 15 trees alive the t year. GD and index I (Shroder, 1978, Eq. 3.2) – used to discriminate potential avalanche and non-avalanche events – were defined according to the sample size following the recommendations of Butler and Sawyer (2008) and Corona et al. (2012).

$$I_t = \left(\left(\sum_{i=1}^{n} R_t\right) \Big/ \left(\sum_{i=1}^{n} A_t\right)\right) * 100 \qquad \textbf{(Eq. 3.2)}$$

where ΣR is the number of trees responding to an event in year *t*, and ΣA represents the number of trees alive in year *t* at the path scale, where the extension of each individual path is delineated according to Sect 3.1. In other words, the detection of avalanche events is made in each path independently, and with a definition of each path corresponding to avalanche flow physics.

In addition to the procedure described in Favillier et al. (2017), lowered thresholds were adopted to maximize the number of detected events without including exogenous noise. Additional events were only added if they exceeded the I threshold and if the number of GD was less than 1 under the GD threshold. According to the second step of the procedure (Fig. 2), climatic and ecological signals interfering with the dendrogeomorphic signal were identified. In total, 17 larch budmoth (LBM, *Zeiraphera diniana* Gn.; cf. Baltensweiler et al., 1977, and Kress et al., 2009) outbreak years (see Tab. 3.1) have been reconstructed and 34 characteristic narrow rings have been identified in the Southern/Intermediate French Alps since 1720 CE according to Saulnier et al. (2017). Similarly, 20 years with negative May-September anomalies of temperature and precipitation (with values exceeding 1.5 SD below the average) have been considered as

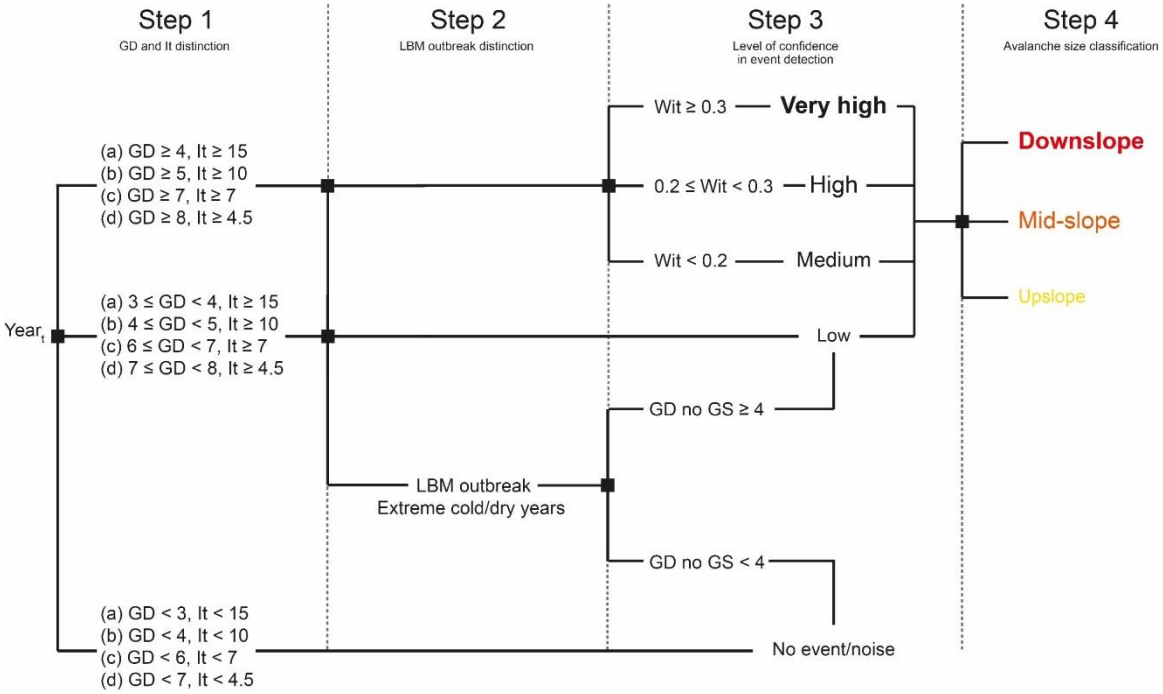

Figure 3.2 – Synoptic diagram of the 4-step approach used for the detection of avalanche events in tree-ring series, adapted from Favillier et al. (2017).

Table 3.1 – Larch budmoth events and pointer years (according to Saulnier et al., 2017), as well as extremely cold and dry summers (Efthymiadis et al., 2006) in the French Alps. All these years have been carefully analyzed due to probable interferences between snow avalanche damage in trees, as well as LBM and climatic signals that may induce growth reductions comparable to those observed after snow avalanches in the tree-ring series.

2005**	*1923*	1892*	1862*	*1828*	**1811**	*1775*
1980	*1918*	*1891*	**1857**	*1827*	*1810*	*1774*
1971	**1917**	*1890**	**1856**	1823*	1804**	*1758*
1963	1914*	*1884**	**1847**	*1821*	*1803*	*1757*
1962	1911*	*1883*	**1846**	*1820*	**1802**	**1741**
1943	*1910*	*1876*	1845*	*1819*	*1795*	**1740**
1936	**1909**	*1868*	1843*	1818*	**1794**	**1733**
1935	*1908*	**1867**	*1839*	1815*	*1793*	*1732*
1926	*1900*	*1866*	*1830*	**1812**	*1784*	*1723*

LBM-outbreak year, *Pointer year*, * Extreme cold summer, ** Drought year

extreme dry/cold years (Tab. 3.1) during the period 1720–2003 and according to the gridded HISTALP point temperature information (Efthymiadis et al., 2006) closest to the study site. Potential avalanche events detected in step 1 coinciding with LBM outbreak episodes or extremely cold/dry years were examined in more detail to avoid misclassification. According to the procedure, we systematically excluded growth suppressions from the account of GDs. Avalanche and non-avalanche years were discriminated at the path scale based on a threshold of 3 GDs (Fig. 3.2).

In the third step, levels of confidence – very high (vHLC, Wit > 0.3), high (HLC, 0.3 > Wit > 0.2) and medium (MLC, Wit < 0.2) –were distinguished for each detected event based on a weighted index factor (Wit, Eq. 3.3) accounting for the type and intensity of GDs (Favillier et al., 2017).

$$W_{it} = \frac{[(\sum_{i=1}^{n} T_i * 7) + (\sum_{i=1}^{n} T_s * 5) + (\sum_{i=1}^{n} T_m * 3) + (\sum_{i=1}^{n} T_w * 1)]}{\sum_{i=1}^{n} A_t} \quad \textbf{(Eq. 3.3)}$$

where, for each year *t*,, T_i is the sum of trees with injuries; T_s is the sum of trees with strong GDs; T_m is the sum of trees with medium-intensity GDs; T_w represents the sum of trees with weak-intensity GDs, and where *A* gives the total number of trees alive in year *t*. Despite the precautions taken at each previous step, each additional event detected during step 1 and events coinciding with an ecological or a climatic year at step 2 were only rated with a low level of confidence (LLC) (Fig. 3.2).

In the last step, avalanche events and corresponding GDs were mapped using the ArcGis 10.2.1 Time Slider (ESRI, 2013; Kennedy, 2013). On the basis of the sampling

transects, avalanche reaching the upper, intermediate, and lower transects were rated as eXtra-Large (XL), Large (L), Medium, (M) or Small (S), respectively. At the path scale, the annual probability for an avalanche event was computed by dividing the number of reconstructed events by the period covered by the reconstruction.

4. Results

4.1. Delineation of avalanche paths at Ravin de la Salce

At Ravin de la Salce, precise geomorphic mapping including field observations, interpretation of aerial photographs (CLPA), extent of past avalanche events derived from the EPA and flow extensions simulated with the RAMMS numerical snow avalanche simulations revealed a minimum of four distinct avalanche paths, namely (from west to east): E1 (19.7 ha, 1075 m long, 240 m wide, release area 2110-2180 m asl), E2 (25.3 ha, 1130 m long, 255 m wide, 2140-2340 m asl), C1 (42 ha, 1515m long, 300 m wide, 2290-2520 m asl), and C2 (55 ha, 1725 m long, 366 m wide, 2430-2620 m asl) (Figs. 3.1b, 3.3; see Tab. 3.2). According to the performed RAMMS simulations, the maximum velocities and pressures are significantly lower on E1/E2 (<10 $m.s^{-1}$ and 100 kPa) than on C1/C2 (>30$m.s^{-1}$, >300 kPa). E1 and E2 are covered by a dense larch forest from the top of the slope to the runout zones. A characteristic transverse vegetation pattern can be observed across C1 and C2: the inner zone is colonized by herbaceous and shrubby (*R. ferrugineum*, *J. communis*) formations, whereas *L. decidua* is dominant in the outer zone.

4.2. Snow avalanches recorded in historical archives

Archival data on past events at Ravin de la Salce go back to 1930. The EPA inventoried 10 events on avalanche paths E1 and E2, namely in 1930, 1947, 1951, 1959, 1961, 1973, 1977, 1986, 2003, and 2009. According to the EPA database in which E1 and

Table 3.2 – Geomorphic characteristics and soil occupation of the studied avalanche paths and their release zones.

	Avalanche path						Release area				
Path	Aspect	Length (m)	Width (m)	Area (ha)	Mean slope (°) (SD)	Release altitude (m)	Deposit altitude (m)	Mean slope (°) (SD)	Area (ha)	Forest cover in 1945 (%)	Forest cover in 2015 (%)
E1	WN	1240	240	19.7	25.1 (9.2)	2110-2200	1745	34.5 (2.4)	4.3	76.4	100
E2	WN	1290	255	25.3	27.8 (5.6)	2140-2340	1745	35.0 (2.3)	6.4	46.9	54.7
C1	WN	1580	300	42	26.4 (6.6)	2290-2520	1760	33.1 (3.3)	6.9	1.9	1.5
C2	WN	1600	366	55	26.6 (7.3)	2430-2620	1790	32.5 (3.9)	6.9	0	0
Echalp	W	1200	200	*n.p.*	32 (*n.p.*)	2100-2450	1700	36 (*n.p.*)	*n.p.*	*n.p.*	*n.p.*

n.p. not provided

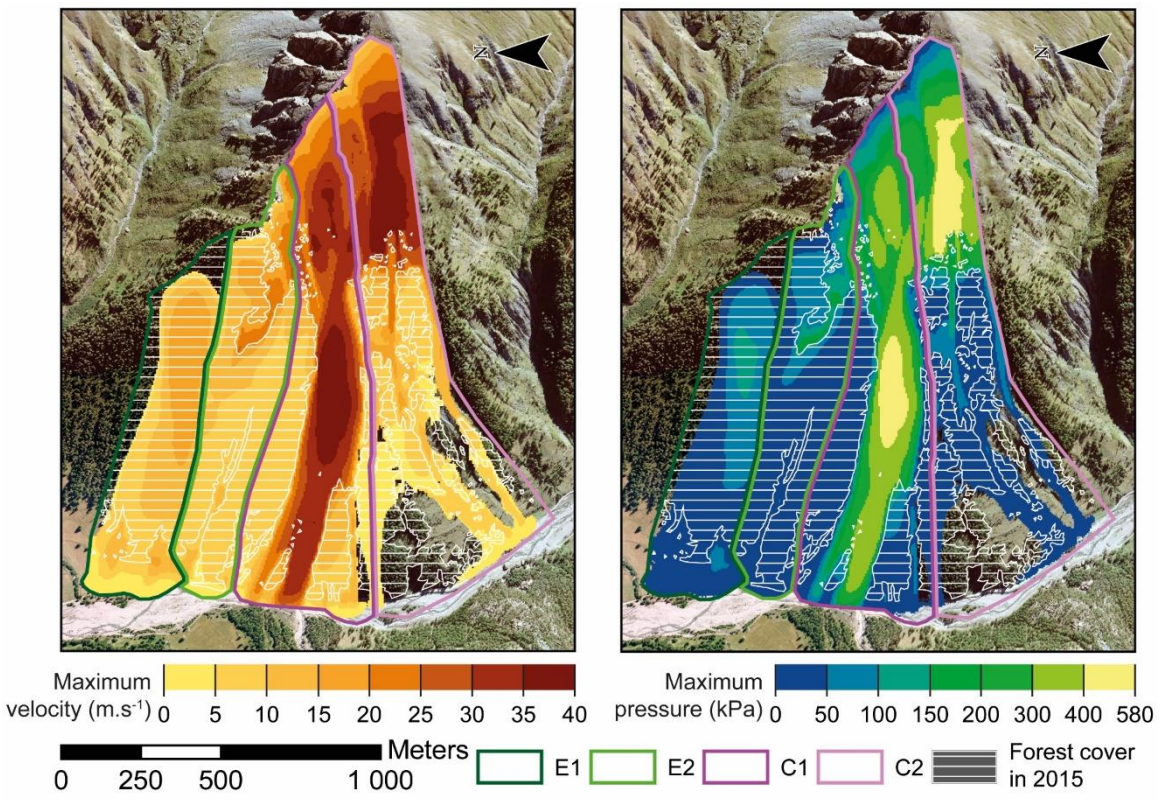

Figure 3.3 – (a) Maximum velocities and (b) maximum pressures computed with the RAMMS snow avalanche model. Avalanche extensions obtained with RAMMS are used in this study to delineate avalanche paths E1-C2.

E2 paths were grouped in a unique couloir, the longest events would have occurred on 25 February 1947, 24 February 1951, and 1959 (undated), reaching an altitude of < 1550 m asl. Damage to the forest stands are reported for the snow avalanches that occurred in 1977 (undated) and on 16 December 2008. For the period 1930-2008, the mean recurrence intervals between two consecutive events is 8 years based on EPA records. The absence of avalanche events between 1930 and 1947 is probably due to the absence of systematic observations during the interwar period and World War II. Similarly, due to the absence of elements at risk, avalanche paths C1 and C2 do not contain any records of past events in the EPA. However, one event was retrieved from the CLPA datasheet, pointing to an avalanche that would have occurred on 16 December 2008 in at least one of these couloirs. In addition, according to the diachronic comparison of aerial photographs, evidence for at least two snow avalanche events can be found indirectly as they apparently destroyed parts of forested stands C1-C2 between 1957–1962 and 2003–2009.

4.3. Age structure of the stands

Visual cross-dating of tree-ring samples was carried out by means of the skeleton plot method and primarily based on the narrow rings of 1500, 1643, 1668, 1741, and 1906.

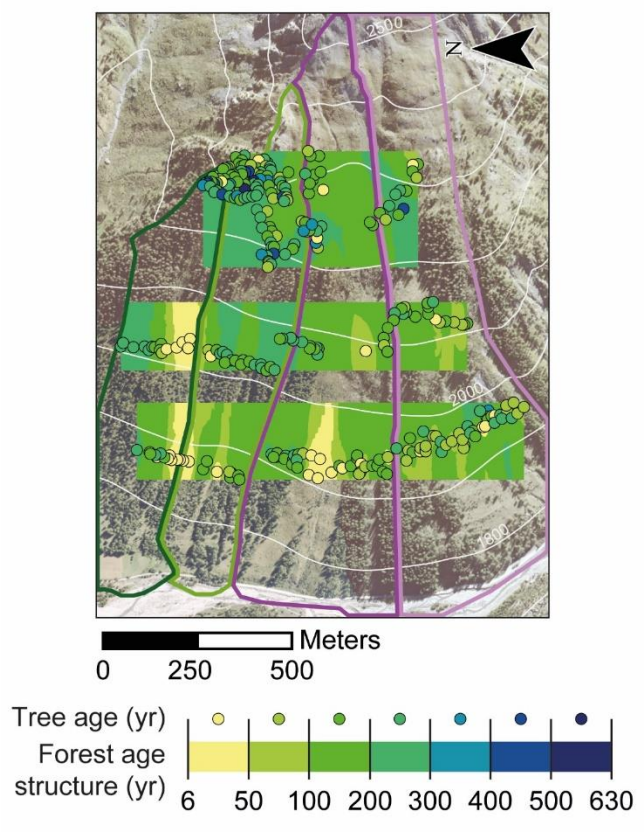

Figure 3.4 – Age structure of the forest stand growing at the Ravin de la Salce slope.

After cross-dating, data on pith ages at breast height indicate that the 306 trees sampled on the Ravin de la Salce slope are on average 171 years old (± 102 years). The oldest tree selected for analysis attained sampling height in 1398 (618 rings in 2016) while the youngest tree reached breast height in 2010. Figure 3.4 shows that trees older than 300 years are mainly located along the upper transect (T1) where the average age of individuals is 206 years (± 114 years). On T3, the mean age of sampled trees is lower, especially for E1 and C1 paths (126 ± 81 years). The number of trees (n=15) considered as a minimum for analysis in our 4-step procedure was exceeded in 1779 at E1, 1720 at E2, 1813 at C1 and 1791 at C2. The sample size shows a clear increase in the 1860-70s at E1, E2, and C1, and in the 1920s at C2. A second step or increase is observed in the 1980s at E1 (Fig. 3.5).

4.4. Distribution of growth disturbances and chronology of avalanche events

Sampled cores allowed identification of 1591 GD in the tree-ring series for the period 1720–2016, of which 314 (19.4%) were considered strong avalanche indicators (Classes 3 or 4). Table 3 summarizes the types of GD as well as their intensity. TRDs and CW were the GDs most frequently (76.6%) identified in the samples, followed by growth suppressions (GS; 20%). By contrast, only 51 injuries were sampled, which represents 3.2 % of the dated disturbances. In total, 60.6% of the GDs were rated as weak, 20.0% as median and 16.2% as strong. The oldest GD identified in the tree-ring series was dated to 1496 CE, the most recent to 2016. Nearly every year exhibited GD in a small number of trees for the period 1780-2016 at E1 and E2. GDs were scarcer before1920 at C1 and C2.

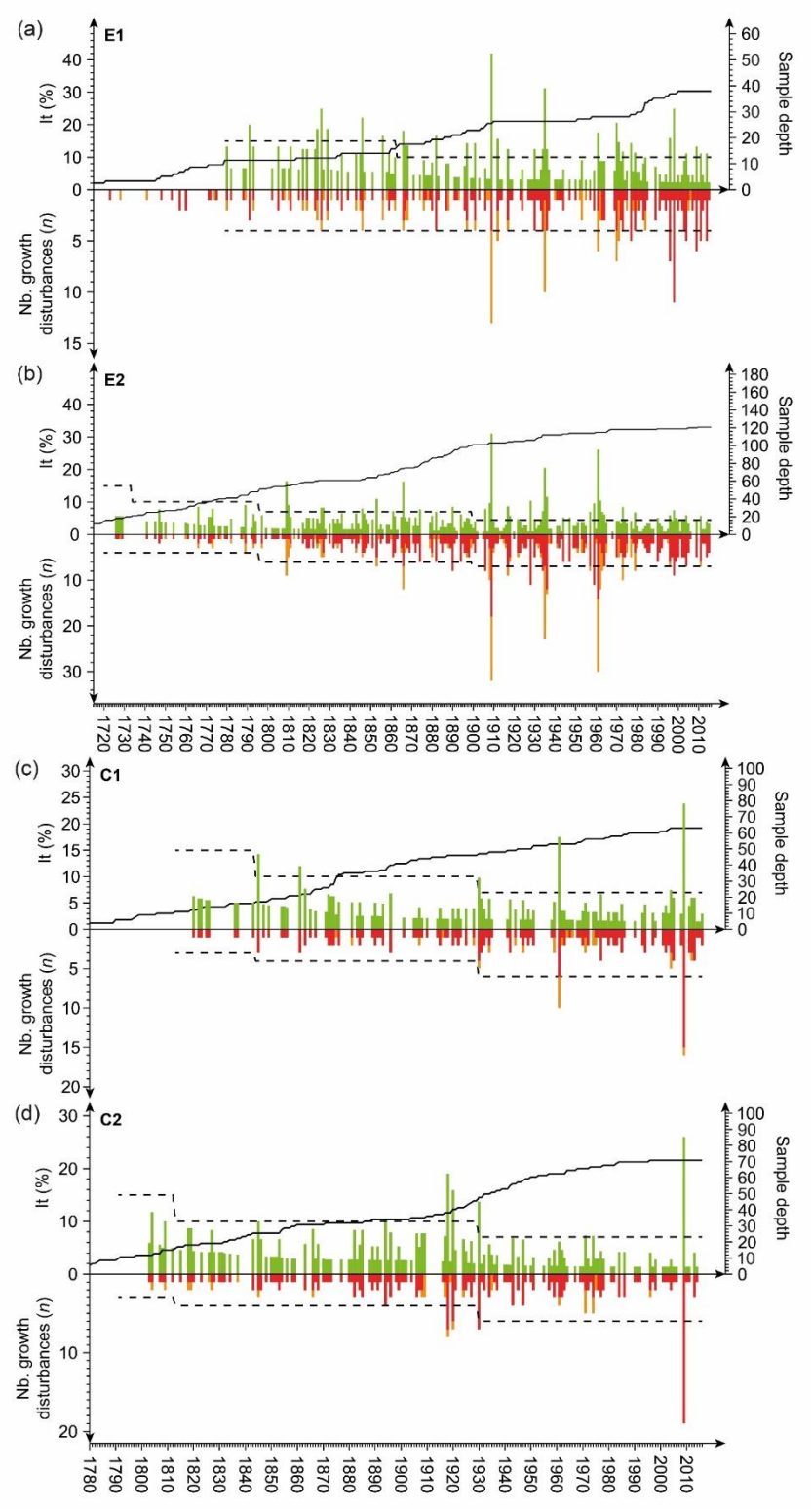

Figure 3.5 – Event-response histograms showing the total number of growth disturbances (GD, in red and orange) and the percentage of trees responding to an event (in green) at each of the four paths. Orange bars show the total number of growth reductions which are possibly related to larch budmoth outbreaks or to climatic extremes. The dashed lines denote the GD and It thresholds used to reconstruct past avalanche events. The solid lines denote sample depth, i.e. the number of trees available for analysis for each year of the reconstruction.

The event-response histograms depicted in Figure 3.5 summarize all reactions recorded in the trees along the four avalanche paths. In total, 22 (1779-2016), 23 (1720-2016), 2 (1812-2016), and 5 (1894-2016) avalanche events were reconstructed at sites E1, E2, C1, and C2, respectively. The highest percentages of disturbances were recorded in 1909 with It of 41.94 and 31.1 and a Wit of 1.39 and 0.78 at paths E1 and E2, respectively. In 2009, growth disturbances reached It values of 13.33 (Wit: 0.31), 23.88 (Wit: 0.93), and 26.03 (Wit: 1) at paths E1, C1, and C2, respectively. Finally, a large proportion of disturbances were dated to 1961 at paths E1, E2, and C1 (It: 17.65, 26.09, 17.54%; Wit: 0.47, 0.66, 0.53). Based on potential interferences between the avalanche and exogenous signals in the dendrochronological series (step 2), and on the basis of the Weighted Index Factor (Wit; step 3, Fig. 3.6) that includes simultaneously for the type and intensities of

Table 3.3 – Intensity of reactions and types of growth disturbances (GD) assessed in the 306 larch trees selected for analysis.

Type / intensity	1	2	3	4	Total
Injuries	-	-	-	53 (3.2%)	53 (3.2%)
TRD, CT, CW	810 (51.3%)	220 (13.9%)	187 (11.4%)	-	1217 (76.6%)
GS	147 (9.4%)	97 (6.1%)	77 (4.7%)	-	321 (20.2%)
Total	957 (60.6%)	317 (20%)	264 (16.2%)	53 (3.2%)	1591 (100%)

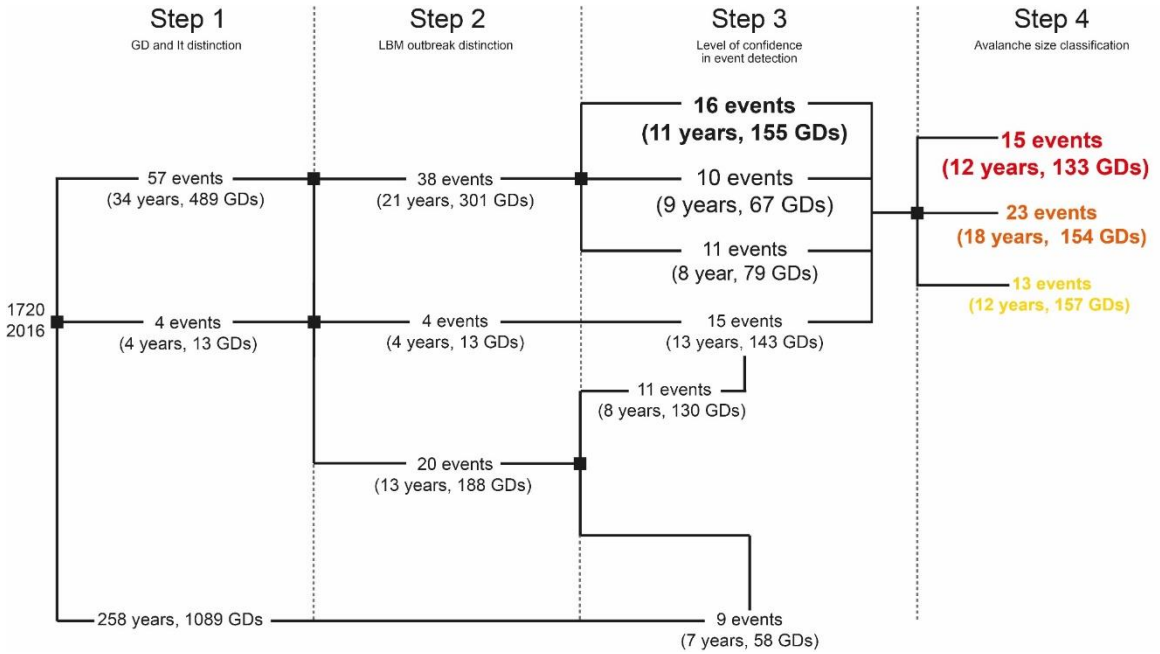

Figure 3.6 – Results of the 4-step procedure. Reconstructed event characteristics consider possible interference with climate or larch budmoth outbreaks and include the level of confidence and the minimum slide extent.

growth disturbances, 16 and 10 events occurring during 19 different years were assigned with very high and high levels of confidence, respectively. By comparison, 24 events (22 years) characterized by a majority of weak and medium GDs, were reconstructed with a medium and low level of confidence. Amongst the 20 potential events that coincide with LBM outbreak episodes or extreme climatic years, 9 were excluded from the reconstruction and 11 were rated with a low level of confidence. With respect to the 1791-2014 and 1809-1998 periods – delimited by the first and the last observed events – and at the level of the slope scale, the mean recurrence intervals of snow avalanches are 10 and 9 years at E1 and E2, respectively. They exceed 20 years (24 years, 1961-2009; and 23 years, 1894-2009) at C1 and C2. The decades 1931-1940 (7 events) and 1971-1980 (6 events) are characterized by the highest avalanche activity; conversely, no event was reconstructed for the periods 1829-1853 and 1937-1956. In total, nine events occurred synchronously at E1 and E2, namely in 1909, 1934, 1936, 1961, 1973, 1979, 1998, 2004, and 2011 (Fig. 3.7).

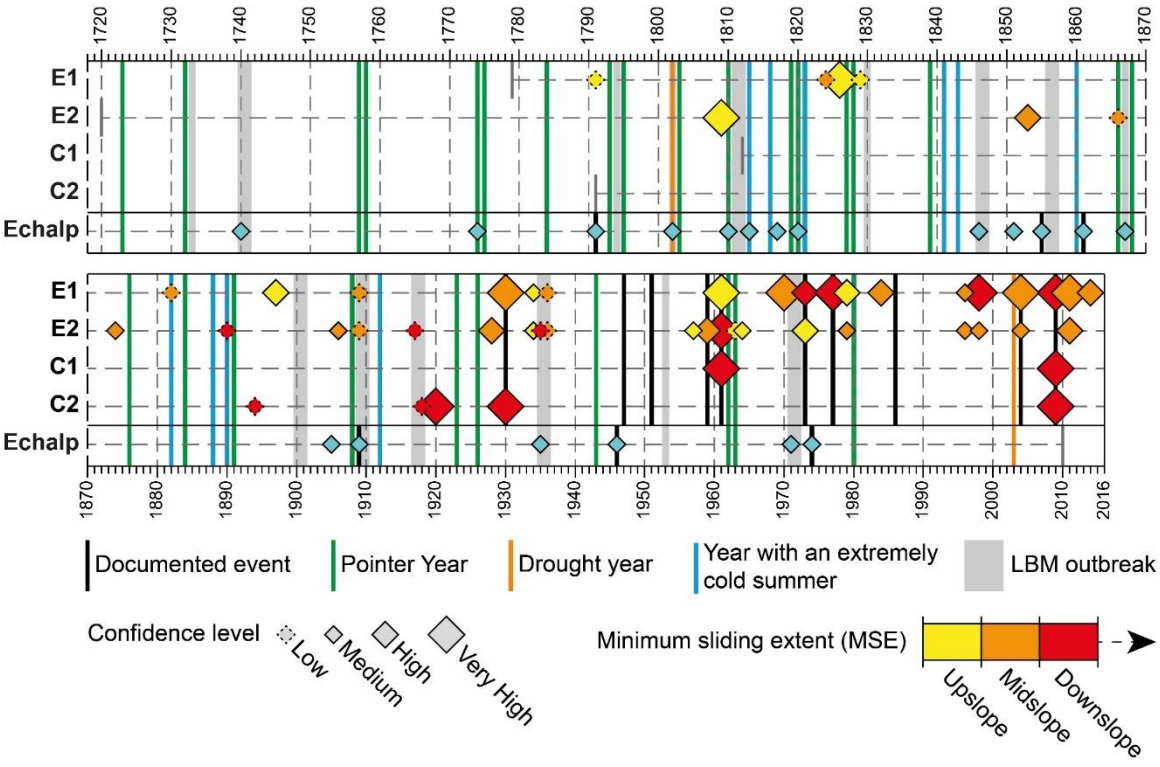

Figure 3.7 – Avalanche events reconstructed for the period 1720-2016 at the four avalanche paths. Symbol sizes are proportional to the level of confidence, whereas the color range denotes the minimum slide extent. Grey bands represent years associated to LBM outbreaks. Vertical lines show snow avalanche events documented in historical archives (black), as well as extremely dry (orange), cold (blue) summers and pointer years (green).

4.5. Spatial extent of reconstructed events

Sampling along transects only allows a partial reconstruction of the spatial extent of past avalanche events and an estimation of the minimum longitudinal extent of past events. In total, 15 events reached the distal segment of the talus, 24 were reconstructed at the median transect level and 13 were limited to the upper part of the avalanche paths (Fig. 3.7). All the events retrieved at C1 and C2 reached the lowest transect. Conversely, at E1 and E2, 37 out of 45 (82%) snow avalanches were limited to the upper (35.1%) or the median (64.9%) transects.

Figure 3.8 shows two high-magnitude events reconstructed from the dendrogeomorphic approach in 1962 and 2009. Based on the EPA inventory, we could reasonably attribute the 30 and 10 GDs observed at E2 and C1, respectively, to the event reported on 7 February 1961. This hypothesis is further supported by the diachronic analysis of the aerial photographs of 1956 and 1962 showing that a large part of the stands was destroyed at C1 and that larch trees were removed from the main track and in the lowest portion of E2 (Fig. 3.8). In the same way, the snow avalanche documented on 17 December 2008 was retrieved through tree-ring analyses at C1 (16 GDs) and C2 (19 GDs) and could be precisely delineated based on the aerial photographs from 2005 and 2010.

Before 1945, aerial photographs are not available for our study site. The topographic maps of 1896 and 1930 did not provide insights into possible changes in the spatial extent of the forest stand. As a consequence, the events reconstructed with a high level of confidence in 1897, 1920, 1928, and 1930 could not be confirmed through diachronic analysis.

5. Discussion

5.1. Accuracy of the reconstructions

The study we report here employs dendrogeomorphic techniques on four adjacent, albeit differently structured, avalanche paths from the Queyras massif (French Alps), with the aim to compare their potential for a continuous reconstructions of past avalanche activity. In the global warming context, such reconstructions have proven to be particularly important to complement incomplete historical record and for the detection of potential climate-related trends in avalanche activity (Ballesteros-Cánovas et al., 2018). To reach this goal, we used the 4-step procedure developed by Favillier et al. (2017 –chapter 1) (i) to disentangle snow avalanche signals in tree-ring series from signals induced by other external disturbances and (ii) to estimate the robustness of our tree-ring based snow

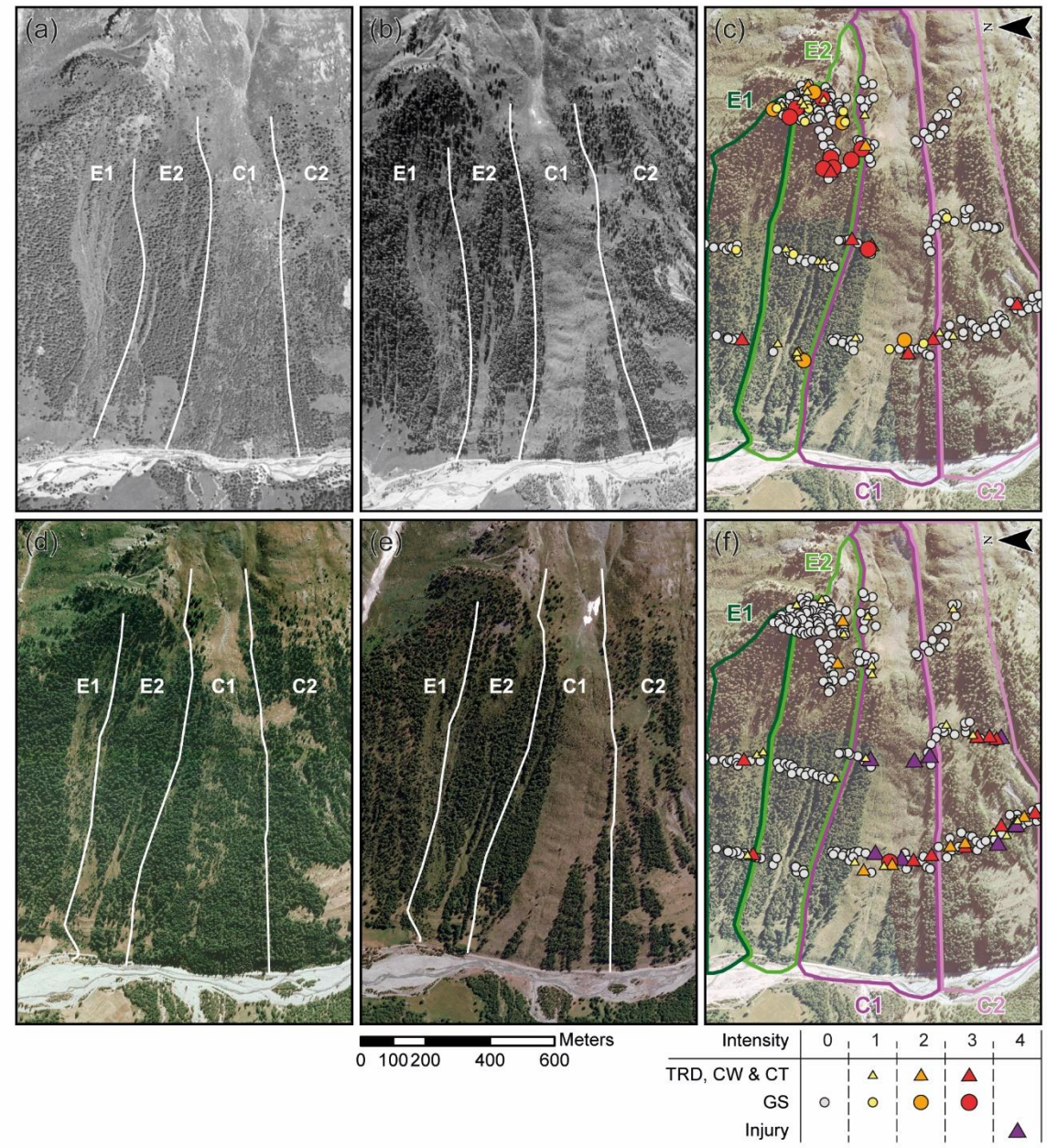

Figure 3.8 – Location of trees disturbed in 1961 and 2008 and presumably corresponding to avalanches that occurred (c) on February 7, 1961 and (f) on December 17, 2008 and diachronic comparisons of aerial photographs (IGN) highlighting the evolution of the forest stand between 1956 and 1962 (a, b) and between 1988 and 2009 (d,e).

avalanche reconstruction depending on the total number of disturbances (GD) and the percentage of trees impacted. Based on this procedure, 52 snow avalanche events were reconstructed in 38 different avalanche years. The reconstruction therefore complemented the historical chronology significantly with 10 new snow avalanche winters between 1930 and 2008, and by extending the series back to 1791 CE at E1. In total, 70% of the avalanche years listed in the EPA were retrieved, especially on paths E1 and/or E2 with the dendrogeomorphic approach, namely in 1930 (E1, C2), 1959 (E2), 1961 (E1, E2, C2), 1973 (E1, E2), 1977 (E1), 2003 (E1), and 2009 (E1, C1, C2). Amongst these avalanche years, five could be reconstructed with very high levels of confidence. In particular, the extreme avalanche cycle of 16 December 2008, when 10 snow avalanches were reported in the Ristolas municipality (Eckert et al., 2010c; Gaucher et al., 2009), could be reconstructed with the highest level of confidence on paths E1, C1, and C2. On C1 and C2, the absence of EPA records renders a comparison impossible. On paths E1 and E2, the convergence rate between the EPA and the tree-ring reconstruction significantly exceeds those reported by previous studies made in the French Alps by Corona et al. (2012, 43%), Corona et al. (2013, 43%), Schläppy et al. (2013, 38%) and Schläppy et al. (2014, 33-45%). This synchronicity confirms the potential of forested avalanche paths for a detailed reconstruction of past avalanche activity. Albeit the fact that GDs were observed in tree-ring series in 1947 (14), 1951 (8), and 1986 (8), these events listed in historical records were not confirmed with dendrogeomorphic analysis as the It, GD, or Wit values did not exceed the required thresholds. This lack may be attributed to the stringency of the procedure employed here, designed to limit the introduction of noise but could equally be related to an over-sensibility of the dendrogeomorphic approach. Indeed, one should indeed keep in mind that the It, GD, and Wit thresholds used in the first and third steps are empirical. As no consensus exist in literature, they have been synthesized from Corona et al. (2014), Favillier et al. (2017), Kogelnig-Mayer et al. (2011) and Schneuwly-Bollschweiler et al. (2013) but cannot be considered as absolute values suitable for all sites. Similarly, in the second step, the threshold of four mechanical disturbances was arbitrary chosen to disentangle snow avalanche events from climate and larch budmoth outbreaks (Favillier et al., 2017 – chapter 1) and may therefore lead to the omission of minor events and to an underestimation of past avalanche activity. In addition, (i) snow avalanches reported in historical chronicles have to be of sufficient magnitude to have impacts on trees, but (ii) not too major as they would then destroy large parts of the forest stand and thereby remove evidence of past and subsequent events or disturb tree growth in such a way that

younger events cannot be identified in the tree-ring record (e.g. Carrara, 1979; Kogelnig-Mayer et al., 2011). As a consequence, and despite our high success rate, the number of reconstructed events has to be seen as a minimum frequency of natural avalanche activity.

5.2. Two different avalanche dynamics

In this study, we deliberately chose contiguous avalanche paths with different morphometric characteristics and forest cover, with the aim to detect differences in their potential to record past events in trees. On the one hand, paths E1 and E2 are characterized by forested release areas, located at altitudes <2340 m asl and the presence of a very dense shrub cover (mainly *R. ferrugineum*), with an average height of about 0.70 m. Both paths have limited areas (<25ha), their length does not exceed 1000 m, and they are almost completely covered by open larch stands. On the other hand, on paths C1 and C2, snow avalanches are commonly triggered naturally from unforested release zones located above 2290 m asl and covered by shrubby grassland. Their lengths exceed 1500 m and they show a marked transverse vegetation zonation (Malanson and Butler, 1986) with an inner zone colonized by shrubs and shade-intolerant pioneer tree species and forest vegetation (mainly European larch) in the outer zone. The performed snow avalanche simulations reveal that maximum velocities and maximum pressures are significantly higher in these paths than on paths E1 and E2.

As expected, avalanche dynamics strongly differ from C1/C2 to E1/E2. On paths C1 and C2, all snow avalanches reach the lower sections of the slope and are reconstructed with a high level of confidence. Avalanches in paths C1 and C2 are often accompanied by large forest removal, such as in the 1960s and after 2009 according to archival documents and reveal the intense and destructive nature of snow avalanches in these paths. Paradoxically, the recurrence intervals calculated on path C1 (24 years over the period 1961-2009) and C2 (23 years over the period 1894-2009) are much lower than those calculated for paths E1 and E2. This paradox can neither be explained by path characteristics nor by the vegetation structure that could plead for a higher frequency of snow avalanches on paths C1 and C2. By contrast, we can reasonably hypothesize that they result from a gap in the dendrogeomorphic approach. More explicitly, it is likely that the periodic destruction of the forest stands by high-magnitude snow avalanches, comparable to those observed in 1962 or 2009, jointly limits the length of the reconstruction as well as the number of the reconstructed events (Corona et al., 2012). In addition, despite the presence of multi-century-old larch trees along the outer margins of both paths, no

avalanches could be reconstructed prior to the end of the 19th century, thus suggesting that the lateral extents of snow avalanches during the Little Ice Age did not exceed those of the 20th century.

On the contrary, on paths E1 and E2, the reconstructions derived from tree-ring analyses span longer periods (1791-2016 and 1809-1998, respectively), and exceed those derived for paths C1 and C2 by more than one century. Comparable decadal avalanche recurrence intervals, 2.5 times higher than on paths C1/C2, are reconstructed on paths E1/E2. We assume that the intensity of past avalanche events has been more moderate. This assumption is supported by a vast body of evidence such as (1) the lower altitude of vegetated release areas, (2) higher forest coverage, (3) the output of the RAMMS simulations, (4) the presence of older trees, (5) the diachronic analysis of aerials photographs showing only limited changes in forest cover, and (6) more heterogeneous runout distances with 29, 46, and 25% of the reconstructed event reaching the upper, medium, and lower sampling transects, respectively.

These results have strong implications for dendrogeomorphic studies. Indeed, to evidence the potential impacts of global warming on snow avalanches, tree-ring reconstructions aim at investigating snow avalanche–climate linkages (Casteller et al., 2011; Decaulne et al., 2014; Dubé et al., 2004; Gądek et al., 2017; Germain et al., 2009, 2005; Hebertson and Jenkins, 2003; Martin and Germain, 2017, 2016; Muntán et al., 2009; Schläppy et al., 2016; Voiculescu et al., 2016) and at comparing current activity with colder periods such as the Little Ice Age (see e.g., Ballesteros-Cánovas et al., 2018; Corona et al., 2013; Giacona et al., 2018). These studies generally focus on long-lived stands and should rely on reconstructions that are as complete and continuous as possible. In this context, our study confirms that a careful selection of avalanche paths is a very critical prerequisite as it conditions both the length and the reliability of the reconstructions. In detail, it shows the great potential of forested slopes affected by snow avalanches of low to medium magnitudes, as they have the best boundary conditions to yield comprehensive, long-range reconstructions that can then be used for the detection of climate-driven trends or shifts. Although we are aware that our approach does not cover the entire avalanche regime (i.e. from very small to extremely large events), these results are all the more interesting as avalanche activity on these paths is more susceptible to be strongly affected by global warming as (1) warmer winter temperatures and decreasing days with a minimum snow depth required for avalanches will probably further reduce the importance of avalanche disturbances in forested terrain in the future (Castebrunet et al., 2014) and (2) warmer

temperature during the growing season will probably further facilitate forest expansion and productivity (Bebi et al., 2009) at these sites. One should yet keep in mind that these recommendations are strictly focused on comprehensiveness of all avalanches, regardless of whether they represent a hazard or not, and that the time-consuming sampling methodology presented here, may not be necessary or appropriate for locations where the priority is on identifying the largest magnitude, most hazardous snow avalanches that cause the greatest impacts to people and infrastructure.

6. Conclusions

In this study, a dendrogeomorphic approach has been used to reconstruct past avalanche activity on four contiguous paths located in the upper Guil valley (Queyras massif, French Alps), and characterized by different structures and forest covers. In total, 306 *Larix decidua* Mill. trees were sampled along three altitudinal transects to reconstruct 52 avalanche events. Despite the fact that several limitations may persist in terms of the arbitrary thresholds chosen for the detection of events and the exclusion of noise from reconstructions, our results show very different avalanche dynamics in different avalanche couloirs of the same slope. Unsurprisingly, on paths C1 and C2, characterized by high-altitude release areas that are only covered by shrubby vegetation, high-magnitude events reach the lower transect and cause damage to the forest stand. By contrast, on paths E1 and E2, a forest covers up to the release areas limits the intensity and the spatial extent of past events. More interestingly, the frequency of events reconstructed on the latter paths is 2.5 times higher, reconstructions cover a longer time span and the convergence rate with events listed in the EPA archive attests clearly to the reliability of the reconstructed avalanche history. These results have particularly important implications for avalanche reconstructions aiming at deciphering avalanche activity fluctuations in the current context of global warming. They suggest that a careful selection of the couloirs is essential and that a priority should be given to forested paths since (i) they allow for exhaustive and (ii) reliable reconstructions over (iii) long periods of time.

CHAPITRE 4

Non-stationarities induced by land-cover changes in dendrogeomorphic reconstructions of snow avalanche activity

Non-stationarities induced by land-cover changes in dendrogeomorphic reconstructions of snow avalanche activity: Insights from the Queyras massif (French Alps)

Ce chapitre est en totalité constitué de l'article soumis dans la revue : *Anthropocene.*

Les résultats présentés dans ce chapitre sont basés sur les données dendrogéomorphologiques récoltées dans le cadre du travail d'étude et de recherches réalisé par R. Mainieri (2015). Celles-ci ont ensuite été complétées avec 605 nouveaux individus échantillonnés (4 couloirs supplémentaires) et l'ensemble des résultats ont été recalculés et réinterprétés. L'article a été rédigé sur la base des nouveaux résultats obtenus.

Co-auteurs et affliations :

Robin Mainieri[1], **Adrien Favillier**[2], Jérôme Lopez-Saez[3,4], Nicolas Eckert[5], Taline Zgheib[5], Pauline Morel[1,5], Mélanie Saulnier[6], Jean-Luc Peiry[7], Markus Stoffel[3,4,8], Christophe Corona[2]

1. University Grenoble Alpes, IRSTEA, UR LESSEM, 2 rue de la Papeterie-BP76, F-38402 Saint-Martin-d'Hères, France.
2. Université Clermont Auvergne, CNRS, Université de Limoges, GEOLAB, F-63000 Clermont-Ferrand, France.
3. University of Geneva - Institute for Environmental Sciences, Climatic Change and Climate Impacts, 66 Boulevard Carl-Vogt –CH-1205 Geneva, Switzerland.
4. Dendrolab.ch, Department of Earth Sciences, University of Geneva, rue des Maraîchers 13, CH-1205 Geneva, Switzerland.
5. Faculty of Forestry and Wood Sciences, Czech University of Life Sciences, Kamýcká 129, 16521 Prague, Czech Republic.
6. University Grenoble Alpes, IRSTEA, UR ETNA, 2 rue de la Papeterie-BP76, F-38402 Saint-Martin-d'Hères, France.
7. CNRS, UMI3189, "Environnement, Santé, Sociétés", Faculté de Médecine, UCAD, BP 5005, DAKAR-FANN, Sénégal.
8. Department F.-A. Forel for Environmental and Aquatic Sciences, University of Geneva, 66 Boulevard Carl-Vogt, CH-1205 Geneva, Switzerland.

Remerciements et financement

The authors wish to address special thanks to Michaël Deschâtres for his assistance in the field. This work was initiated with the support of the Irstea grant DENDROAVAL (Premex project) and further supported by Université Grenoble Alpes ("RARETES", avalanche risk as revealer of long-range interactions between environment and society, AGIR-PEPS 2016 program); and the French government IDEX-ISITE initiative 16-IDEX-0001 (CAP 20-25). Irstea is a member of Labex OSUG@2020.

Abstract

Dendrogeomorphic analyses typically provide long and continuous chronologies of mass movements and can thus contribute to the detection of trends potentially related to climate change. However, the non-stationarities found in tree-ring based chronologies of mass movements may also be related to socio-environmental changes. In this paper, growth disturbances in tree-ring series were used to reconstruct snow avalanche events for 6 contiguous paths located in the Grand Bois de Souliers slope (Queyras massif, French Alps) with the aim to detect and illustrate such confounding effects and to identify their origin. The resulting reconstruction covers the period 1750-2016 and evidences two clearly different trends: on the three southern avalanche paths, a sharp increase in the frequency of reconstructed events is observed since the 1970s. The distribution of tree ages, in combination with old topographic maps, allows an attribution of this non-stationarity to the destruction of a large part of the forest stand in the 1910-20s, presumably related to a devastating avalanche event. This extreme event induced a sudden change in the capability of newly colonizing trees to yield dendrogeomorphic records as information on previous or subsequent events has been removed. By contrast, on the three northern paths, snow avalanche activity is truly characterized by a strong reduction since the 1930s related to the progressive afforestation of the paths since the mid-18th century and to the colonization of the release areas since World War 2. Even if we cannot rule out the possibility that global warming may have played a certain, yet likely minor, role in the evolution of these avalanche-forest ecosystem, we conclude that the contrasted evolutions observed between the avalanche paths can, above all, be explained by socio-environmental factors (e.g., forest and grazing management) during the 18th century that have gained in importance by the rural exodus and the abatement of pastoral practices during the 20th century. In that sense, our results evidence quite clearly the crucial need for future studies aimed at detecting changes in mass-movement activity from tree-ring analyses to systematically interpret trends in activity considering interrelations between forest evolution, global warming, social practices and process activity itself.

Keywords: Snow avalanches, tree-ring analysis, land cover changes, French Alps.

Résumé

La dendrogéomorphologie permet de reconstruire des chronologies longues et continues des mouvements de masse et contribuent ainsi à la détection des tendances potentiellement liées au changement climatique. Cependant, les non-stationnarités observées dans les chronologies reconstruites peuvent également être liées à des changements socio-environnementaux. Dans cet article, les événements d'avalanches de six couloirs d'avalanche contigus du versant du Grand Bois de Souliers (massif du Queyras, Alpes françaises) ont été reconstruits afin de détecter, d'illustrer et d'identifier l'origine des non-stationnarités. La reconstruction proposée couvre la période 1750–2016 et met en évidence deux tendances très différentes : sur les trois couloirs d'avalanches les plus au sud, une forte augmentation de la fréquence des événements reconstruits est observée depuis les années 1970. La structure d'âge de la forêt et les documents topographiques anciens suggèrent que cette tendance est liée à la destruction d'une grande partie du peuplement forestier dans les années 1910-2020, vraisemblablement à la suite d'une avalanche dévastatrice. Cet événement extrême est à l'origine d'un changement soudain dans la capacité des arbres à enregistrer les événements d'avalanches en supprimant les indices précédents ou en empêchant l'enregistrement des événements suivant en perturbant durablement la croissance des arbres survivants. A l'opposé, sur les trois couloirs les plus au nord, l'activité des avalanches diminue véritablement depuis les années 1930 à la suite du boisement progressif des couloirs d'avalanches depuis le milieu du 18ème siècle et à la colonisation des zones de départ depuis la Seconde Guerre mondiale. Même si l'on ne peut pas exclure le rôle certain, mais probablement mineur, du réchauffement climatique dans l'évolution de ces écosystèmes de forêt exposés aux avalanches, nous concluons que les évolutions contrastées observées entre les couloirs s'expliquent principalement par des facteurs socio-environnementaux (par exemple, la gestion forestière et pastorale) au 18ème siècle qui ont gagné en importance avec l'abandon des pratiques agro-sylvo-pastorales durant le 20ème siècle. En ce sens, nos résultats soulignent le besoin crucial d'études visant à détecter les changements dans l'activité des mouvements de masse, issue d'une approche dendrogéomorphologique, pour interpréter systématiquement les tendances de l'activité en tenant compte des interrelations entre l'évolution des forêts, le réchauffement climatique, l'activité humaine et l'activité des processus eux-mêmes.

Mots-clefs : avalanches ; dendrogéomorphologie ; changements d'occupation du sol ; Alpes françaises

1. Introduction

Climate warming in Europe has been marked since the end of the Little Ice Age (or LIA) around ~1850; this trend has accelerated more markedly since ~1985 (IPCC, 2013). High mountain environments experience an even stronger response to climate change with even faster average warming as compared to the global mean (Mountain Research Initiative EDW Working Group et al., 2015). This evolution has resulted in rapid changes in the cryosphere (Beniston et al., 2018) and related changes in hydro-geomorphic process activity (Stoffel and Huggel, 2012). As a result of the ongoing warming, available *in situ* snow depth data indicate an elevation-dependent decreasing trend in snow amounts, snow cover duration and snow water equivalent in the Alps (e.g. Bormann et al., 2018; Falarz, 2004; Laternser and Schneebeli, 2003; Marty et al., 2017; Morán-Tejeda et al., 2013). At the same time, many mountain regions across Europe have been affected by the abandonment of traditional farming systems since the mid-19th century, and even more so after World War II. The abatement of traditional farming has favored grassland abandonment, subsequent forest encroachment (Gellrich et al., 2007; O'Rourke, 2006) and the progressive disappearance of mosaics of landscape features reflecting traditional mixed farming management (MacDonald et al., 2000).

Changes in snow cover characteristics are expected to induce changes in spontaneous avalanche activity (Castebrunet et al., 2012; Stoffel and Corona, 2018) including changes in friction and flow regime (Naaim et al., 2013; Köhler et al., 2018). Tree-ring and historical archives are used to infer longer-term changes of avalanche activity (Corona et al., 2013; Giacona et al., 2017), and to possibly detect the impacts of climate change on snow avalanche activity. In this regard, Ballesteros-Cánovas et al. (2018) reported increased avalanche activity on some slopes of the Western Indian Himalaya over the past decades and related the changes in process behavior to the increased frequency of wet-snow conditions. In the European Alps, past changes in avalanche numbers and runout distance as well as avalanche activity in forested areas were demonstrated to be negatively correlated with temperature changes and positively correlated with snow depth changes (Eckert et al. 2013, Teich et al., 2012). These studies also suggest that avalanche mass and run-out distance have decreased over past decades, with a decrease of avalanches with a powder part since the 1980s, a decrease of avalanche numbers below 2000 m, but an increase of snow avalanches at higher elevations (Eckert et al., 2013; Lavigne et al., 2015; Gadek et al., 2017). At the same time, a positive trend in the proportion of avalanches

involving wet snow has been shown over the last decades and for the months of December through to February (Pielmeier et al., 2013; Naaim et al., 2016).

Similarly, changes in traditional agricultural systems are susceptible to impact avalanche activity as they can favor passive colonization of release areas with shrubs and trees, with potentially marked consequences on avalanche frequency and runout distances. Yet, to date, the impact of land abandonment and marginalization has been poorly considered with respect to mass-movement activity, with the exception of García-Hernández et al. (2017) who noticed that passive reforestation has been the main factor influencing the evolution of avalanche damage over the last fifty years in the Spanish Pyrenees. Similarly, Giacona et al. (2018) reported that progressive land abandonment and decreased anthropogenic pressure have reduced the exposure of properties (high-altitude farms in particular) to avalanche risk significantly in the Vosges massif.

The lack of long-term studies is usually attributed to the scarcity of continuous records of past avalanche activity (see e.g. Corona et al., 2012). On wooded paths, dendrogeomorphology (Alestalo, 1971) can be used to identify and date growth disturbances in ring width series and to provide, at least theoretically, continuous, annually resolved snow avalanche reconstructions to complement historical sources. Dendrogeomorphic approaches have been applied repeatedly over the last decades in numerous mountainous regions worldwide to reconstruct multi-decadal to multi-centennial chronologies of snow avalanche events (see Favillier et al., 2017 – chapter 1 – for a recent review). Yet, dendrogeomorphic reconstructions can be affected by non-stationarities that will then have an impact on the reconstructed time series and trends therein. For this reason, Corona et al. (2012) proposed to adjust thresholds aimed at detecting past process activity in tree-ring records so as to account for the reduced frequency of reconstructed events related to the decreasing number of living trees back in time. Similarly, Favillier et al. (2018 – chapter 2) attributed the overrepresentation of avalanche events in their reconstructions since the mid-20th century to the difficulty to retrieve ancient hidden scars (Stoffel and Perret, 2006), invisible on the stem surface, thus rendering the determination of suitable sampling positions a difficult task (Trappmann and Stoffel, 2013). Finally, age- and diameter-dependent sensitivities of trees observed in hydro-geomorphic processes are yet another factor to be considered (Tichavský and Šilhán, 2016), and thus represent a third source of non-stationarity in tree-ring reconstructions.

In this study, a dendrogeomorphic approach has been deployed on a slope of the upper Guil valley (Chateau-Ville-Vieille municipality, French Alps) in the Queyras massif

with the aim to (i) evidence and (ii) quantify potential non-stationarities in snow avalanche reconstructions as well as to (iii) disentangle, if possible, real fluctuations in avalanche activity from trends inherent to tree-ring approaches. The slope was selected as it is composed of six different avalanche paths with similar morphology (altitude of the starting zone and length), but differences in terms of forest cover (i.e. densely forested paths upstream and corridors characterized by a marked transverse zonation downstream), thus allowing comparison between reconstructions. The evolution of the forest stand within each path is documented with a diachronic analysis of historical maps, aerial photographs and tree ages as estimated from the sampled trees. Comparison of the different sources of information this enables discussion of potential non-stationarities in the tree-ring reconstruction induced by (i) forest recolonization after destructive avalanche events or (ii) afforestation related to recent socio-environmental changes at the study site. We demonstrate that a more careful inclusion and consideration of socio-environmental changes – be they related to the pastoral decline or rural exodus – so as to better understand and explain ongoing trends in snow avalanche activity.

2. Study site

The site under investigation is on the territory of Château-Ville-Vieille (Queyras massif, French Alps), 1.5 km to the northwest of a hamlet called Souliers. The study site is locally known as Grand Bois (44° 47'N, 6° 46'E, Fig. 4.1) and consists of a west-facing slope (135 ha) extends from the Crépaud ridge (2580 m asl) to the Souliers torrent (1900 m asl). Naturally triggered snow avalanches are common on the slope and released from several starting zones located between 2300 and 2580 asl. We delineated six avalanches paths (S1-S4, A1-A2) based on the mapping of erosional and depositional avalanche features in the field as well as on the interpretation of aerial photographs. The morphometric characteristics of each path – summarized in Table 4.1 – were derived from a 5-m Digital Elevation Model (DEM) extracted from the IGN RGE ALTI® database. With respect to land cover, a north-south gradient of afforestation is observed on the selected paths, meaning that the forest cover increases from 31.2% at A2 to 65.1% at S2. Characteristic transverse vegetation patterns – as defined by Malanson and Butler (1984)– are observed across paths S3-S4 and A1-A2: the inner zone of these paths is colonized by dense shrubs with flexible stems, such as European rowan (*Sorbus aucuparia* L.) or common juniper (*Juniperus comunis*); in the outer zones, European larch (*Larix decidua* Mill.) is dominant. Understory vegetation is mostly composed by rhododendron (*Rhododendron ferrugineum*

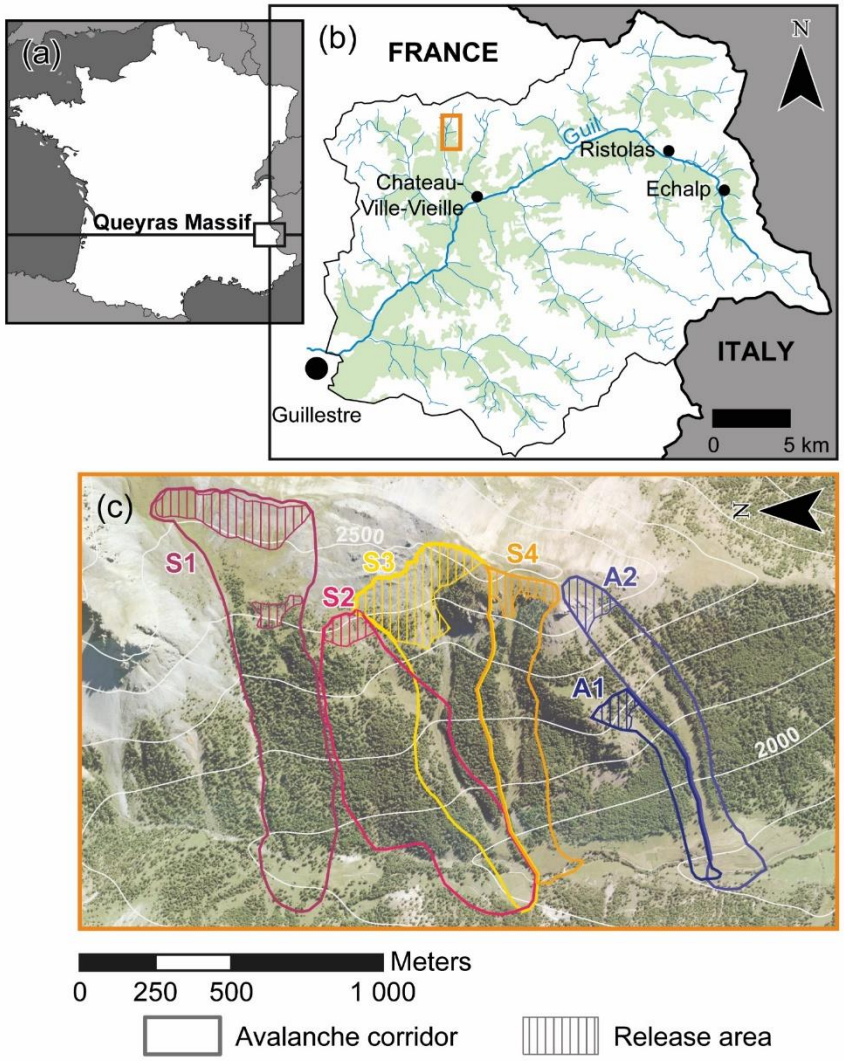

Figure 4.1 – Location of the studied paths: (a) overview of the Queyras massif (French Alps), (b) detailed view of the Chateau-Ville-Vieille locality within the Queyras massif and the study site (c) detailed view of the six avalanche paths delineated on the Grand Bois de Souliers slope.

Table 4.1 – Main characteristics of the studied avalanche paths. Numerical values correspond to the areas delineated in Figure 4.1c and derived from crossed a 5-m DEM.

	Avalanche path						Release area		
Path	Aspect	Length (m)	Mean width (m)	Area (ha)	Mean slope (°)	Forest cover in 2015 (%)	Release altitude (m)	Mean slope (°)	Area (ha)
S1	W	1231	250	39.1	22.4	45.92	2390-2570	28.1	7.9
S2	W	990	350	35.6	24.8	65.13	2350-2420	26.7	1.5
S3	W	1107	250	27.6	28	43.53	2300-2515	31.1	7.5
S4	W	950	180	16.5	28.8	55.49	2380-2490	29.6	2.1
A1	W-S	695	92	6.02	27	50.33	2150-2250	34.4	1.2
A2	W-S	1105	160	15.6	28.4	31.20	2375-2490	34.8	2

L.) and bilberries (*Vaccinium myrtillus* L.). By contrast, transverse vegetation patterns were absent at A1-A2 where the occurrence of past avalanches was revealed mainly by tree stand physiognomy (i.e. candelabra-shaped or broken-crown trees). According to Saulnier (2012), the Grand Bois de Souliers slope has been used intensively for pastoralism since the mid-19th century. Despite a sharp decline in pastoral activities, the forest was used over large parts of the 20th century and until pastoralism disappeared in 1971 (Saulnier et al., 2015).

At the meteorological station of Saint-Véran (44°41'N, 6°52'E, 2039 m asl), located 12 km southeast of Grand Bois, mean annual precipitation and temperature are 709.6 mm and 5.3°C (1981–2010), with a winter (Dec-Apr) mean temperature of -0.2°C and winter precipitation totaling 237 mm on average. Due to its remoteness and the lack of objects at risk, the northernmost portion (S1-S4) of the Grand Bois de Souliers slope has neither been included in the EPA (Enquête Permanente sur les Avalanches; Bourova et al., 2016; Mougin, 1922) database nor mapped in the CLPA (Carte de Localisation des Phénomènes Avalancheux; Bonnefoy et al., 2010). Conversely, in the case of paths A1-A2, CLPA maps exist for two events: one in 1972 covering the Souliers road and torrent over a distance of 80 m. The second record is from December 2008 when a powder-snow avalanche destroyed 50 m^3 of wood. The 2008 event occurred during an intense avalanche cycle that affected the Queyras between December 14 and December 17, 2008 (Eckert et al., 2010c). It is attributed to southerly atmospheric fluxes that progressively evolved into an easterly return causing important snowfall for three days. Cold temperatures and drifting snow aggravated the situation and caused the occurrence of 209 avalanches over a period of 5 days according to the EPA avalanche database. Some avalanches had very long runout distances and exceeded the historical limits recorded in the CLPA (Gaucher et al., 2009).

3. Material and methods

3.1. Sampling strategy, dating and classification of growth disturbances

A total of 884 increment cores was sampled in summers 2011 (S1-S2) and 2016 (S3-S4, A1-A2) from 825 European larch (*Larix decidua* Mill.) trees growing in the 6 avalanche paths. In the field, tree-ring samples were collected following the recommendations of Šilhán and Stoffel (2015) and Stoffel and Corona (2014) with respect to the number and the spatial distribution of sampled trees as well as to the balance between older and younger trees. The position of each tree was recorded with a 1-m precision GPS device and a series of data was recorded for each tree including its diameter at breast height

(DBH) and the the nature of the disturbance (type, height). In the lab, samples were processed following standard dendrochronological procedures (Stoffel and Bollschweiler, 2008). Growth disturbances were identified in the tree-ring series and cross-dated against two local reference chronologies (Corona et al., 2012; Saulnier et al., 2019). Injuries and callus tissues (CT) (Stoffel et al., 2010), tangential rows of traumatic resin ducts (TRD) (Schneuwly et al., 2009b, 2009a), compression wood (CW) and sharp growth suppression (GS; Kogelnig-Mayer et al., 2013) were considered the most reliable indicators of past avalanche activity. Individual series of disturbed trees were cross-dated against the Souliers and Echalp reference chronologies (Corona et al., 2012; Saulnier et al., 2019) with the aim to correct the tree-ring records of affected trees in case of missing or false tree rings. Intensities were then assigned to GDs in order to emphasize features that are obviously associated with avalanche activity (Stoffel et al., 2013). GDs were classified based on their visual aspect according to the classification proposed by Kogelnig-Mayer et al. (2011): weak (intensity class 1), medium (intensity class 2), strong (intensity class 3) reactions and clear evidence of injuries (intensity class 4).

3.2. Detection of past avalanche events in growth disturbance series

To detect past snow avalanche events in GD series, we employed the four-step procedure proposed by Favillier et al. (2017); please refer to Figure 4.2 for details. The avalanche reconstruction was restricted to the period for which at least 10 trees were alive. In addition, we adjusted the minimum number of GDs and Shroder's It index (Shroder, 1978) in a way to account for changes in sample depth (Butler and Sawyer, 2008; Corona et al., 2012). Definition of these thresholds depends on the nature of the avalanche path and the type of vegetation, and sometimes needs to be adjusted to the study site. For this reason, we employed thresholds that were less rigid than those proposed by Favillier et al. (2017) so as to (1) to maximize the frequency of reconstructed events while still (2) taking sufficient care not to include noise in the reconstruction.

In a second step (Fig. 4.2), we identified years with larch budmoth (LBM) outbreaks and climatic extremes (cold/dry years) as they could potentially bias the avalanche reconstruction. LBM outbreak years at the study site have been recorded by Saulnier et al. (2017). Extremely cold and dry summers were retrieved from the homogenized temperature (1780-2014) and precipitation (1800-2002) records from the HISTALP grid points located nearest to the study site (Chimani et al., 2013; Efthymiadis et al., 2006). The list of LBM events and extreme summers found at the study site is shown in Table 4.2. In case that

potential avalanche events detected in step 1 coincide with LBM years or climatic extremes, tree-ring records were analysed again to avoid erroneous reconstruction of snow avalanches. In these years, abrupt growth suppressions were excluded systematically from the GD record. In addition, a minimum threshold of 3 GDs was used to discriminate avalanche from non-avalanche events (Fig. 4.2). In a third step, levels of confidence were assigned to each avalanche event based on the weighted index factor (Wit) proposed by Kogelnig-Mayer et al. (2011) accounting for GD type and intensity as follows: very high (vHLC, Wit > 0.3), high (HLC, 0.3 > Wit > 0.2) and medium (MLC, Wit < 0.2) (Favillier et al., 2017). To increase the stringency of the approach further, each event detected during step 1 and events coinciding with LBM or climatic events in step 2 were systematically rated with a low level of confidence (LLC) (Fig. 4.2). In a last step, avalanche events and associated GDs were mapped using the ArcGIS 10.2.1 Time Slider (ESRI, 2013; Kennedy, 2013). On the basis of the position of impacted trees, avalanches with a length <600 m, 600-800m, 800-1000m, 1000-1200m, 1200-1400m, and <1400 m were categorized as eXtra-Small (XS), Small (S), Medium (M), Large (L), eXtra-Large (XL), eXtra- eXtra-Large (XXL) avalanches, respectively. All the thresholds employed in the four-step procedure with respect to the minimal number of GDs, their intensity and the minimum percentage of disturbed trees are summarized in Figure 4.2. At the scale of individual paths,

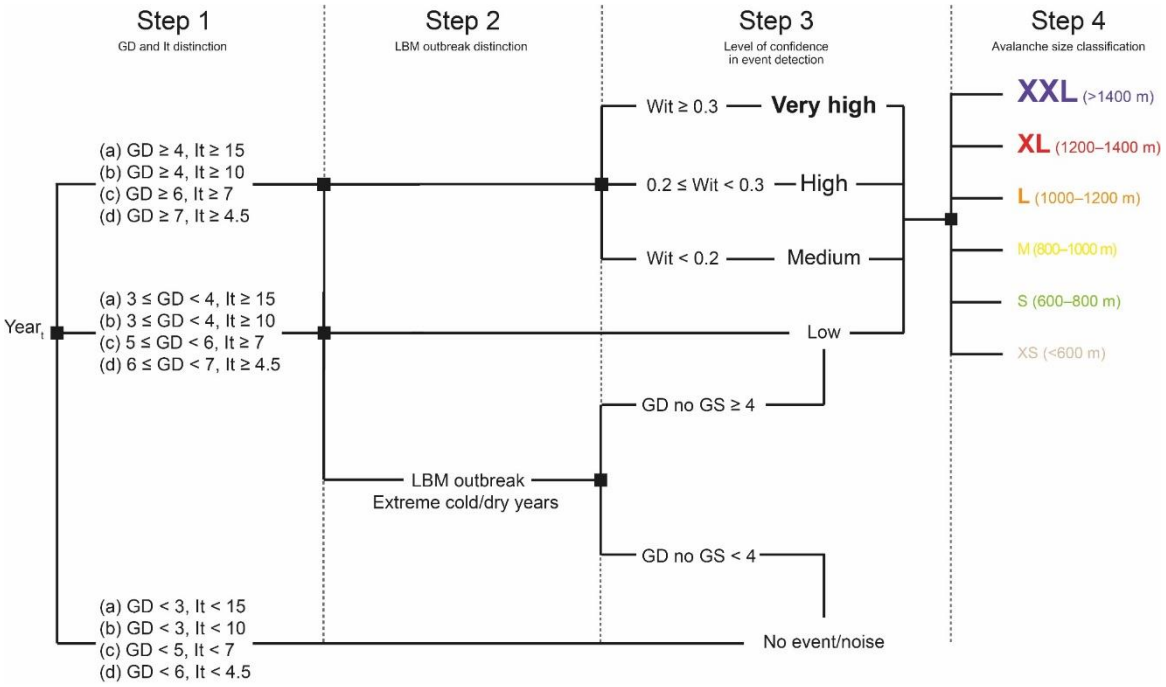

Figure 4.2 – Synoptic diagram of the 4-step approach used for the detection of avalanche events in tree-ring series, adapted from Favillier et al. (2017). Growth disturbance (GD) and intensity (It) thresholds vary according to the sample size: (a) <20 trees; (b) 20 to 49 trees; (c) 50 to 99 trees; and (d) >= 100 trees.

Table 4.2 – Larch budmoth events and pointer years (according to Saulnier et al., 2017), as well as extremely cold and dry summers (Efthymiadis et al., 2006; Saulnier et al., 2011) in the French Alps. All these years have been carefully analyzed due to probable interferences between snow avalanche damage in trees with LBM and/or climatic signals that may induce growth reductions comparable to those observed after snow avalanches in the tree-ring series.

2003**	*1926*	*1848*	*1801*
1997	*1925*	**1847**	**1795**
1996	*1918*	1843*	**1794**
1991**	1912*	1841*	*1779*
1980	**1910**	**1830**	*1766*
1972	*1909**	*1821**	*1758*
1963	1902	*1820*	*1750*
1950**	**1901**	1816*	
1947**	1888*	*1813**	
1945	*1867*	**1812**	
1937	1860*	*1803*	
1936	**1857**	**1802****	

LBM-outbreak year, Extreme cold * and dry ** summers

the annual probability for an avalanche event was computed by dividing the number of reconstructed events by the period covered by the reconstruction.

3.3. Documentation of forest dynamics

Spatio-temporal dynamics of forest stands are typically analyzed with time series of cartographic documents (cadastral, topographic maps, aerial photographs; Houghton et al., 2012). In France, the oldest map yielding data on evolution is the Napoleonic cadastral map from the early 19th century. This map has been created for taxation purposes (Eynard-Machet, 1993) and therefore offers a precise and detailed record of land ownership and use at the level of allotments (Coughlan, 2013). At Souliers, the Napoleonic cadastral map is dated to 1827 and is used here as a baseline for the documentation of forest cover changes. In addition, we analyzed pictures from 5 aerial flight campaigns from the French National Geographic Institute (IGN; <1:30,000) to detect forest changes, namely in 1945, 1971, 1981, 2003 and 2015. Image interpretation was realized with standard photographic keys (i.e., tone, texture, pattern, shape, and size) and supplemented with secondary information on geomorphology, historical vegetation maps, and ground truth data. Based on these physiographic constraints, visual interpretation and digitalization (Kennedy, 2013) was realized at the path scale to generate maps of forest cover patterns for each of the dates, allowing quantification of forest cover changes between 1945 and 2015 for each path and for 100-m elevation bands using ArcGIS 10.2.1 (ESRI, 2013). In addition, data from 11 aerial flight campaigns with lower-resolution images (>1:30,000) were used to detect evidence of high-magnitude snow avalanches that would have destroyed the forested stands partially between 1945 and 2016.

Forest dynamics were also assessed for each path through an estimation of the age structure of the stands. This was done by approximating the number of tree rings in each of the selected trees. Whenever the pith was not present on a core, we estimated the number of missing rings using the "*Estimate Distance and Rings to Pith*" function of the coo-recorder 9.0 software (Larsson, 2016). In this study, sampling positions ranged from 0.2 to 1.5 m above ground level. To compensate for the time elapsed from germination until a tree reaches sampling height, we added an age correction factor (Stoffel et al., 2010). Age at sampling height was estimated in comparison to nearby *L. decidua* trees with according heights, for which the age could be easily determined by counting branch whorls (Sorg et al., 2010).

4. Results

4.1. Evolution of the forest cover

Trees sampled in the six paths were, on average, 186.1±126 years old. The oldest tree sampled in path S2, was 628 years old whereas the youngest tree (S3) reached sample height in 2010. Amongst the individuals sampled on the Grand Bois de Souliers slope, 40.6% of the sampled trees were less than 100 years old and 26.7% had between 200 and 300 growth rings at sampling height. One-fifth of all trees was older than 300 years (19.2%) and 8.3% of the sampled trees were at least 400-

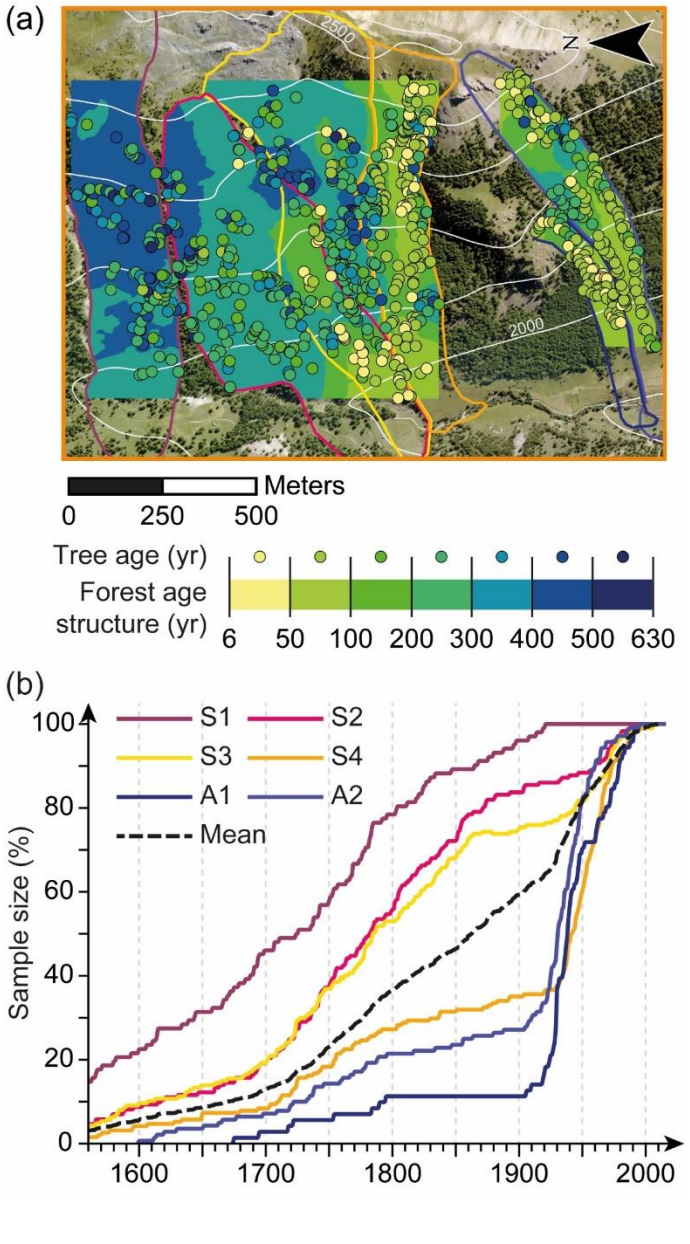

Figure 4.3 – Age structure of the forest stand growing at Grand Bois de Souliers: (a) spatial distribution of individual tree and interpolated stand ages; (b) evolution of the sample size at the six avalanche paths. The black line represents the mean sample size evolution.

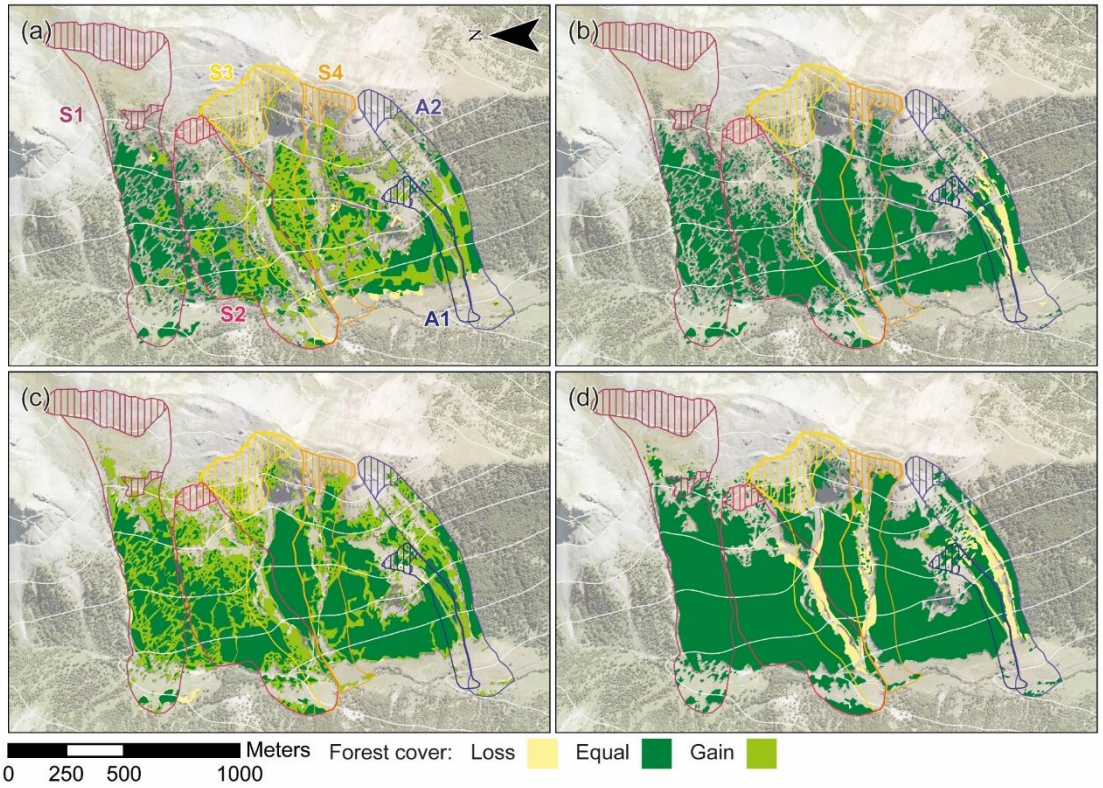

Figure 4.4 – Diachronic evolution of the forest stands at Grand Bois de Souliers between 1945 and 2015: (a) 1945-1971, (b) 1971-1981, (c) 1981-2003, and (d) 2003-2015.

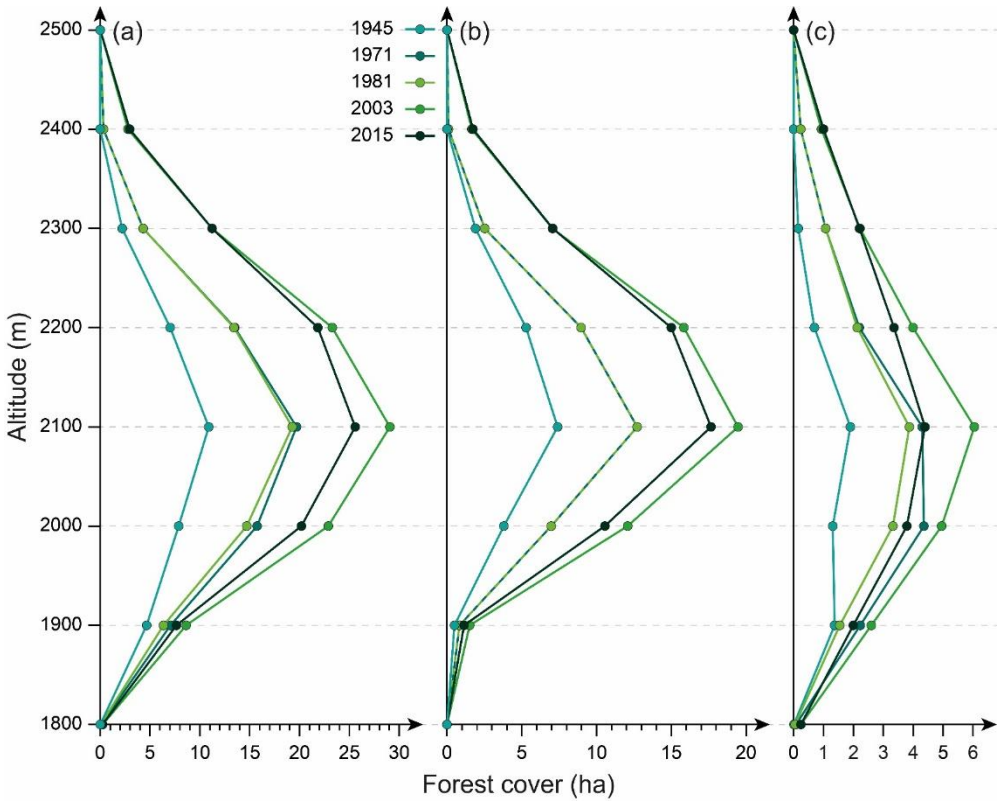

Figure 4.5 – Evolution of the surfaces occupied by larch stands, computed for 100-m elevation bands, (a) at Grand Bois de Souliers; within (b) avalanche paths S1-S3; and (c) paths S4, A1 and A2 as delineated in Figure 4.1.

year-old. The spatial distribution of trees shows clear spatial patterns with three homogeneous areas (Fig. 4.3a): (1) an old-growth forest stand mainly composed of >300-year old trees in the northern part of the slope (S1-S2), (2) a cluster (S2-S3) where the distribution of tree ages ranges between 100 and 300 years but does not exceed 100 years at the margins of the main tracks, and (3) several clusters of senescent trees above 2200-2300 m asl.

Tree-ring data also provide valuable information on forest dynamics for the last century (Fig. 4.3a). Tree ages are significantly higher in paths S1 (306±122 yrs), S2 (229±122 yrs) and S3 (225±128 yrs) than in S4, A1 and A2 where tree ages averaged 137±120, 92±70 and 128±97 yrs, respectively. In paths S1-S3, sample depth exceeds 10% after 1620 CE and steadily increased between 1730 and 1860 (Fig. 4.3b). In these three paths, >70% of the sampled trees were present in 1860. Sample size evolved only moderately during the 20th century. By contrast, in paths S4 and A1-A2, sample size evolves moderately from 18.3, 5.5, and 14.3% in 1750 CE to 36.1, 16.9, and 33.6% in 1920, respectively. The number of sampled trees remains <40% before 1920 but sharply increases during the interwar period to exceed 80% after World War II. Here, results suggest a rapid colonization of the central part of the paths between the 1920s and the 1960s.

At the slope scale, historical maps and aerial photographs usefully supplement tree-ring data to document forest evolution since the mid-19th century. At the Grand Bois de Souliers slope, the Napoleonian Cadastral map from 1827 shows a binary landscape with allotments (Getrille and Clos de la Chaussole) between 2100 and 2300 m asl mainly occupied by larch stands, whereas rocks and scree covered with shrubs and herbs take over above 2300 m asl. Landscape changes appears rather limited between 1827 and 1945, but resolution obviously differs between the cadastral map and the aerial photographs. Between 1945 and 1971 (Fig. 4.4), diachronic comparison of aerial pictures reveals rapid forest sprawl, mostly in paths S1-S3, and an increase of forested areas between 2100 and 2300 m asl by 9 ha (+71.1%, Fig. 4.5). In addition, the expansion of young trees on bare areas is clearly visible above 2300 m asl in S1-S3 (+0.72 ha). Between 1981 and 2015, forest colonization was ongoing above 2300 m asl (+9.6 ha), i.e. in a zone where avalanches are usually released. Over the full period covered by aerial pictures (1945–2015), the forested surface has more than doubled at Grand Bois de Souliers (89.7 vs. 32.7 ha or +274.3%).

4.2. Past snow avalanche activity

Comparison of the 16 additional aerial photographs available for the period 1945-2016 allowed retrieving signs of past avalanche events through the identification of avalanche-induced forest damage or avalanche deposits. The events listed in the CLPA for 1972 and 2008 could be delineated precisely by comparing the aerial photographs of 1971–1974 and 2003–2009, respectively. No additional events could be retrieved in the 10 other photographs covering the periods 1945–1948, 1952–1971, 1974–2003, and 2009–2013 (Fig. 4.4).

Analysis of the 825 trees sampled in the six paths allowed identification and dating of 2,460 GDs (1750-2016) with annual resolution. The number and type of GDs identified at the slope and path scales are summarized in Table 4.3. The mean number of GDs per tree is significantly lower in paths S1-S3 (1.85, 2.1, and 1.7 GD.tree^{-1}, respectively) as compared to paths S4, A1-A2 (3.7, 3.8, and 4.8 GD.tree^{-1}, respectively). Figure 4.6 shows types of GDs computed for the time windows 1750-1825, 1826-1900,1901-1950, and 1951-2013 in S1-S3 (Fig. 4.6a) and S4-A1-A2 (Fig. 4.6b). In S1-S3, the mean number of GDs progressively decreased from 39.7 GD.decade^{-1} (n=298 GDs) in 1750-1825 to 26.2 GD.decade^{-1} (n=131 GDs) in 1950-2000. Conversely, in paths S4-A1-A2, it shows a

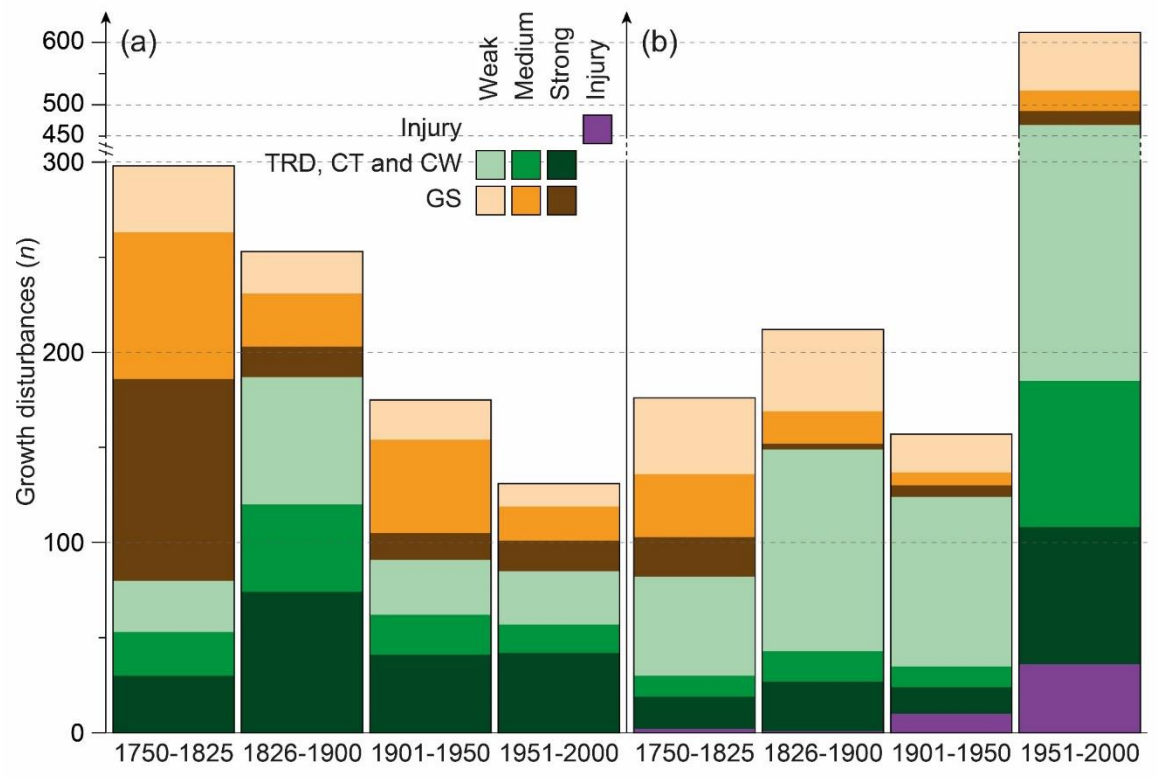

Figure 4.6 – Barplots showing the distributions of GD types and intensities between 1750 and 2000 for paths (a) S1-S3 and (b) S4-A1-A2.

significant increasing trend from 31.4 GD.decade^{-1} (n=176 GDs) in 1750-1825 to 123.2 GD.decade^{-1} (n=616 GDs) in 1950-2000. For all paths, a clear shift is observed in the spectrum of mechanical damage: the percentage of growth suppression in the spectrum of mechanical damage decreased inversely proportional to the percentage of callus tissue, tangential rows of traumatic resin ducts and compression wood. In addition, in paths S4 and A1-A2, the spectrum is characterized by an increasing proportion of injuries during the 19th century. Based on the 4-step procedure, 974 GDs (40%) have been used for the reconstruction of past events. The remaining 60% (n=1460) were considered noise that was not related to snow avalanches and hence excluded from analysis. Amongst the 974 GDs, 314 had intensities of 3 or 4 are thus considered the more robust indicators of snow avalanching.

Dendrogeomorphic analysis allowed the dating of 97 snow avalanches (Fig. 4.7) occurring in 67 different years. Except for path A1 where the number of trees is insufficient to reconstruct avalanches before 1908, the sample depth exceeds the minimal threshold (n=10) for the period 1750-2016. In total, 6, 11, 11, 23, 10, and 36 avalanche events were reconstructed in paths S1, S2, S3, S4, A1 and A2, respectively. The oldest event was dated to 1756 on S2 whereas the most recent avalanche occurred in paths A1-A2 in 2015. Based on possible interferences between avalanche activity, climatic, and LBM signals in the tree-ring record (step 2), and based on the Weighted Index Factor (Wit; step 3, Figs. 4.7-4.8), we assigned very high and high levels of confidence to 28 and 30 events, respectively. By comparison, 22 events with a Wit<0.2, and characterized by a majority of weak and medium GDs, were therefore reconstructed with a LLC. Amongst the 30 potential events that coincide with LBM outbreak episodes or extreme climatic years, 13 were excluded from the reconstruction and 17 were rated with an LLC (Fig. 4.7). At the annual scale, the

Table 4.3 – Intensities of reactions and types of growth disturbances (GD) assessed in the 825 larch trees selected for analysis.

		Mechanical disturbances (*n*) TRD, CT, CW			Growth suppression (*n*)			
Path	**Impact scars (n)**	*strong*	*medium*	*weak*	*strong*	*medium*	*weak*	**Total**
S1	0 (0%)	45 (1.8%)	11 (0.4%)	21 (0.9%)	57 (2.3%)	42 (1.7%)	13 (0.5%)	189 (7.7%)
S2	0 (0%)	70 (2.8%)	48 (2%)	88 (3.6%)	81 (3.3%)	96 (3.9%)	54 (2.2%)	437 (17.8%)
S3	0 (0%)	46 (1.9%)	17 (0.7%)	22 (0.9%)	31 (1.3%)	49 (2%)	26 (1.1%)	191 (7.8%)
S4	48 (2%)	80 (3.3%)	44 (1.8%)	218 (8.9%)	43 (1.7%)	86 (3.5%)	182 (7.4%)	701 (28.5%)
A1	4 (0.2%)	31 (1.3%)	32 (1.3%)	128 (5.2%)	12 (0.5%)	12 (0.5%)	53 (2.2%)	272 (11.1%)
A2	17 (0.7%)	84 (3.4%)	65 (2.6%)	305 (12.4%)	33 (1.3%)	55 (2.2%)	111 (4.5%)	670 (27.2%)
Total	69 (2.8%)	356 (14.5%)	217 (8.8%)	782 (31.8%)	257 (10.4%)	340 (13.8%)	439 (17.8%)	2460 (100%)

highest frequencies of events are observed in the years 1808, 1908, 1933, 1971, 1972, 1984 and 2004 during which snow avalanches were reconstructed in 3 out of 6 paths. Interestingly, the two events mentioned in the CLPA for 1972 and 2008 were retrieved with an LLC in S4-A1-A2 and with a vHLC in S4-A2, respectively.

Considering all reconstructed events, the mean recurrence interval of avalanches at Grand Bois de Souliers is 2.8 years (or 3.6 events per decade) for the period 1750–2016. The recurrence interval is not constant over time but shows a clear decrease from 5.9 years for the periods 1750–1850 and 1851-1950 to 2 years between 1950 and 2015. Maximum decadal frequencies are observed from 1772 to 1793 (9 events), 1804–1810 (8 events), 1825-1837 (7), 1932-1937 (5), 1970-1986 (13), and 1999-2009 (10) (Fig. 4.8). Conversely, the number of reconstructed events decreased drastically between 1838 and 1861 (1), 1884–1900 (1), 1912–1930 (1), 1938–1959 (2), 1964–1969 (0), and 1987–1998 (5) (Fig. 4.8). At the path scale, the frequency of events sharply increased in A1 and A2 since 1970. In these paths, the number of reconstructed events increased from 0 to 10 and from 6 to 18 for the periods 1924-1969 and 1970-2015, respectively. By contrast, no event was retrieved from tree-ring analyses in paths S1 and S2 since 1933 and 1974 whereas only 2 avalanches were reconstructed with LLC in S3 since 1974 (Fig. 4.8). Decadal frequency of events ranged between 0.3 (S1) and 0.68 events.decade^{-1} (S4, A2) for the period 1750-1882 but is very

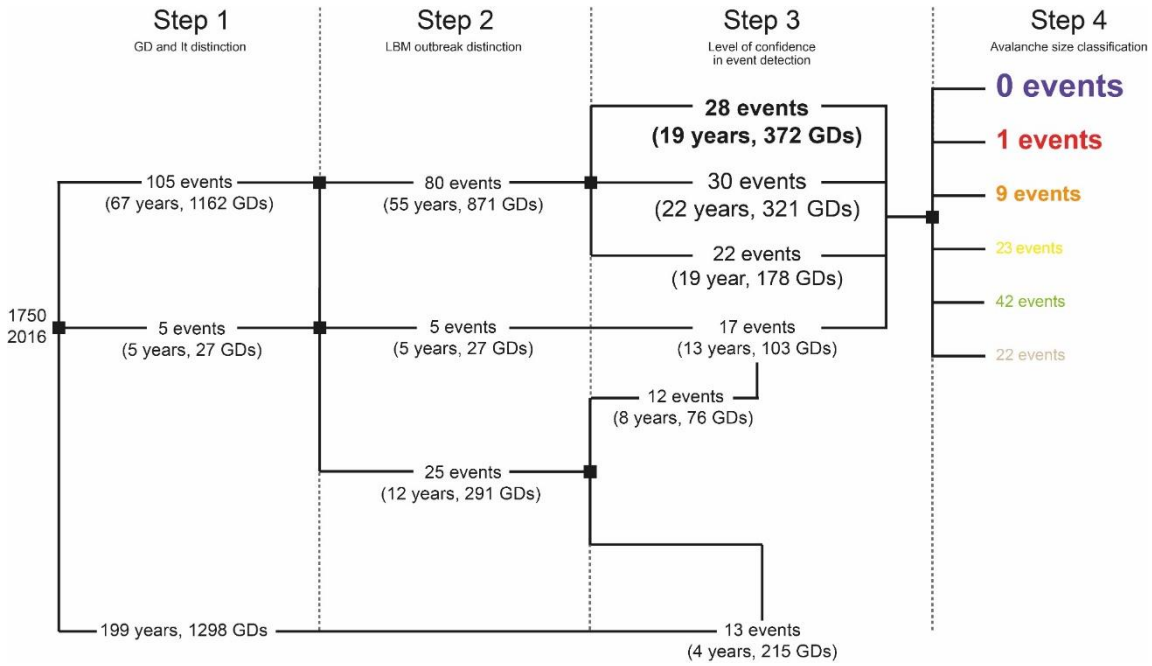

Figure 4.7 – Synoptic diagram showing the characteristics of the reconstructed snow avalanche events and possible interferences with climate or larch budmoth outbreaks, level of confidence, and minimum slide extent.

heterogeneous between paths: while it is <0.2 event.decade^{-1} in paths A1-A2, values exceeds 1 event.decade^{-1} in S4 (1.1) and S2 (2.04) for the period 1883-2015.

5. Discussion

The study we report here employs dendrogeomorphic techniques in six avalanche paths at Grand Bois de Souliers with the aim to discuss interrelations between forests stand dynamic and snow avalanche activity as documented by tree rings. To meet this objective, the detection procedure developed by Favillier et al. (2017 – chapter 1) was used (1) to disentangle snow avalanche signs in tree-ring records from signals induced by climatic or ecological disturbances and (2) to qualify the robustness of our tree-ring based snow avalanche reconstruction. Based on this procedure, 97 snow avalanche events were reconstructed in 67 different avalanche years back to 1750 CE. In parallel, the evolution of the forest cover was quantified with a diachronic analysis of cartographic documents and age estimates of the stand structure and allowed illustration of the afforestation process in

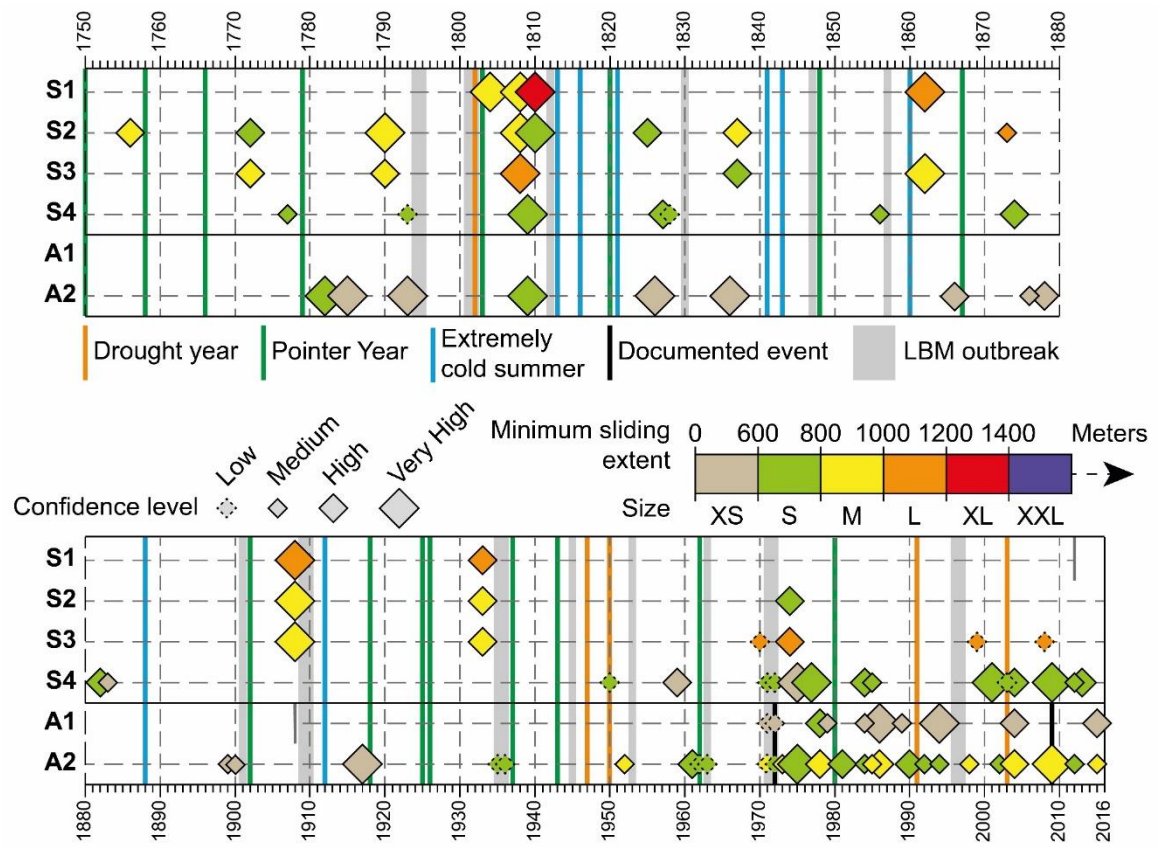

Figure 4.8 – Avalanche events reconstructed for the period 1750–2015 in six paths at Grand Bois de Souliers. Symbol sizes are proportional to the level of confidence. The color range highlights the minimum slide extent determined from the position of impacted trees. Grey bands represent years associated to LBM outbreaks. Vertical lines show snow avalanches documented in chronicles (black), as well as extremely dry (orange) and cold (blue) summers.

the selected paths since the mid-18th century. In detail, our study reveals a strong dichotomy between paths S1, S2, and S3 (Group 1, G1) where the progressive disappearance of snow avalanche activity is observed since the 1930s on one side and paths A1, A2 and to a lesser extent S4 (Group 2, G2) for which the recurrence intervals drastically increased since the 1970s on the other side. This difference is further reinforced by forest cover evolution which gradually increased in paths S1, S2, and S3 since 1750 whereas it showed an abrupt extension only around the 1920s in the other paths.

5.1. Non-stationarity of the dendrogeomorphic reconstruction potential in paths A1, A2 and S4

For the paths of Group 2, we attribute the increase in the avalanche frequency over the last decades to a non-stationarity in the potential of dendrogeomorphic approaches to capture past snow avalanches. As such, this non-stationarity could be related to the underestimation of hidden scars as reported by Stoffel and Perret (2006): As conifers mask scars of past events effectively, the existence and/or position of old scars can often not be detected on the stem surface, rendering determination of suitable sampling positions a difficult task. Older events can thus be missed on increment cores of *L. decidua*, and older trees will tend to yield data on fewer impacts relative to their age (Trappmann and Stoffel, 2013). Secondly, the tipping point observed in the reconstructions of Group2 paths in the 1970s could also be attributed to forest recolonization after an avalanche event destroying large parts of the forest stands, thereby removing evidence of past and subsequent events (e.g. Carrara, 1989, 1979; Corona et al., 2012; Kogelnig-Mayer et al., 2011). Evidence for such an extreme event could not be retrieved from GDs detected between 1880 and 1920 in trees from paths S4, A1 and A2. Yet, its occurrence is supported by the distribution of tree ages in paths A1-A2 and S4 showing a sharp increase in sample depth during the 1930s and signs of forest recolonization on topographic maps between 1896 and 1933 (Fig. 4.9b, c). Based on observations at the site that was cleared by powder-snow avalanche in 2008, *L. decidua* seedlings tend to recolonize avalanche paths at Grand Bois de Souliers within only a few years after a geomorphic event. One may therefore reasonably assume that an avalanche that would have occurred in the early 1910–1920 could have given rise to a new forest stand which would have recovered its "dendrogeomorphic potential" in the 1970s. This assumption and the lag are in line with observations of a sharp increase in avalanche activity as observed in reconstructions realized at Täsch (Swiss Alps; Favillier et al., 2018 – chapter 2). Here the increase in reconstructed avalanche activity in the 1960s was proven

the result of an extreme avalanche event that destroyed a 400×800 m forest strip in 1920. It thus seems reasonable to suggest that up to 50–60 years are required for a forest stand to recover its dendrogeomorphic potential after an extreme event.

5.2. Non-stationarity of the snow avalanche activity related to slope afforestation

In the paths of Group 1, the frequency of GDs and avalanche events detected in the tree-ring series has been shown to decrease since the 1930s. In these three paths, the oldest trees are more than 500 years old and a majority of the trees sampled exceed 200 years. In addition, continuous forest expansion is observed since 1540, and especially during the 18th century. The presence of multi-centennial trees in avalanche paths suggests the absence of extreme events since the mid-16th century as otherwise extreme avalanches would have destroyed the forest stand. Furthermore, evidence for more moderate snow avalanching as compared to Group2 exists via the more limited number of GDs (n=798) identified and dated in the tree-ring series from the 461 trees sampled in this sector and via the absence of injuries (intensity 4 damage). By contrast to Group1, the dendrogeomorphic potential in the paths of Group2 is considered constant over time and reconstructions should thus properly reflect the natural fluctuations of avalanche activity. Yet, the conservation of the forest should not be dissociated from human activity at Souliers. Saulnier (2012) reports that specific silvicultural rules existed since “immemorial times” at Grand Bois de Souliers to maintain the protective function of the forest stand. Interestingly, Roman (1887) and Gadoud (1917) indicate a multiplication of protective regulations between the 13th and 15th centuries in the Queyras massif aimed at preventing forest overexploitation or destruction. The proclamation of these regulations coincides with the age of the oldest trees in paths S1 and S2.

From a perspective of process dynamics, our reconstruction shows a moderate, yet continuous avalanche activity in paths S3 and S2 – and to a lesser extent in S1 – between the mid-18th century to the 1930s that decreased sharply thereafter. This evolution is most likely related to the afforestation of several release areas that is clearly visible through the analysis of aerial photographs since 1945. Indeed, the presence of trees is a decisive factor stabilizing snowpack by (1) increasing terrain roughness (2) intercepting falling snow, (3) modifying radiation and temperature regimes and by (4) reducing near-surface analysis of aerial photographs since 1945. Indeed, the presence of trees is a decisive factor stabilizing

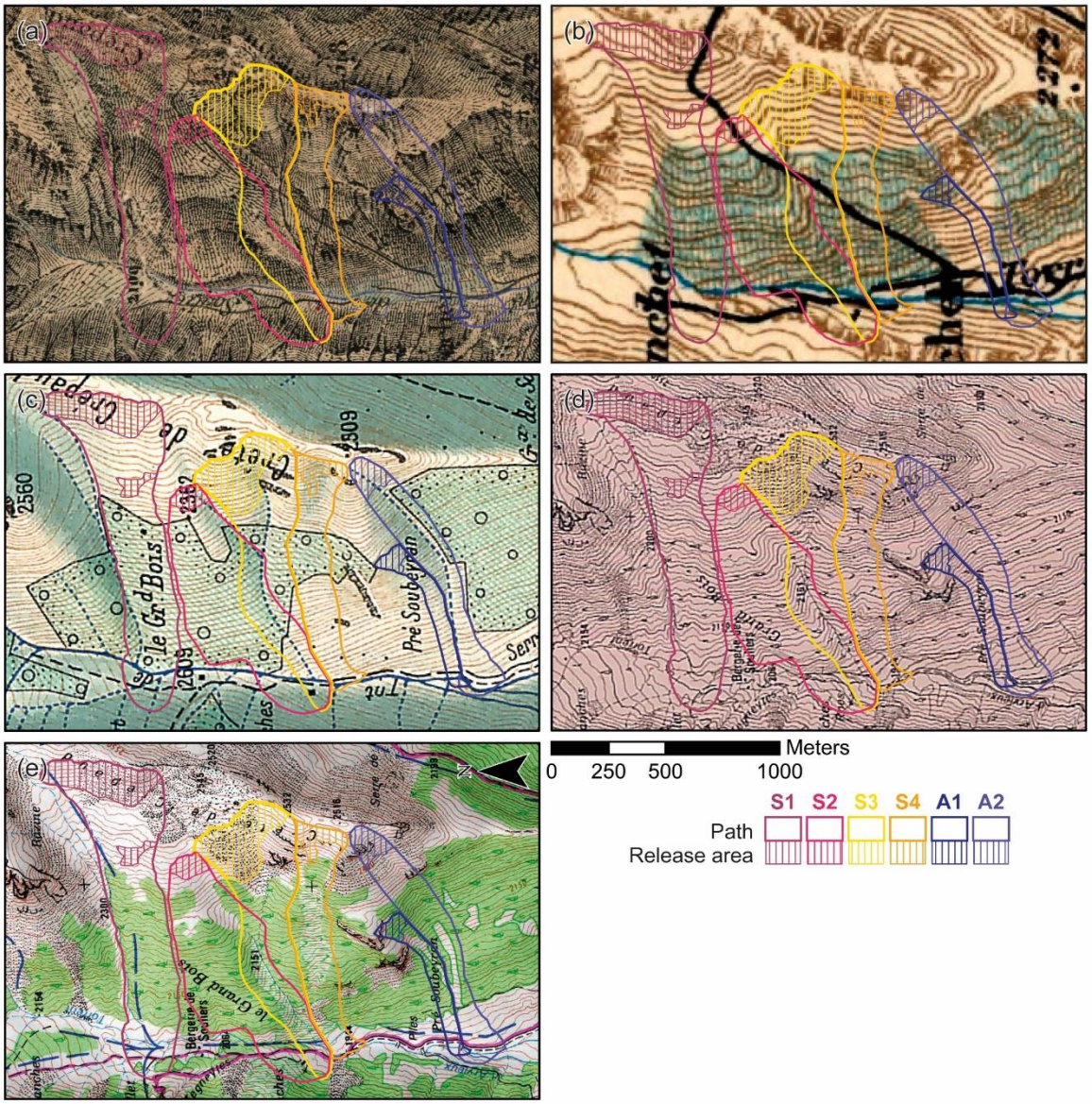

Figure 4.9 – Diachronic comparison of topographical maps of (a) 1866, (b) 1896, (c) 1933, (d) 1971, and (e) 2015. Germination dates of sampled trees suggest that a devastating avalanche in the 1910s or 1920s would have cleared the forested surface in paths S1-A1-A2. This interpretation is supported by topographic maps showing the absence of forests (c) in 1933 and an almost complete (re)colonization (d) in 1971 and (e) in 2015.

snowpack by (1) increasing terrain roughness (2) intercepting falling snow, (3) modifying radiation and temperature regimes and by (4) reducing near-surface wind speeds (de Quervain, 1978; Leitinger et al., 2008; McClung, 2003; Salm, 1978). These effects have been demonstrated to considerably limit avalanche formation to the steepest slopes (>35°; Schneebeli and Bebi, 2004).

Even if the interrelations between a decrease of snow avalanche activity and forest expansion are undoubted, the causes for this evolution are less easily understood. Indeed, one should keep in mind that forest colonization in paths S1-S3 dates back to medieval times as testified by the age structure of sampled trees and that the forest expanded continuously, especially during the 18th and 19th centuries. This trend is in line with the forest expansion observed at Chateau-Ville-Vieille (and at the scale of the Queyras massif), where forested areas increased from 357 ha (4400 ha in the Queyras massif) in 1747 to 2,325 ha (16,000 ha) in 1908 (Gadoud, 1917). Pre-industrial afforestation cannot reasonably be attributed to anthropogenic global warming. According to Touflan et al. (2010) and Chauchard et al. (2010), the significant recruitment of *L. decidua* during the 18th and the 19th centuries is related to forest and grazing managements. Larch is not only an early successional species, but also favored by shepherds because of its compatibility with grazing activities. The deciduous foliage of larch, with its soft needles and its low tree density, ensures high grass productivity and offers shelter from rain and intense sunlight to both cattle and sheep (Carrer and Urbinati, 2001; Chauchard et al., 2010; Motta and Lingua, 2005). In addition, larch is probably more resistant to trampling as compared to Cembran pine or Silver fir and its wood is also more valued for its natural decay resistance, high density and aesthetic value (Chauchard et al., 2010). In addition, the progressive extensification of livestock grazing in the Queyras was marked by a strong decrease in livestock from 6808 units (LU) in 1836 (Granet-Abisset, 1994), 3015 LU in 1961 (Leynaud and Georges, 1965), and 1994 LU in 2010 (AGRESTE, 2012), as a result of a rural exodus (Chauchard et al., 2007; Didier, 2001; Motta and Garbarino, 2003). The reduced livestock pressure and rural exodus certainly explains part of the upward shift of larch trees at Souliers as it coincides with the demographic evolutions in (1) the Chateau-Ville-Vieille municipality where the number of inhabitants decreased from 1440 in 1763 to 766 in 1911 and (2) in the Queyras massif where the 1911 census population (4094 inhabitants) was lower to the one of 1700 (5310 inhabitants) (Blanchard, 1915).

Finally, we cannot exclude that decreasing trends in snow cover depth (Beniston et al., 2018; Durand et al., 2009a; Reid et al., 2016) and snow cover duration (Beniston, 1997;

Uhlmann et al., 2009) may have played a role in the avalanche-forest interactions through direct impacts on avalanche frequency (Eckert et al., 2010d; Ballesteros-Cánovas et al., 2018) and the nature (Pielmeier et al., 2013; Naaim et al., 2016) of snow avalanches. At Grand Bois de Souliers slope, it is therefore possible that the increase in the treeline in the 20th century was a mere bounce-back to a level without depression by previous anthropogenic activity (Gehrig-Fasel et al., 2007), rather than a climatically induced advance of the treeline. Similarly, (i) the absence of clear trends in avalanche frequency in Group2 since the 1970s, (ii) the rather weak decrease in snow amounts and snow cover duration documented so far in the Southern French Alps (Durand et al., 2009a; Castebrunet et al., 2014) at the altitudes at which the avalanche release areas are located, and (iii) the rather limited changes documented over the last decades in avalanche occurrence numbers around the study area (Eckert et al., 2013; Lavigne et al., 2015) further suggest limited impacts of global warming.

6. Conclusion

In this study, we used dendrogeomorphic techniques to document past avalanche activity in six contiguous paths in the Queyras massif (French Alps). By using the 4-step procedure designed by Favillier et al. (2017 – chapter 1), we aimed at disentangling signals induced by snow avalanches from other disturbances (e.g., climatic extremes and larch budmoth outbreaks). Two distinct types of non-stationarities have been identified in the reconstructed avalanche activity: (1) in three paths located in the southern part of the slope, a strong increase in avalanche frequency has been evidenced since the 1970s. The distribution of tree ages retrieved from dendrogeomorphic techniques in combination with old topographic maps allowed attributing this non-stationarity to rapid afforestation of the snow avalanche paths. (2) In the northern paths, the frequency of reconstructed events decreased in S1 during the 1930s, and in S2-S3 after World War 2. This non-stationarity indicates a real decrease in snow avalanche activity related to the densification of the forest stands in these paths since the 18th century and to the colonization of the release areas during the 20th century. Even if we cannot exclude that global warming may play a role in this evolution by speeding up forest colonization or weakly decreasing available snow amounts in S1-S3, we explain both dynamics by socio-environmental factors and their impact on forest cover dynamics, namely through forest and grazing management during the 18th century, and the rural exodus and abatement of grazing throughout the 20th century. In that sense, our results evidence the crucial need for future tree-ring studies of mass-

movement changes to take potential impacts of socio-environmental changes into account, both in terms of the potential of forest stands to yield data on past events as well as in terms of process activity. More widely, this study calls for more systemic approaches in tree-ring reconstructions to adequately tackle the complex interrelations between forest evolution, global warming, social practices and process activity.

CHAPITRE 5

Complex signals in regional tree-ring reconstructions of snow avalanches

Complex signals in regional tree-ring reconstructions of snow avalanches: lessons from the Goms valley (Swiss alps)

Ce chapitre est un article en préparation pour la revue :

Progress in Physical Geography

Les résultats présentés dans ce chapitre sont basés sur les séries dendrogéomorphologiques récoltées et analysées par S. Guillet et les équipes de Dendrolab.ch, dans le cadre la rédaction de rapports d'expertise à destination du Canton du Valais (Stoffel et al., 2015, 2016). J'ai ensuite analysé les séries de perturbations de croissance et identifié les événements d'avalanche à Oberwald (chapitre 1), Münster et Geschinen à l'aide de l'approche en 4-étapes développée dans le chapitre 1. La chronologie d'événements a ensuite été homogénéisée à l'aide de la modélisation bayésienne hiérarchique conçue par N. Eckert. Le travail de fouille et la compilation de la base de données d'archive ont été réalisés par F. Giacona et G. Zenhäusern. À partir de la base de données d'archives et des résultats de modélisation, j'ai effectué la totalité des tests statistiques et des comparaisons. Sur la base des résultats obtenus, j'ai conçu l'ensemble des figures et rédigé l'article.

Co-auteurs et affliations :

A. Favillier[1], S. Guillet[2,3], J. Lopez-Saez[2,3], F. Giacona[4], N. Eckert[4], G. Zenhäusern[5], J.L. Peiry[6], M. Stoffel[2,3,7], C. Corona[1]

1. Université Clermont Auvergne, CNRS, Université de Limoges, GEOLAB, F-63000 Clermont-Ferrand, France
2. University of Geneva – Institute for Environmental Sciences, Climatic Change and Climate Impacts, 66 Boulevard Carl-Vogt –CH-1205 Geneva, Switzerland.
3. Dendrolab.ch, Department of Earth Sciences, University of Geneva, rue des Maraîchers 13, CH-1205 Geneva, Switzerland.
4. University Grenoble Alpes, IRSTEA, UR ETNA, 2 rue de la Papeterie-BP76, F-38402 Saint-Martin-d'Hères, France.
5. Forschungsinstitut zur Geschichte des Alpenraums, CH-3900 Brig, Switzerland.
6. CNRS, UMI3189, "Environnement, Santé, Sociétés", Faculté de Médecine, UCAD, BP 5005, DAKAR-FANN, Sénégal.
7. Department F.-A. Forel for Environmental and Aquatic Sciences, University of Geneva, 66 Boulevard Carl-Vogt, CH-1205 Geneva, Switzerland.

Abstract

One of the purposes of dendrogeomorphic studies is to provide long and continuous reconstructions of mass movements with the aim to detect potential trends notably related to climate change. To this end, the development of regional chronologies – that aggregate results from different sites – is a crucial prerequisite to overcome local specificities and extract a common signal possibly driven by climate fluctuations. Yet, such chronologies are scarce in literature and no consensus exists neither on the way to compute them nor on the method to extract a common signal. With respect to snow avalanches, a large majority of studies thus include less than ten paths and discriminate the years of high/low activity on the basis of an index that represents the proportion of trees showing disturbances at the regional scale. This index, independent from the paths, does not to account for potential non-stationarities recently evidenced in local tree-ring reconstructions and related to e.g. increasing sample depth over time, changing dendrogeomorphic potential in the aftermath of extreme events or socio-environmental changes. In this paper, growth disturbances in tree-ring series were used to reconstruct snow avalanche events for 11 paths located in the Goms valley (Swiss Alps). Reconstructions were first computed at the path scale based on the 4-step procedure developed by Favillier et al. (2017 – chapter 1) to disentangle the potential effects of snow avalanches from disturbance pulses caused by climatic or exogenous factors. They were processed within a Bayesian hierarchical spatio-temporal framework specifically designed to remove trends related to the decreasing number of living trees over time and to infer robust spatio-temporal trends in mean annual/regional behaviour.

Despite the stringency of our procedure, the comparison of the homogenized regional reconstruction with several snow avalanche chronologies available for the Obergoms municipality, Switzerland and the French Alps are poorly conclusive. In addition, we failed to find robust climatic drivers for snow avalanche fluctuations. Such results question the relevance of tree-ring reconstructions to document the impacts of climatic fluctuations on snow avalanche activity and raise the issues of the number and the selection of paths to be included in a regional chronology to increase the signal/noise ratio.

Keywords: Snow avalanches, tree-ring analysis, regional snow avalanche activity, hierarchical Bayesian modelling, Swiss Alps

Résumé

L'un des objectifs de l'approche dendrogéomorphologique est de fournir des reconstructions longues et continues des mouvements de masse dans le but de détecter les tendances potentielles notamment liées au changement climatique. À cette fin, le développement de chronologies régionales – regroupant des séries d'événements de différents sites – est une condition préalable cruciale pour surmonter les biais locaux et extraire un signal commun, peut-être en lien avec fluctuations climatiques. Pourtant, celles-ci sont rares dans la littérature et aucun consensus n'existe sur la façon de les calculer ni sur la méthode d'extraction d'un signal commun. Dans le cas des avalanches, la grande majorité des études intègrent moins de dix couloirs et discriminent les années de forte/basse activité sur la base d'un indice représentant la proportion d'arbres présentant des perturbations de croissance à l'échelle régionale. Cet indice, indépendant des couloirs, ne tient pas compte des non-stationnarités potentielles récemment mises en évidence dans les reconstructions locales et liées, par exemple, à l'augmentation de la profondeur d'échantillonnage au cours du temps, au changement du potentiel dendrogéomorphologique à la suite d'événements extrêmes ou des changements socio-environnementaux. Dans ce chapitre, les séries perturbations identifiées dans les cernes de croissance ont été utilisées pour reconstruire les avalanches dans 11 couloirs de la vallée de Goms (Canton du Valais, Alpes suisses). Les chronologies d'événements ont d'abord été établies à l'échelle des couloirs à l'aide de la procédure en quatre étapes mise au point par Favillier et al. (2017 – chapitre 1) pour discriminer les avalanches des perturbations causées par des facteurs climatiques ou exogènes. Les chronologies obtenues ont, ensuite, été traités dans un cadre spatio-temporel bayésien hiérarchique spécifiquement conçu pour éliminer les tendances liées à la diminution du nombre d'arbres vivants au fil du temps, puis déduire des tendances spatio-temporelles robustes du régime annuel/régional moyen.

Malgré la rigueur de l'approche, la comparaison de la reconstruction régionale homogénéisée avec plusieurs bases de données d'avalanches disponibles pour la commune d'Obergoms, les Alpes suisses, puis françaises est peu concluante. De plus, aucuns facteurs climatiques robustes expliquant les fluctuations des avalanches de neige n'a été identifié. De tels résultats interrogent la pertinence des reconstructions dendrogéomorphologiques pour documenter les impacts des fluctuations climatiques sur l'activité avalancheuse et soulèvent la question du nombre et de la sélection des couloirs à inclure dans une chronologie régionale pour augmenter le rapport signal/bruit.

Mots-clefs : avalanches, dendrogéomorphologie, activité régionale, modélisation bayésienne hiérarchique, Alpes suisses.

1. Introduction

Mountains systems are particularly affected by the ongoing climate warming which provokes sustained and rapid environmental changes (see e.g. Beniston et al., 2018; Gobiet et al., 2014). Temperature increases in mountain regions twice as much as the global average since the late 19th century (Auer et al., 2007; IPCC, 2013) and significantly alters the cryosphere (Beniston et al., 2018). Since the middle of the 20th century, in the Alps, multiple studies thus report decreasing trends in snow depth (Beniston et al., 2018; Durand et al., 2009a; Reid et al., 2016), snow cover duration (Beniston, 1997; Uhlmann et al., 2009), snow water equivalent (Marty et al., 2017) and snow extremes (Marty and Blanchet, 2012; Nicolet et al., 2018, 2016). In the future, climate models forecast that snow depth will be significantly reduced (Jylhä et al., 2008) – especially at the mean snow-rain transition altitude – and that snow properties (Castebrunet et al., 2014), such as snow stability (Castebrunet et al., 2014; Martin et al., 2001), will be modified. Such changes are expected to strongly affect snow avalanche activity (Mock and Birkeland, 2000).

In order to document potential climatically driven trends in avalanche activity, systematic and continuous inventories have been used. Based on 50-yr avalanche records, Schneebeli et al. (1997) investigated possible changes in the number of catastrophic avalanches in the vicinity of Davos (Switzerland), but could not observe changes over the course of the 20th century. Similarly, Laternser and Schneebeli (2002) did not show significant changes in avalanche activity between 1950 and 2000 in Switzerland. On the other hand, in the French Alps, Eckert et al., (2013, 2010a,b) highlighted significant changes in avalanche series from the EPA (Enquête Permanente sur les Avalanches; Bourova et al., 2010) since 1950, notably in avalanche runout altitudes. Over the same time period and region, Castebrunet et al. (2012) showed that regional annual avalanche activity indicators can be related successfully to modelled snow and weather covariates using regression models that represent trends and high/low peaks, whereas Lavigne et al. (2012, 2015) point to altitudinal controls in avalanche regimes.

On longer timescales, historical archives have been used to document potential trends in avalanche chronicles (Laternser and Pfister, 1997). Yet, numerous difficulties remain in accessing, organizing and homogenizing these data, or to use them all together as they were collected over different timeframes and with different purposes (Giacona et al., 2017). For instance, old archival data was not designed for scientific use (Ibsen and Brunsden, 1996) and many discontinuities exist in long time series concerning hazard, vulnerability, sources, or

perception (Martin et al., 2015). Furthermore, one should keep in mind that these records are usually biased towards events with a direct impact on either property or human lives, thus representing only a partial avalanche history (Casteller et al., 2011). Paleo-environmental proxies such as lichens (Jomelli and Pech, 2004; McCarroll, 1993), lake sediments (Fouinat et al., 2018; Nesje et al., 2007; Vasskog et al., 2011) or colluvial sedimentary successions (Blikra and Selvik, 1998) have been used to document avalanche activity over centuries to millennia. Yet, these studies are based on decadal to centennial-resolved series and remain limited to sites where proxies have been preserved.

On forested paths, archival and proxy records can theoretically be supplemented with dendrogeomorphic techniques (Alestalo, 1971; Stoffel et al., 2010; Stoffel and Bollschweiler, 2008). Evidences of avalanches will be conserved in tree morphology in the form of candelabra growth, tilted stems, impact scars, or root breakage. In addition, growth disturbances are recorded in the tree-ring series (Stoffel and Bollschweiler, 2008), which in turn allow avalanche histories on sites where long and extensive time series of events are lacking. Among the 67 tree-ring based avalanche reconstructions, listed through an exhaustive inventory of existing literature, 20 studies explored the relation between meteorological variables and snow avalanches (Figure 5.1). Several authors found significant relations between snow avalanche activity and meteorological parameters or avalanche-prone weathers (Dubé et al., 2004; Germain et al., 2005, 2008; Schläppy et al., 2016; Voiculescu et al., 2016), the increase of mean air temperature during the 20th century (Ballesteros-Cánovas et al., 2018; Gądek et al., 2017), large-scale circulation patterns such as El Niño Southern Oscillation (ENSO) (Casteller et al., 2011) or the North Atlantic Oscillation (NAO) (Martin and Germain, 2017; Muntán et al., 2009). In these studies, time-implicit approaches have been developed to directly model avalanche activity as combinations of snow and weather covariates. By contrast, except for Ballesteros-Cánovas et al. (2018), no study specifically investigated relationships between climatic and snow avalanche trends, at decadal to centennial scales, in a time-explicit approach that considers time as a covariate.

Several limitations question the ability of the above-mentioned dendrogeomorphic studies to decipher the impacts of climatic fluctuations on avalanche activity. They are related with (i) the limited number of paths included in a large majority of the reconstructions ($n < 4$ for 80% of the 67 listed studies, $n > 10$ for only 9%) that precludes from a robust assessment of trends in snow avalanche activity and subsequently significant relationships between climatic and avalanche fluctuations. In addition, (ii) no consensus exist on the methods to aggregate local tree-ring reconstruction in a regional chronology. Germain et al. (2005), Muntán et al.

(2009) and Voiculescu et al. (2016), for example, summed up the event-years retrieved at the path scale and considered the peaks in the resulting chronology as regional events. Following Dubé et al. (2004), several studies (Germain et al., 2008; Decaulne et al. 2012, 2014; Voiculescu et al., 2016; Martin and Germain, 2017) used a regional avalanche activity index (RAAI) that represents, for each year (t) the ratio between the sum of local avalanche activity indices (i.e. the proportion of damaged trees in year t) and the number of paths that could potentially record an avalanche in year t. At the range scale, they discriminate period of high/low avalanche activity on the basis of a RAAI threshold (generally ranging from 10 to 20%). (iii) Several non-stationarities evidenced in site-specific chronologies and intrinsic to the dendrogeomorphic approach are susceptible to blur the climatic signal in the regional chronology. The latter are related to increasing sample size over time (Butler, 1987; Butler and Sawyer, 2008; Corona et al., 2012), the difficulty to sample old scars (Stoffel and Perret, 2006; Trappmann and Stoffel, 2013), the overrepresentation of visible injuries in the growth disturbance spectrum (Favillier et al., 2017 – chapter 1) or the modification of the dendrogeomorphic potential in the aftermath of extreme destructive events (Corona et al., 2012; Favillier et al., 2018 – chapter 2; Mainieri et al., submitted – chapter 4). In addition, de Bouchard d'Aubeterre et al. (2019 – chapter 3) demonstrated that geomorphological characteristics of the avalanche paths could affect significantly the comprehensiveness and the reliability of tree-ring avalanche reconstructions. Finally, (iv) socio-environmental factors such as forest, grazing managements, rural exodus and the extensification of pastoral practices are also susceptible to interfere with climate-induced trends (Mainieri et al., submitted – chapter 4).

In that context, in order to illustrate the multiplicity of signals embedded in dendrogeomorphic reconstructions of snow avalanches at the regional scale, making the detection of the climatic forcing on avalanche activity complex, this study will (i) aggregate 11 snow avalanche chronologies available at the path scale in a regional chronology covering the Goms valley (canton of Valais, Swiss Alps); use an innovative Bayesian hierarchical spatio-temporal logistic regression approach in order (ii) to remove trends related to the decreasing number of living trees over time so as to (iii) extract a common signal of past changes in avalanche activity at the regional scale and (iv) confront it with independent historical series and past climate and land use conditions.

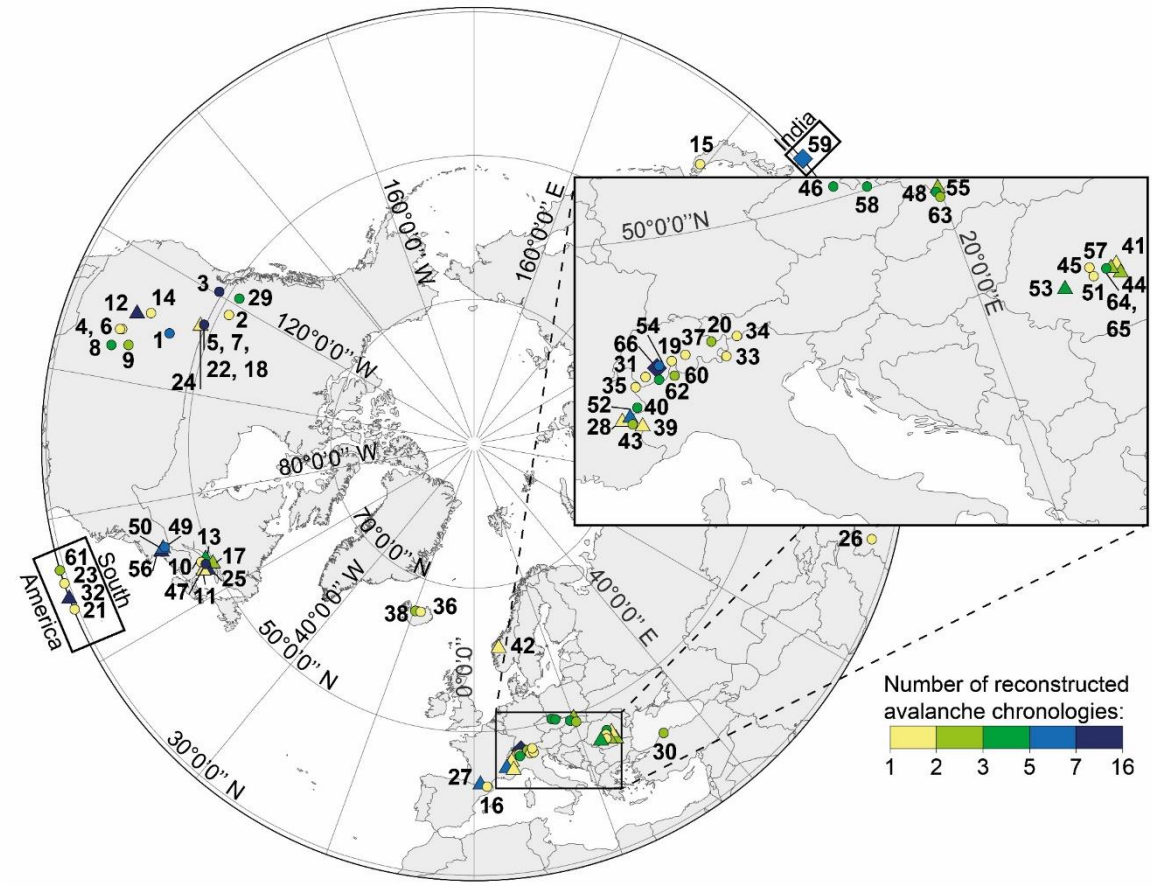

Figure 5.1 – Synthesis of tree-ring based avalanche reconstructions. Small and white dots represent dendrogeomorphic snow avalanche studies that do not assess the linkage between snow avalanche activity and climate parameters. Colored lozenges represent dendrogeomorphic snow avalanche studies assessing the relation between snow avalanche activity and climatic parameters while triangles represent studies assessing relations between snow avalanche activity and meteorological parameters or avalanche-prone weathers. Colored dots represents other dendrogeomorphic snow avalanche studies.

1. Potter (1969); **2**. Schaerer (1972); **3**. Smith (1973); **4**. Ives et al. (1976); **5**. Butler (1979); **6**. Carrara (1979); **7**. Butler and Malanson (1985); **8**. Bryant et al. (1989); **9**. Rayback (1998); **10**. Larocque et al. (2001); **11**. Boucher et al. (2003); **12**. Hebertson and Jenkins (2003); **13**. Dubé et al. (2004); **14**. Jenkins and Hebertson (2004); **15**. Kajimoto et al. (2004); **16**. Muntán et al. (2004); **17**. Germain et al. (2005); **18**. Pederson et al. (2006); **19**. Stoffel et al. (2006); **20**. Casteller et al. (2007); **21**. Mundo et al. (2007); **22**. Butler and Sawyer (2008); **23**. Casteller et al. (2008); **24**. Reardon et al. (2008); **25**. Germain et al. (2009); **26**. Laxton and Smith (2009); **27**. Muntán et al. (2009); **28**. Corona et al. (2010); **29**. Johnson and Smith (2010); **30**. Köse et al. (2010); **31**. Szymczak et al. (2010); **32**. Casteller et al. (2011); **33**. Garavaglia and Pelfini (2011); **34**. Kogelnig-Mayer et al. (2011); **35**. Corona et al. (2012); **36**. Decaulne et al. (2012); **37**. Püntener et al. (2012); **38**. Arbellay et al. (2013); **39**. Corona et al. (2013); **40**. Schläppy et al. (2013); **41**. Voiculescu and Onaca (2013); **42**. Decaulne et al. (2014); **43**. Schläppy et al. (2014); **44**. Voiculescu and Onaca (2014); **45**. Chiroiu et al. (2015); **46**. Tumajer and Treml (2015); **47**. Germain (2016); **48**. Lempa et al. (2016); **49**. Martin and Germain (2016a); **50**. Martin and Germain (2016b); **51**. Pop et al. (2016); **52**. Schläppy et al. (2016); **53**. Voiculescu et al. (2016); **54**. Favillier et al. (2017); **55**. Gądek et al. (2017); **56**. Martin and Germain (2017); **57**. Pop et al. (2017); **58**. Šilhán and Tichavský (2017); **59**. Ballesteros-Cánovas et al. (2018); **60**. Bollati et al. (2018); **61**. Casteller et al. (2018); **62**. Favillier et al. (2018); **63**. Krause and Křížek (2018); **64**. Meseșan et al. (2018a); **65**. Meseșan et al. (2018b); **66**. This study.

2. Regional settings

Our study site is located in the Goms valley (Fig. 5.2), in the upper part of the Rhone valley extending from the Brig municipality to the Rhone glacier (Swiss Alps). Based on (1) the existence of old forest stands presenting avalanche-related damages, (2) the absence of possible interferences between snow avalanches and other mass movements and (3) the hazard maps available for the regions, three avalanche slopes were selected on the S-E facing slope of the valley, namely in the municipality of Münster (MU, 46°29'14N, 8°15'44E), Geschinen (GE, 46°29'44N, 8°16'49E) and Oberwald (OB, 46°32'05N, 8°20'54E). On these slopes, 11 paths – that exceed 1000 m in length and a difference in elevation ranging from ~430 to 730 m – have been delineated using (i) technical reports from the Wasser Schnee Lawinen engineering office (cited in Stoffel et al., 2015, 2016) complemented by the (ii) mapping of erosional and depositional avalanche features in the field as well as on the interpretation of (iii) Lidar data and aerial photographs available from the Federal Office of Topography Swisstopo. The characteristics of each path are given in Table 5.1.

At MU and OB slopes, four and five avalanche paths have been identified with release areas ranging from 1810 and 2170 m asl. All these paths directly threaten human settlements, the Matterhorn-Gotthard Bahn (MGB) railway line as well as the road between Brig (canton of Wallis) and Andermatt (canton of Uri). As a consequence, since the 19th century, great efforts have been made to limit snow avalanche activity. Several rows of avalanche barriers have been installed in the release areas of avalanche paths in Münster (MU2, MU3) since the end of the 19th century (Coaz, 1910). These protection structures were maintained and completed with additional rows of snow bridges built in the release zone of MU3 and MU4 in 1958, 1984, 1985, 1986, 1987, 1988, and in 1998. Snow bridges and wind baffle were also constructed at MU1 release area to prevent the formation of snow cornice formation in 1990. In total, 77 snow bridges and snow rakes, as well as the 8 wind baffles, prevent the snow accumulation in the release zones of MU avalanche paths (Fig. 5.2). At OB, based on the analysis of historical aerial photographs, snow bridges and snow glide tripods were installed in the release zones of OB3 (1750–1850 m asl) between 1944 and 1960. During the same period, an avalanche deflecting dam was built in the deposit area of OB2 and OB3 paths in order to protect the village. Between 1960 and 1967, rows of snow rakes were constructed in the forest between 1500 and 1700 m asl on OB1 and OB2 paths to prevent small avalanche release. Finally, between 1967 and 1988, wind baffles and snow dams were constructed in OB3 release area.

At GE, snow avalanches are released from two zones located between 1850 and 2100 m asl. Several rows of wall terraces and avalanche barriers have been installed in the starting zones at

the end of the 19th century to protect the municipality (Torrenté, 1888). The comparison of historical maps (available at map.geo.admin.ch, Swisstopo) shows that additional snow bridges and snow rakes were built at the beginning of 20th century mainly in the upper part of the slope between 1770 m and 2010 m asl. Since 1990s, snow bridges above 1980 m asl were no longer maintained. Nowadays, 29 snow rakes, built between 1995 and 2005, and 25 snow glide tripods, built between 2001 and 2006, in the southern part of forest prevent from snow avalanche release between 1800 m and 2000 m asl.

According to the meteorological series from Ulrichen (46°5'N, 8°31'E, 1346 m asl), annual temperature and precipitation totals in the Goms Valley are on average 3.7°C and 1212 mm for the period 1981-2010. During winter, mean air temperature (DJF) is -6.6°C and between November and April precipitation falls primarily as snow with an average annual snowfall reaching 578 cm for the period 1999–2010 (the average snow cover period is 171 days).

3. Methods

3.1. Sampling strategy and detection of past avalanche events in tree-ring series

For this study, additional tree-ring series were collected at Munster (4 paths) and Geschinen (2 paths) and combined with the series developed at Oberwald (5 paths, Favillier et al., 2017 – chapter 1). In total of 2256 increment cores and 20 cross-sections were sampled during summers 2014 and 2015 from 1014 European Larch (*Larix decidua* Mill.) and Norway spruce (*Picea abies* (L.) Karst.) in the 11 selected paths. In the field, tree-ring material was collected following recommendations from Šilhán and Stoffel (2015) and Stoffel and Corona (2014) with respect to the number and the spatial distribution of sampled trees as well as the balance between old and young trees. In the laboratory, the material was processed following standard dendrochronological procedures (Stoffel and Bollschweiler, 2008). Growth disturbances were identified in the tree-ring series and cross-dated against two local reference chronologies (Corona et al., 2012). Injuries and callus tissues (CT) (Stoffel et al., 2010), tangential rows of traumatic resin ducts (TRD) (Schneuwly et al., 2009a,b), compression wood (CW) and sharp growth suppressions (GS; Kogelnig-Mayer et al., 2013) were considered as the most reliable indicators of past avalanche activity. Intensities were assigned to GDs in order to emphasize features that are obviously associated with avalanche activity (Stoffel et al., 2013). GDs were classified based on the visual quality of the evidence of reactions according to the classification proposed by Kogelnig-Mayer et al. (2011): weak (intensity class 1), medium (intensity class 2), strong (intensity class 3) reactions and clear evidence of injuries (intensity class 4). To detect past snow avalanche events – which correspond to the occurrence of one

Table 5.1 – Main characteristics of the studied avalanche paths.

	Avalanche path					Forest characteristics		
Path	Lenght (m)	Mean slope (°)	Mean slope of the release area (°)	Mean release alt. (m)	Deposit alt. (m)	Sampled trees (n)	Mean age (yr)	Oldest tree (yr)
MU 1	1258	28.36	36.58	2170	1571	52 (+7)	230.5	432
MU 2	1571	29.98	40	2060	1390	32 (+8)	240.9	493
MU 3	1255	29.84	36.71	1941	1326	80 (+27)	225.1	513
MU 4	1000	27.79	34.28	1823	1338	50	228.4	497
GE 1	1104	32.52	38.33	2050	1388	135	146.2	554
GE 2	1147	32.49	36.87	2050	1370	140	205.2	678
OB 1	1253	27.67	27.24	1878	1363	127	235.2	584
OB 2	1562	25.9	28.16	1970	1370	135	222.6	579
OB 3	1838	26.07	33.37	2100	1368	74 (+26)	197.23	561
OB 4	1358	26.68	33.04	2018	1368	115 (+10)	188.7	584
OB 5	1155	25.38	39.06	1810	1380	74 (+3)	198.9	489
Total	**1318.27**	**28.43**	**34.88**	**1988.18**	**1384.72**	**1014**	**205.9**	**678**

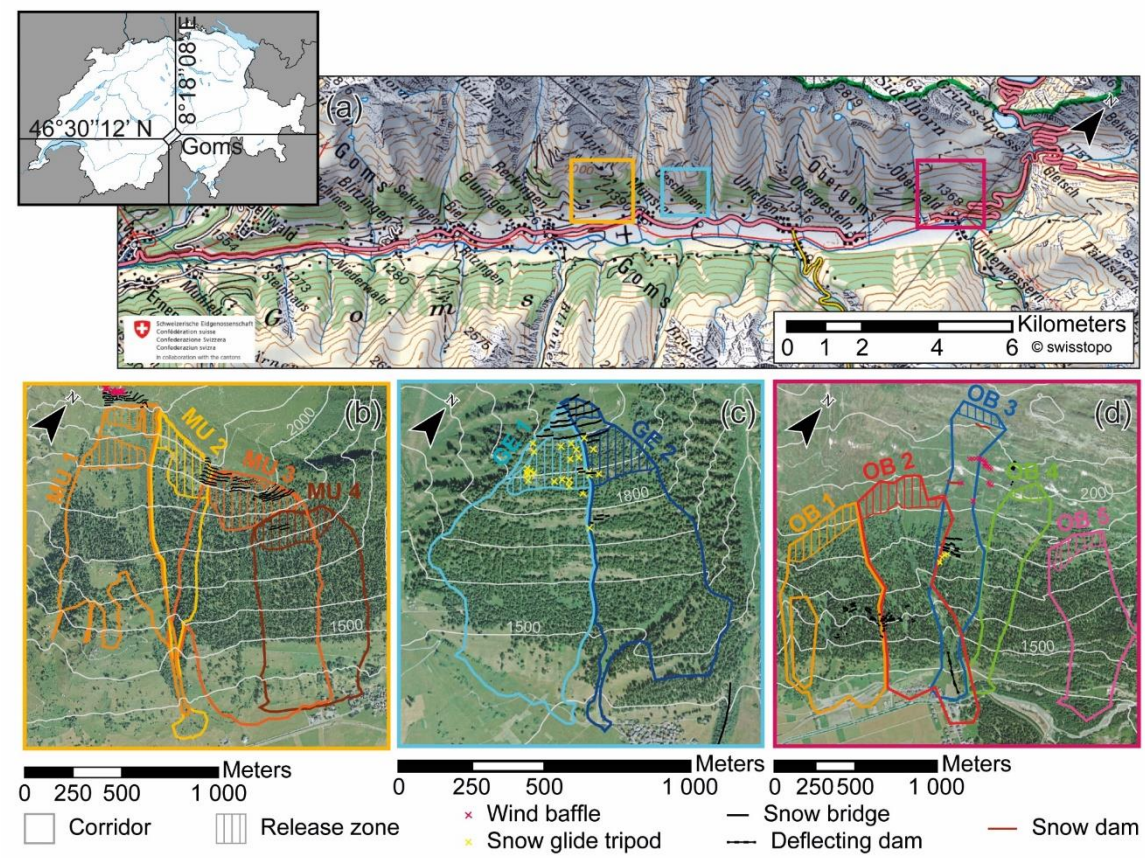

Figure 5.2 – Location of the study sites: (a) the Goms Valley in the Canton of Valais, Switzerland, the (b) Münster, Geschinen (c) and Oberwald (d) avalanche paths.

snow avalanche at least per year in each selected path – in the GD series, we adopted the four-step procedure proposed by Favillier et al. (2017 – chapter 1). This procedure underlines the necessity to disentangle the potential effects of snow avalanches from disturbance pulses caused by climatic or exogenous factors, such as cold/dry years or larch budmoth (LBM) outbreaks. The triplets of LBM outbreak years (i.e. three consecutive years) have been reconstructed in the Goms Valley according to Esper et al. (2007) and Büntgen et al. (2009). Extremely cold and dry summers were retrieved from Battipaglia et al. (2010) and Efthymiadis et al. (2006) (see Favillier et al., 2017 – chapter 1, for more details). Unlike previous regional reconstructions aforementioned in the introduction section, past avalanche events were first determined at the path scale and path chronologies were aggregated at the valley scale.

In order to detect potential recolonization patterns after extreme avalanche events, the age structure of the forests at each slope has been assessed by counting the number of tree-rings in the sampled trees and mapped using an inverse distance weighted method. Yet, one should keep in mind that these ages are systematically underestimated and do not reflect inception or germination dates due to sampling height and to frequently rotten innermost rings especially in older individuals.

3.2. Estimation of the regional snow avalanche activity since 1880 using a hierarchical Bayesian modelling approach

3.2.1. Principle

Hierarchical Bayesian Modelling (HBM) is a flexible framework to deal with spatio-temporal data (Cressie and Wikle, 2011; Wikle et al., 1998). For this reason, it was rapidly incorporated in climate science (e.g., Wikle, 2003), statistical geophysics (e.g., Berliner, 2003) and, more generally, in a growing range of applications related to mountain risks and climate (e.g., Eckert et al., 2007, 2011; Jomelli et al., 2015, 2019; Lavigne et al., 2012; Rabatel et al., 2013). This increasing popularity originates from several advantages. First, it respects the spatio-temporal data structure (in our case, occurrence or non-occurrence of an avalanche in a given tree ring record a given year) and makes it possible to avoid the major drawbacks of "standard" regional studies: the impoverishment of the data available by transformation of repeated observation series into a single regional series. Hence, with dependant replicates of the same "common effects" in space and time, the HBM framework compensates for short data series, making it possible to infer robust spatio-temporal trends in mean annual/regional behaviour. For instance, the mean common temporal effect over all paths where avalanche activity has been reconstructed should be relatively free from local artefacts, thus providing a

fair estimate of the temporal variations of avalanche activity over the sample of studied paths. Symmetrically, the interannual mean local effect representing local environmental constraints (altitude, etc.) is more easily inferred with repeated observations over several years than with data corresponding to given (annual or mean over several years) environmental condition. Eventually, HBM has the advantage of easily coping for series of uneven length, with the missing year-path couplets being simply treated as additional unknown (Tanner, 1992). For doing so, HBM accommodates complexity in a series of simpler conditional models which are inferred altogether, making the overall model structure much more flexible than a "traditional" Generalised Linear Model (GLM). This provides robust quantification at each sublevel of the model of the different sources of variability/uncertainty (limited quantity of available data, natural interannual and/or inter-path variability, etc.).

Concretely, within this framework, we develop a new specific hierarchical spatio-temporal logistic regression approach that removes potential trends in tree-ring based avalanche chronologies related to the increasing number of living trees during recent decades. Doing such, we aim at producing a homogenised/detrended assessment of past changes in mean avalanche activity over the studied path sample to be confronted to past climate and land use conditions. Also, in this reconstructed homogenised activity, we distinguish year-to-year variability from the lower frequency smoothed signal with a non-parametric regression. This has the additional advantage of providing more robust estimates of past changes in avalanche activity due to the so-called shrinkage effect of hierarchical Bayesian models (i.e. the information transfer from one year to another through the inferred temporal structure), especially for the old years for which information is missing on several paths.

3.2.2. Hierarchical Bayesian model specification

Avalanche occurrence in path *i* (over N paths in total) in year *t* (over T years in total) is classically expressed as a binary Bernoulli variable (event/no event) with a probability p_{it}:

$$y_{it} = \{0,1\} \sim B(p_{it}) \qquad \textbf{(Eq. 5.1)}$$

The time-space decomposition at the non-observable logit level is written as:

$$\text{logit}(p_{it}) = a_0 + POT_{it} + v_i + g_t + z_t \qquad \textbf{(Eq. 5.2)}$$

where a_o is a constant, v_i is the spatial component of the signal (which in our case is attributable to geomorphologic variables such as altitude, exposition, etc. that makes each path more or less active), $g_t + z_t$ is the detrended temporal anomaly we are interested in (smooth trend and year-to year fluctuations, respectively) and POT_{it} the "potential" function that

accounts for changes in living trees in each path over the study period. The constraints $\sum_{i=1}^{N} v_i = 0$ and $\sum_{t=1}^{T} z_t = 0$ are set for identifiability purposes. By construction (see below) $\sum_{t=1}^{T} g_t = 0$.

We express the potential function as:

$$POT_{it} = a_{1i}\left(\frac{n_{it}}{n_{iT}}\right)^{a_{2i}} \quad \textbf{(Eq. 5.3)}$$

where n_{it} is the number of living trees in a given path a given year and n_{iT} is the (maximal) number of living trees in the considered path, which is the one of the last years of the study period (sampling year). a_{i1} and a_{i2} are two free parameters quantifying the strength and shape of the detrending in each path. Hence, the standardized potential belonging to 0–1 and quantifying the capacity of the local tree stand to register avalanche activity a given year writes:

$$POTnorm_{it} = \frac{POT_{it}}{POT_{iT}} = \left(\frac{n_{it}}{n_{iT}}\right)^{a_{2i}} \quad \textbf{(Eq. 5.4)}$$

Eventually, the detrended spatio-temporal avalanche activity is obtained while setting this standardised potential to 1. This leads the detrended mean probability of avalanche occurrence in each path:

$$p_{iT} = \frac{\exp\left(a_0 + a_{1i} + v_i + g_t + z_t\right)}{1 + \exp\left(a_0 + a_{1i} + v_i + g_t + z_t\right)} \quad \textbf{(Eq. 5.5)}$$

and, by averaging over the different paths, the detrended annual probability of avalanche occurrence, considering the full temporal variability:

$$p'_t = \frac{\exp\left(a_0 + \frac{1}{N}\sum_{i=1}^{N} a_{1i} + g_t + z_t\right)}{1 + \exp\left(a_0 + \frac{1}{N}\sum_{i=1}^{N} a_{1i} + g_t + z_t\right)} \quad \textbf{(Eq. 5.6)}$$

or, alternatively, only the smooth component of the temporal signal:

$$p'_{smooth_t} = \frac{\exp\left(a_0 + \frac{1}{N}\sum_{i=1}^{N} a_{1i} + g_t\right)}{1 + \exp\left(a_0 + \frac{1}{N}\sum_{i=1}^{N} a_{1i} + g_t\right)} \quad \textbf{(Eq. 5.7)}$$

This highlights that the detrended mean inter-annual avalanche probability is simply:

$$p_o = \frac{\exp\left(a_0 + \frac{1}{N}\sum_{i=1}^{N} a_{1i}\right)}{1+\exp\left(a_0 + \frac{1}{N}\sum_{i=1}^{N} a_{1i}\right)} \quad \textbf{(Eq. 5.8)}$$

The smooth trend is captured with the model proposed by Wahba (1978) who proposed an *a priori* distribution for the vector $g = (g_1, \ldots\ g_T)$ such that its Bayesian posterior expectation is a cubic smoothing spline. Speckman and Sun (2003) show that such a *prior* can be written as an intrinsic conditional autoregressive model (iCAR, where each value is the weighted mean of its neighbors), with improper density:

$$p\left(g \middle| \sigma_g^2, A\right) = \frac{|A|_+^{1/2}}{\sigma_g^{T-2}} \exp\left(\frac{-1}{2\sigma_g^2} g^{tr} A g\right) \quad \textbf{(Eq. 5.9)}$$

where A is a chosen semi-positive definite matrix with two null eigenvalues, and "$|.|$" and "^{tr}"denote the matrix determinant and transposition operators. Here, we simply take A such that g is a second-order random walk, since Rue and Held (2005) showed that this approximation of Wahba (1978)'s *prior* leads to a smooth posterior mean. The "variance" parameter σ_g^2 controls the level of smoothing.

Eventually, classically, v_i and z_t are modeled as centered white noises, *i.e.*:

$$p\left(v_i \middle| \sigma_v^2\right) = \frac{1}{\sqrt{2\pi}\sigma_v} \exp\left(-\frac{v_i^2}{2\sigma_v^2}\right) \quad \textbf{(Eq. 5.10)}$$

$$p\left(z_t \middle| \sigma_z^2\right) = \frac{1}{\sqrt{2\pi}\sigma_z} \exp\left(-\frac{z_t^2}{2\sigma_z^2}\right) \quad \textbf{(Eq. 5.11)}$$

3.2.3. Variance decomposition

One important advantage of this model is that it allows easy quantification of the fraction of the total variability captured by the different terms. Indeed, the way the model is constructed makes all components independent. Hence, the total variance (*VAR*) at the logit layer is:

$$VAR\left(\text{logit}\left(p_{it}\right)\right) = VAR\left(POT_{it}\right) + VAR\left(g_t\right) + \sigma_v^2 + \sigma_z^2 \quad \textbf{(Eq. 5.12)}$$

with $VAR(g_t)$ to be computed from the vector $g = (g_1, \ldots\ g_T)$ and $VAR(POT_{it})$ from the matrix POT_{it}.

By analogy to the classical R^2 adjustment statistics, variance ratios can thus be computed to evaluate the respective weight of the different terms in the modelled variability of avalanche occurrences:

$$R^2_{time\,trend} = VAR(g) / VAR\left(\text{logit}(p_{it})\right) \quad \textbf{(Eq. 5.13)}$$

$$R^2_{time\,noise} = \sigma_z^2 / VAR\left(\text{logit}(p_{it})\right) \quad \textbf{(Eq. 5.14)}$$

$$R^2_{space} = \sigma_v^2 / VAR\left(\text{logit}(p_{it})\right) \quad \textbf{(Eq. 5.15)}$$

$$R^2_{POT} = VAR(POT_{it}) / VAR\left(\text{logit}(p_{it})\right) \quad \textbf{(Eq. 5.16)}$$

with the equality $R^2_{time\,trend} + R^2_{time\,noise} + R^2_{space} + R^2_{POT} = 1$.

Note that the specific weight of the detrending term in each path can be evaluated as:

$$R^2_{POT_i} = VAR(POT_{i.}) / \left(VAR(POT_{i.}) + VAR(g_t) + \sigma_z^2\right) \quad \textbf{(Eq. 5.17)}$$

where $VAR(POT_{i.})$ is the variance of the detrending term evaluated the considered path only.

Eventually, the ratio:

$$R^2_{temp} = VAR(g_t) / \left(VAR(g_t) + \sigma_z^2\right) \quad \textbf{(Eq. 5.18)}$$

is the classical signal-to-noise statistics within the temporal component.

3.2.4. Model inference and posterior estimates

Inference challenge is solved using standard Bayesian Markov chain Monte Carlo methods (MCMC; Gilks et al., 1995). Classical poorly informative *priors* were used, with the common assumption of *a priori* independence between the *prior* marginal distributions of each parameter. Robustness of the inferences was checked on long simulation runs using tests based on starting different simulation runs at different points of the parameter space (Brooks and Gelman, 1998). The posterior distributions of all variance ratios were evaluated by computing their values at each point of the MCMC sequence. In addition, we also evaluated the posterior distributions of different avalanche numbers to be confronted to the actual total number of reconstructed avalanches: $y_{tot_i} = \sum_{t=1}^{T} y_{it}$ and $y_{tot} = \sum_{i=1}^{N} \sum_{t=1}^{T} y_{it}$ correspond to the number of avalanche which would have been reconstructed if there were no missing values in the chronologies, in each path of in total, respectively. In addition, sampling the predictive distribution $p(y_{iT}) = dBern(p_{iT})$ lead estimates of the total detrended avalanche activity at the path scale or all over the set of sampled paths. From all *posterior* distributions, we retained

posterior means as point estimates and 95% credibility intervals to evaluate the corresponding uncertainty.

3.3. Compilation of historical archives

At the site scale, the reliability of our regional tree-ring reconstruction was tested by graphical comparison with historical chronicles of snow avalanche compiled for Obergoms and Münster municipalities. Series were extracted from several documentary sources such as (i) local and regional newspapers (i.e. Confédéré, Walliser Bote, Le Nouvelliste, Journal et Feuille d'avis du Valais), ecclesiastical archives and stakeholder chronicles. In addition, (ii) the annual winter reports from the Institute for Snow and Avalanche Research (Institut für Schnee und Lawinenforschung–SLF), available since 1935 for the Goms Valley, and (iii) the historical database (1880–2015) from the Forschungsinstitut zür Geschichte des Alpenraums (FGA), as well as (iv) the Swiss-scale database from Laternser and Pfister (1997) were reviewed in detail.

3.4. Documentation of land cover changes and climatic fluctuations

The evolution of forest cover in the selected avalanche slopes – susceptible to reveal the occurrence of past destructive events and to interfere at decadal to centennial timescales with avalanche activity – was documented for the three studied avalanche slopes between 1881 and 2015 through the diachronic analysis of cartographic documents (Houghton et al., 2012). In detail, aerial flight campaigns of 1949 and 2015 – available from the Federal Office of Topography (Swisstopo; 1:20,000) – and the Siegfried map (Obergesteln, 490, edition 1881) of 1881 were digitized. The evolution of surfaces covered by forest at each slope was then computed for 100-m elevation bands using ArcGIS (ESRI, 2013; Kennedy, 2013).

Finally, potential climatic linkages were deciphered by comparing snow avalanche activity to climatic records from Andermatt (46°38'N, 8°35'E; 1438 m asl), uninterrupted since 1875 (temperature) and 1881 (precipitation). To this end, the decadal snow avalanche activity (p'_{smooth}) was regressed against smoothed mean winter (DJFMAM) temperature and precipitation totals – processed using a low pass filter (Yang and Zurbenko, 2010).

4. Results

4.1. Age structure and land cover changes

In total, 525 (51.8%), 275 (27.1%) and 214 (21.1%) trees were sampled at Oberwald, Geschinen and Münster slopes (see Tab. 5.1). After cross-dating, sampled trees aged on average 204 years (SD ±113 yr., Tab. 5.1). The oldest and youngest trees were sampled in Geschinen (GE2) and Oberwald (OB3) (Fig. 5.3). They reached sampling height in 1336 and

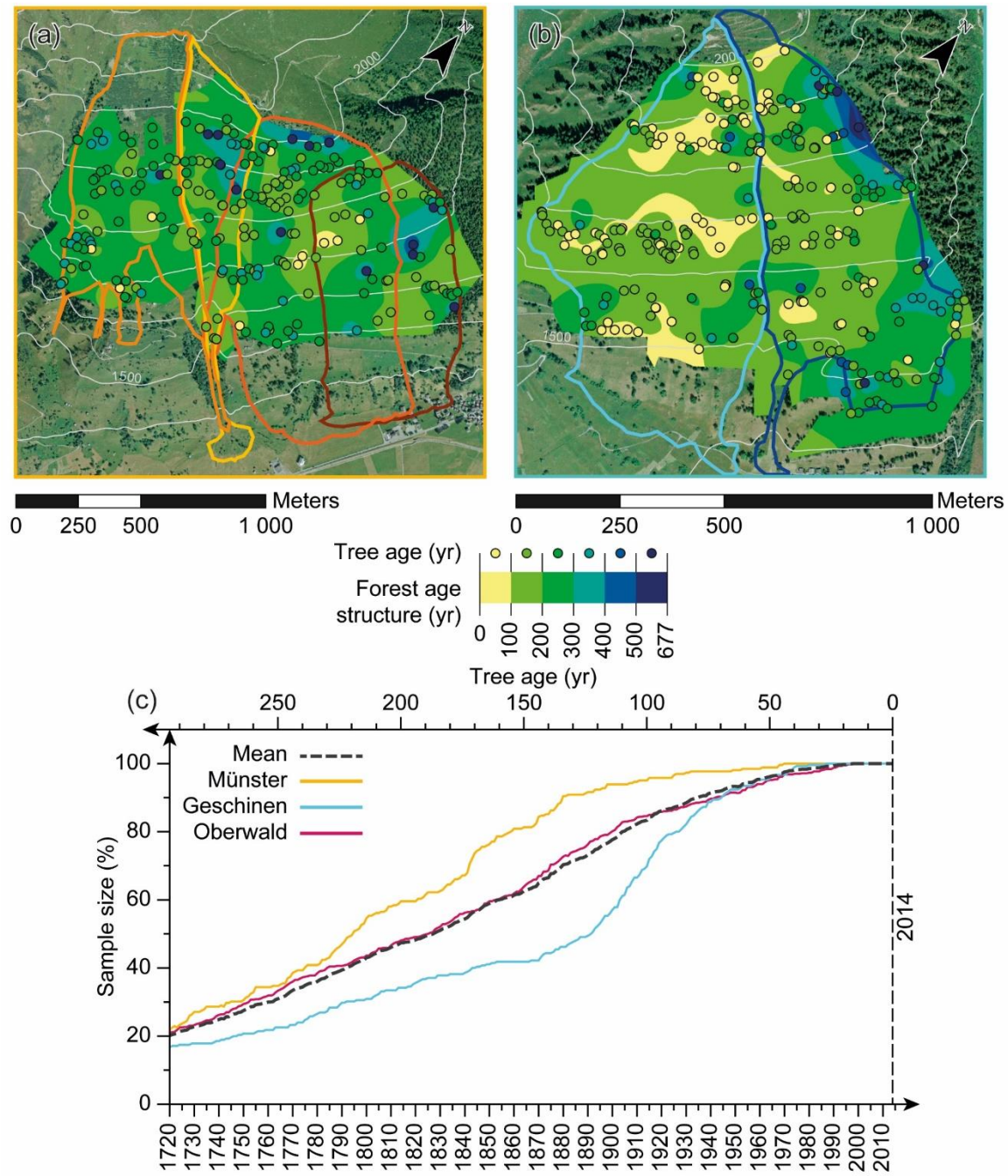

Figure 5.3 – Age structure of the forest stands growing in the Goms valley: spatial distribution of individual tree and interpolated age at Münster (a) and Geschinen (b); (c) evolution of the sample size at the three avalanche slopes. The black dashed line represents the mean sample size evolution. Age structure maps and spatial distribution of sampled trees for Oberwald are given in Favillier et al. (2017).

1998. At Munster and Oberwald, the forest stands are dominated 100–300-yr old trees (68.0%). By contrast, 0–100-year-old trees, have been scarcely sampled and do not show any specific pattern suggesting forest recolonization after high-magnitude events. At Geschinen, and more specifically at GE1, the tree stand is younger and 57.8% of sampled trees are <150 years. Figure 5.3 confirms the continuous densification of the forest stand at Münster and Oberwald between 1720 and 1900 but clearly shows an abrupt increase of the sample size between 1900 and 1940 at Geschinen.

The comparison of aerial photographs and maps for the period 1881–2015 shows significant variations in the extent of the forest stands, especially in Geschinen (Fig. 5.4). According to the Siegfried map – dated back to 1881 – the surfaces covered by forest stands were 102.1, 17.3 and 114.4 ha for Münster, Geschinen and Oberwald avalanche slopes, respectively. Between 1881 and 2015, the forest cover increases by 13.9 ha at Münster in relation with an upslope colonisation process above 1800-m asl. Below this altitudinal limit, the forest expansion is more limited and is related to the closure of the avalanche channels. Comparable evolution is observed at OB where forest areas increase of 12.5 ha and 10 ha below 1500 m and above 1800 m asl, respectively, between 1881 and 2015. By contrast, at GE paths, the forest surface almost doubled between 1881 (17.3 ha) and 1945 (32.9ha) as well as between 1945 and 2015 (58.8 ha). Highest afforestation rates were observed above 1700 m asl where forest cover has been multiplied by 20 between 1881 and 2015.

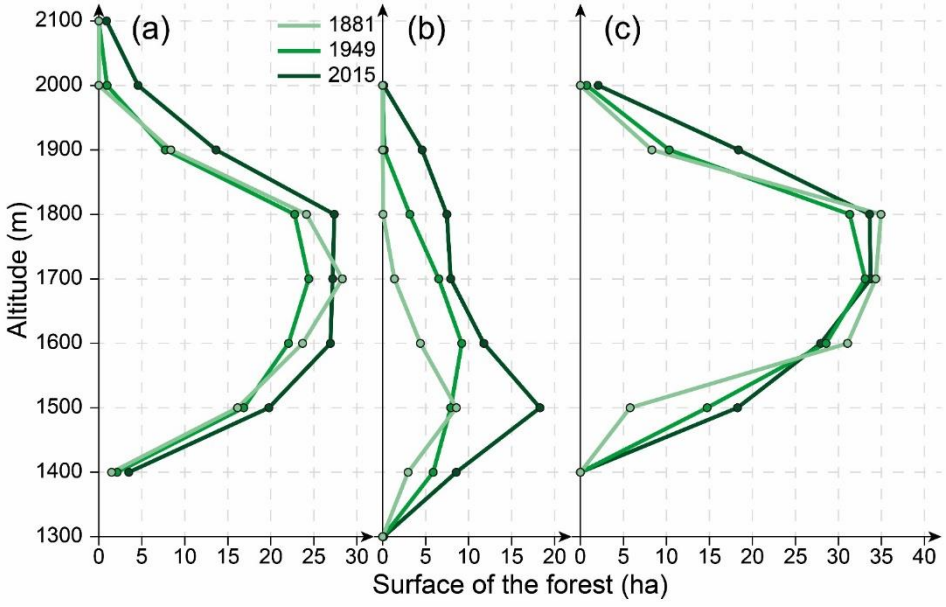

Figure 5.4 – Evolution of the forest cover (1881-2015) at (a) Münster, (b) Geschinen and (c) Oberwald.

Table 5.2 – Intensity and types of growth disturbances (GD) identified in the 1014 sampled trees.

Type	Intensity	MU 1	MU 2	MU 3	MU 4	GE 1	GE 2	OB 1	OB 2	OB 3	OB 4	OB 5	Total
Injuries	very strong	4	1	9	8	14	10	8	12	9	18	8	101 (1.8%)
TRD, CT and CW	strong	15	13	28	16	82	85	58	71	45	57	46	516 (9.4%)
	medium	60	45	78	50	125	120	88	77	47	74	36	800 (14.5%)
	weak	129	114	192	132	331	287	270	211	60	125	65	1916 (34.8%)
GS	strong	19	8	21	14	26	22	30	29	27	48	29	273 (5.0%)
	medium	90	37	99	59	134	130	67	75	70	119	55	935 (17.0%)
	weak	29	16	56	32	92	116	176	110	73	191	70	961 (17.5%)
Total		**346 (6.3%)**	**234 (4.3%)**	**483 (8.8%)**	**311 (5.7%)**	**804 (14.6%)**	**770 (14.0%)**	**697 (12.7%)**	**585 (10.6%)**	**331 (6.0%)**	**632 (11.5%)**	**309 (5.6%)**	**5502 (100%)**

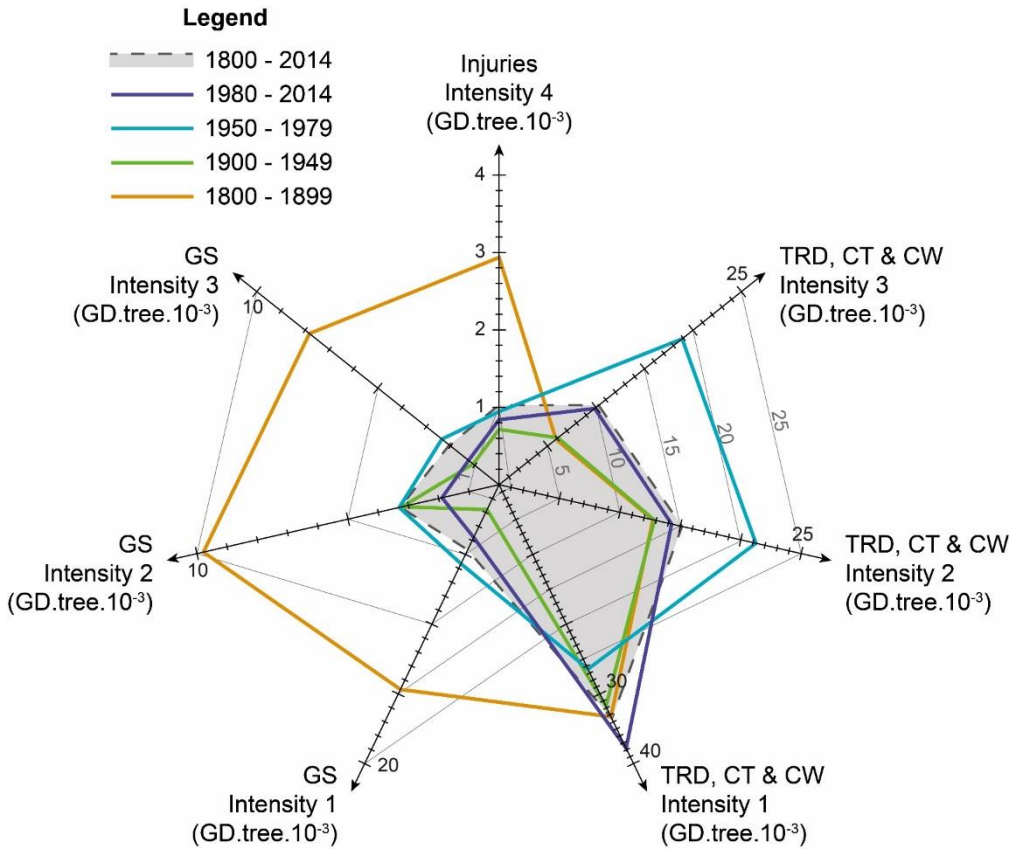

Figure 5.5 – Radar chart showing the distributions of GD types and intensities between 1800 and 2014. The figure only shows GDs attributed to snow avalanche events.

4.2. Growth disturbances and snow avalanche activity

In total, 5,502 GDs (1511 at MU, 1650at GE and the 2764 used for OB reconstructions, Favillier et al., 2017 – chapter 1) were identified in the tree-ring series. Table 5.2 summarizes the types and the intensity of GDs by path. TRDs, CT and CW were the most frequent (58.7%) GDs identified within the samples followed by growth suppression (39.4%). By contrast, only 101 injuries were sampled. In total 52.3% of the GDs were rated as weak (intensity 1) and 31.5% as medium (intensity 2). Strong GDs and injuries, rated intensities 3 and 4, represent 14.3% and 1.8% of the total number of GDs, respectively. The oldest GD identified in tree-ring series dated back to 1383. For 9 out of 11 paths, the frequencies of GDs range between 0.032 and 0.043 $GD.yr^{-1}$ (mean = 0.041). The lowest frequency was computed at OB5 (0.027 $GD.yr^{-1}$), the highest at GES1 (0.060 $GD.yr^{-1}$). The number of GDs detected in tree-ring series only slightly increases from 0.018 $GD.tree^{-1}.yr^{-1}$ for the 19th century to 0.029 $GD.tree^{-1}.yr^{-1}$ for the period 1980-2014. By contrast, the spectra of GDs used to reconstruct avalanche events show a clear overrepresentation of growth suppressions (GS) during the late 19th century (Fig. 5.5). For the periods 1900–1949 and 1980–2014, a majority of TRDs, CT and CW with weak to medium intensities were retrieved in the tree-ring series. By contrast, between 1950 and 1979, growth disturbances were more intense (Fig. 5.5).

On the basis of our 4-step procedure, these disturbances allowed for the identification of 107 events (73 avalanche years) between 1720 and 2014 at the 11 avalanche paths (Fig. 5.6). The oldest (1772) and the most recent events (2014) were recorded at the GE2. In total, 43 snow avalanches (40.2%) were identified at OB (5 paths), 24 (22.4%) at MU (4 paths) and 40 (37.4%) at GE (2 paths). At the path scales, higher snow avalanche frequencies were computed at GE1 (23 events between 1795 and 2009), and GE2 (17 events, 1772–2013). By contrast, 0, 5 (1794–2012), 4 (1911–1994) and 6 events (1834-2006) were retrieved at OB5, MU1, MU3 and MU4, respectively.

At step 2 of our procedure, 90 potential events that coincide with LBM outbreak episodes or extreme climatic years were detected. Amongst these potential events, 60 were excluded from the reconstruction and 30 were rated with a LLC. At step 3, 13 and 18 events were rated with HLC and MLC, respectively. By comparison, 76 events with a Wit<0.2 – characterized by a majority of weak and medium GDs – were reconstructed with a LLC. Events rated with high and medium level of confidence were mainly retrieved at GE1 (4 HLC, 3 MLC) OB4 (3 HLC, 4 MLC), OB3 (2 HLC, 4 MCL). By contrast, GDs were less frequent and less intense at GE2 (15 LLC), OB1 (10 LLC), OB2 (9 LLC) and MU2 (7 LLC).

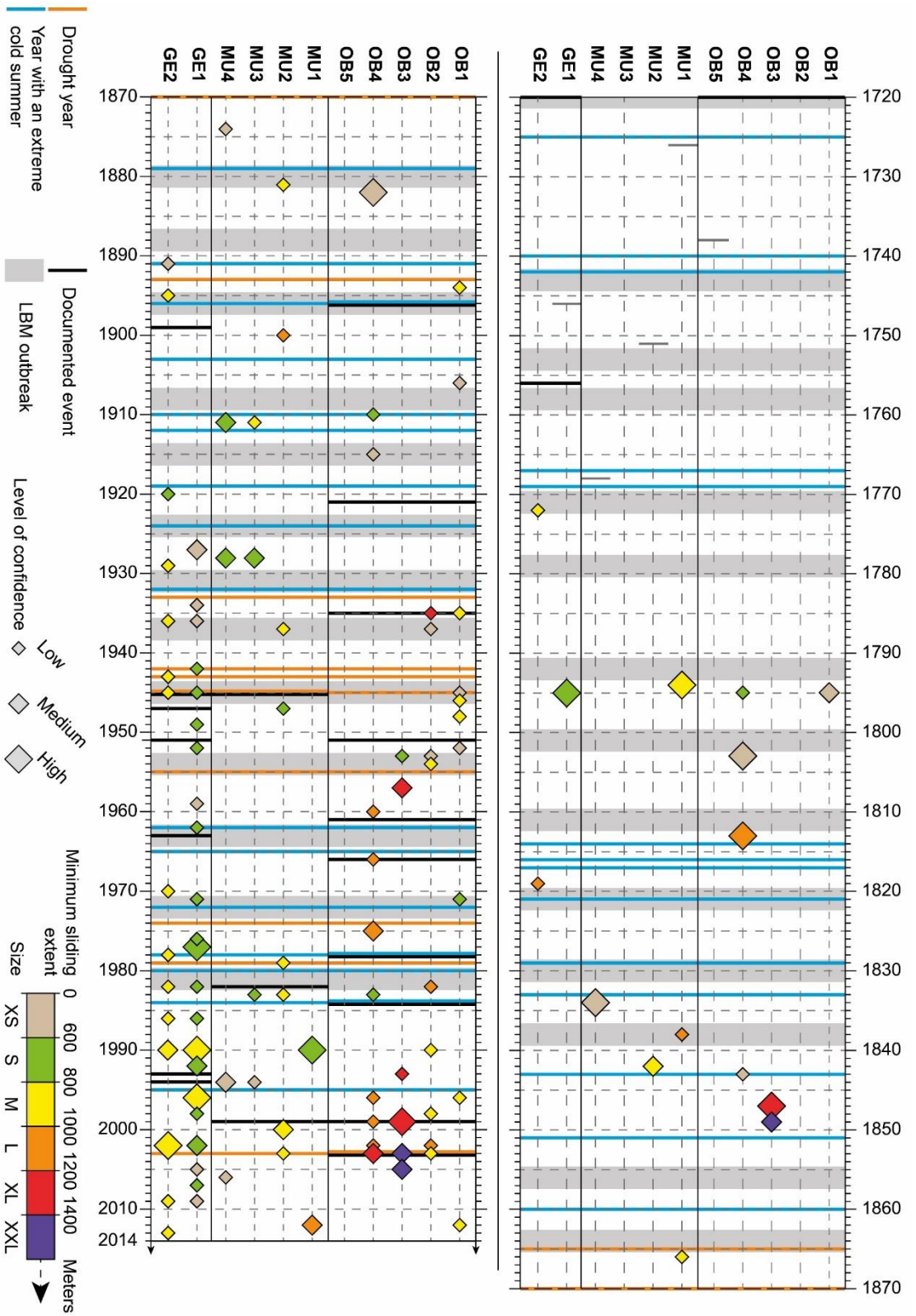

Figure 5.6 – Avalanche events reconstructed for the period 1720–2014 in studied avalanche paths based on the 4-step procedure developed by Favillier et al. (2017 – chapter 1). Symbol sizes are proportional to the level of confidence. The colour range highlights the minimum slide extent determined from the position of impacted trees. Grey bands represent triplets of years associated to LBM outbreaks. Vertical lines show snow avalanche events documented in site-specific historical chronicles (black), as well as extremely dry (orange) and cold (blue) summers.

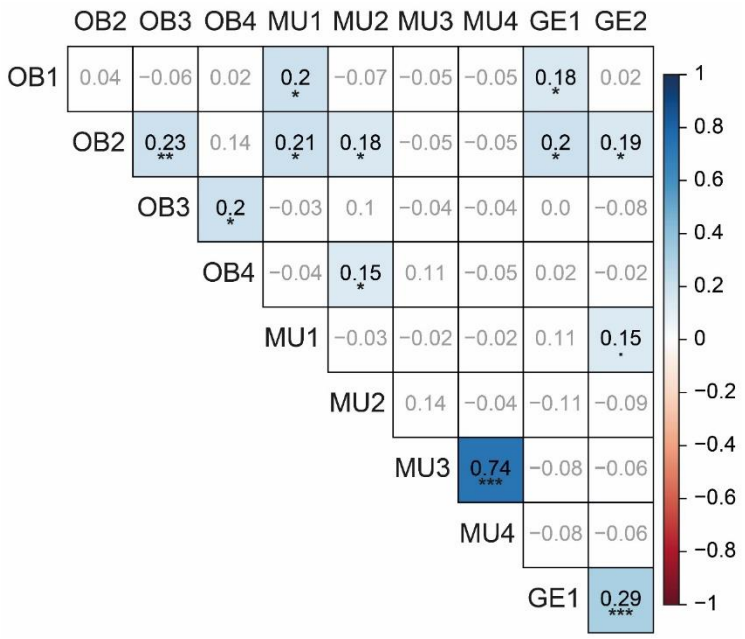

Figure 5.7 – Comparison of raw snow avalanche activity at path scale for the period 1880–2014. Non-significant correlation coefficients are in gray. Significance levels are rated by a **.** (α=0,1), ***** (α=0,05), ****** (α=0,01), ******* (α=0,001).

At the Goms valley scale, the chronology was considered as robust since 1880 when the sample size exceeded 60% (Fig. 5.3). In total, 91 events were reconstructed, for the period 1880–2014. Mean recurrence interval – which represents the mean time period between two avalanche events – is 1.5 yr. (6.51 event.decade^{-1}). Higher decadal frequencies are observed for the periods 1940–1949 (9 events), 1970–1979 and 1980–1989 (8 events). By comparison, lower decadal activities were observed during the periods 1880–1889 (2 events), 1900–1909 (2 events), 1890–1899 (3 events) and 1960–1969 (3 events).

The correlation matrix (Fig. 5.7) was computed between path reconstructions for the period 1880–2014. The highest correlation ($r > 0.74$, $\alpha < 0.001$) was computed between MU3 and MU4 chronologies. Lower ($r \approx 0.2$) albeit significant correlations were calculated between OB2-OB3-OB4 and GE1-GE2. For its most part; the matrix shows weak and not statistically significant correlations thus demonstrating asynchronous variations of avalanche activity between paths and slopes.

4.3. Comparison with historical chronicles

Analysis of historical archives yielded data on 23 avalanche events (16 years) on the 10 studied paths for the period 1880-2014. In total, 5 (31% out the 16 avalanche years retrieved from site-specific historical chronicles were reconstructed from tree-ring records, namely in 1935 (OB2), 1945 (GE), 1966 (OB), 1999 (0B3) and 2003 (OB3). An insufficient number of GDs and/or possible interferences with external events (LBM outbreaks, cold

summer and drought) as well as limitations inherent to the dendrogeomorphic approach did not permit to retrieve witnesses for the other events. For example, although historical archives reported snow avalanches in 1951 on OB1, OB3 and GE1, no evidence from these high-magnitude events was observed in the tree-ring series.

At the same time, 202 avalanche events (65 avalanche years, Fig. 5.8) have been reported in the historical chronicles at the Obergoms municipality scale. In total, 35 out of the 65 years (54%) listed in the historical database were detected in tree-ring series. In addition, tree-ring and historical chronologies share 46 common years in which no avalanche event was reported. Pearson's Chi-squared test suggest that both avalanche chronologies are not independent ($\alpha < 0.05$). At the municipality scale, the collected database reveals that major avalanche winters occurred in 1896 (25), 1951 (13), 1967 (9), 1978 (8) and 1999 (29) (Fig. 5.8). Amongst these winters, only 1978 and 1999 have been reconstructed through tree-ring analysis with 1 (GE2) and 2 events (OB3, OB4), respectively (Figs. 5.7, 5.8). Conversely, extreme events in our reconstruction (1911, 1928, 1945, 1953, 1971, 1982, 1983, 1990, 1996 and 2002–2003) did not appear as exceptional in the archive database.

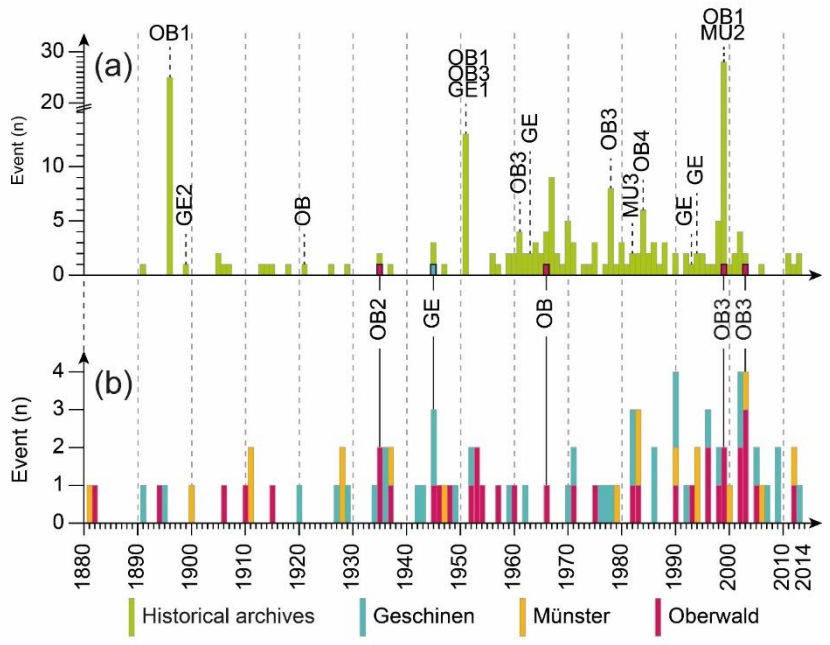

Figure 5.8 – Comparison of the historical archives with the snow avalanche chronology derived from tree-ring series. Green bars represent the number of snow avalanches recorded in the historical database. Blue, orange and pink bars indicate the number of snow avalanche events reconstruted at Geschinen, Münster and Oberwald, respectively.

4.4. Hierarchical modelling of snow avalanche activity at the regional scale

The Bayesian hierarchical model described in section 3.2 has been used in order to homogenise the regional snow avalanche reconstruction between 1880 and 2014 (Fig. 5.9). Global parameters of the model indicate that the variations of the dendrogeomorphic potential explain 41.1% of the variability in regional snow avalanche activity. The smoothed (decadal) temporal trend and the year-to-year fluctuations (p') of avalanche activity represent 37.9% and 5.7% of the modelled variability, respectively. Both components share 86.6% of common variability. Finally, the spatial component v_i only explains 15.3% of the variance.

In total, the Bayesian hierarchical model estimates that 2 events (with a 95% confidence level ranging from 0 to 28 events) on average were missed in the regional chronology due to the insufficient length of reconstructions OB2, OB3, MU3 and GE1. Including the decreasing dendrogeomorphic potential (e.g. decreasing sample size) in the past, the model estimates that 109 [78–150] snow avalanches, on average, occurred during the 1880–2014 period, which corresponds, after homogenization, to a mean annual snow avalanche probability p_0 of 0.054.

From a spatial point of view, the correction factor (1.2) used to compensate for decreasing dendrogeomorphic potential is maximum in GE1. On this path, POT increased from 0.65 in 1880 to 1 in 1987 (Fig. 5.10). On the other paths, the correction close to 0,

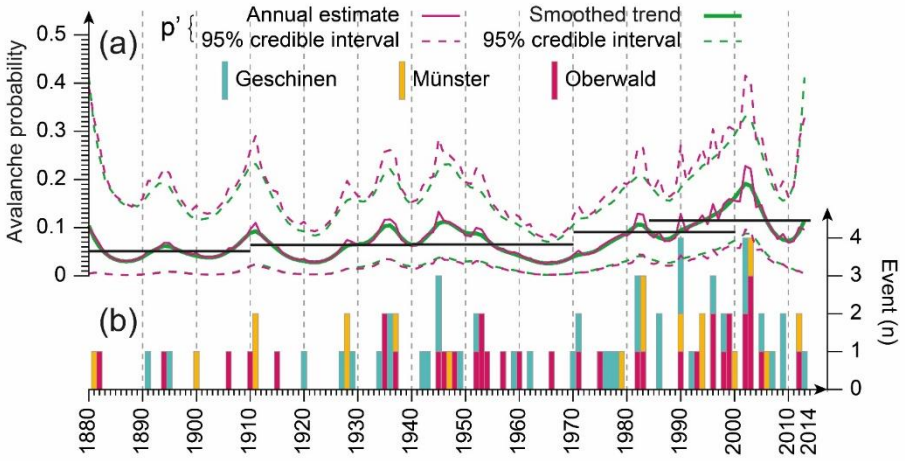

Figure 5.9 – (a) Regional snow avalanche activity computed from the dendrogeomorphological reconstruction using the hierarchical Bayesian approach. . The violet and green lines represent the annual and the decadal snow avalanche probability. Dashed lines indicate the 95% confidence level. The horizontal black lines represent the mean probability of snow avalanche computed form 30-yr periods. Reconstructed snow avalanche events are represented with blue, orange and purple bars for Geschinen, Münster and Oberwald slopes, respectively.

thus showing an absence of trend in tree-ring reconstruction related to decreasing sample size over time. For the latter, POTs exceed 0.8 since 1888. After detrending, GE1 (0.18, [0.10–0.30]), GE2 (0.08, [0.04–0.15]) and OB2 (0.07, [0.03–0.13]) paths are characterized by the higher snow avalanche probabilities. By contrast, lowest probabilities are modelled on MU4 (0.02, [0.00–0.05]), MU3 (0.02, [0.00–0.05]) and OB1 (0.05, [0.02–0.10]) paths (Fig. 5.10).

On a temporal plan, the years 2002 (p'=0.22), 2003 (0.22), 1999 (0.16), 2000 (0.15) and 2001 (0.15) have the higher annual probability of event (Fig. 5.9). By contrast, these probabilities are up to 10 times lower in 1965 (0.03), 1964 (0.03), 1967 (0.03), 1922 (0.03) and 1921 (0.03). At the decadal scale, the decades 1996-2005 (p'_{smooth} = 0.15), 1944–1953 (0.1) and 1906–1915 (0.08). Conversely, the periods 1883-1892 (p'_{smooth} = 0.03), 1918–1927 (0.03) and 1961–1970 (0.03) are characterized by significantly lower avalanche activity. Over the entire period, the 30-yr snow avalanche probability (Fig. 5.9) continuously increased from 0.052 (1880–1909) to 0.065 (1910–1939), 0.066 (1940–1969), 0.092 (1970–1999) and 0.12 (1985–2014). According to the Mann-Kendall test, this trend (+0.00046 per year) is statistically significant. One should yet keep in mind that uncertainties are on average 0.17 on the 1880–2014 period, with minimum and maximum

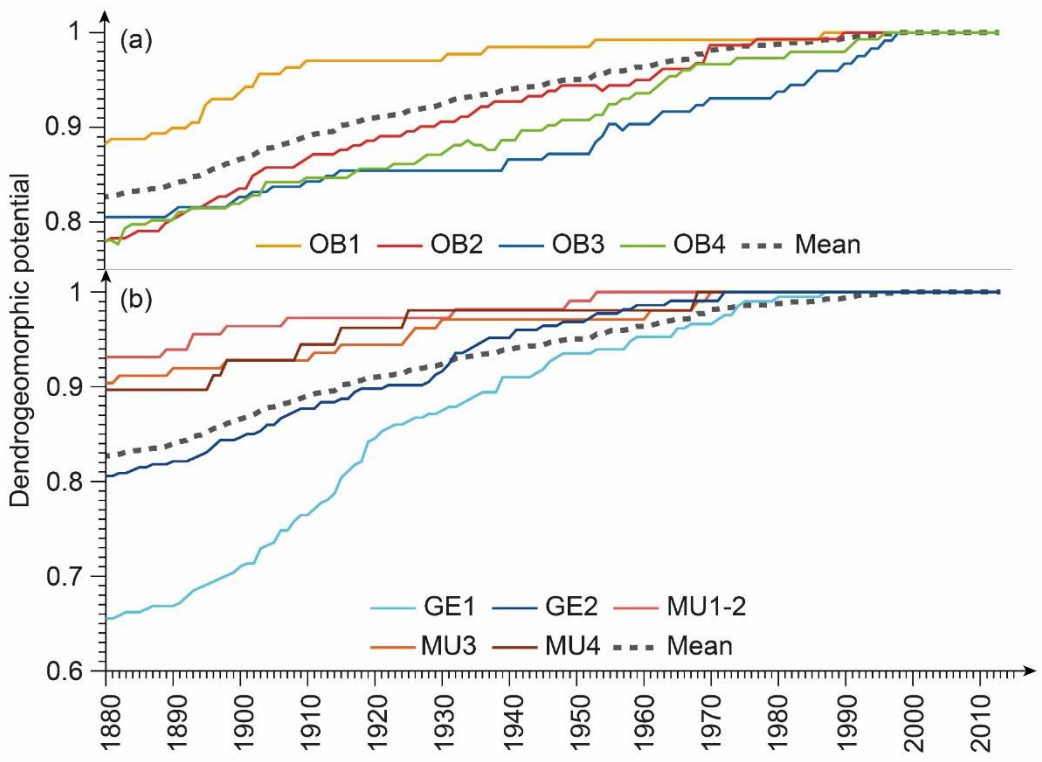

Figure 5.10 – Evolution of the dendrogeomorphic potential (POT) at (a) Oberwald, (b) Münster and Geschinen. The grey dashed line indicates the mean evolution of the dendrogeomorphic potential.

95% confidence intervals observed over the decades 1961–1969 (0.08) and 1996–2005 (0.25), respectively.

4.5. Impacts of climatic fluctuations on the regional avalanche activity

For the period 1881–2014, a significant correlation was computed between the decadal fluctuations of snow avalanche activity and smooth winter temperatures series from the Andermatt meteorological station ($r = 0.66$, $\alpha < 0.001$). A significant albeit weaker correlation was also computed with the precipitation records ($r = 0.24$, $\alpha < 0.01$). Despite these results, according to Figure 5.11, above-average probabilities of snow avalanches observed in the detrended reconstruction in 1996–2005, 1906–1915, 1928–1937 and 1944–1953 do not coincide obviously, with the exception of 1906–1915, with abnormally wet or cold decades. Similarly, the decades 1918–1927 and 1921–1970, both characterized by low avalanche activity, are characterized by differing climatic conditions wet and warm for the first one, cool with no clear precipitation anomaly for the second.

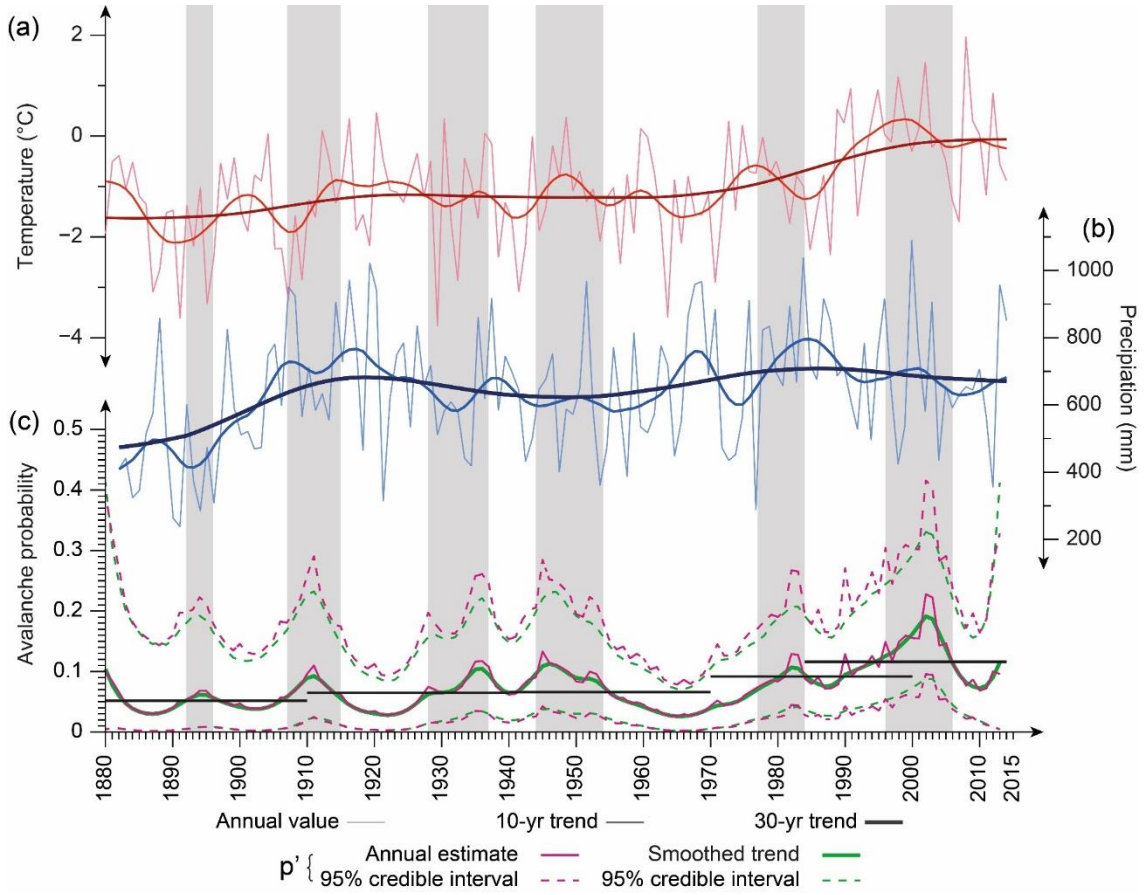

Figure 5.11 – Comparison of winter (a) mean temperatures and (b) precipitations fluctuations with (c) the standardized snow avalanche activity. The violet and green lines represent the annual and the decadal snow avalanche probability. Dashed lines indicate the 95% confidence level. The horizontal black lines represent the mean probability of snow avalanche computed form 30-yr periods.

5. Discussion

The study we report here aims at illustrating the multiplicity of signals embedded in a regional tree-ring reconstruction of snow avalanches. To meet this objective, a 60% new (with respect to Favillier et al., 2017 – chapter 1), unique (with respect to the number of paths included and the period covered) and breakthrough (with respect to the methodology used to homogenize avalanche records) regional tree-ring reconstruction was elaborated from 1014 multi-centennial old trees sampled on 11 avalanche paths located in the Goms Valley (Swiss Alps). Events were detected at the path scale using the procedure developed by Favillier et al. (2017 – chapter 1) that enables to (1) disentangle snow avalanche signals in tree-ring series from other external disturbances and (2) associate a qualitative level of confidence to each reconstructed event. Based on this procedure, 107 snow avalanche events were reconstructed in 73 different avalanche years between 1720 and 2014. Most previous studies (Germain et al., 2008; Decaulne et al. 2012, 2014; Voiculescu et al., 2016; Martin and Germain, 2017) discriminated avalanche/non avalanche years on the basis of an arbitrary threshold for the proportion of disturbed trees at the regional scale. Unlike these studies, we used a Bayesian hierarchical model that provides a reliable estimate of the temporal (interannual and decadal) variations of avalanche activity free from local artefacts so that no threshold needs to be set to distinguish active/inactive years. The advantages and drawbacks of this modelling approach, briefly summarized in the methodological section of this paper, have been extensively discussed in Jomelli et al. (2015).

Here, this model includes a new, specifically developed, hierarchical spatio-temporal logistic regression approach designed to remove potential trends in tree-ring based avalanche chronologies related to the increasing number of living trees during recent decades. According to this regression, over the period 1880-2014, only 18 events were potentially missed in the regional chronology. This limited number of missed events results from high dendrogeomorphic potentials that exceed 0.8 in 9 out of 10 avalanche paths since 1888. The way the model is constructed makes the spatial component (v_i) and the temporal component ($g_t + z_t$) independent. Variance ratios computed to evaluate the respective weight of the different terms in the modelled variability of avalanche probabilities reveal that the temporal term explains a larger part of the total variability of reconstructed avalanche occurrences (44%) than the spatial term (15%). According to the homogenized reconstruction, the decadal fluctuations of avalanche activity remain limited over the 20th century and shared a high common proportion of variance with interannual fluctuations.

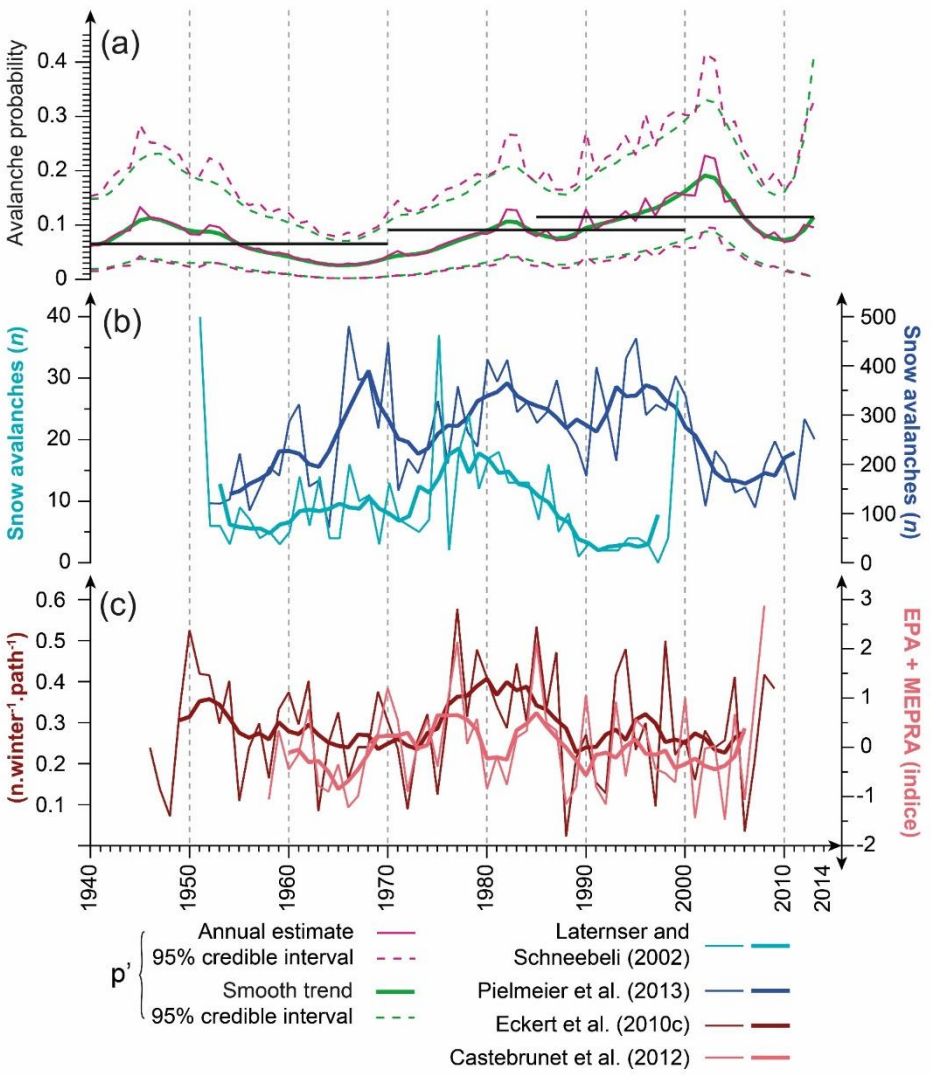

Figure 5.12 – Comparison between (a) the regional avalanche activity and (b) the avalanche activity indicators for the Swiss (Laternser and Schneebeli, 2002; Pielmeier et al., 2013) (c) and French (Castebrunet et al., 2012; Eckert et al., 2010c) Alps. . The violet and green lines represent the annual and the decadal snow avalanche probability. Dashed lines indicate the 95% confidence level. The horizontal black lines represent the mean probability of snow avalanche computed form 30-yr periods.

Since the mid-20th century, our reconstruction thus shows a minimum in avalanche probabilities during the decades 1961–1970 and a maximum between 1996 and 2005.

Despite the stringency of our approach with respect to the detection of past events and our efforts to extract a common signal from the regional reconstruction, the comparisons with historical archives, meteorological series and several snow avalanche chronologies available for Switzerland and the French Alps are poorly conclusive (Fig. 5.12):

(i) The rate of convergence (31%) at Goms is significantly lower than those reported by previous studies made in the French Alps by Corona et al. (2012, 43%), Corona et al. (2013, 43%), Schläppy et al. (2013, 38%), Schläppy et al. (2014, 33-45%) and de Bouchard

d'Aubeterre et al. (2019 – chapter 3, >70%). We assume that our reconstruction only represents a partial record of the complete avalanche activity (Casteller et al., 2011; Corona et al., 2012, 2013; Favillier et al., 2018 – chapter 2) that strongly underestimates the frequency of (extreme destructive) events.

(ii) The correlation between the homogenized chronology and series from the Andermatt meteorological station failed to identify precipitation totals as robust climatic drivers for the reconstructed evolution. In addition, we hypothesize that the positive significant correlation computed between the decadal fluctuations of avalanche activity and winter temperatures is an artifact that may result from comparable increasing trends existing in the tree-ring reconstruction – resulting from an underestimation of snow avalanche activity in the late 19th, early 20th century – and in winter temperatures. Yet, owing to the absence of significant trend in the GD spectra (Fig. 5.5) – similar to those evidenced by Trappmann and Stoffel (2013), Ballesteros-Cánovas et al. (2018) and Favillier et al. (2017) – the stringency of the statistical framework used to detrend the tree-ring chronologies, and the upper elevation of the release areas of the studied paths (>2300 m), we cannot exclude that the trend observed in the regional chronology might result from global warming. Increasing air temperatures in winter and early spring could have favored the wetting of snow and an increasing proportion of wet snow avalanches (Pielmeier et al., 2013, Ballesteros-Cánovas et al., 2018) recorded in trees. In the absence of snow cover series at the vicinity of the release areas of the studied path, the distinction between correlation and causality yet remains difficult.

(iii) Finally, the fluctuations of avalanche activity reconstructed from tree-ring analysis are only partly in line with other alpine studies (Fig. 5.12) from Eckert et al. (2013), that point to a decrease in avalanche activity in systematic inventories during the 1960s and from Schneebeli et al. (1997), Laternser and Schneebeli (2002), Eckert et al. (2013) and Pielmeier et al. (2013) that failed to detect a significant trend in the number of winters with low/high activity in the French and the Swiss Alps since the 1990s. Even though increasing avalanche activity could not be exluded given the elevation of the release areas of the studied paths (Lavigne et al., 2012), this absence of decreasing trend since the 1990s is rather surprising as (i) important efforts have been made in the course of the 20th century to install countermeasures designed to limit avalanche activity in the majority of the studied paths, especially after the second world war, (ii) an increase and a densification of the forest cover in the upper part of the avalanche couloirs at MU, OB and especially GE has been documented since the end of the 19th century.

6. Conclusion

In this study, we used dendrogeomorphic techniques to document past avalanche activity in 11 avalanche paths from the Goms Valley (Swiss Alps). The 4-step procedure designed by Favillier et al. (2017 – chapter 1) with the specific purpose to disentangle signals related to snow avalanche from other ecological disturbances (climatic extremes and larch budmoth outbreaks) enabled to reconstruct snow avalanche activity, at the path scale, since 1880 but show a clear increasing trend since the 1980s. In order to remove this trend, potentially related to the increasing number of trees over time and to extract common fluctuations from the regional chronology, a specific statistical framework based on hierarchical Bayesian modelling has been developed. Despite the stringency of this approach, the homogenized regional avalanche chronology does not portray a clear climatic signal and only show a poor convergence with avalanche chronicles existing for the Obergoms valley as well as for the Swiss and French Alps. This limited synchronicity with other records question the use of our chronology, and more generally of tree-ring reconstructions, to document the impacts of climatic fluctuations on snow avalanche activity. In particular, they raise the issue of the number of paths to be aggregated to derive a tree-ring reconstruction sufficiently robust to portray a climatic signal. In that sense, our study suggests that 10 paths – number that exceeds a large majority of previously published studies – are not enough to represent the spatio-temporal variability of the Goms valley and plaids for the inclusion of more sites in future researches. Similarly, the aggregation of poorly correlated path reconstructions (Fig. 5.7), with asynchronous non-stationarities related to e.g. afforestation, has probably hampered a robust detection of the climatic signal in our reconstruction. For this reason, we really believe that the implementation of a sampling strategy at the regional scale will be a crucial prerequisite to improve the robustness of future studies.

CHAPITRE 6

Impacts des fluctuations climatiques sur l'activité des avalanches dans le Queyras

1. Introduction

Dans les espaces de montagne, les avalanches constituent un aléa majeur qui cause chaque année des dommages aux infrastructures, aux bâtiments, aux voies de communication et aux populations (Fuchs et al., 2007, 2004; Schneebeli et al., 1997). Elles se caractérisent par un écoulement gravitaire rapide de neige dont le déclenchement et la rhéologie résultent d'interactions complexes entre la topographie, l'occupation du sol, le manteau neigeux et les paramètres météorologiques (Ancey, 2006; Jomelli et al., 2007; Schweizer, 2003).

De nombreuses études ont mis en évidence les impacts du réchauffement climatique récent sur le régime nivo-météorologique (Beniston et al., 2018; IPCC, 2013), la mise en place, la structure et la persistance du manteau neigeux (Beniston, 1997; Uhlmann et al., 2009). Dans les Alpes, le réchauffement observé est près de deux fois supérieur à celui observé à l'échelle globale depuis la fin du 19ème siècle (Auer et al., 2007; IPCC, 2014, 2013) – avec une augmentation des températures pouvant atteindre localement +1,7°C (Gobiet et al., 2014). La diminution du manteau neigeux est observée dans toutes les tranches altitudinales mais est particulièrement importante entre 1500 et 2500 mètres d'altitude, où la température conditionne fortement la nature des précipitations (Jomelli et al., 2004). Un nombre croissant d'hivers chauds et humides, tels que l'hiver 2017–2018 (Stoffel et Corona, 2018), caractérisé par un enneigement déficitaire a ainsi été observé dans cette tranche d'altitude au cours des dernières décennies. Il a été démontré, de manière théorique et empirique, que cette évolution du climat induit des modifications de l'activité des avalanches (Mock et Birkeland, 2000). L'analyse statistique des données contenues dans l'Enquête Permanente sur les Avalanches (EPA ; Bourova et al., 2016; Mougin, 1922) a permis de mettre en évidence une augmentation de l'altitude atteinte par les avalanches de forte magnitude depuis les années 1980 (Eckert et al., 2013, 2010a). De même, une augmentation de la proportion d'avalanches de neige humide a été observée par Eckert et al. (2013) et Naaim et al. (2016) depuis le début des années 1970, dans les Alpes françaises. Toutefois, bien que significatives, ces tendances sont limitées par la durée des données historiques, très lacunaires avant les années 1950.

A l'échelle pluriséculaire, les approches lichénométrique (Jomelli et Pech, 2004; McCarroll, 1993) et sédimento-palynologique (Fouinat et al., 2018; Nesje et al., 2007; Vasskog et al., 2011) suggèrent une augmentation de la fréquence des avalanches dans le Nord et l'Ouest de l'Europe durant le Petit Age Glaciaire. Néanmoins la portée de ces études est limitée par leur résolution temporelle (décennale à séculaire) et leur extension

spatiale (un seul versant). Les archives historiques ne permettent pas de mettre en évidence de relations significatives entre l'activité avalancheuse et les fluctuations climatiques en raison de leur caractère discontinu, souvent lacunaire et centré sur les événements extrêmes (Casteller et al., 2011; Corona et al., 2012; Ibsen et Brunsden, 1996; Laternser et Pfister, 1997).

Sur les versants forestiers, la dendrogéomorphologie (Alestalo, 1971; Stoffel et al., 2010; Stoffel et Corona, 2014; Favillier et al., 2017 – chapitre 1, 2018 – chapitre 2) permet de reconstruire en continu l'activité des avalanches, à l'échelle pluriséculaire, avec une résolution annuelle (Butler et Sawyer, 2008). Sur la base de ces reconstructions, plusieurs études ont cherché à mettre en évidence les covariables nivo-météorologiques expliquant les variations interannuelles de l'activité avalancheuse (se reporter à la figure 5.1 pour une synthèse détaillée). En revanche, à l'exception de Ballesteros-Cánovas et al. (2018) – qui démontrent une corrélation significative entre l'augmentation du nombre d'avalanches observées sur un versant himalayen et l'augmentation des températures hivernales moyennes depuis le début des années 1970 – l'impact des fluctuations climatiques sur l'activité des avalanches a rarement été analysé. Cette lacune s'explique en partie par (i) le caractère local des études majoritairement réalisées sur un seul versant ou un nombre restreint de couloirs, ce qui ne permet pas de s'affranchir des caractéristiques locales ; (ii) l'absence de prise en compte de non-stationnarités liées à l'approche dendrogéomorphologique (de Bouchard d'Aubeterre et al., 2019 – chapitre 3 ; Mainieri et al., sous presse – chapitre 4) ou de potentielles interférences entre la dynamique avalancheuse, les changements de l'occupation des sols et les fluctuations climatiques (García-Hernández et al., 2017; Giacona et al., 2017; Mainieri et al., sous presse – chapitre 4) ; (iii) la période couverte par les reconstructions, qui excède rarement un siècle, ne permet pas de documenter l'activité avalancheuse des dernières décennies avec des périodes très différentes d'un point de vue climatique, telles que la période préindustrielle ou les phases froides du Petit Age Glaciaire.

Dans ce contexte, afin de cerner l'impact du réchauffement climatique récent sur l'activité des avalanches, (i) les reconstructions dendrogéomorphologiques obtenues sur les 10 couloirs des versants de Souliers (Mainieri et al., sous presse – chapitre 4) et du ravin de la Salce (de Bouchard d'Aubeterre, 2019 – chapitre 3) et sur le couloir de l'Echalp (Corona et al., 2013) ont été agrégées en une reconstruction régionale couvrant le massif du Queyras (Alpes françaises) ; (ii) cette reconstruction a été homogénéisée au moyen d'une approche bayésienne hiérarchique développée pour la vallée de Goms (chapitre 5)

afin de corriger les tendances induites par la diminution du potentiel dendrogéomorphologique dans le passé ; enfin, (iii) les variations décennales à centennales détectées dans la reconstruction homogénéisée ont été comparées aux fluctuations des températures moyennes et des totaux pluviométriques hivernaux.

2. Sites d'étude

Afin de reconstruire l'activité des avalanches, deux secteurs ont été sélectionnés dans le massif du Queyras : le versant du Ravin de la Salce, dans la haute Vallée du Guil (chapitre 3 ; Fig. 6.1c) et la haute vallée de Souliers (chapitre 4 ; Fig. 6.1d).

2.1. Vallée du Haut Guil

Le versant du Ravin de la Salce est localisé à l'amont du hameau de l'Echalp, sur la rive droite du Guil (44°44'47''N, 6°59'42''E ; 1740 m d'altitude ; Fig. 6.1b, chapitre 3). Le versant s'étend depuis le talweg du Guil, à 1740 m, jusqu'à la crête des Baysses, à 2700 m d'altitude. La pente moyenne du versant est comprise entre 27 et 32° ; les pentes varient entre 20-25° dans la partie distale du versant et 35-40° dans les parties apicales. La géologie est dominée par des alternances schisto-calcaires avec la présence de plusieurs failles orientées Sud-Nord et Sud-Ouest-Nord-Est. Quatre couloirs d'avalanche, d'une longueur moyenne de 1428 m et d'une pente moyenne de 26°, ont été mis en évidence lors de l'analyse géomorphologique du versant. Les couloirs E1 et E2 sont sous-forêt, avec un sous-bois dominé par des espèces herbacées et des arbustes – en particulier le rhododendron ferrugineux (*Rhododendron ferrugineum* L.) et le myrtillier commun (*Vaccinium myrtillus* L.) –, depuis leurs zones de départ, situées entre 2110 et 2340 m d'altitude, pour une pente moyenne de 32°, jusqu'à leur zone de dépôt située à proximité immédiate du torrent du Guil, entre 1740 et 1750 m d'altitude. Les couloirs C1 et C2 sont majoritairement asylvatiques. Leurs zones de départ sont situées entre 2290 et 2620 m d'altitude et sont dépourvues de couvert ligneux. Les avalanches se déclenchant dans ces couloirs se déposent au niveau du talweg du Guil entre 1760 et 1790 m d'altitude.

2.2. Vallée de Souliers

Le versant de Souliers (chapitre 4) se situe à l'amont du hameau de Souliers dans la vallée du même nom (commune de Château-Ville-Vieille, Hautes Alpes) (Fig. 6.1a, c). Orienté vers l'ouest et d'une surface de 130,35 ha, ce versant, d'une longueur de 1500 mètres, s'étend de la bergerie de Souliers (2070 m), au pied du Grand Bois, jusqu'au Pré Soubeyran (1900 m, Fig. 6.1c). Son altitude est comprise entre 1900-2050 m au niveau du

talweg du torrent de Souliers et atteint 2400-2580 m au niveau de la Crête du Crépaud. Au total, sept zones de départ, situées entre 2300 m et 2580 m d'altitude et dont la pente moyenne est de 30,8°, ont été identifiées sur le versant de Souliers au moyen d'analyses géomorphologique et diachronique. Six couloirs avalancheux, forestiers, d'une longueur moyenne de de 900 m et d'une pente moyenne de 24° ont été délimités : quatre (S1-S4) sont limités à l'aval par le torrent de Souliers, deux (A1-A2) ont une zone de dépôt (pente moyenne 8°) située au lieu-dit Pré Soubeyran. Pour les deux versants, les caractéristiques de chaque couloir sont résumées dans le Tableau 6.1.

Les couloirs identifiés sont, pour la plupart, caractérisés par une zonation transversale de la végétation (Malanson et Butler, 1984). La zone centrale, où les périodes de retour sont les plus faibles, est en général colonisée par des espèces herbacées et des ligneux bas pionniers, héliophiles, tels que le sorbier européen (*Sorbus aucuparia* L.) ou le genévrier (*Juniperus comunis*). Dans les portions plus externes, où les avalanches sont moins fréquentes, la végétation forestière est exclusivement composée de mélèzes d'Europe (*Larix decidua* Mill), entre 2050 et 2400 m d'altitude. Le sous-bois est dominé par des

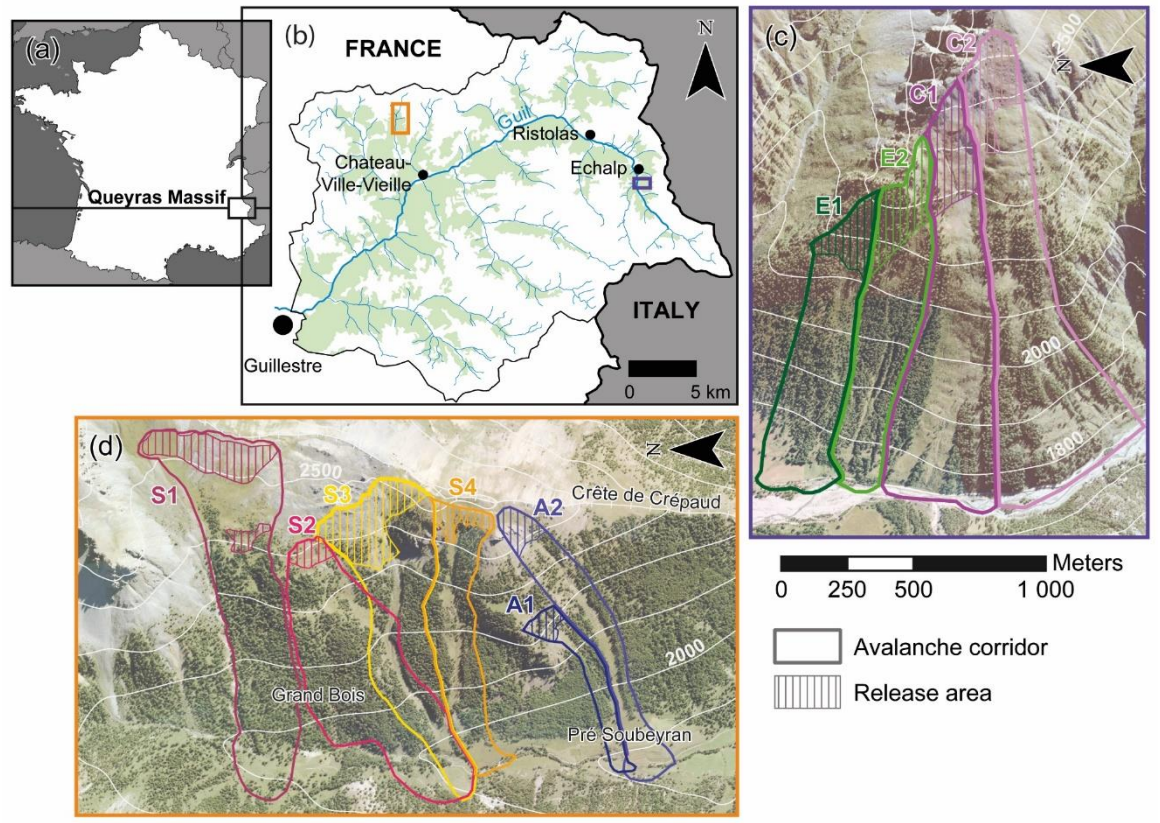

Figure 6.1 – Localisation des versants de (b) la haute vallée du Guil et de (c) de la vallée de Souliers, dans (a) le massif du Queyras, Hautes-Alpes, France.

Tableau 6.1 – Principales caractéristiques morphologiques des couloirs d'avalanches étudiés.

		Couloirs d'avalanche					Zone de départ			
Couloir		Expo.	Longueur (m)	Largeur moy. (m)	Surface (ha)	Pente moy. (°)	Alt. de départ. (m)	Alt. d'arrêt(m)	Pente moy. (°)	Surface (ha)
Souliers	S1	O	1231	250	39,1	22,4 (6,2)	2390–2570	2090	28,1 (±4,1)	7,9
	S2	O	990	350	35,6	24,8 (4,6)	2350–2420	1990	26,7 (±3,8)	1,5
	S3	O	1107	250	27,6	28,0 (7,7)	2300–2515	1990	31,1 (±6,9)	7,5
	S4	O	950	180	16,5	28,8 (7,5)	2380–2490	1990	29,6 (±8,8)	2,1
Ravin de la Salce	A1	S-O	695	92	6,02	27,0 (7,4)	2150–2250	1908	34,4 (±1,2)	1,2
	A2	S-O	1105	160	15,6	28,4 (7,9)	2375–2490	1908	34,8 (±5,3)	2,0
	E1	N-O	1240	240	19,7	25,1 (9,2)	2110–2200	1745	32,1 (±4,0)	4,3
	E2	N-O	1290	255	25,3	27,8 (5,6)	2140–2340	1745	32,2 (±5,1)	6,4
	C1	N-O	1580	300	42,0	26,4 (6,6)	2290–2520	1760	32,2 (±4,5)	6,9
	C2	N-O	1600	366	55,0	26,6 (7,3)	2430–2620	1790	32,5 (±5,3)	6,9
Echalp		O	1200	200	*n.p.*	32,0	2400	1700	36,0	*n.p.*

n.p. : non communiqué

espèces herbacées et des arbustes, notamment le rhododendron ferrugineux (*Rhododendron ferrugineum* L.) et le myrtillier commun (*Vaccinium myrtillus* L.).

Selon les données de la station météorologique la plus proche, située à Saint-Véran (44°41'54''N, 6°52'06''E, 2039 m, 1928–2019), la température annuelle est de 5,3°C et le cumul annuel de précipitations s'élève à 710 mm, pour la période 1980–2010. De décembre à avril, la température moyenne est de -0.2°C. Les précipitations cumulées atteignent 237 mm et tombent principalement sous forme de neige.

3. Matériel et méthodes

Ce chapitre décrit les méthodes statistiques employées pour analyser les relations entre l'activité des avalanches et les fluctuations du climat. En ce qui concerne, les reconstructions dendrogéomorphologiques, le lecteur se référera aux sections matériels et méthodes des chapitres précédents.

3.1. Estimation de l'activité régionale des avalanches

La régression logistique à double composante spatiale et temporelle présentée dans le chapitre 5 a été utilisée afin d'éliminer les tendances induites dans les reconstructions dendrogéomorphologiques par l'augmentation du nombre d'arbres vivant au cours des dernières décennies. Cette approche développée dans un cadre bayésien hiérarchique permet de standardiser et d'homogénéiser les reconstructions, préalables indispensables à une confrontation avec les données climatiques ou d'occupation des sols. Cette approche permet également, sur la base d'un lissage au moyen d'une régression non-paramétrique,

de distinguer l'activité interannuelle (p') et l'activité décennale des avalanches (p'_{smooth}). Elle est donc particulièrement adaptée à l'identification des co-variables nivo-météorologiques à l'origine des fluctuations interannuelles de l'activité avalancheuse mais également à la détection de tendance d'origine climatique. Les équations constituant le modèle bayésien hiérarchique utilisé sont décrites dans le chapitre 5, section 3.2.

3.2. Influence des fluctuations du climat sur l'activité avalancheuse

Afin de mettre en évidence les impacts des fluctuations du climat sur l'activité des avalanches dans le massif du Queyras : (i) les températures moyennes (1781-2014) et les cumuls mensuels de précipitations (1802-2014) ont été extraits de la base de données HISTALP (Efthymiadis et al., 2006) pour les points de grille les plus proches de chacun des versants (Souliers : 44°45'N, 6°45'E ; Ravin de la Salce : 44°45' N, 6°60'E) ; (ii) les moyennes de températures et les cumuls de précipitations hivernaux, pour les mois de décembre à mai (DJFMAM), ont été calculés à partir des données mensuelles puis transformées en z-score (nombre d'écarts-types au-dessus ou en dessous de la moyenne) ; (iii) les anomalies de températures et de précipitations (z-scores) ont été lissées au moyen d'un filtre passe-bas (Yang et Zurbenko, 2010) afin de mettre en évidence les fluctuations décennales ; (iv) les fluctuations décennales de l'activité avalancheuse (p'_{smooth}) ont été finalement corrélées avec les séries climatiques lissées.

4. Résultats

4.1. Structure d'âge des peuplements

Sur les versants étudiés, 1131 mélèzes d'Europe (*Larix decidua* Mill.) ont été échantillonnés au cours des automnes 2011 et 2016, puis durant l'été 2017 sur les versants de Souliers et du Ravin de la Salce (Tab. 6.2). Après interdatation, les arbres échantillonnés ont un âge moyen de 186 ans (±125 ans ; Tab. 6.2). L'individu le plus âgé, prélevé dans le couloir S2, a atteint la hauteur de prélèvement en 1382 ; le plus jeune (couloir E2) a atteint la hauteur d'échantillonnage en 2010. Les peuplements forestiers échantillonnés sont dominés par des individus de moins de 150 ans (46,3%). Néanmoins, 27% des arbres ont entre 200 et 300 ans, 16,4% ont plus de 300 ans et 7,2% plus de 400 ans. Le plus vieux peuplement forestier est situé sur le couloir S1 (306.1 ±122,1 ans), le plus jeune sur A1 (91,7 ±70,3 ans) (Tab. 6.2). La Figure 6.2 présente la cartographie de la structure d'âge des peuplements échantillonnés pour chaque couloir.

Tableau 6.2 – Caractéristiques des peuplements forestiers échantillonnés

Couloirs d'avalanche		Arbres (n)	Echantillons (n)	Âge moyen (a)
Souliers	S1	102		306,1 (±122,1)
	S2	208	428	229,1 (±122,0)
	S3	113 (+74)		225,2 (±128,0)
	S4	191	224	136,6 (±120,0)
	A1	71	75	91,7 (±70,3)
	A2	140	157	127,8 (±97,5)
	Sous-total	*824*	*884*	*190,0 (±132,4)*
Ravin de la Salce	E1	45	52	163,3 (±122,6)
	E2	121	127	201,3 (±105,6)
	C1	67	77	141,8 (±78,4)
	C2	73	86	148,7 (±88,6)
	Sous-total	*306*	*342*	*170,6 (±102,4)*
Echalp		163	366	402
Total		**1294**	**1592**	**198**

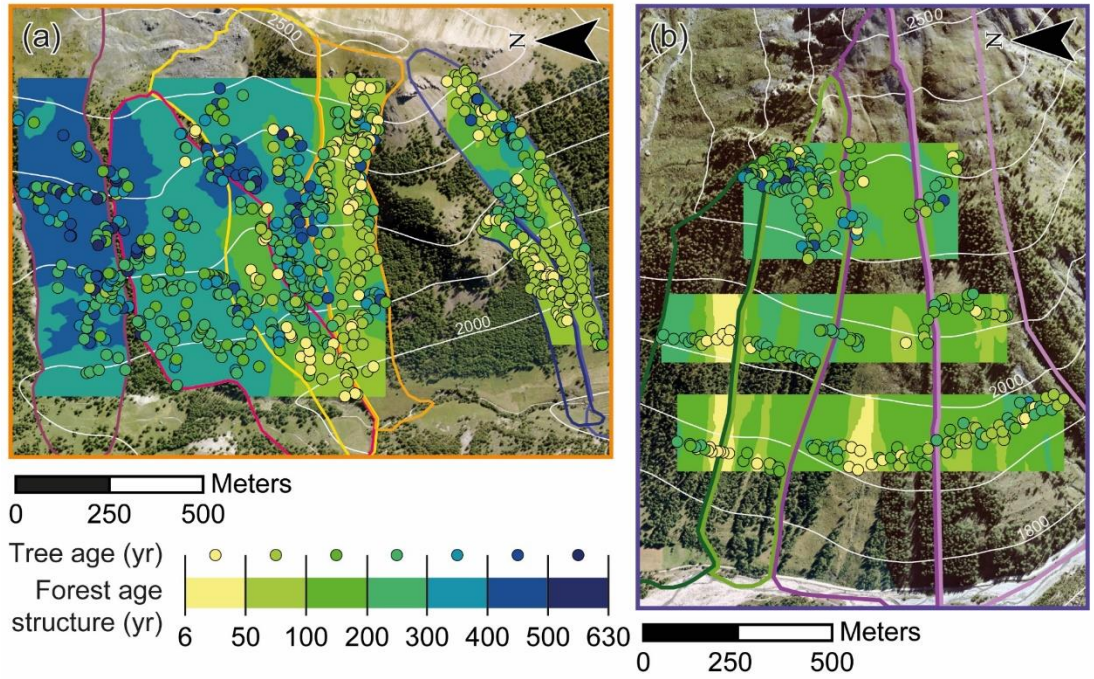

Figure 6.2 – Structure d'âge des populations forestières de (a) Souliers et du (b) Ravin de la Salce, Queyras, France.

4.2. Reconstruction de la chronologie des avalanches dans le Queyras

Au total 4 630 perturbations de croissance (GDs) ont été identifiées et datées dans les échantillons prélevés, 2986 à Souliers, 1644 sur le versant du Ravin de la Salce. Parmi ces perturbations de croissance, 1200, classées d'intensité 3 ou 4 sont considérées comme les meilleurs indicateurs de l'activité avalancheuse passée (1560-2016). Le Tableau 6.3 résume les types et l'intensité des perturbations de croissance pour chacun des couloirs. Les TRD (lignes tangentielles de canaux résinifères traumatiques), CT (le tissu calleux) et CW (le bois de compression) sont les perturbations les plus fréquemment observées (61,5%). Les réductions de croissance (GS) représentent 35,8% du total. Seules 122 cicatrices d'impacts (SC) ont été identifiées dans les séries de cernes de croissance. La majorité des perturbations identifiées sont d'intensité faible (1 ; 51,4%). Les perturbations de croissance d'intensités moyenne (classe 2) ou forte (classes 3 et 4) représentent respectivement 22,7%, 2,6% et 23,3% du total.

Tableau 6.3 – Type et intensité des perturbations de croissance (GD) détectées dans les 1131 mélèzes d'Europe échantillonnés pour chaque couloir des deux versants étudiés, pour la période 1560–2016. Les données non-précisées sont notées n.p.

			Perturbations mécaniques - TRD, CT, CW (n)			**Réductions de croissance (n)**			
Couloirs		**Cicatrice d'impact (n)**	Fort	Moyen	Faible	Fort	Moyen	Faible	**Total**
Souliers	S1	0 (0%)	56 (1,2%)	23 (0,5%)	29 (0,6%)	95 (2,1%)	60 (1,3%)	16 (0,3%)	279 (6%)
	S2	0 (0%)	79 (1,7%)	58 (1,3%)	90 (1,9%)	113 (2,4%)	113 (2,4%)	66 (1,4%)	519 (11,2%)
	S3	0 (0%)	87 (1,9%)	48 (1%)	61 (1,3%)	66 (1,4%)	92 (2%)	59 (1,3%)	413 (8,9%)
	S4	48 (1%)	90 (1,9%)	60 (1,3%)	229 (4,9%)	53 (1,1%)	97 (2,1%)	205 (4,4%)	782 (16,9%)
	A1	4 (0,1%)	31 (0,7%)	32 (0,7%)	133 (2,9%)	12 (0,3%)	12 (0,3%)	55 (1,2%)	279 (6%)
	A2	17 (0,4%)	92 (2%)	68 (1.5%)	324 (7%)	38 (0,8%)	59 (1,3%)	116 (2,5%)	714 (15,4%)
	Sous-total	*69 (1,5%)*	*435 (9,4%)*	*289 (6,3%)*	*866 (18,6%)*	*377 (8,1%)*	*433 (9,4%)*	*517 (11,1%)*	*2986 (64,4%)*
Ravin de la Salce	E1	10 (0,2%)	36 (0,8%)	30 (0,6%)	187 (4%)	28 (0,6%)	17 (0,4%)	49 (1,1%)	357 (7,7%)
	E2	14 (0,3%)	64 (1,4%)	111 (2,4%)	416 (9%)	31 (0,7%)	65 (1,4%)	80 (1,7%)	781 (16,9%)
	C1	12 (0,3%)	32 (0,7%)	36 (0,8%)	123 (2,7%)	10 (0,2%)	6 (0,1%)	13 (0,3%)	232 (5%)
	C2	17 (0,4%)	56 (1,2%)	51 (1,1%)	117 (2,5%)	9 (0,2%)	12 (0,3%)	12 (0,3%)	274 (5,9%)
	Sous-total	*53 (1,2%)*	*188 (4,1%)*	*228 (4,9%)*	*843 (18,2%)*	*78 (1,7%)*	*100 (2,2%)*	*154 (3,4%)*	*1644 (35,6%)*
	Echalp	*n.p.*	*n.p.*	*n.p.*	*n.p.*	*n.p.*	*n.p.*	*n.p.*	+553
	Total	**122 (2,6%)**	**623 (13,5%)**	**517 (11,2%)**	**1709 (36,9%)**	**455 (9,8%)**	**533 (11,5%)**	**671 (14,5%)**	**4630 (100%)**

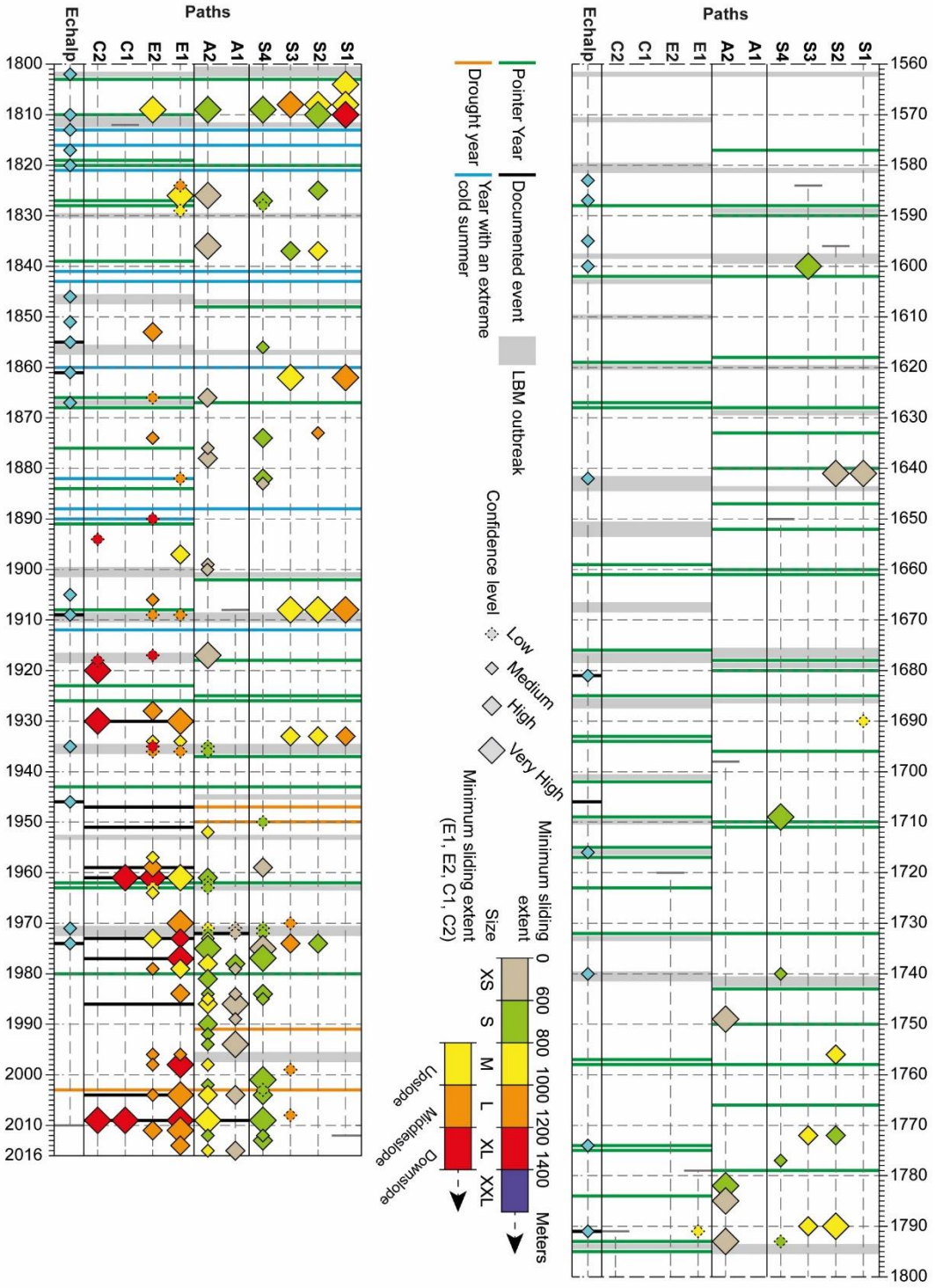

Figure 6.3 – Avalanches reconstruites pour la période 1560-2017 dans les dix couloirs d'avalanches étudiés. La taille des symboles est proportionnelle au niveau de confiance, les couleurs indiquent l'extension minimale de chaque événement estimée à partir de la disposition spatiale des arbres blessés dans les couloirs. Les bandes grises représentent les années d'épidémies de tordeuse grise. Les lignes verticales indiquent les avalanches de neige documentées dans les archives historiques (noir), les étés extrêmement secs (orange) et froids (bleu) ainsi que les cernes étroits observés dans les chronologies de référence élaborées à partir d'arbres non impactés(vert).

Ces perturbations de croissance ont permis de reconstruire 156 événements avalancheux (93 années) sur les versants de Souliers et du Ravin de la Salce entre 1560 et 2016 (Fig. 6.3, Tab. 6.4). A ces derniers, s'ajoutent 26 événements (17 années) reconstruits par Corona et al. (2013) au hameau de l'Echalp (commune de Ristolas). Ces événements ont été arbitrairement considérés avec un niveau de confiance faible en raison des critères de discrimination moins contraignants utilisés pour la détection. Au total, 66,6% des événements détectés ont été identifiées dans les six couloirs de Souliers. Le couloir A2 (37 avalanches reconstruites) représente 23,7% du total. Les couloirs S4, E1 et E2 représentent respectivement 16, 14,1 et 14,7% du total, avec 25, 22 et 23 événements reconstruits. Les proportions d'avalanches reconstruites sur les couloirs S1 (n=8, 5,1%, 1641-1933), C1 (n=2, 1,3%, 1961-2009) et C2 (n=5, 3,2%, 1894-2009) sont plus faibles (Tab. 6.4).

Parmi ces événements, 31,4% (49) et 25,6% (40) ont été classés avec des niveaux de confiance très élevés (vHLC) ou élevés (HLC). Par comparaison, 21,8% (34) et 21,2% (33) des événements ont été reconstruits avec un niveau de confiance moyen (MLC) ou faible (LLC). Les événements avec un niveau de confiance très élevé ou élevé ont été reconstruits en majorité dans les couloirs A2 (10 vHLC, 8 HLC), E1 (9 vHLC, 5 HLC) et S4 (6 vHLC, 7 HCL) ; 75,8% des événements assortis d'un niveau de confiance faible ont été reconstruits dans les couloirs E2 (7 LLC), E1 (6 LLC), A2 (6 LLC) et S4 (7 LLC).

Tableau 6.4 – Niveau de confiance et nombre d'événements d'avalanche détectés dans les séries de perturbations de croissance, par couloir.

	Couloirs	**vHLC**	**HLC**	**MLC**	**LLC**	**Total**
Souliers	S1	6 (3,3%)	1 (0,5%)	0 (0%)	1 (0,5%)	8 (4,4%)
	S2	5 (2,7%)	6 (3,3%)	1 (0,5%)	0 (0%)	12 (6,6%)
	S3	4 (2,2%)	5 (2,7%)	0 (0%)	3 (1,6%)	12 (6,6%)
	S4	6 (3,3%)	7 (3,8%)	6 (3,3%)	6 (3,3%)	25 (13,7%)
	A1	2 (1,1%)	3 (1,6%)	3 (1,6%)	2 (1,1%)	10 (5,5%)
	A2	10 (5,5%)	8 (4,4%)	13 (7,1%)	6 (3,3%)	37 (20,3%)
	Sous-total	*33 (18,1%)*	*30 (16,3%)*	*23 (12,5%)*	*18 (9,8%)*	*104 (57,1%)*
Ravin de la Salce	E1	9 (4,9%)	5 (2,7%)	2 (1,1%)	6 (3,3%)	22 (12,1%)
	E2	2 (1,1%)	5 (2,7%)	9 (4,9%)	7 (3,8%)	23 (12,6%)
	C1	2 (1,1%)	0 (0%)	0 (0%)	0 (0%)	2 (1,1%)
	C2	3 (1,6%)	0 (0%)	0 (0%)	2 (1,1%)	5 (2,7%)
	Sous-total	*16 (8,7%)*	*10 (5,4%)*	*11 (6%)*	*15 (8,2%)*	*52 (28,5%)*
	Echalp	-	-	-	26 (14,3%)	26 (14,3%)
	Total	**49 (26,9%)**	**40 (22%)**	**34 (18,7%)**	**59 (32,4%)**	**182 (100%)**

L'intervalle de récurrence moyen à l'échelle de l'ensemble des couloirs étudiés est de 10,6 ans, pour la période 1600–1800, de 2,7 ans pour la période 1801–1900 et de 2,3 ans pour la période 1901–2000. Les maximas d'activité sont observés au cours des périodes 1789–1793 (6 avalanches, soit un intervalle de récurrence de 0,67 années), 1804–1813 (11, 0,82 a), 1824–1829 (7, 0,71 a), 1905–1909 (8, 0,50 a), 1928–1936 (14, 0,57 a), 1957–1964 (11, 0,63 a), 1970–1986 (33, 0,48 a) et 1998–2015 (26, 0,65 a) (Fig. 6.3). Au contraire, aucune avalanche n'a été reconstruite au cours des périodes 1601–1640, 1645–1680, 1691–1708, 1710–1739 et 1758–1770. Pour les 19ème et le 20ème siècles, les minimas d'activité sont observés au cours des périodes 1794–1808 (2 avalanches, soit un intervalle de récurrence de 7 années), 1814–1824 (3, 3,3 a), 1830–1854 (6, 4 a), 1884–1900 (5, 1,2 a), 1910–1929 (5, 3,8 a), 1937–1958 (4, 5,3 a), 1965–1969 (0) et 1987–1997 (7, 1,4 a) (Fig. 6.3).

Sur le plan spatial, la matrice de corrélation (1790-2016, Fig. 6.4) entre les reconstructions brutes à l'échelle des couloirs met en évidence un fonctionnement synchrone des couloirs S1, S2, S3 ($r > 0.5$, $\alpha < 0{,}001$) et, dans une moindre mesure, E1-E2 ($\alpha < 0.05$). Les corrélations entre les couloirs du versant de la Salce et de la vallée de Souliers ne sont, en revanche, pas (ou faiblement) significatives.

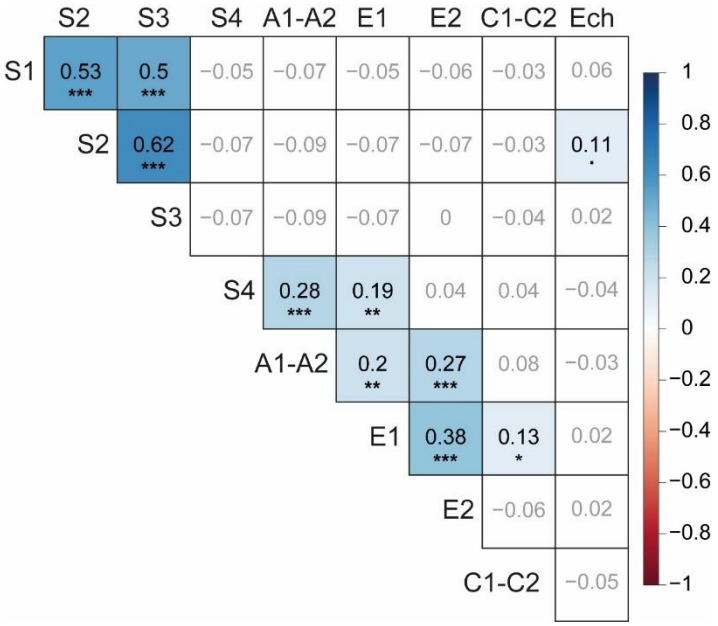

Figure 6.4 – Comparaison de l'activité des avalanches par couloir pour la période 1790–2016. Les couloirs A1 et C1 ont été respectivement appariés avec A2 et C2 pour permettre leur comparaison avec les autres couloirs pour la même période. Les coefficients de régression non-significatifs apparaissent grisés. Les niveaux de significativité des p valeurs sont représentés par un **.** (α=0,1), ***** (α=0,05), ****** (α=0,01), ******* (α=0,001).

4.3. Standardisation de la chronologie régionale au moyen de la modélisation bayésienne hiérarchique

Les paramètres du modèle indiquent que la variabilité de l'activité avalancheuse est expliquée à 50% par l'évolution du potentiel dendrogéomorphologique, à 7.3% par la composante spatiale et à 42.9% par les composantes temporelles, interannuelles (37,4%) et décennales (5,5%). Ces dernières ont un pourcentage commun de variance très élevé (87%). Au total, 167 événements ont été reconstruits entre 1750 et 2016. Le modèle bayésien hiérarchique permet d'estimer qu'en moyenne 5 événements (0 à 14 pour l'intervalle de confiance 2,5–97,5%) n'ont pas été reconstruits du fait de chronologies trop courtes pour les couloirs S1, A1, E1, C1, C2 et de l'Echalp. Après intégration de la diminution du potentiel de reconstruction, lié à la diminution du nombre d'arbres dans le passé, le nombre moyen d'avalanches estimé atteint 465,9 (308–680), ce qui correspond à une probabilité moyenne annuelle d'observation d'avalanches (p_0) de 0,068.

Sur le plan spatial, les couloirs A2 (0,36, [0,20-0,56]), E1 (0,27, [0,10–0,55]), S4 (0,25, [0,10–0,47]) et A1 (0,21, [0,07–0,44]) ont les probabilités annuelles de déclenchement corrigées les plus fortes. Par comparaison, les couloirs S1 (0,01, [0,004–0.03]), C2 (0.02, [0,004–0,08]) et C1 (0,02, [0,00–0,12]) apparaissent beaucoup moins

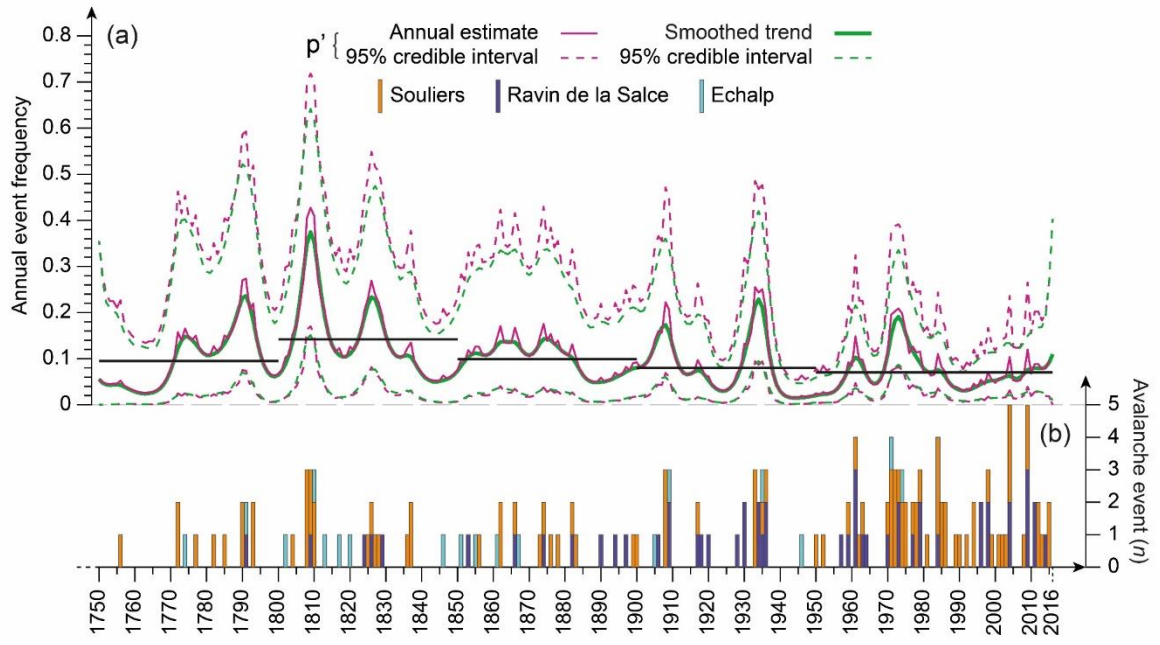

Figure 6.5 – Standardisation (a) de la reconstruction dendrogéomorphologique (b) au moyen de l'approche bayésienne hiérarchique. Sur le graphique supérieur (a), les lignes violettes et vertes pleines représentent les probabilités annuelles et décennales de déclenchement ; les lignes hachurées l'intervalle de confiance à 95% des deux chronologies standardisées. Les lignes horizontales noires indiquent les probabilités annuelles moyennes calculées pour des périodes de 50 ans. Sur le panneau du bas (b), les barres violettes, oranges et bleues représentent les avalanches reconstruites sur les versants du Ravin de la Salce, de Souliers et de l'Echalp.

actifs. Les facteurs de correction (a_1) du potentiel dendrogéomorphologique (POT) les plus élevés ont été utilisés sur les couloirs A2 (4,8, [2,8–7,5]), E1 (4,4 ; [2,3–7,1]), S4 (4,3 ; [2,3–7,3]), A1 (4,1 ; [1,9–7,1]) et E2 (4,1 ; [2,1–7,1]). Les tendances (a_2) les plus fortes (augmentation récente de l'activité) ont été observées sur C1, E2 et A1, les plus faibles sur les couloirs S2, A2 et de l'Echalp.

La chronologie régionale standardisée (Fig. 6.5) fait ressortir les fluctuations (pluri)décennales de l'activité avalancheuse. Les maximas d'activité sont observés pour les périodes 1805–1814 (0,28), 1785–1794 (0,18), 1822–1831 (0,18), 1971–1980 (0.15) et 1929–1938 (0,15). L'activité avalancheuse est en revanche minimale au cours des décennies 1940–1949 (0,01), 1758–1767 (0.028), 1987–1996 (0,037) et 1919–1928 (0.043). Malgré des incertitudes croissantes (0,16 pour la période 1965–2016, 0,29, pour la période 1750–1800), la chronologie montre que la probabilité de déclenchement au cours de la première partie du 19ème siècle (0,14 pour la période 1801–1850) est significativement supérieure à celle calculée pour les dernières décennies (0,08 pour la période 1967–2016).

4.4. Relations avalanche–climat.

Pour la période 1800-2014, les fluctuations décennales de l'activité avalancheuse et les séries de températures ($r = -0,192$, $\alpha \leq 0,01$), et de précipitations ($r = 0,197$, $\alpha \leq 0,01$) hivernales lissées au moyen d'un filtre passe-bas sont significativement corrélées. Les coefficients de corrélation avec les cumuls de précipitations ($r = 0,67$, $\alpha \leq 0,001$) et les températures hivernales ($r = -0,33$, $\alpha \leq 0,01$) sont supérieurs pour la période 1920-2008. Plusieurs décennies caractérisées par une fréquence avalancheuse forte coïncident avec des conditions climatiques anormalement humides et généralement plutôt froides : 1805–1814 (z-score précipitation = +0.1 ; z-score températures = -0.48), 1822–1831(+0.13 ; +0.19), 1929–1938 (+0.14, -0.46) et 1971–1980 (+1.09, 0.06, Fig. 6.6). Inversement, en 1815–1824 (-0.3 ; +0.05), 1919–1928 (-0.16 ; +0.38), 1940–1949 (-0.2 ; + 0.08) et 1987-1996 (-0.15 ; + 1.12), l'activité avalancheuse plus faible coïncide avec des séries d'hivers plutôt chauds et secs. Au cours de la décennie 1900-1909, caractérisée par une fréquence avalancheuse élevée (p=0.13), des conditions climatiques sèches (z-score précipitation = -0.31) mais plutôt fraîches (-0.58) sont observées. Enfin, une probabilité moyenne de déclenchement faible (p=0.07) est observée entre 1911-1920, décennie pourtant la plus humide (z-score précipitation = +0.76) depuis 1800.

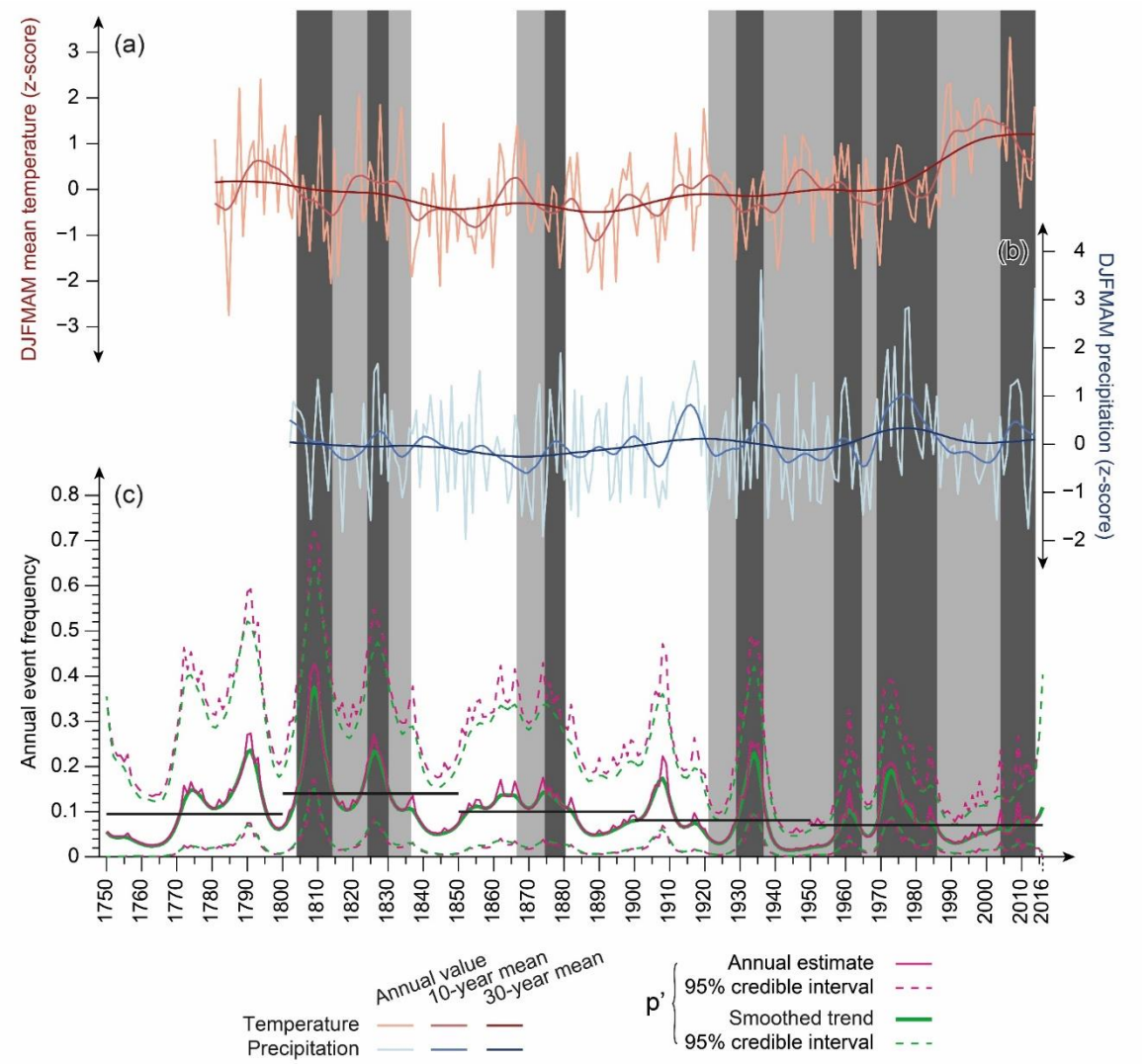

Figure 6.6 – Comparaison des fluctuations (a) des températures et (b) des précipitations hivernales (DJFAM) et de des reconstructions avalancheuses standardisées. Les lignes violettes et vertes pleines représentent les probabilités annuelles et décennales de déclenchement ; les lignes hachurées l'intervalle de confiance à 95% des deux chronologies. Les lignes horizontales noires représentent les fréquences annuelles moyennes d'événement pour les périodes 1750–1800, 1801–1850, 1851–1900, 1901–1950 et 1951–2016.

5. Discussion et conclusion

5.1. Robustesse de la reconstruction

L'approche dendrogéomorphologique utilisée dans 10 couloirs d'avalanches du massif du Queyras (versants de Souliers et du ravin de la Salce) a permis de reconstruire l'activité des avalanches au cours de la période 1560–2016. La datation de 4630 perturbations de croissance dans les séries de largeur de cernes de 1131 mélèzes d'Europe (*Larix decidua* Mill.) ont permis d'identifier, par le biais de la méthode de détection en 4 étapes présentée dans le chapitre 1 (Favillier et al. 2017), 93 années avalancheuses depuis 1560. En ajoutant les 26 avalanches, reconstruites par Corona et al. (2013) sur le versant de l'Echalp, la chronologie régionale (11 couloirs) compte 182 événements. La rigueur de la méthode de détection utilisée garantit une inclusion de bruit limitée – lié à de potentielles interférences entre l'activité avalancheuse et des signaux exogènes (climatiques, épidémies de tordeuses) – dans la reconstruction. Elle permet en outre d'estimer, de manière qualitative, le niveau de confiance associé à chaque événement reconstruit. Ainsi, avec 89 événements (48,9% du total) classés vHLC ou HLC, la chronologie du Queyras apparaît plus robuste que celle de la vallée de Goms (chapitre 5) où 29% des événements seulement ont été assortis de niveaux de confiance équivalents. Cette robustesse est liée à la fréquence élevée des perturbations de croissance de forte et de très forte intensités (notées 3 ou 4) datées dans les séries de largeur de cernes.

Malgré la qualité de la chronologie, cette dernière reste caractérisée par une tendance très marquée puisque 59% des avalanches ont été reconstruites durant le 20ème siècle et 43% après 1950. Comme nous l'avons mis en évidence dans les chapitres précédents, cette non-stationnarité s'explique par (i) l'augmentation du nombre d'arbres vivants au cours des dernières décennies, (ii) la difficulté à retrouver les impacts après cicatrisation (Favillier et al., 2017 – chapitre 1, 2018 – chapitre 2 ; Trappmann et Stoffel, 2013), mais également par (iii) un échantillonnage souvent trop important des blessures visibles (Favillier et al., 2018 – chapitre 2 ; de Bouchard d'Aubeterre et al., 2019 – chapitre 3). De plus, la matrice des corrélations démontre des fonctionnements synchrones à l'échelle de quelques couloirs (S1-S2-S3, S4-A1-A2, E1-E2) mais également l'absence de corrélations significatives entre des couloirs voisins (S3-S4) et entre les couloirs du versant de Souliers et ceux du Ravin de la Salce. Ce synchronisme limité peut être attribué aux caractéristiques morphologiques de chaque couloir, comme nous l'avons mis en évidence sur le versant du ravin de la Salce (de Bouchard d'Aubeterre et al., 2019 – chapitre 3) mais

également, à Souliers, à des non-stationnarités induites par l'exploitation puis la déprise sylvo-pastorale (Mainieri et al., sous presse – chapitre 4).

5.2. Modélisation de l'activité régionale des avalanches

Afin de limiter les biais induits dans la chronologie régionale par la diminution du potentiel dendrogéomorphologique dans le passé, cette dernière a été homogénéisée au moyen d'une régression logistique bayésienne à double composante spatiale et temporelle (voir chapitre 5). L'analyse des tendances centennales de la reconstruction régionale homogénéisée montre qu'un maxima avalancheux a été observé dans le Queyras entre 1770 et 1836 puis que l'activité décroît progressivement depuis le milieu du 19^{e} siècle. Malgré des incertitudes croissantes, la probabilité de déclenchement au cours de la première partie du 19ème siècle apparaît ainsi significativement supérieure à celle calculée pour les cinquante dernières décennies. Ces résultats sont en adéquation avec les analyses lichénométriques réalisées sur des blocs rocheux déposés dans les zones d'arrêt d'avalanches dans le Massif des Ecrins (Jomelli et Pech, 2004) notamment pour les périodes 1780–1830 puis 1830–1950 caractérisées respectivement par une activité avalancheuse forte, puis plus modérée. De la même manière, le minima identifié dans les données lichénométriques entre 1830 et 1850 est clairement observé dans la reconstruction dendrogéomorphologique. Ils convergent également avec les analyses sédimentologiques réalisées dans le lac du Lauvitel (Massif des Ecrins, Fouinat et al., 2018) montrant des hausses marquées de la fréquence avalancheuse à la fin du 18^{e} siècle puis un maximum au cours des décades 1800-1820. A l'échelle décennale, des maximas sont observées durant les périodes 1805–1814, 1822–1831, 1929–1938 et 1971–1980. L'activité avalancheuse est significativement plus faible au cours des décennies 1940–1949, 1758–1767, 1987–1996 et 1919–1928. Avant 1950, les inventaires historiques parcellaires (p.ex. Tivollier et Isnel, 1938) ou très locaux (p.ex. Le Gallou et Guignard 2011), disponibles dans le Queyras (chapitre 4), ne permettent pas de valider les fluctuations reconstruites. Depuis le milieu du 20ème siècle, la comparaison de l'activité régionale modélisée avec les données recensées, de manière exhaustive, dans l'EPA montre que le maxima détecté dans la reconstruction dendrogéomorphologique standardisée au début des années 1970 est plus tardif dans la chronique EPA alpine (1976-1987, Eckert et al., 2013) et n'apparaît pas clairement à l'échelle des Alpes du Sud (Castebrunet et al., 2012) (Fig. 6.7).

Plusieurs facteurs peuvent expliquer le synchronisme limité entre les deux chronologies notamment (i) le nombre limité de couloirs inclus dans la reconstruction

dendrogéomorphologique ce qui induit (ii) une variabilité spatiale limitée (chapitre 5) ; (iii) un taux de convergence qui en général n'excède pas 50% entre les données historiques et dendrogéomorphologiques (Corona et al., 2010, 2012, 2013 ; Schläppy et al., 2016 ; de Bouchard d'Aubeterre et al., 2019 – chapitre 3).

5.3. Fluctuations du climat et activité des avalanches

Les paramètres globaux du modèle indiquent le poids important de la composante temporelle qui explique plus de 40% de la variabilité avalancheuse. Ils montrent également que les composantes temporelles, interannuelles et décennales ont un pourcentage commun de variance très élevé. Ces paramètres, indépendants de l'effet de site, suggèrent l'existence d'un contrôle climatique sur l'activité avalancheuse. Cette hypothèse est validée par (i) les probabilités de déclenchement élevées observées entre les années 1780 et 1830, durant le minimum solaire de Dalton caractérisé par des températures plutôt froides et des avancées glaciaires significatives dans les Alpes (voir p. ex. Brönnimann et al., 2019), tendent à valider cette hypothèse ; (ii) la diminution de l'activité avalancheuse depuis le milieu des années 1980 synchrones avec une hausse des températures mais également avec deux

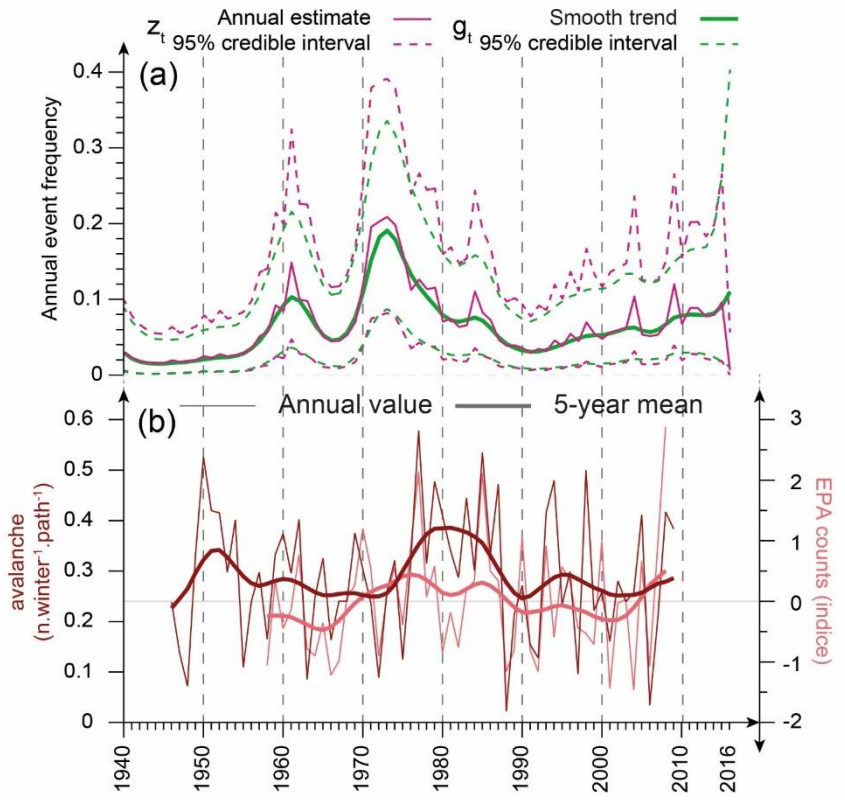

Figure 6.7 – Comparaison de (a) des moyennes à 5 ans, 10 ans et 30 ans de l'activité des avalanches dans le Queyras (rouge) avec (b) l'activité observée des avalanches (b) dans les Alpes françaises entre 1940 et 2016. L'activité des avalanches est représentée à l'échelle de l'ensemble du massif (rouge sombre), d'après Eckert et al.(2013), et à l'échelle des Alpes françaises du Sud (rouge clair), d'après Castebrunet et al. (2012).

décades, 1985-2004, plutôt sèches. La comparaison de la chronologie avalancheuse avec les séries hivernales de températures (1781–2014) et précipitations (1802–2014) extraites de la base de données HISTALP (Auer et al., 2007; Efthymiadis et al., 2006), confirment la corrélation significative entre les fluctuations décennales des températures (1781–2014, $r = -0{,}192$, $\alpha \leq 0{,}01$) et des précipitations (1802–2014, $r = 0{,}197$, $\alpha \leq 0{,}01$) et celles de l'activité avalancheuse. Pour la période 1920–2014, les corrélations avec les précipitations ($r = 0{,}67$, $\alpha \leq 0{,}001$) et les températures ($r = -0{,}33$, $\alpha \leq 0{,}001$) augmentent significativement. En particulier, au cours du 20ème siècle, plusieurs décennies caractérisées par une fréquence avalancheuse forte (1929–1938, 1971–1980) coïncident avec des précipitations hivernales excédentaires. A l'inverse, au cours des décennies 1919–1928, 1940–1949 et 1987-1996, plutôt sèches, la probabilité de déclenchement décroît significativement.

Malgré le caractère particulièrement prometteur de ces résultats, il faut cependant garder à l'esprit que : (i) la chronologie régionale élaborée pour le massif du Queyras, unique à l'échelle alpine, ne repose que sur deux versants et 11 couloirs avalancheux. Elle ne représente donc que partiellement la variabilité spatio-temporelle de l'activité avalancheuse ; (ii) malgré l'utilisation de méthodes de détection particulièrement rigoureuses (Favillier et al., 2017 – chapitre 1) et de l'approche bayésienne hiérarchique afin d'homogénéiser les reconstructions (chapitre 5), l'approche dendrogéomorphologique tend à sous-estimer fortement l'activité avalancheuse ; (iii) les non-stationnarités locales, liées à l'exploitation puis à la déprise sylvo-pastorale ou aux caractéristiques morphologiques des couloirs, n'ont pas été prises en compte ; enfin, (iv) la reconstruction homogénéisée a été comparée aux séries de la base de données HISTALP qui ne représentent qu'imparfaitement l'évolution climatique dans le Queyras, notamment avant le début du 20ème siècle pour lesquelles les données ont été interpolées à partir de stations météorologiques situées en dehors du massif alpin (Hiebl, 2006). De plus, HISTALP ne fournit pas de données d'enneigement. Les données utilisées (températures et précipitations) ne permettent donc d'estimer que très grossièrement l'évolution du manteau neigeux dans les zones de départ des couloirs étudiés.

SYNTHÈSE GÉNÉRALE

1. Principaux résultats

1.1. Elaboration de deux chronologies régionales inédites

Ce travail de thèse vise à mettre en évidence l'impact des fluctuations climatiques, notamment du réchauffement récent, et des changements socio-économiques sur l'aléa avalancheuse dans les Alpes. Afin d'atteindre cet objectif, l'élaboration de chronologies régionales, à haute résolution temporelle et, dans la mesure du possible, continues, constituait un prérequis crucial afin de : (1) s'affranchir des signaux locaux, (2) détecter des tendances robustes d'évolution de l'activité avalancheuse, et (3) identifier le rôle respectif du réchauffement climatique et de la déprise agro-sylvo-pastorale dans les fluctuations de l'activité avalancheuse détectées. Dans le cadre de cette thèse, l'approche dendrogéomorphologique a ainsi été utilisée pour reconstruire l'activité pluriséculaire des avalanches dans deux régions alpines (Fig. S.1) :

- Dans la vallée de Goms (Valais, Suisse), 1014 L. decidua et P. abies ont été échantillonnés sur 11 couloirs d'avalanches des versants de Münster, Geschinen et Oberwald. Les 5502 perturbations de croissance identifiées dans les prélèvements ont permis la détection de 107 événements d'avalanches (73 années) entre 1720 et 2014 ;
- Dans le massif du Queyras (Hautes-Alpes, France), 1131 *L. decidua* ont été prélevés sur deux versants exposés aux avalanches de la haute-vallée du Guil et de la vallée de Souliers. Les 4630 perturbations de croissance identifiées dans les cernes annuels ont permis la reconstruction de 156 avalanches entre 1560 et 2016 dans les 10 couloirs délimités. De plus, les 26 avalanches détectées entre 1560 et 2010 par Corona et al. (2013) sur le versant du hameau de l'Echalp, voisin, ont été ajoutées à la chronologie régionale. Au total, la chronologie d'avalanche du Queyras se compose de 182 (110 années) événements d'avalanches entre 1560 et 2016.

Ces deux chronologies régionales sont inédites à l'échelle des Alpes, mais aussi à l'échelle globale, en raison du nombre d'arbres échantillonnés et du nombre de couloirs inclus dans chaque chronologie. Pluriséculaires, elles excèdent également largement la période couverte par les inventaires systématiques et sont très complémentaires des archives historiques pour documenter l'activité des avalanches durant les périodes pré- et post-industrielles, très différentes d'un point de vue climatique (minima du Petit Âge de Glace et dernières décennies). La construction de ces chronologies repose sur de

nombreuses campagnes de prélèvements et a nécessité un temps de traitement et d'analyse particulièrement important, mais a également donné lieu à plusieurs développements méthodologiques, permettant notamment d'améliorer la détection et la cartographie des événements passés, de prendre en compte les non-stationnarités induites par la structure d'âge des arbres échantillonnés dans les chronologies ou de détecter les fluctuations de l'activité des avalanches.

1.2. Amélioration de la détection des événements passés

Les analyses dendrogéomorphologiques initialement réalisées sur le versant d'Oberwald (vallée de Goms, Valais, Suisse) ont permis de démontrer que de nombreuses avalanches potentielles coïncidaient avec des épidémies de tordeuse grise (*Zeiraphera diniana* gn.), un lépidoptère ravageur du Mélèze d'Europe. **Cette concomitance nous a permis de réaliser que les interférences pouvant exister dans les reconstructions dendrogéomorphologiques, entre le signal avalancheux et des signaux exogènes (épidémies de ravageurs, tempête, extrêmes climatiques), n'avaient jamais été considérées dans la littérature scientifique.** Afin de prendre en compte ces interférences et d'attribuer un niveau de confiance aux événements reconstruits, une nouvelle méthode de détection, en quatre étapes, a été développée (Favillier et al., 2017 – chapitre 1). Cette dernière intègre (i) le nombre d'arbres perturbés, (ii) l'intensité des perturbations observées, (iii) le synchronisme entre les événements reconstruits et l'occurrence de perturbations exogènes ainsi que (iv) la répartition spatiale des arbres impactés. Cette procédure nous a conduit à rejeter 31 des 74 événements initialement reconstruits au cours de la période 1780-2014 confirmant ainsi le biais important qui pouvait être engendré par la confusion des différents signaux. Cette confusion est particulièrement importante dans les reconstructions réalisées à partir de *Larix decidua* Mill., les plus fréquentes en milieu alpin du fait de la répartition spatiale de cette espèce et de son caractère longévif, du fait des pullulations récurrentes de la tordeuse grise.

1.3. Dendrogéomorphologie et cartographie de l'aléa avalancheux

Les travaux réalisés sur le versant de Täsch (canton du Valais, Alpes suisses), où les avalanches menacent la route menant à Zermatt, nous ont également conduit à nous interroger sur l'utilisation de l'approche dendrogéomorphologique pour le zonage de cet aléa. Paradoxalement, la synthèse bibliographique préalable à ce travail de thèse nous avait démontré que, malgré les apports théoriquement importants pour la prédétermination de la période de retour et de l'extension spatiale des événements potentiellement dommageables,

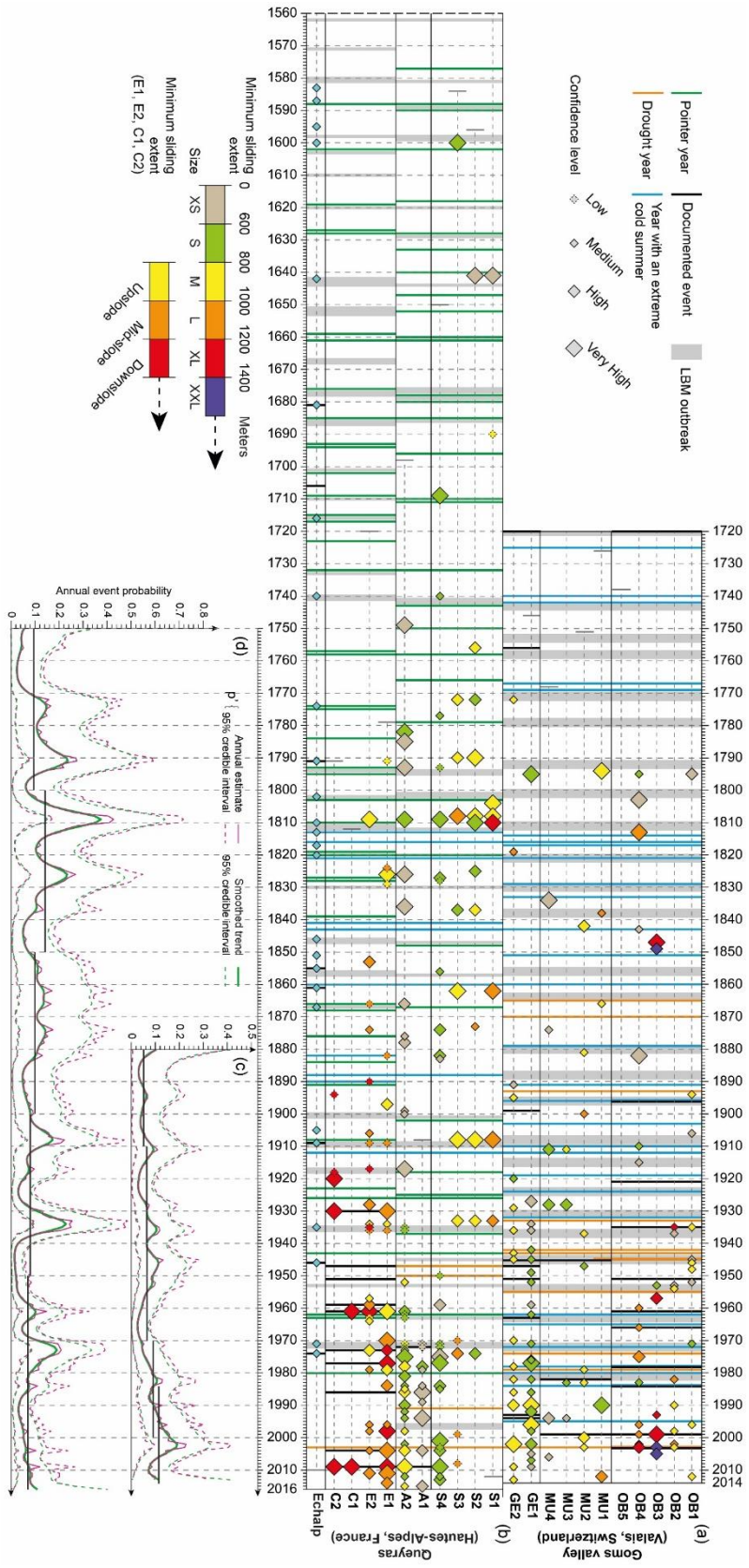

Figure S.1 – Chronologies des événements d'avalanche de (a, c) la vallée de Goms et (b, d) du massif du Queyras et leur activité homogénéisée au moyen de l'approche bayésienne hiérarchique. Les lignes horizontales noires représentent les fréquences annuelles moyennes d'événement pour des périodes de (c) 30 ans et (d) de 50 ans.

l'approche n'avait été que très rarement utilisée dans une perspective spatiale. De plus, les rares cartographies proposées ne représentaient qu'une interpolation anisotropique de la fréquence locale de perturbations observée au niveau de chaque arbre échantillonné et non une réelle période de retour, c'est à dire la probabilité annuelle d'occurrence d'une avalanche d'intensité donnée en chaque point du versant. Afin de proposer une alternative à l'interpolation, l'emprise spatiale de chaque événement reconstruit a tout d'abord été déterminée grâce à la position des arbres impactés. Puis, l'intervalle de récurrence a été calculé en tout point du versant comme le ratio de la période couverte par la reconstruction et du nombre d'emprises superposées. Cette approche permet de reproduire des patrons spatiaux cohérents avec le processus avalancheux, notamment une augmentation de l'intervalle de récurrence de l'amont vers l'aval et du centre vers les marges des couloirs. Néanmoins, malgré son apparente précision, cette cartographie comporte encore des incertitudes liées : (1) à la cartographie des emprises, réalisées à dire d'expert sur la base de la disposition spatiale des arbres échantillonnés et impactés, ce qui peut induire des incertitudes d'ordre plurimétriques ; (2) à la sous-estimation de la fréquence réelle des avalanches par l'approche dendrogéomorphologique ; et (3) au fait qu'un point du versant peut être atteint par plusieurs zones de départ. Malgré ces limitations, nos résultats ont permis de démontrer les apports de la dendrogéomorphologie pour la cartographie de l'aléa sur des couloirs forestiers, pour lesquelles la documentation historique est souvent très limitée et lacunaire. En fournissant des intervalles de récurrence de l'aléa, elle apparaît très complémentaire mais indépendante des approches traditionnellement utilisées pour la prédétermination telles que : (1) la méthode « norvégienne » (Lied and Bakkehøi, 1980) dans laquelle les distances d'arrêt sont estimées à partir de covariables topographiques et d'une base de données élaborée à l'échelle régionale afin de pallier l'absence de données spécifiques au site étudié. Cette méthode est complexe à mettre en œuvre en milieu alpin, du fait de la diversité topographique des couloirs avalancheux ; de plus elle est très dépendante de la quantité et de la robustesse des données utilisées pour établir la distribution des distances d'arrêt et nécessite souvent une extrapolation afin d'évaluer la distance d'arrêt des avalanches ayant les périodes de retour les plus longues ; (2) la méthode « suisse », dans laquelle des chutes de neige de période de retour 30, 100 et 300 ans sont propagées numériquement, en utilisant le modèle de Voellmy (1955) et des valeurs de coefficients de friction adaptés au versant étudié, puis transformées en distance d'arrêt en utilisant (Bartelt et al., 1999). L'un des principaux inconvénients de cette approche est d'estimer la période de retour d'une chute de neige et non d'un événement avalancheux.

1.4. Mise en évidence de non-stationnarités dans les reconstructions

Malgré la rigueur de notre approche et le soin apporté à la détection des événements, l'analyse des chronologies obtenues a mis en évidence des non-stationnarités récurrentes dans les reconstructions. Nous avons démontré que leur origine pouvait être différente selon les sites. A Oberwald, la tendance à l'augmentation de l'activité avalancheuse depuis le milieu du 20ème siècle a été attribuée à la diminution du nombre d'arbres vivants dans le passé mais également à un biais lors de l'échantillonnage ayant conduit à une surreprésentation des cicatrices et des lignes tangentielles de canaux résinifères traumatiques récentes dans le spectre des perturbations de croissance. En d'autres termes, l'existence de cette tendance résulte de la difficulté d'échantillonner des blessures anciennes, masquées, dans des arbres de gros diamètres, souvent pluri-centenaires. Sur les versants de Täsch (Favillier et al., 2018 – chapitre 2) et de Souliers (couloirs S4–A1–A2, Mainieri et al., soumis – chapitre 4), l'absence d'événements reconstruits pendant plusieurs décennies ont permis de mettre en évidence la perte du signal dendrogéomorphologique à la suite d'un événement de forte magnitude. A ces non-stationnarités intrinsèques à l'approche dendrogéomorphologique s'ajoutent celles liées aux mutations socio-économiques. Ces dernières ont été mises en évidence sur les couloirs de Souliers (S1-S3) où la diminution de la fréquence des avalanches depuis les années 1930 a été attribuée à la recolonisation des zones de départ en lien avec la déprise sylvo-pastorale et l'exode rural depuis le milieu du 19ème siècle.

L'existence de ces non-stationnarités, souvent asynchrones et spatialement hétérogènes, limite les corrélations entre les reconstructions, à l'échelle d'un même versant ou entre les versants d'un même massif (Figs. 5.7, 6.4). Ces différences sont renforcées par le potentiel dendrogéomorphologique susceptible de varier fortement entre deux couloirs voisins. Nous avons en effet pu démontrer (de Bouchard d'Aubeterre et al., 2019 – chapitre 3), sur le versant du Ravin de la Salce (massif du Queyras), que les caractéristiques morphométriques et la structure du couvert forestier pouvait fortement affecter la fréquence, la durée et la robustesse des reconstructions. Ainsi sur les couloirs forestiers, de pente limitée, caractérisés par l'occurrence d'avalanches de faible magnitude (E1-E2), les reconstructions sont plus longues, les taux de convergence avec les archives historiques supérieures et les récurrences plus élevées que sur les couloirs voisins (C1-C2) en pente raide, très actifs où la couverture forestière réduite est régulièrement détruite par des événements de forte magnitude. Ces différences ont des implications particulièrement importantes pour la reconstruction de l'activité des avalanches dans le contexte de

réchauffement du climat. **Elles démontrent que la sélection des couloirs est cruciale et que les couloirs forestiers, affectés par des avalanches de faible magnitude, sont plus propices à une reconstruction continue de l'aléa sur de longues périodes temporelles.** Plus généralement, la mise en évidence de ces non-stationnarités nous ont progressivement conduit à nous interroger sur la procédure d'agrégation des reconstructions en chronologies régionales.

1.5. Reconstruction régionale de l'activité des avalanches

Nos recherches bibliographiques ont démontré que les reconstructions à l'échelle régionale (c'est à dire incluant deux couloirs avalancheux ou plus) étaient peu nombreuses dans la littérature : parmi les 67 reconstructions de l'activité avalancheuse recensées, 80% sont basées sur moins de quatre couloirs et 9% seulement sur 10 couloirs ou plus. Deux approches ont généralement été utilisées afin de combiner les reconstructions locales en chronologies régionales : Germain et al. (2005), Muntán et al. (2009) and Voiculescu et al. (2016) ont simplement additionné les événements retrouvés à l'échelle de chaque couloir puis comparé les pics d'activité avalancheuse avec les données nivo-météorologiques. Sur la base de la méthodologie proposée par Dubé et al. (2004), plusieurs études (Germain et al., 2009; Decaulne et al. 2012, 2014; Voiculescu et al., 2016; Martin and Germain, 2017) ont utilisé un index d'activité régional des avalanches (RAAI) qui représente pour chaque année (t) le ratio entre le pourcentage d'arbres endommagés à l'échelle régionale et le nombre de couloirs susceptibles d'enregistrer un événement. La distinction entre années avalancheuse et non-avalancheuse est ensuite réalisée sur la base d'un seuil (en général compris entre 10 et 20%). Ces reconstructions ne prennent pas en compte les non-stationnarités précédemment évoquées et ont un caractère dichotomique, les années avalancheuses à l'échelle régionale étant discriminées sur la base d'un seuil. Elles ne mettent que partiellement en évidence les variations interannuelles à décennales de l'activité des avalanches.

Afin de pallier ces biais et de prendre en compte les non-stationnarités liées à la réduction du potentiel dendrogéomorphologique dans le passé une approche bayésienne hiérarchique a été utilisée. Cette approche particulièrement adaptée, en raison de sa flexibilité à l'analyse de données à composante spatio-temporelle, a été fréquemment utilisée par les sciences du climat et dans de nombreuses études consacrées aux relations aléas/climat (Eckert et al., 2007b, 2011 ; Jomelli et al., 2015, 2019 ; Lavigne et al., 2012 ; Rabatel et al., 2013). Dans le cadre de la thèse, une régression logistique spatio-temporelle

permettant d'enlever les tendances potentiellement liées à l'augmentation du nombre d'arbres a été développée et utilisée afin d'homogénéiser les reconstructions de la vallée de Goms et du Queyras. Cette régression permet également de distinguer les variabilités annuelles et décennales de l'activité des avalanches sans utiliser de seuils arbitraires et de quantifier le pourcentage de variance respectif associé aux différentes co-variables spatiales et temporelles.

Dans la vallée de Goms, le modèle bayésien indique que plus de 40% de la variabilité des avalanches est expliquée par les fluctuations du potentiel dendrogéomorphologique et d'estimer que 109 événements se sont probablement produits entre 1880 et 2014 alors que 91 ont été reconstruits. Les composantes temporelles et spatiales expliquent respectivement 38 et 15% de cette variabilité. Les fluctuations décennales, sont peu marquées et fortement corrélées aux fluctuations interannuelles. A l'échelle décennale, les probabilités maximales d'occurrence sont observées entre 1996 et 2005, 1944 et 1953, et 1906 et 1915. Les périodes 1883-1896, 1918-1927 et 1961-1970, sont en revanche caractérisées par des fréquences avalancheuses beaucoup plus faibles. **Sur des périodes de 30 ans, une tendance significative à l'augmentation des avalanches est observée et on ne peut pas conclure à une diminution de l'activité des avalanches au cours des dernières décennies.**

Dans le Queyras, les paramètres du modèle indiquent que la variabilité de l'activité avalancheuse est expliquée à 50% par l'évolution du potentiel dendrogéomorphologique, à 7.3% par la composante spatiale et à 43% par les composantes temporelles. Au total, 167 événements ont été reconstruits entre 1750 et 2016. Le modèle bayésien hiérarchique permet d'estimer qu'entre 308 et 680 se sont produites pendant cette période. Les maximas de la chronologie régionale standardisée sont observés pour les périodes 1805–1814, 1785–1794, 1822–1831, 1971–1980 et 1929–1938. L'activité avalancheuse est en revanche minimale au cours des décennies 1940–1949, 1758–1767, 1987–1996 et 1919–1928. **Malgré des incertitudes croissantes, la chronologie montre que la probabilité de déclenchement au cours de la première partie du 19ème siècle est significativement supérieure à celle calculée pour les dernières décennies.** La Figure S.1 (c,d) ne montre que peu de synchronisme entre les deux reconstructions régionales homogénéisées.

1.6. Variations de l'activité avalancheuse *vs.* fluctuations du climat

Parmi les 67 études relatives à la reconstruction des avalanches au moyen d'une approche dendrogéomorphologique que nous avons recensées, seules 20 ont analysé les

relations entre les fluctuations de l'activité avalancheuse et des covariables nivo-météorologiques (Muntán et al.,2009 ; Casteller et al.,2011 ; Schläppy et al., 2015 ; Gądek et al., 2017 ; Martin et Germain, 2017). A l'exception de Ballesteros-Canovas et al. (2017) qui montrent une relation significative entre l'augmentation des températures, le changement de la nature des avalanches et l'augmentation de la fréquence sur un versant Himalayen, la relation avalanche/climat n'a pas été réellement abordée. **La confrontation de nos chronologies régionales homogénéisées avec les données climatiques illustre les interférences existant avec les évolutions socio-économiques et paysagères des régions étudiées et l'impact des non-stationnarités induites par l'approche dendrogéomorphologique.**

Ainsi, dans la vallée de Goms, la comparaison entre l'activité des avalanches et les fluctuations du climat est peu concluante. De la même manière, la convergence avec les inventaires systématiques disponibles pour les Alpes suisses et françaises et les archives historiques recensées dans la commune d'Obergoms sont faibles. Enfin, malgré les nombreux aménagements réalisés sur les versants et un processus d'afforestation marquée au cours du 20ème siècle, une tendance à l'augmentation de l'activité avalancheuse est observée. Même si on ne peut pas exclure, compte-tenu de l'altitude de départ, que cette tendance reflète une augmentation de la fréquence des avalanches de fonte (Castebrunet et al., 2014), ce synchronisme limité et l'absence de tendance suggère que la chronologie régionale ne reflète que très partiellement le forçage climatique. En d'autres termes, **malgré le caractère exhaustif de notre reconstruction, il est possible que cette dernière ne reflète que très imparfaitement les fluctuations de l'activité avalancheuse dans la vallée de Goms et/ou n'inclue pas suffisamment de couloirs pour permettre de s'affranchir des signaux locaux et discriminer un signal commun.**

Dans le massif du Queyras, la comparaison de l'activité régionale des avalanches avec les données de la base de données HISTALP (Efthymiadis et al., 2006) depuis 1802, montre une corrélation significative entre l'activité des avalanches, et les précipitations hivernales. Plusieurs décennies caractérisées par une fréquence avalancheuse forte coïncident avec des conditions climatiques anormalement humides et généralement plutôt froides : 1805–1814,1822–1831, 1929–1938 et 1971–1980. A l'inverse, les décennies 1815–1824, 1919–1928, 1940–1949, et 1987–1996, caractérisées par une activité avalancheuse plus faible, coïncident avec des séries d'hivers plutôt chauds et secs. **Ces résultats, encore très préliminaires, suggèrent un lien entre le réchauffement**

climatique et la diminution de la probabilité de déclenchement observée au cours des dernières décennies, significativement inférieure à celle de la période préindustrielle.

2. Perspectives de recherches

Ce travail a permis de lever plusieurs verrous méthodologiques concernant notamment la détection et la cartographie des événements avalancheux. Les résultats obtenus nous ont conduit à reconsidérer des limites de l'approche dendrogéomorphologique et ont fait émerger de nouvelles perspectives de recherche.

2.1. Ajustement des seuils de détection des événements

Une méthode en quatre étapes qualifiant l'incertitude des chronologies reconstruites, qui tient compte du nombre et de l'intensité des perturbations de croissance, mais aussi des interférences avec les autres signaux écologiques et climatiques, a été proposée. Bien que testée sur de nombreux couloirs, cette dernière repose sur des seuils de détection (nombre de blessures, pourcentage d'arbres impactés) fixés arbitrairement susceptibles d'influencer la fréquence des événements reconstruits. Dans le futur, ces seuils devront nécessairement être affinés notamment sur des couloirs où l'activité avalancheuse est documentée par les archives historiques. Nous sommes conscients que les couloirs forestiers comparables à celui des Pèlerins dans la vallée de Chamonix, utilisé par Corona et al. (2012) sont très rares à l'échelle des Alpes. Une première alternative pour ajuster les seuils dendrogéomorphologiques des chronologies historiques composites serait de travailler en étroite collaboration avec les historiens afin d'améliorer les chroniques existantes. Une seconde consisterait à utiliser différentes générations d'événements (anciens, récents, très récents) survenus sur différents couloirs de la même région.

2.2. Densification de l'échantillonnage à l'échelle régionale

Les reconstructions régionales réalisées dans les vallées de Goms et du Queyras ont nécessité un investissement important, sur le terrain, lors de la phase de collecte des échantillons, et encore plus lors de la phase d'analyse. Malgré le caractère unique des reconstructions régionales obtenues et la mise en œuvre de l'approche bayésienne hiérarchique, la détection du forçage climatique potentiel doit encore être améliorée. Une des solutions envisagées pour s'affranchir des signaux locaux consistent à augmenter le nombre de couloirs dans chaque reconstruction afin d'améliorer le ratio signal/bruit. Compte-tenu du coût/bénéfice élevé des reconstructions dendrogéomorphologiques, une stratégie d'échantillonnage prenant en compte non seulement la structure du peuplement

forestier (peuplements pluri-centenaires dans l'idéal) et son évolution (Mainieri et al., soumis – chapitre 4) mais également la topographie des couloirs (de Bouchard d'Aubeterre et al., 2019 – chapitre 3) et leur caractère représentatif de la région étudiée devra nécessairement être mise en place. Afin de limiter les phases de terrain et d'analyse, le nombre de prélèvements pourra être limité à une centaine par couloir conformément aux recommandations de Stoffel et Corona (2013).

2.3. Meilleure intégration des non-stationnarités liées à l'approche dendrogéomorphologique et des impacts des changements socio-économiques

Différentes sources de non-stationnarités ont été mises en évidence dans les reconstructions locales. Ces dernières sont liées à la variabilité du potentiel dendrogéomorphologique conditionné par l'occurrence d'événements extrêmes pouvant limiter le potentiel de reconstruction pendant plusieurs décennies (Favillier et al., 2017 ; de Bouchard d'Aubeterre et al., 2019 ; Mainieri et al., soumis), à la difficulté d'échantillonner des blessures anciennes (Favillier et al., 2017), à la structure des couloirs étudiés (de Bouchard d'Aubeterre et al., 2019) ou à la réduction du nombre d'arbres vivants dans le passé. A l'exception de cette dernière, ces sources n'ont pas été intégrées dans les reconstructions régionales. De la même manière, nous avons pu démontrer que les évolutions socio-économiques – déprise sylvo-pastorale du milieu du 19ème siècle dans le Queyras (Mainieri et al., soumis), campagne de reboisements et installation de dispositifs paravalanche dans la vallée de Goms – étaient susceptibles de jouer un rôle déterminant dans l'évolution de l'activité avalancheuse. Ces évolutions ont été discutées de manière qualitative dans le cadre de cette thèse mais n'ont pas été intégrés dans la modélisation bayésienne hiérarchique. Dans le futur, ces variables environnementales pourraient être intégrées dans le modèle ce qui permettrait de quantifier leur impact sur la variabilité de l'activité avalancheuse. Ce type d'approche utilisée dans les bassins versants torrentiels des Alpes françaises a par exemple permis de déterminer que la pente expliquait 20% de la variance des séries de laves torrentielles (Jomelli et al., 2015).

2.4. Améliorations des chronologies régionales par convergence avec d'autres sources d'informations

Sur les couloirs E1/E2 du versant du Ravin de la Salce, le taux de convergence entre la reconstruction dendrogéomorphologique et les archives de l'Enquête Permanente sur les Avalanches atteint 60%. Il s'explique par une activité avalancheuse modérée liée à une couverture forestière dense et à des couloirs de faible extension longitudinale et de pente

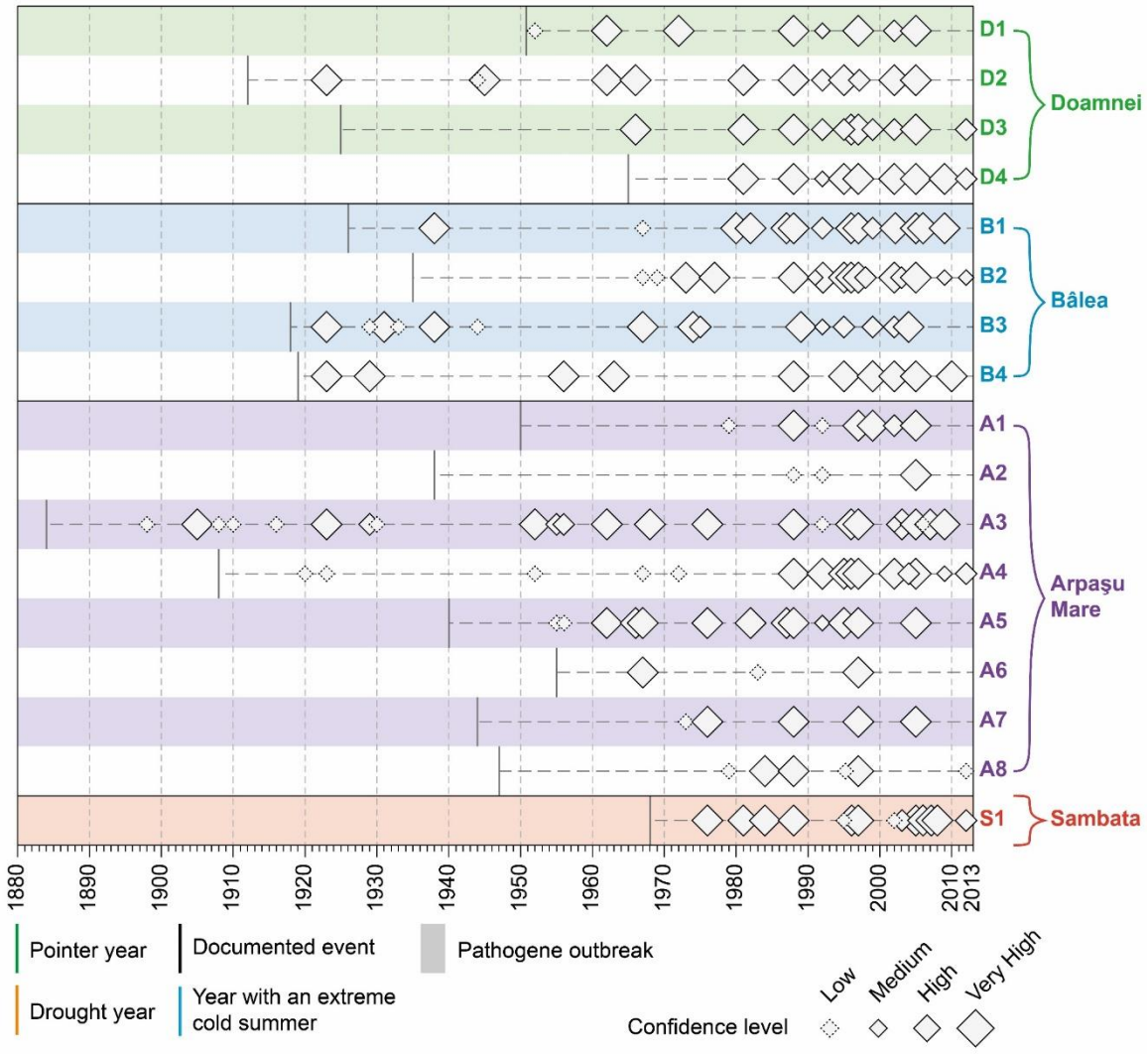

Figure S.2 – Chronologie régionale de l'activité des avalanches pour 17 couloirs du massif des Făgăraş (Roumanie) pour la période 1884–2013. La taille des symboles est proportionnelle au niveau de confiance.

réduite. Il est significativement supérieur à celui mesurée dans les autres études réalisées dans les Alpes françaises par Corona et al. (2012, 43%), Corona et al. (2013, 43%), Schläppy et al. (2013, 38%) et Schläppy et al. (2014, 33-45%). Plusieurs explications ont été avancées afin d'expliquer ces différences notamment la difficulté de distinguer deux événements qui se sont produits la même année dans les cernes d'arbres, la difficulté à retrouver les événements extrêmes ayant détruits le peuplement forestier ou au contraire de trop faible intensité pour endommager la forêt (Corona et al., 2012). Dans tous les cas, et malgré les avancées proposées ici pour une sélection des couloirs permettant d'optimiser la convergence avec la documentation historique, les reconstructions ne reflètent que très imparfaitement l'activité « réelle » des avalanches. Dans le futur, afin d'améliorer l'exhaustivité des chronologies, un couplage systématique devra être envisagé. Ce dernier devra nécessaire intégrer les spécificités inhérentes aux deux approches.

2.5. Utilisation de l'approche dans d'autres contextes bioclimatiques

A ce jour, les deux chronologies présentées dans le cadre de cette thèse sont inédites par leur durée et le nombre de couloirs qu'elles incluent. Elles permettent de mettre en évidence des différences significatives entre les deux régions étudiées. Dans le futur, l'approche proposée ici pourra bien entendu être répliquée dans d'autres massifs et dans d'autres contextes bioclimatiques. Une chronologie régionale est ainsi en cours de construction pour le massif des Făgăraş (Roumanie) à partir de 17 couloirs d'avalanches prélevés dans les vallées de Doamnei, Bâlea, Arpaşu Mare et de Sambata (Fig. S.2) (collaboration avec l'université de Timisoara). Malgré de nombreuses interactions avec les activités agro-sylvo-pastorales, un fort potentiel existe également dans les massifs forestiers de moyenne altitude (Préalpes, Pyrénées, Vosges, Jura) où l'enneigement fortement déficitaire au cours des dernières décennies est susceptible d'avoir modifié, encore plus que dans les Alpes, l'activité des avalanches (Giacona et al., 2018).

BIBLIOGRAPHIE

A

AGRESTE, 2012. *Recensement Agricole 2010 – Résultats – Données chiffrées*. Ministère de l'Agriculture et de l'Alimentation, Paris, France.

ALDRICH J., NELSON F., 1984. *Linear Probability, Logit and Profit Models, Quantitative Application in the Social Sciences*. Sage Publications, Beverly Hills, CA.

ALESTALO J., 1971. Dendrochronological interpretation of geomorphic processes. *Fennia* 105, 1–139.

ALPINE CONVENTION, 2015. *Demographic Changes in the Alps. The Fifth Report on the State of the Alps*. Permanent Secretariat of the Alpine Convention, Innsbruck.

ANCEY, C., 1998. *Guide Neige et avalanches : Connaissances, pratiques, sécurité*. Quae.

ANCEY, C., 2004. Powder snow avalanches: Approximation as non-Boussinesq clouds with a Richardson number–dependent entrainment function. *J. Geophys. Res.-Earth* 109, F01005. doi: 10.1029/2003JF000052

ANCEY, C., 2006. *Dynamique des avalanches. Presses polytechniques et universitaires romandes*. Cemagref, Lausanne ;Antony (France).

ANCEY, C., 2012. Are there "dragon-kings" events (i.e. genuine outliers) among extreme avalanches? *Eur. Phys. J. Spec. Top.* 205, 117–129. doi: 10.1140/epjst/e2012-01565-7

ANCEY, C., CHARLIER, C., 1996. Quelques réflexions autour de la classification des avalanches / Some thoughts on a classification of avalanches. *Rev. Géogr. Alp.* 84, 9–21. doi: 10.3406/rga.1996.3844

ANCEY, C., MEUNIER, M., 2004. Estimating bulk rheological properties of flowing snow avalanches from field data. *J. Geophys. Res.-Earth* 109, F01004. doi: 10.1029/2003JF000036

ANCEY, C., GERVASONI, C., MEUNIER, M., 2004. Computing extreme avalanches. *Cold Reg. Sci. Technol.* 39, 161–180. doi: 10.1016/j.coldregions.2004.04.004

ANENA, 2018. *Bilan des accidents d'avalanches 2017-2018*. Consulté le 01.06.2018 [http://www.anena.org/10529-bilan-des-accidents-d-avalanche-2017-2018.htm].

ARBELLAY, E., STOFFEL, M., DECAULNE A., 2013. Dating of snow avalanches by means of wound-induced vessel anomalies in sub-arctic Betula pubescens. *Boreas* 42, 568–574. doi: 10.1111/j.1502-3885.2012.00302.x

ARPA, CEMAGREF, 2008. *Projet n°165 PROVIALP : Protection de la Viabilité Alpine – Rapport Final (Rapport Final)*. ARPA, CEMAGREF, Torino (Ita).

ASTRADE, L., LUTOFF, C., NEDJAI, R., PHILIPPE, C., LOISON, D., BOTTOLLIER-DEPOIS, S., 2007. Péri-urbanisation et risques naturels : Évolution d'un espace montagnard périurbain et conscience des risques naturels par ses habitants : le bassin du Lavanchon (agglomération de Grenoble, France). *Rev. Géogr. Alp.*, 9–18. doi: 10.4000/rga.125

AUER, I., BÖHM, R., JURKOVIC, A., LIPA, W., ORLIK, A., POTZMANN, R., SCHÖNER, W., UNGERSBÖCK, M., MATULLA, C., BRIFFA, K., JONES, P., EFTHYMIADIS, D., BRUNETTI, M., NANNI, T., MAUGERI, M., MERCALLI, L., MESTRE, O., MOISSELIN, J.-M., BEGERT, M., MÜLLER-WESTERMEIER, G., KVETON, V., BOCHNICEK, O., STASTNY, P., LAPIN, M., SZALAI, S., SZENTIMREY, T., CEGNAR, T., DOLINAR, M., GAJIC-CAPKA, M., ZANINOVIC, K., MAJSTOROVIC, Z., NIEPLOVA, E., 2007. HISTALP—historical instrumental climatological surface time series of the Greater Alpine Region. *Int. J. Climatol.* 27, 17–46. doi: 10.1002/joc.1377

B

BADOUX, A., ANDRES, N., TECHEL, F., HEGG, C., 2016. Natural hazard fatalities in Switzerland from 1946 to 2015. *Nat. Hazards Earth Syst.* 16, 2747–2768. doi: 10.5194/nhess-16-2747-2016

BAKKEHØI, S., 1987. Snow avalanche prediction using probabilistic method. Avalanche formation, movement and effect. *IAHS Spec. Publ.* 549–556.

BALLESTEROS-CÁNOVAS, J.A., TRAPPMANN, D., MADRIGAL-GONZÁLEZ, J., ECKERT, N., STOFFEL, M., 2018. Climate warming enhances snow avalanche risk in the western Himalayas. *P. Natl. Acad. Sci. USA* 115, 3410–3415. doi: 10.1073/pnas.1716913115

BALTENSWEILER, W., BENZ, G., BOVEY, P., DELUCCHI, V., 1977. Dynamics of Larch Bud Moth Populations. *Annu. Rev. Entomol.* 22, 79–100. doi: 10.1146/annurev.en.22.010177.000455

BARBOLINI, M., KEYLOCK, C.J., 2002. A new method for avalanche hazard mapping using a combination of statistical and deterministic models. *Nat. Hazards Earth Syst.* 2, 239–245

BARBOLINI, M., GRUBER, U., KEYLOCK, C.J., NAAIM, M., SAVI, F., 2000. Application of statistical and hydraulic-continuum dense-snow avalanche models to five real European sites. *Cold Reg. Sci. Technol.* 31, 133–149. doi: 10.1016/S0165-232X(00)00008-2

BARTELT, P., STÖCKLI, V., 2001. The influence of tree and branch fracture, overturning and debris entrainment on snow avalanche flow. *Ann. Glaciol.* 32, 209–216. doi: 10.3189/172756401781819544

BARTELT, P., SALM, B., GRUBER, U., 1999. Calculating dense-snow avalanche runout using a Voellmy-fluid model with active/passive longitudinal straining. *J. Glaciol.* 45, 242–254. doi: 10.3189/S002214300000174X

BATTIPAGLIA, G., FRANK, D., BÜNTGEN, U., DOBROVOLNÝ, P., BRÁZDIL, R., PFISTER, C., ESPER, J., 2010. Five centuries of Central European temperature extremes reconstructed from tree-ring density and documentary evidence. *Glob. Planet. Chang.* 72, 182–191. doi: 10.1016/j.gloplacha.2010.02.004

BEBI, P., KIENAST, F., SCHÖNENBERGER, W., 2001. Assessing structures in mountain forests as a basis for investigating the forests' dynamics and protective function. *For. Ecol. Manag.* 145, 3–14. doi: 10.1016/S0378-1127(00)00570-3

BEBI, P., KULAKOWSKI, D., RIXEN, C., 2009. Snow avalanche disturbances in forest ecosystems—State of research and implications for management. *For. Ecol. Manag.*, Disturbances in Mountain Forests: Implications for Management 257, 1883–1892. doi: 10.1016/j.foreco.2009.01.050

BEBI, P., SEIDL, R., MOTTA, R., FUHR, M., FIRM, D., KRUMM, F., CONEDERA, M., GINZLER, C., WOHLGEMUTH, T., KULAKOWSKI, D., 2017. Changes of forest cover and disturbance regimes in the mountain forests of the Alps. *For. Ecol. Manag.* 388, 43–56. doi: 10.1016/j.foreco.2016.10.028

BÉLANGER, L., CASSAYRE, Y., 2004. Projects for Past Avalanche Observation and Zoning in France, After 1999 Catastrophic Avalanches. *Proceedings of the International Snow Science Workshop 2004.* Jackson Hole, Wyoming, 416–421.

BENISTON, M., 1997. Variations of Snow Depth and Duration in the Swiss Alps Over the Last 50 Years: Links to Changes in Large-Scale Climatic Forcings. In: DIAZ, H.F., BENISTON, M., BRADLEY, R.S. (EDS.), *Climatic Change at High Elevation Sites*. Springer Netherlands, Dordrecht, pp. 49–68. doi: 10.1007/978-94-015-8905-5_3

BENISTON, M., 2005. Warm winter spells in the Swiss Alps: Strong heat waves in a cold season? A study focusing on climate observations at the Saentis high mountain site. *Geophys. Res. Lett.* 32. doi: 10.1029/2004GL021478

BENISTON, M., FARINOTTI, D., STOFFEL, M., ANDREASSEN, L.M., COPPOLA, E., ECKERT, N., FANTINI, A., GIACONA, F., HAUCK, C., HUSS, M., HUWALD, H., LEHNING, M., LÓPEZ-MORENO, J.-I., MAGNUSSON, J., MARTY, C., MORÁN-TEJÉDA, E., MORIN, S., NAAIM, M., PROVENZALE, A., RABATEL, A., SIX, D., STÖTTER, J., STRASSER, U., TERZAGO, S., VINCENT, C., 2018. The European mountain cryosphere: a review of its current state, trends, and future challenges. *Cryosphere* 12, 759–794. doi: 10.5194/tc-12-759-2018

BERLINER, L.M., 2003. Physical-statistical modeling in geophysics. *J. Geophys. Res.-Atmos.* 108. doi:10.1029/2002JD002865

BLANCHARD, R., 1915. Le Haut Dauphiné à la fin du XVIe siècle, d'après les procès-verbaux de la Révision des Feux de 1700. *Rev. Géogr. Alp.* 3, 337–419. doi: 10.3406/rga.1915.4846

BLIKRA, H., SELVIK, F., 1998. Climatic signals recorded in snow avalanche-dominated colluvium in western Norway: depositional facies successions and pollen records. *The Holocene* 8, 631–658. doi: 10.1191/095968398674390284

BÖHM, R., JONES, P.D., HIEBL, J., FRANK, D., BRUNETTI, M., MAUGERI, M., 2009. The early instrumental warm-bias: a solution for long central European temperature series 1760–2007. *Climate Change* 101, 41–67. doi: 10.1007/s10584-009-9649-4

BOLLATI, I., CROSA LENZ, B., GOLZIO, A., MASSEROLI, A., 2018. Tree rings as ecological indicator of geomorphic activity in geoheritage studies. *Ecol. Indic.* 93, 899–916. doi: 10.1016/j.ecolind.2018.05.053

BOLLSCHWEILER, M., STOFFEL, M., SCHNEUWLY, D.M., 2008a. Dynamics in debris-flow activity on a forested cone — A case study using different dendroecological approaches. *CATENA* 72, 67–78. doi: 10.1016/j.catena.2007.04.004

BOLLSCHWEILER, M., STOFFEL, M., SCHNEUWLY, D.M., BOURQUI, K., 2008b. Traumatic resin ducts in Larix decidua stems impacted by debris flows. *Tree Physiol.* 28, 255–263. doi: 10.1093/treephys/28.2.255

BONNEFOY, M., BARRAL, L., CABOS, S., ESCANDE, S., GAUCHER, R., PASQUIER, X., RICHARD, D., 2010. The localization map of avalanche phenomena (CLPA): Stakes and prospects. *Proceedings of the International Snow Science Workshop 2010*. Squaw Valley, California, 699–705.

BORMANN, K.J., BROWN, R.D., DERKSEN, C., PAINTER, T.H., 2018. Estimating snow-cover trends from space. Nat. *Climate Change* 8, 924. doi: 10.1038/s41558-018-0318-3

BOUCHER, D., FILION, L., HETU, B., 2003. Reconstitution dendrochronologique et fréquence des grosses avalanches de neige dans un couloir subalpin du mont Hog's Back, en Gaspésie centrale (Québec). *Géogr. Phys. Quat.* 57, 159–168. doi: 10.7202/011311ar

BOUROVA, E., MALDONADO, E., LEROY, J.-B., ALOUANI, R., ECKERT, N., BONNEFOY-DEMONGEOT, M., DESCHATRES, M., 2016. A new web-based system to improve the monitoring of snow avalanche hazard in France. *Nat. Hazards Earth Syst. Sci.* 16, 1205–1216. doi: 10.5194/nhess-16-1205-2016

BOZHINSKIY, A.N., NAZAROV, A.N., CHERNOUSS, P.A., 2001. Avalanches: a probabilistic approach to modelling. *Ann. Glaciol.* 32, 255–258.

BRIQUEL, V., 2001. L'avancée de la périurbanisation dans les Alpes du Nord françaises et ses liens avec la croissance récente de la population. *Rev. Géogr. Alp.* 89, 21–40. doi: 10.3406/rga.2001.3020

BRÖNNIMANN, S., FRANKE, J., NUSSBAUMER, S.U., ZUMBÜHL, H.J., STEINER, D., TRACHSEL M., HEGERL G.C., SCHURER A., WORNI M., MALIK A., FLÜCKIGER J., RAIBLE C.C., 2019. Last phase of the Little Ice Age forced by volcanic eruptions. *Nat. Geoscience*, 10. doi : 10.1038/s41561-019-0402-y

BROOKS, S.P., GELMAN, A., 1998. General methods for monitoring convergence of iterative simulations. *J. Comput. Graph. Stat.* 7, 434–455. doi: 10.1080/10618600.1998.10474787

BRÜNDL, M., ETTER, H.-J., STEINIGER, M., KLINGLER, C., RHYNER, J., AMMANN, W.J., 2004. IFKIS - a basis for managing avalanche risk in settlements and on roads in Switzerland. *Nat. Hazards Earth Syst. Sci.* 4, 257–262.

BRÜNDL, M., BARTELT, P., SCHWEIZER, J., KEILER, M., GLADE, T., 2010. Review and future challenges in snow avalanche risk analysis. In ALCÁNTARA-AYALA I. AND GOUDIE A. (EDS.), *Geomorphological Hazards and Disaster Prevention.* Cambrige University Press, Cambrige, 49–61

BRYANT, C.L., BUTLER, D.R., VITEK, J.D., 1989. A statistical analysis of tree-ring dating in conjunction with snow avalanches: Comparison of on-path versus off-path responses. *Environ. Geol. Water S.* 14, 53–59. doi: 10.1007/BF01740585

BÜNTGEN, U., ESPER, J., FRANK, D.C., NICOLUSSI, K., SCHMIDHALTER, M., 2005. A 1052-year tree-ring proxy for Alpine summer temperatures. *Clim. Dynam.* 25, 141–153. doi: 10.1007/s00382-005-0028-1

BÜNTGEN, U., FRANK, D., LIEBHOLD, A., JOHNSON, D., CARRER, M., URBINATI, C., GRABNER, M., NICOLUSSI, K., LEVANIC, T., ESPER, J., 2009. Three centuries of insect outbreaks across the European Alps. *New Phytol.* 182, 929–941. doi: 10.1111/j.1469-8137.2009.02825.x

BURROWS, C.J., BURROWS, V.L., 1976. Procedures for the study of snow avalanche chronology using growth layers of woody plants: Boulder, Colorado. *Inst. Arct. Alpine Res.*, Occasional Paper, 54p.

BUTLER, D.R., 1979. Snow Avalanche Path Terrain and Vegetation, Glacier National Park, Montana. *Arct. Alpine Res.* 11, 17–32. doi: 10.2307/1550456

BUTLER, D.R., 1986. Snow avalanches hazards in Glacier National Park, Montana, meteorological and climatological aspects. *Phys. Geogr.* 7, 72–87.

BUTLER, D.R., 1987. Teaching General Principles and Applications of Dendrogeomorphology. *J. Geol. Educ.* 35, 64–70. doi: 10.5408/0022-1368-35.2.64

BUTLER, D.R., MALANSON, G.P., 1985a. A History of High-Magnitude Snow Avalanches, Southern Glacier National Park, Montana, U.S.A. *Mt. Res. Dev.* 5, 175–182. doi: 10.2307/3673256

BUTLER, D.R., MALANSON, G.P., 1985b. A Reconstruction of Snow-Avalanche Characteristics in Montana, U.S.A., Using Vegetative Indicators. *J. Glaciol.* 31, 185–187. doi: 10.3189/S0022143000006444

BUTLER, D.R., SAWYER, C.F., 2008. Dendrogeomorphology and high-magnitude snow avalanches: a review and case study. *Nat. Hazards Earth Syst.* 8, 303–309. doi: 10.5194/nhess-8-303-2008

BUTLER, D.R., SAWYER, C.F., MAAS, J.A., 2010. Tree-ring dating of snow avalanches in Glacier National Park, Montana, USA. In: STOFFEL, M., BOLLSCHWEILER, M., BUTLER, D.R., LUCKMAN, B.H. (EDS.), *Tree Rings and Natural Hazards – A State-of-the-Art*. Springer, Dordrecht, pp. 33–44.

C

CARRARA, P.E., 1979. The determination of snow avalanche frequency through tree-ring analysis and historical records at Ophir, Colorado. *Geol. Soc. Am. Bull.* 90, 773–780. doi: 10.1130/0016-7606(1979)90<773:TDOSAF>2.0.CO;2

CARRARA, P.E., 1989. Late quaternary glacial and vegetative history of the Glacier National Park region, Montana (USGS Numbered Series No. 1902), Bulletin. U.S. G.P.O. ; For sale by the Books and Open-File Reports Section, U.S. Geological Survey. doi : 10.3133/b1902

CARRER, M., URBINATI, C., 2001. Assessing climate-growth relationships: a comparative study between linear and non-linear methods. *Dendrochronologia* 1, 57–65.

CASTEBRUNET, H., ECKERT, N., GIRAUD, G., 2012. Snow and weather climatic control on snow avalanche occurrence fluctuations over 50 yr in the French Alps. *Clim. Past.* 8, 855–875. doi: 10.5194/cp-8-855-2012

CASTEBRUNET, H., ECKERT, N., GIRAUD, G., DURAND, Y., MORIN, S., 2014. Projected changes of snow conditions and avalanche activity in a warming climate: a case study in the French Alps over the 2020–2050 and 2070–2100 periods. *Cryosphere* 8, 581–640. doi: 10.5194/tcd-8-581-2014

CASTELLER, A., STÖCKLI, V., VILLALBA, R., MAYER, A.C., 2007. An Evaluation of dendroecological indicators of snow avalanches in the Swiss alps. *Arct. Antarct. Alp. Res.* 39, 218–228. doi: 10.1657/1523-0430(2007)39[218:AEODIO]2.0.CO;2

CASTELLER, A., CHRISTEN, M., VILLALBA, R., MARTÍNEZ, H., STÖCKLI, V., LEIVA, J.C., BARTELT, P., 2008. Validating numerical simulations of snow avalanches using dendrochronology: the Cerro Ventana event in Northern Patagonia, Argentina. *Nat. Hazards Earth Syst. Sci.* 8, 433–443. doi: 10.5194/nhess-8-433-2008

CASTELLER, A., VILLALBA, R., ARANEO, D., STÖCKLI, V., 2011. Reconstructing temporal patterns of snow avalanches at Lago del Desierto,southern Patagonian Andes. *Cold Reg. Sci. Technol.* 67, 68–78. doi: 10.1016/j.coldregions.2011.02.001

CASTELLER, A., HÄFELFINGER, T., CORTÉS DONOSO, E., PODVIN, K., KULAKOWSKI, D., BEBI, P., 2018. Assessing the interaction between mountain forests and natural hazards at Nevados de Chillán, Chile, and its implications for Ecosystem-based Disaster Risk Reduction. *Nat. Hazards Earth Syst. Sci.* 1173–1186. doi: 10.5194/nhess-18-1173-2018

CHAUCHARD, S., CARCAILLET, C., GUIBAL, F., 2007. Patterns of Land-use Abandonment Control Tree-recruitment and Forest Dynamics in Mediterranean Mountains. *Ecosystems* 10, 936–948. doi: 10.1007/s10021-007-9065-4

CHAUCHARD, S., BEILHE, F., DENIS, N., CARCAILLET, C., 2010. An increase in the upper tree-limit of silver fir (Abies alba Mill.) in the Alps since the mid-20th century: A land-use change phenomenon. *For. Ecol. Manag.* 259, 1406–1415. doi: 10.1016/j.foreco.2010.01.009

CHIMANI, B., MATULLA, C., BÖHM, R., HOFSTÄTTER, M., 2013. A new high resolution absolute temperature grid for the Greater Alpine Region back to 1780. *Int. J. Climatol.* 33, 2129–2141. doi: 10.1002/joc.3574

CHIROIU, P., STOFFEL, M., ONACA, A., URDEA, P., 2015. Testing dendrogeomorphic approaches and thresholds to reconstruct snow avalanche activity in the Făgăraş Mountains (Romanian Carpathians). *Quat. Geochronol.* 27, 1–10. doi: 10.1016/j.quageo.2014.11.001

CHRISTEN, M., KOWALSKI, J., BARTELT, P., 2010. RAMMS: Numerical simulation of dense snow avalanches in three-dimensional terrain. *Cold Reg. Sci. Technol.* 63, 1–14. doi: 10.1016/j.coldregions.2010.04.005

COAZ, J., 1910. *Statistik und Verbau der Lawinen in den Schweizeralpen*. Im Auftrag des eidgenössischen Departementes des Innern, Stämpfli, Bern.

CONOVER, W.J., 1999. *Practical Nonparametric Statistics, 3rd edition*. John Wiley & Sons, New York.

COOK, E.R., 1987. The decomposition of tree-ring series for environmental studies. *Tree-Ring Bull.*

CORONA, C., ROVÉRA, G., LOPEZ-SAEZ, J., STOFFEL, M., PERFETTINI, P., 2010. Spatio-temporal reconstruction of snow avalanche activity using tree rings: Pierres Jean Jeanne avalanche talus, Massif de l'Oisans, France. *CATENA* 83, 107–118. doi: 10.1016/j.catena.2010.08.004

CORONA, C., LOPEZ-SAEZ, J., STOFFEL, M., BONNEFOY, M., RICHARD, D., ASTRADE, L., BERGER, F., 2012. How much of the real avalanche activity can be captured with tree rings? An evaluation of classic dendrogeomorphic approaches and comparison with historical archives. *Cold Reg. Sci. Technol.* 74–75, 31–42. doi: 10.1016/j.coldregions.2012.01.003

CORONA, C., LOPEZ-SAEZ, J., STOFFEL, M., ROVÉRA, G., EDOUARD, J.-L., BERGER, F., 2013. Seven centuries of avalanche activity at Echalp (Queyras massif, southern French Alps) as inferred from tree rings. *The Holocene* 23, 292–304. doi: 10.1177/0959683612460784

CORONA, C., LOPEZ-SAEZ, J., STOFFEL, M., 2014. Defining optimal sample size, sampling design and thresholds for dendrogeomorphic landslide reconstructions. *Quat. Geochronol.* 22, 72–84. doi: 10.1016/j.quageo.2014.02.006

COUGHLAN, M.R., 2013. Errakina: Pastoral fire use and landscape memory in the Basque region of the French western Pyrenees. *J. Ethnobiol.* 33, 86–104. doi: 10.2993/0278-0771-33.1.86

COUTTS, M.P., 1983. Root architecture and tree stability. *Plant Soil* 71, 171–188. doi: 10.1007/BF02182653

CRAMER, V., HOBBS, R., STANDISH, R., 2008. What's new about old fields? Land abandonment and ecosystem assembly. *Trends Ecol. Evol.* 23, 104–112. doi: 10.1016/j.tree.2007.10.005

CRESSIE, N., WIKLE, C.K., 2011. Statistics for Spatio-Temporal Data. John Wiley & Sons.

D

DALE, M.R.T., FORTIN, M.-J., 2014. *Spatial Analysis: A Guide for Ecologists, 2nd edn*. Cambridge University Press, Cambridge.

DE BOUCHARD D'AUBETERRE, G., FAVILLIER, A., MAINIERI, R., LOPEZ SAEZ, J., ECKERT, N., SAULNIER, M., PEIRY, J.-L., STOFFEL, M., CORONA, C., 2019. Tree-ring reconstruction of snow avalanche activity: Does avalanche path selection matter? *Sci. Total Environ.* 684, 496–508. doi: 10.1016/j.scitotenv.2019.05.194

DE QUERVAIN, M., 1978. Wald und Lawinen. In: *Proceedings of the IUFRO*. Presented at the Seminar Mountain Forests and Avalanches, Davos, Switzerland, pp. 219–231.

DE QUERVAIN, M., MEISTER, R., 1987. 50 years of snow profiles on the Weissfluhjoch and relations to the surrounding avalanche activity (1936–1985). In: Proceedings of the IAHS Symposium. Presented at the IAHS Davos 1986, IAHS, Davos, Switzerland, pp. 161–181.

DECAULNE, A., EGGERTSSON, Ó., SÆMUNDSSON, Þ., 2012. A first dendrogeomorphologic approach of snow avalanche magnitude–frequency in Northern Iceland. *Geomorphology* 167–168, 35–44. doi: 10.1016/j.geomorph.2011.11.017

DECAULNE, A., EGGERTSSON, Ó., LAUTE, K., BEYLICH, A.A., 2014. A 100-year extreme snow-avalanche record based on tree-ring research in upper Bødalen, inner Nordfjord, western Norway. *Geomorphology* 218, 3–15. doi: 10.1016/j.geomorph.2013.12.036

DER, G., EVERITT, B.S., 2009. *A Handbook of Statistical Analyses using SAS*, 3rd ed. Chapman and Hall/CRC, Boca Raton.

DESLOGES, J.R., RYDER, J.M., 1990. Neoglacial history of the Coast Mountains near Bella Coola, British Columbia. *Can. J. Earth Sci.* 27, 281–290. doi: 10.1139/e90-027

DIDIER, L., 2001. Invasion patterns of European larch and Swiss stone pine in subalpine pastures in the French Alps. *For. Ecol. Manag.* 145, 67–77. doi: 10.1016/S0378-1127(00)00575-2

DUBÉ, S., FILION, L., HÉTU, B., 2004. Tree-ring reconstruction of high-magnitude snow avalanches in the northern Gaspé peninsula, Québec, Canada. *Arct. Antarct. Alp. Res.* 36, 555–564. doi: 10.1657/1523-0430(2004)036[0555:TROHSA]2.0.CO;2

DURAND, Y., GIRAUD, G., LATERNSER, M., ETCHEVERS, P., MÉRINDOL, L., LESAFFRE, B., 2009a. Reanalysis of 47 Years of Climate in the French Alps (1958–2005): Climatology and Trends for Snow Cover. *J. Appl. Meteorol. Climatol.* 48, 2487–2512. doi: 10.1175/2009JAMC1810.1

DURAND, Y., LATERNSER, M., GIRAUD, G., ETCHEVERS, P., LESAFFRE, B., MERINDOL, L., 2009b. Reanalysis of 44 Yr of Climate in the French Alps (1958–2002): Methodology, Model Validation, Climatology, and Trends for Air Temperature and Precipitation. *J. Appl. Meteorol. Climatol.* 48, 429–449. doi: 10.1175/2008JAMC1808.1

E

ECKERT, N., PARENT, E., RICHARD, D., 2007a. Revisiting statistical–topographical methods for avalanche predetermination: Bayesian modelling for runout distance predictive distribution. *Cold Reg. Sci. Technol.* 49, 88–107. doi: 10.1016/j.coldregions.2007.01.005

ECKERT, N., BAYA, H., DESCHATRES, M., 2010a. Assessing the Response of Snow Avalanche Runout Altitudes to Climate Fluctuations Using Hierarchical Modeling: Application to 61 Winters of Data in France. *J. Clim.* 23, 3157–3180. doi: 10.1175/2010JCLI3312.1

ECKERT, N., NAAIM, M., PARENT, E., 2010b. Long-term avalanche hazard assessment with a Bayesian depth-averaged propagation model. *J. Glaciol.* 56, 563–586. doi: 10.3189/002214310793146331

ECKERT, N., PARENT, E., BELANGER, L., GARCIA, S., 2007b. Hierarchical modelling for spatial analysis of the number of avalanche occurrences at the scale of the township. *Cold Reg. Sci. Technol.* 50, 97–112. doi: 10.1016/j.coldregions.2007.01.008

ECKERT, N., PARENT, E., NAAIM, M., RICHARD, D., 2008. Bayesian stochastic modelling for avalanche predetermination: from a general system framework to return period computations. *Stoch. Env. Res. Risk A.* 22, 185–106. doi: 10.1007/s00477-007-0107-4

ECKERT, N., COLEOU, C., CASTEBRUNET, H., DESCHATRES, M., GIRAUD, G., GAUME, J., 2010c. Cross-comparison of meteorological and avalanche data for characterising avalanche cycles: The example of December 2008 in the eastern part of the French Alps. *Cold Reg. Sci. Technol.* 64, 119–136. doi: 10.1016/j.coldregions.2010.08.009

ECKERT, N., PARENT, E., KIES, R., BAYA, H., 2010d. A spatio-temporal modelling framework for assessing the fluctuations of avalanche occurrence resulting from climate change: application to 60 years of data in the northern French Alps. *Climatic Change* 101, 515–553. doi: 10.1007/s10584-009-9718-8

ECKERT, N., BAYA, H., THIBERT, E., VINCENT, C., 2011. Extracting the temporal signal from a winter and summer mass-balance series: application to a six-decade record at Glacier de Sarennes, French Alps. *J. Glaciol.* 57, 134–150. doi: 10.3189/002214311795306673

ECKERT, N., KEYLOCK, C.J., CASTEBRUNET, H., LAVIGNE, A., NAAIM, M., 2013. Temporal trends in avalanche activity in the French Alps and subregions: from occurrences and runout altitudes to unsteady return periods. *J. Glaciol.* 59, 93–114. doi: 10.3189/2013JoG12J091

EFTHYMIADIS, D., JONES, P.D., BRIFFA, K.R., AUER, I., BÖHM, R., SCHÖNER, W., FREI, C., SCHMIDLI, J., 2006. Construction of a 10-min-gridded precipitation data set for the greater alpine region for 1800–2003. *J. Geophys. Res.* 111. doi: 10.1029/2005JD006120

EINHORN, B., ECKERT, N., CHAIX, C., RAVANEL, L., DELINE, P., GARDENT, M., BOUDIÈRES, V., RICHARD, D., VENGEON, J.-M., GIRAUD, G., SCHOENEICH, P., 2015. Changements climatiques et risques naturels dans les Alpes: Impacts observés et potentiels sur les systèmes physiques et socio-économiques. *Rev. Géogr. Alp.* doi: 10.4000/rga.2829

ESPER, J., BUNTGEN, U., FRANK, D.C., NIEVERGELT, D., LIEBHOLD, A., 2007. 1200 years of regular outbreaks in alpine insects. *Proc. R. Soc. B-Biol. Sci.* 274, 671–679. doi: 10.1098/rspb.2006.0191

ESRI, 2013. *ArcGIS 10.2.1*. ESRI, Redlands, CA.

EYNARD-MACHET, R., 1993. Anciens cadastres et évolution des paysages. Cartographie historique de l'occupation des sols dans les Alpes de Savoie, France. *Rev. Géogr. Alp.* 81, 51–66. doi: 10.3406/rga.1993.3719

F

FALARZ, M., 2004. Variability and trends in the duration and depth of snow cover in Poland in the 20th century. *Int. J. Climatol.* 24, 1713–1727. doi: 10.1002/joc.1093

FAVILLIER, A., GUILLET, S., MOREL, P., CORONA, C., LOPEZ-SAEZ, J., ECKERT, N., BALLESTEROS CÁNOVAS, J.A., PEIRY, J.-L., STOFFEL, M., 2017. Disentangling the impacts of exogenous disturbances on forest stands to assess multi-centennial tree-ring reconstructions of avalanche activity in the upper Goms Valley (Canton of Valais, Switzerland). *Quat. Geochronol.* 42, 89–104. doi: 10.1016/j.quageo.2017.09.001

FAVILLIER, A., GUILLET, S., TRAPPMANN, D., MOREL, P., LOPEZ-SAEZ, J., ECKERT, N., ZENHÄUSERN, G., PEIRY, J.-L., STOFFEL, M., CORONA, C., 2018. Spatio-temporal maps of past avalanche events derived from tree-ring analysis: A case study in the Zermatt valley (Valais, Switzerland). *Cold Reg. Sci. Technol.* 154, 9–22. doi: 10.1016/j.coldregions.2018.06.004

FEISTL, T., BEBI, P., CHRISTEN, M., MARGRETH, S., DIEFENBACH, L., BARTELT, P., 2015. Forest damage and snow avalanche flow regime. *Nat. Hazards Earth Syst.* 15, 1275–1288. doi: 10.5194/nhess-15-1275-2015

FOUINAT, L., SABATIER, P., DAVID, F., MONTET, X., SCHOENEICH, P., CHAUMILLON, E., POULENARD, J., ARNAUD, F., 2018. Wet avalanches: long-term evolution in the Western Alps under climate and human forcing. *Clim. Past* 14, 1299–1313. doi: 10.5194/cp-14-1299-2018

FRAZER, G.H., 1985. *Dendrogeomorphic evaluation of snow avalanche history at two sites in Banff National Park*. Department of Geography, University of Western Ontario, London, ON, Canada.

FUCHS, S., BRÜNDL, M., STÖTTER, J., 2004. Development of avalanche risk between 1950 and 2000 in the Municipality of Davos, Switzerland. *Nat. Hazards Earth Syst. Sci.* 4, 263–275. doi: 10.5194/nhess-4-263-2004

FUCHS, S., THÖNI, M., MCALPIN, M.C., GRUBER, U., BRÜNDL, M., 2007. Avalanche hazard mitigation strategies assessed by cost effectiveness analyses and cost benefit analyses—evidence from Davos, Switzerland. *Nat. Hazards* 41, 113–129. doi: 10.1007/s11069-006-9031-z

FUCHS, S., RÖTHLISBERGER, V., THALER, T., ZISCHG, A., KEILER, M., 2017. Natural hazard management from a coevolutionary perspective: exposure and policy response in the European Alps. *Ann. Am. Assoc. Geogr.* 107, 382–392. doi: 10.1080/24694452.2016.1235494

G

GADEK, B., KACZKA, R.J., RĄCZKOWSKA, Z., ROJAN, E., CASTELLER, A., BEBI, P., 2017. Snow avalanche activity in Żleb Żandarmerii in a time of climate change (Tatra Mts., Poland). *CATENA* 158, 201–212. doi: 10.1016/j.catena.2017.07.005

GADOUD, M., 1917. *Les forêts du Haut-Dauphiné à la fin du XVIIe siècle et de nos jours*. Imprimerie Allier Frère, Grenoble.

GARAVAGLIA, V., PELFINI, M., 2011. The role of border areas for dendrochronological investigations on catastrophic snow avalanches: A case study from the Italian Alps. *CATENA* 87, 209–215. doi: 10.1016/j.catena.2011.06.006

GARCÍA-HERNÁNDEZ, C., RUIZ-FERNÁNDEZ, J., SÁNCHEZ-POSADA, C., PEREIRA, S., OLIVA, M., VIEIRA, G., 2017. Reforestation and land use change as drivers for a decrease of avalanche damage in mid-latitude mountains (NW Spain). *Glob. Planet. Change* 153, 35–50. doi: 10.1016/j.gloplacha.2017.05.001

GAUCHER, R., PASQUIER, X., BONNEFOY, M., ECKERT, N., DESCHATRES, M., 2009. Quelques exemples d'avalanches exceptionnelles. *Neige Avalanche* 10–14.

GAUME J., ECKERT, N., CHAMBON G., ECKERT N., NAAIM M., BEL, L., 2013. Mapping extreme snowfalls in the French Alps using Max-Stable processes. *Water Resour. Res.* 49(2), 1079–1098. doi: 10.1002/wrcr.20083

GEHRIG-FASEL, J., GUISAN, A., ZIMMERMANN, N.E., 2007. Tree line shifts in the Swiss Alps: Climate change or land abandonment? *J. Veg. Sci.* 18, 571–582. doi: 10.1111/j.1654-1103.2007.tb02571.x

GELLRICH, M., BAUR, P., KOCH, B., ZIMMERMANN, N.E., 2007. Agricultural land abandonment and natural forest re-growth in the Swiss mountains: A spatially explicit economic analysis. *Agric. Ecosyst. Environ.* 118, 93–108. doi: 10.1016/j.agee.2006.05.001

GEORGE, J.-P., GRABNER, M., KARANITSCH-ACKERL, S., MAYER, K., WEIßENBACHER, L., SCHUELER, S., 2017. Genetic variation, phenotypic stability, and repeatability of drought response in European larch throughout 50 years in a common garden experiment. *Tree Physiol.* 37, 33–46. doi: 10.1093/treephys/tpw085

GERMAIN, D., 2016. A statistical framework for tree-ring reconstruction of high-magnitude mass movements: case study of snow avalanches in eastern Canada. *Geogr. Ann. A* 98, 303–311. doi: 10.1111/geoa.12138

GERMAIN, D., FILION, L., HÉTU, B., 2005. Snow avalanche activity after fire and logging disturbances, northern Gaspé Peninsula, Quebec, Canada. *Can. J. Earth Sci.* 42, 2103–2116. doi: 10.1139/e05-087

GERMAIN, D., FILION, L., HÉTU, B., 2008. Snow avalanche regime and climatic conditions in the Chic-Choc Range, eastern Canada. *Climate Change* 92, 141–167. doi: 10.1007/s10584-008-9439-4

GIACONA, F., ECKERT, N., MARTIN, B., 2017. A 240-year history of avalanche risk in the Vosges Mountains based on non-conventional (re)sources. *Nat. Hazards Earth Syst.* 17, 887–904. doi: 10.5194/nhess-17-887-2017

GIACONA, F., ECKERT, N., MAINIERI, R., MARTIN, B., CORONA, C., LOPEZ-SAEZ, J., MONNET, J.-M., NAAIM, M., STOFFEL, M., 2018. Avalanche activity and socio-environmental changes leave strong footprints in forested landscapes: a case study in the Vosges medium-high mountain range. *Ann. Glaciol.* 59, 111–133. doi: 10.1017/aog.2018.26

GILKS, W.R., RICHARDSON, S., SPIEGELHALTER, D., RICHARDSON, S., SPIEGELHALTER, D., 1995. *Markov Chain Monte Carlo in practice*. Chapman and Hall/CRC, New York, 512. doi: 10.1201/b14835

GOBIET, A., KOTLARSKI, S., BENISTON, M., HEINRICH, G., RAJCZAK, J., STOFFEL, M., 2014. 21st century climate change in the European Alps—A review. *Sci. Total Environ.* 493, 1138–1151. doi: 10.1016/j.scitotenv.2013.07.050

GRANET-ABISSET, A.-M., 1994. *La route réinventée : les migrations des Queyrassins aux XIXe et XXe siècles*. La pierre et l'écrit, Presses universitaires de Grenoble, Grenoble.

GRANET-ABISSET, A.-M., 2006. Mémoire et gestion des risques naturels. L'exemple des sociétés alpines (XIXe-XXe siècle). In: Walter, F., Fantini, B., Delvaux, P. (Eds.), *Les cultures du risque (XVIe-XXIe Siècle)*. Travaux d'histoire Suisse, Presses d'Histoire Suisse, Genève, 117–138.

GRUBER, U., BARTELT, P., 2007. Snow avalanche hazard modelling of large areas using shallow water numerical methods and GIS. *Environ. Model. Softw.* 22, 1472–1481. doi: 10.1016/j.envsoft.2007.01.001

H

HAEBERLI, W., HOELZLE, M., PAUL, F., ZEMP, M., 2007. Integrated monitoring of mountain glaciers as key indicators of global climate change: the European Alps. *Ann. Glaciol.* 46, 150–160. doi: 10.3189/172756407782871512

HEBERTSON, E.G., JENKINS, M.J., 2003. Historic climate factors associated with major avalanche years on the Wasatch Plateau, Utah. *Cold Reg. Sci. Technol.* 37, 315–332. doi: 10.1016/S0165-232X(03)00073-9

HEFFERNAN, O., 2018. Coming down the tracks. *Nat. Clim. Change* 8, 937–939. doi: 10.1038/s41558-018-0306-7

HIEBL, J., 2006. *The early instrumental climate period (1760–1860) in Europe. Evidence from the alpine region and Southern Scandinavia*. Diploma thesis, Department of Geography and Regional Research, University of Vienna, Vienna.

HOUGHTON, R.A., HOUSE, J.I., PONGRATZ, J., VAN DER WERF, G.R., DEFRIES, R.S., HANSEN, M.C., LE QUÉRÉ, C., RAMANKUTTY, N., 2012. Carbon emissions from land use and land-cover change. *Biogeosciences* 9, 5125–5142. doi: 10.5194/bg-9-5125-2012

I

IBSEN, M.-L., BRUNSDEN, D., 1996. The nature, use and problems of historical archives for the temporal occurrence of landslides, with specific reference to the south coast of Britain, Ventnor, Isle of Wight. *Geomorphology* 15, 241–258. doi: 10.1016/0169-555X(95)00073-E

IPCC, 2013. *Climate Change 2013: The Physical Science Basis*. Contribution of Working Group I to the Fifth Assessment Report of the Intergovernmental Panel on Climate Change, Cambridge University Press. ed. Intergovernmental Panel on Climate Change, Cambridge, United Kingdom ; New York, NY, USA.

IPCC, 2014. *Climate Change 2014: Synthesis Report*. Contribution of Working Groups I, II and III to the Fifth Assessment Report of the Intergovernmental Panel on Climate Change, IPCC. ed. Geneva, Switzerland.

IVES, J.D., MEARS, A.I., CARRARA, P.E., BOVIS, M.J., 1976. Natural hazards in Mountain Colorado. *Ann. Assoc. Am. Geogr.* 66, 129–144. doi: 10.1111/j.1467-8306.1976.tb01076.x

J

JAMARD, A.L., GARCIA, S., BELANGER, L., 2002. *L'enquête permanente sur les Avalanches (EPA). Statistique descriptive générale des événements et des sites*. DESS Ingénierie Mathématique option Statistique, Université Joseph Fourrier, Grenoble, France.

JENKINS, M.J., HEBERTSON, E.G., 2004. A practitioner's guide for using dendroecological techniques to determine the extent and frequency of avalanches. In: *Proceedings of the International Snow Science Workshop*, Jackson, Wyoming, Jackson, 423–431

JOHNSON, E.A., 1987. The Relative Importance of Snow Avalanche Disturbance and Thinning on Canopy Plant Populations. *Ecology* 68, 43. doi: 10.2307/1938803

JOHNSON, A.L., SMITH, D.J., 2010. *Geomorphology* of snow avalanche impact landforms in the southern Canadian Cordillera: *Geomorphology* of snow avalanche impact landforms. *Can. Geogr-Géogr. Can.* 54, 87–103. doi: 10.1111/j.1541-0064.2009.00275.x

JOMELLI, V., PECH, P., 2004. Effects of the Little Ice Age on avalanche boulder tongues in the French Alps(Massif des Ecrins). *Earth Surf. Process. Landf.* 29, 553–564. doi: 10.1002/esp.1050

JOMELLI, V., PECH, P., CHOCHILLON, C., BRUNSTEIN, D., 2004. Geomorphic Variations of Debris Flows and Recent Climatic Change in the French Alps. *Climate Change* 64, 77–102. doi: 10.1023/B:CLIM.0000024700.35154.44

JOMELLI, V., DELVAL, C., GRANCHER, D., ESCANDE, S., BRUNSTEIN, D., HETU, B., FILION, L., PECH, P., 2007. Probabilistic analysis of recent snow avalanche activity and

weather in the French Alps. *Cold Reg. Sci. Technol.* 47, 180–192. doi: 10.1016/j.coldregions.2006.08.003

JOMELLI, V., PAVLOVA, I., ECKERT, N., GRANCHER, D., BRUNSTEIN, D., 2015. A new hierarchical Bayesian approach to analyse environmental and climatic influences on debris flow occurrence. *Geomorphology* 250, 407–421. doi: 10.1016/j.geomorph.2015.05.022

JOMELLI, V., PAVLOVA, I., GIACONA, F., ZGHEIB, T., ECKERT, N., 2019. Respective influence of geomorphologic and climate conditions on debris-flow occurrence in the Northern French Alps. *Landslides*. doi: 10.1007/s10346-019-01195-7

JURASINSKI, G., KREYLING, J., 2007. Upward shift of alpine plants increases floristic similarity of mountain summits. *J. Veg. Sci.* 18, 711–718. doi: 10.1111/j.1654-1103.2007.tb02585.x

JYLHÄ, K., FRONZEK, S., TUOMENVIRTA, H., CARTER, T.R., RUOSTEENOJA, K., 2008. Changes in frost, snow and Baltic sea ice by the end of the twenty-first century based on climate model projections for Europe. *Climate Change* 86, 441–462. doi: 10.1007/s10584-007-9310-z

K

KAJIMOTO, T., DAIMARU, H., OKAMOTO, T., OTANI, T., ONODERA, H., 2004. Effects of Snow Avalanche Disturbance on Regeneration of Subalpine Abies mariesii Forest, Northern Japan. *Arct. Antarct. Alp. Res.* 36, 436–445. doi: 10.1657/1523-0430(2004)036[0436:EOSADO]2.0.CO;2

KENNEDY, M.D., 2013. *Introducing Geographic Information Systems with ARCGIS: a workbook approach to learning GIS, 3rd edn*. John Wiley & Sons, Hoboken, New Jersey.

KEYLOCK, C.J., 2005. An alternative form for the statistical distribution of extreme avalanche runout distances. *Cold Reg. Sci. Technol.* 42, 185–193. doi: 10.1016/j.coldregions.2005.01.004

KLEIN, G., VITASSE, Y., RIXEN, C., MARTY, C., REBETEZ, M., 2016. Shorter snow cover duration since 1970 in the Swiss Alps due to earlier snowmelt more than to later snow onset. *Climate Change* 139, 637–649. doi: 10.1007/s10584-016-1806-y

KOCH, J., 2009. Improving age estimates for late Holocene glacial landforms using dendrochronology – Some examples from Garibaldi Provincial Park, British Columbia. *Quat. Geochronol.* 4, 130–139. doi: 10.1016/j.quageo.2008.11.002

KOGELNIG-MAYER, B., STOFFEL, M., SCHNEUWLY-BOLLSCHWEILER, M., HÜBL, J., RUDOLF-MIKLAU, F., 2011. Possibilities and limitations of dendrogeomorphic time-series reconstructions on sites influenced by debris flows and frequent snow avalanche activity. *Arct. Antarct. Alp. Res.* 43, 649–658. doi: 10.1657/1938-4246-43.4.649

KOGELNIG-MAYER, B., STOFFEL, M., SCHNEUWLY-BOLLSCHWEILER, M., 2013. Four-dimensional growth response of mature Larix decidua to stem burial under natural conditions. *Trees* 27, 1217–1223. doi: 10.1007/s00468-013-0870-4

KÖHLER, A., FISCHER, J.-T., SCANDROGLIO, R., BAVAY, M., MCELWAINE, J., SOVILLA, B., 2018. Cold-to-warm flow regime transition in snow avalanches. *Cryosphere* 12, 3759–3774. doi: 10.5194/tc-12-3759-2018

KÖSE, N., AYDIN, A., AKKEMIK, Ü., YURTSEVEN, H., GÜNER, T., 2010. Using tree-ring signals and numerical model to identify the snow avalanche tracks in Kastamonu, Turkey. *Nat. Hazards* 54, 435–449. doi: 10.1007/s11069-009-9477-x

KRAUSE, D., KŘÍŽEK, M., 2017. Dating of recent avalanche events in the eastern high Sudetes, Czech Republic. *Quat. Int.* 470, 166–175. doi: 10.1016/j.quaint.2017.09.001

KRESS, A., SAURER, M., BÜNTGEN, U., TREYDTE, K.S., BUGMANN, H., SIEGWOLF, R.T.W., 2009. Summer temperature dependency of larch budmoth outbreaks revealed by Alpine tree-ring isotope chronologies. *Oecologia* 160, 353–365. doi: 10.1007/s00442-009-1290-4

KULAKOWSKI, D., BEBI, P., RIXEN, C., 2011. The interacting effects of land use change, climate change and suppression of natural disturbances on landscape forest structure in the Swiss Alps. *Oikos* 120, 216–225. doi: 10.1111/j.1600-0706.2010.18726.x

KULAKOWSKI, D., BARBEITO, I., CASTELLER, A., KACZKA, R.J., BEBI, P., 2016. Not only climate: Interacting drivers of treeline change in Europe. *Geogr. Pol.* 89, 7–15. doi: 10.7163/GPol.0042

KUNDZEWICZ, Z.W., ROBSON, A.J., 2004. Change detection in hydrological records— a review of the methodology. *Hydrol. Sci. J.* 1, 7–19.

L

LAROCQUE, S.J., HETU, B., FILION, L., 2001. Geomorphic and dendroecological impacts of slushflows in central Gaspé Peninsula (Québec, Canada). *Geogr. Ann. A* 83, 191–201. doi: 10.1111/j.0435-3676.2001.00154.x

LARSSON, L.A., 2016. *CDendro — Cybis Dendro Dating Program*. Cybis Elektron. Data AB Saltsjöbaden, Sweden.

LATERNSER, M., PFISTER, C., 1997. Avalanches in Switzerland 1500-1990. In: FRENZEL B., MATTHEWS J., GLÄSER A., WEISS M. (EDS.), *Rapid Mass Movement since the Holocene*, Palaeoclimate Research, 241–266.

LATERNSER, M., SCHNEEBELI, M., 2002. Temporal trend and spatial distribution of avalanche activity during the last 50 years in Switzerland. *Nat. Hazards* 27, 201–230.

LATERNSER, M., SCHNEEBELI, M., 2003. Long-term snow climate trends of the Swiss Alps (1931-99). *Int. J. Climatol.* 23, 733–750. doi: 10.1002/joc.912

LAUTE, K., BEYLICH, A.A., 2018. Potential effects of climate change on future snow avalanche activity in western Norway deduced from meteorological data. *Geogr. Ann. A* 100, 163–184. doi: 10.1080/04353676.2018.1425622

LAVIGNE, A., BEL, L., PARENT, E., ECKERT, N., 2012. A model for spatio-temporal clustering using multinomial probit regression: application to avalanche counts. *Environmetrics* 23, 522–534. doi: 10.1002/env.2167

LAVIGNE, A., ECKERT, N., BEL, L., PARENT, E., 2015. Adding expert contributions to the spatiotemporal modelling of avalanche activity under different climatic influences. *J. R. Stat. Soc. Ser.-C Appl. Stat.* 64, 651–671. doi: 10.1111/rssc.12095

LAXTON, S.C., SMITH, D.J., 2009. Dendrochronological reconstruction of snow avalanche activity in the Lahul Himalaya, Northern India. *Nat. Hazards* 49, 459–467. doi: 10.1007/s11069-008-9288-5

LAZAR, B., WILLIAMS, M., 2008. Climate change in western ski areas: Potential changes in the timing of wet avalanches and snow quality for the Aspen ski area in the years 2030 and 2100. *Cold Reg. Sci. Technol.* 51, 219–228. doi: 10.1016/j.coldregions.2007.03.015

LEITINGER, G., HÖLLER, P., TASSER, E., WALDE, J., TAPPEINER, U., 2008. Development and validation of a spatial snow-glide model. *Ecol. Model.* 211, 363–374. doi: 10.1016/j.ecolmodel.2007.09.015

LEMOINE, M., TRICART, P., 1986. Les Schistes lustrés des Alpes occidentales: Approche stratigraphique, structurale et sédimentologique. *Eclogae Geol. Helvetiae* 79, 271–294.

LEMPA, M., KACZKA, R.J., RACZKOWSKA, Z., JANECKA, K., 2016. Combining tree-ring dating and geomorphological analyses in the reconstruction of spatial patterns of the runout zone of snow avalanches, Rybi Potok Valley, Tatra Mountains (Poland). *Geogr. Pol.* 89, 31–45. doi: 10.7163/GPol.0044

LEVERS, C., SCHNEIDER, M., PRISHCHEPOV, A.V., ESTEL, S., KUEMMERLE, T., 2018. Spatial variation in determinants of agricultural land abandonment in Europe. *Sci. Total Environ.* 644, 95–111. doi: 10.1016/j.scitotenv.2018.06.326

LEVESQUE, M., SAURER, M., SIEGWOLF, R., EILMANN, B., BRANG, P., BUGMANN, H., RIGLING, A., 2013. Drought response of five conifer species under contrasting water availability suggests high vulnerability of Norway spruce and European larch. *Glob. Chang. Biol.* 19(10), 3184–3199. doi: 10.1111/gcb.12268

LEWIS, D., SMITH, D., 2004. Dendrochronological Mass Balance Reconstruction, Strathcona Provincial Park, Vancouver Island, British Columbia, Canada. *Arct. Antarct. Alp. Res.* 36, 598–606. doi: 10.1657/1523-0430(2004)036[0598:DMBRSP]2.0.CO;2

LEYNAUD, E., GEORGES, M., 1965. Aspects géographiques de l'élevage dans la zone de montagne du département des Hautes-Alpes. *Études Rural* 18, 5–36. doi: 10.3406/rural.1965.1214

LIED, K., BAKKEHØI, K., 1980. Empirical calculations of snow–avalanche run–out distance based on topographic parameters. *J. Glaciol.* 26, 165–177. doi: 10.3189/S0022143000010704

LÓPEZ-MORENO, J.I., GOYETTE, S., BENISTON, M., 2009. Impact of climate change on snowpack in the Pyrenees: Horizontal spatial variability and vertical gradients. *J. Hydrol.* 374, 384–396. doi: 10.1016/j.jhydrol.2009.06.049

LOUP, J., LOVIE, C., 1966. Sur la fréquence des avalanches en haute Tarentaise. *Rev. Géogr. Alp.* 587–604.

M

MACDONALD, D., CRABTREE, J.R., WIESINGER, G., DAX, T., STAMOU, N., FLEURY, P., GUTIERREZ LAZPITA, J., GIBON, A., 2000. Agricultural abandonment in mountain areas of Europe: Environmental consequences and policy response. *J. Environ. Manage.* 59, 47–69. doi: 10.1006/jema.1999.0335

MAGGIONI, M., GRUBER, U., PURVES, R.S., FREPPAZ, M., 2006. Potential Release Areas and Return Period of Avalanches: Is There a Relation? In: STERNBENZ C. AND GREENE N. (EDS.), *Proceedings of the 2006 International Snow Science Workshop*, Telluride, Colorado, 566–571

MAINIERI, R., 2015. *Apport de l'approche dendrogéomorphologique pour la reconstruction pluriséculaire de l'activité spatiotemporelle des avalanches : le cas du couloir de Souliers (Massif du Queyras, Alpes du sud)*. Mémoire de Master, Institut de Géographie Alpine, Université Joseph Fourier Grenoble 1, Grenoble, 78.

MAINIERI, R., FAVILLIER, A., LOPEZ SAEZ, J., ECKERT, N., ZGHEIB, T., MOREL, P., SAULNIER, MELANIE, PEIRY, J.-L., STOFFEL, M., CORONA, C., submitted. Non-stationarities induced by land-cover changes in dendrogeomorphic reconstructions of snow avalanche activity: Insights from the Queyras massif (French Alps). *Glob. Planet. Change.*

MALANSON, G.P., BUTLER, D.R., 1984. Transverse pattern of vegetation on avalanche paths in the northern Rocky Mountains, Montana. *Great Basin Nat.* 44, 453–458.

MALANSON, G.P., BUTLER, D.R., 1986. Floristic Patterns on Avalanche Paths in the Northern Rocky Mountains, USA. *Phys. Geogr.* 7, 231–238. doi: 10.1080/02723646.1986.10642293

MARTIN, J.-P., GERMAIN, D., 2016a. Can we discriminate snow avalanches from other disturbances using the spatial patterns of tree-ring response? Case studies from the Presidential Range, White Mountains, New Hampshire, United States. *Dendrochronologia* 37, 17–32. doi: 10.1016/j.dendro.2015.12.004

MARTIN, J.-P., GERMAIN, D., 2016b. Dendrogeomorphic reconstruction of snow avalanche regime and triggering weather conditions A classification tree model approach. Prog. *Phys. Geogr.* 40, 0309133315625863. doi: 10.1177/0309133315625863

MARTIN, J.-P., GERMAIN, D., 2017. Large-scale teleconnection patterns and synoptic climatology of major snow-avalanche winters in the Presidential Range (New Hampshire, USA). *Int. J. Climatol.* 37, 109–123. doi: 10.1002/joc.4985

MARTIN, E., GIRAUD, G., LEJEUNE, Y., BOUDART, G., 2001. Impact of a climate change on avalanche hazard. *Ann. Glaciol.* 32, 163–167. doi: 10.3189/172756401781819292

MARTIN, B., DRESCHER, A., FOURNIER, M., GUERROUAH, O., GIACONA, F., GLASER, R., HIMMELSBACH, I., HOLLEVILLE, N., RIEMANN, D., SCHONBEIN, J., VITOUX, M.-C., WITH, L., 2015. Les évènements extrêmes dans le fossé rhénan entre 1480 et 2012. Quels apports pour la prévention des inondations ? *Houille Blanche* 2, 82–93. doi: 10.1051/lhb/20150023

MARTY, C., BLANCHET, J., 2012. Long-term changes in annual maximum snow depth and snowfall in Switzerland based on extreme value statistics. *Clim. Change* 111, 705–721. doi: 10.1007/s10584-011-0159-9

MARTY, C., TILG, A.-M., JONAS, T., 2017. Recent Evidence of Large-Scale Receding Snow Water Equivalents in the European Alps. *J. Hydrometeorol.* 18, 1021–1031. doi: 10.1175/JHM-D-16-0188.1

MCCARROLL, D., 1993. Modelling late-holocene snow-avalanche activity: Incorporating a new approach to lichenometry. *Earth Surf. Process. Landf.* 18, 527–539. doi: 10.1002/esp.3290180606

MCCARTHY, D.P., LUCKMAN, B.H., KELLY, P.E., 1991. Sampling Height-Age Error Correction for Spruce Seedlings in Glacial Forefields, Canadian Cordillera. *Arct. Alpine Res.* 23, 451–455. doi: 10.2307/1551687

MCCLUNG, D.M., 1990. A Model for Scaling Avalanche Speeds. *J. Glaciol.* 36(123), 188–198. doi: 10.3189/S0022143000009436

MCCLUNG, D.M., 2003. Magnitude and Frequency of Avalanches in Relation to Terrain and Forest Cover. *Arct. Antarct. Alp. Res.* 35, 82–90. doi: 10.1657/1523-0430(2003)035[0082:MAFOAI]2.0.CO;2

MCCLUNG, D.M., LIED, K., 1987. Statistical and geometrical definition of snow avalanche runout. *Cold Reg. Sci. Technol.* 13, 107–119. doi: 10.1016/0165-232X(87)90049-8

MCCLUNG, D.M., TWEEDY, J., 1993. Characteristics of avalanching: Kootenay Pass, Bristish Columbia, Canada. *J. Glaciol.* 317–322.

MCCLUNG, D.M., SCHAERER, P.A., 2006. *The Avalanche Handbook, 2nd edn*. The Mountaineers Books, Seattle

MEARS, A.I., 1975. Dynamics of dense-snow avalanches interpreted from broken trees. *Geology* 3, 521. doi: 10.1130/0091-7613(1975)3<521:DODAIF>2.0.CO;2

MEȘEȘAN, F., GAVRILĂ, I.G., POP, O.T., 2018a. Calculating snow-avalanche return period from tree-ring data. *Nat. Hazards* 94, 1081–1098. doi: 10.1007/s11069-018-3457-y

MEȘEȘAN, F., MAN, T.C., POP, O.T., GAVRILĂ, I.G., 2018b. Reconstructing snow avalanche extent using remote sensing and dendrogeomorphology in Parâng Mountains. *Cold Reg. Sci. Technol.* 157, 97–109. doi: 10.1016/j.coldregions.2018.10.002

MEUNIER, M., ANCEY, C., 2004. Towards a conceptual approach to predetermining long-return-period avalanche run-out distances. *J. Glaciol.* 50, 268–278. doi: 10.3189/172756504781830178

MILLER, D.H., 1964. *Interception Processes During Snowstorms*. Pacific Southwest Forest and Range Experiment Station, Berkeley, USA.

MITTERER, C., HIRASHIMA, H., SCHWEIZER, J., 2011. Wet-snow instabilities: comparison of measured and modelled liquid water content and snow stratigraphy. *Ann. Glaciol.* 52, 201–208. doi: 10.3189/172756411797252077

MOCK, C.J., BIRKELAND, K.W., 2000. Snow Avalanche Climatology of the Western United States Mountain Ranges. *Bull. Am. Meteorol. Soc.* 81, 2367–2392. doi: 10.1175/1520-0477(2000)081<2367:SACOTW>2.3.CO;2

MOEN, J., AUNE, K., EDENIUS, L., ANGERBJÖRN, A., 2004. Potential Effects of Climate Change on Treeline Position in the Swedish Mountains. *Ecol. Soc.* 9. doi: 10.5751/ES-00634-090116

MORÁN-TEJEDA, E., LÓPEZ-MORENO, J.I., BENISTON, M., 2013. The changing roles of temperature and precipitation on snowpack variability in Switzerland as a function of altitude: role of altitude on swiss snowpack. *Geophys. Res. Lett.* 40, 2131–2136. doi: 10.1002/grl.50463

MOTTA, R., GARBARINO, F., 2003. Stand history and its consequences for the present and future dynamic in two silver fir (Abies alba Mill.) stands in the high Pesio Valley (Piedmont, Italy). *Ann. For. Sci.* 60, 361–370. doi: 10.1051/forest:2003027

MOTTA, R., LINGUA, E., 2005. Human impact on size, age, and spatial structure in a mixed European larch and Swiss stone pine forest in the Western Italian Alps. *Can. J. For. Res.* 35, 1809–1820. doi: 10.1139/x05-107

MOUGIN, P., 1922. *Les avalanches en Savoie. Ministère de l'Agriculture, Direction Générale des Eaux et Forêts*. Service des Grandes Forces Hydrauliques, Paris.

MOUNTAIN RESEARCH INITIATIVE EDW WORKING GROUP, PEPIN, N., BRADLEY, R.S., DIAZ, H.F., BARAER, M., CACERES, E.B., FORSYTHE, N., FOWLER, H., GREENWOOD, G., HASHMI, M.Z., LIU, X.D., MILLER, J.R., NING, L., OHMURA, A., PALAZZI, E., RANGWALA, I., SCHÖNER, W., SEVERSKIY, I., SHAHGEDANOVA, M., WANG, M.B., WILLIAMSON, S.N., YANG, D.Q., 2015. Elevation-dependent warming in mountain regions of the world. *Nat. Clim. Change* 5, 424–430. doi: 10.1038/nclimate2563

MUNDO, I.A., BARRERA, M.D., ROIG, F.A., 2007. Testing the utility of Nothofagus pumilio for dating a snow avalanche in Tierra del Fuego, Argentina. *Dendrochronologia* 25, 19–28. doi: 10.1016/j.dendro.2007.01.001

MUNTAN, E., ANDREU, L., OLLER, P., GUTIERREZ, E., MARTINEZ, P., 2004. Dendrochronological study of the Canal del Roc Roig avalanche path: first results of the Aludex project in the Pyrenees. *Ann. Glaciol.* 38, 173–179. doi: 10.3189/172756404781815077

MUNTAN, E., GARCIA, C., OLLER, P., MARTI, G., GARCIA, A., GUTIERREZ, E., 2009. Reconstructing snow avalanches in the Southeastern Pyrenees. *Nat. Hazards Earth Syst. Sci.* 9, 1599–1612. doi: 10.5194/nhess-9-1599-2009

N

NAAIM, M., DURAND, Y., ECKERT, N., CHAMBON, G., 2013. Dense avalanche friction coefficients: influence of physical properties of snow. *J. Glaciol.* 59, 771–782. doi: 10.3189/2013JoG12J205

NAAIM, M., ECKERT, N., GIRAUD, G., FAUG, T., CHAMBON, G., NAAIM-BOUVET, F., RICHARD, D., 2016. Impact du réchauffement climatique sur l'activité avalancheuse et multiplication des avalanches humides dans les Alpes françaises. *Houille Blanche* 12–20. doi: 10.1051/lhb/2016055

NESJE, A., BAKKE, J., DAHL, S.O., LIE, O., BOE, A.-G., 2007. A continuous, high-resolution 8500-yr snow-avalanche record from western Norway. *The Holocene* 17, 269–277. doi: 10.1177/0959683607075855

NICOLET, G., ECKERT, N., MORIN, S., BLANCHET, J., 2016. Decreasing spatial dependence in extreme snowfall in the French Alps since 1958 under climate change. *J. Geophys. Res.-Atmos.* 121, 8297–8310. doi: 10.1002/2016JD025427

NICOLET, G., ECKERT, N., MORIN, S., BLANCHET, J., 2018. Assessing Climate Change Impact on the Spatial Dependence of Extreme Snow Depth Maxima in the French Alps. *Water Resour. Res.* 54, 7820–7840. doi: 10.1029/2018WR022763

NIKOLOVA, N., FAŠKO, P., LAPIN, M., ŠVEC, M., 2013. Changes in snowfall/precipitation-day ratio in Slovakia and their linkages with air temperature and precipitation. *Contrib. Geophys. Geod.* 43, 141–155. doi: 10.2478/congeo-2013-0009

NÖTHIGER, C., ELSASSER, H., 2004. Natural Hazards and Tourism: New Findings on the European Alps. *Mt. Res. Dev.* 24, 24–27. doi: 10.1659/0276-4741(2004)024[0024:NHATNF]2.0.CO;2

O

O'ROURKE, E., 2006. Changes in agriculture and the environment in an upland region of the Massif Central, France. *Environ. Sci. Policy*, European Rural Landscapes: Land-use, biodiversity, and conservation 9, 370–375. doi: 10.1016/j.envsci.2006.01.008

P

PAULING, A., LUTERBACHER, J., CASTY, C., WANNER, H., 2006. Five hundred years of gridded high-resolution precipitation reconstructions over Europe and the connection to large-scale circulation. *Clim. Dynam.* 26, 387–405. doi: 10.1007/s00382-005-0090-8

PEDERSON, G.T., REARDON, B.A., CARUSO, C.J., FAGRE, D.B., 2006. High resolution tree-ring based spatial reconstructions of snow avalanche activity in Glacier National Park, Montana, USA, In: STERBENZ, C., GREENE, N. (EDS.), *Proceedings of the International Snow Science Workshop 2006.* Telluride, Colorado, 436–443

PELTOLA, H., KELLOMÄKI, S., VÄISÄNEN, H., IKONEN, V.-P., 1999. A mechanistic model for assessing the risk of wind and snow damage to single trees and stands of Scots pine, Norway spruce, and birch. *Can. J. For. Res.* 29, 647–661. doi: 10.1139/x99-029

PIELMEIER, C., TECHEL, F., MARTY, C., STUCKI, T., 2013. Wet snow avalanche activity in the Swiss Alps – trend analysis for mid-winter season. *International Snow Science Workshop 2013.* Grenoble, France, 1240–1246.

POP, O.T., GAVRILĂ, I.-G., ROȘIAN, G., MESEȘAN, F., DECAULNE, A., HOLOBÂCĂ, I.H., ANGHEL, T., 2016. A century-long snow avalanche chronology reconstructed from tree-rings in Parâng Mountains (Southern Carpathians, Romania). *Quat. Int.* 415, 230–240. doi: 10.1016/j.quaint.2015.11.058

POP, O.T., MUNTEANU, A., FLAVIU, M., GAVRILĂ, I.-G., TIMOFTE, C., HOLOBÂCĂ, I.-H., 2017. Tree-ring-based reconstruction of high-magnitude snow avalanches in Piatra Craiului Mountains (Southern Carpathians, Romania). *Geogr. Ann. A* 100, 99–115. doi: 10.1080/04353676.2017.1405715

POTTER, N., 1969. Tree-ring dating of snow avalanche tracks and the geomorphic activity of avalanches, northern Absaroka Mountains, Wyoming. *Geol. Soc. Am. Spec. Pap.* 123, 141–166. doi: 10.1130/SPE123-p141

PÜNTENER, C., STOFFEL, M., SCHNEUWLY-BOLLSCHWEILER, M., 2012. Frequenz und Fliesshöhen der Plattlaui (Uri), rekonstruiert mithilfe von Jahrringen. *Schweiz. Z. Forstwes.* 163, 445–450. doi: 10.3188/szf.2012.0445

R

RABATEL, A., LETRÉGUILLY, A., DEDIEU, J.P., ECKERT, N., 2013. Changes in glacier equilibrium-line altitude in the western Alps from 1984 to 2010: evaluation by remote sensing and modeling of the morpho-topographic and climate controls. *The Cryosphere* 7, 1455–1471. doi: 10.5194/tc-7-1455-2013

RAJCZAK, J., PALL, P., SCHÄR, C., 2013. Projections of extreme precipitation events in regional climate simulations for Europe and the Alpine Region. *J. Geophys. Res.-Atmos.* 118, 3610–3626. doi: 10.1002/jgrd.50297

RAŠKA, P., ZÁBRANSKÝ, V., DUBIŠAR, J., KADLEC, A., HRBÁČOVÁ, A., STRNAD, T., 2014. Documentary proxies and interdisciplinary research on historic geomorphologic hazards: a discussion of the current state from a central European perspective. *Nat. Hazards* 70, 705–732. doi: 10.1007/s11069-013-0839-z

RAYBACK, S.A., 1998. A dendrogeomorphological analysis of snow avalanche in the Colorado Front Range, USA. *Phys. Geogr.* 19, 502–515. doi: 10.1080/02723646.1998.10642664

REARDON, B.A., PEDERSON, G.T., CARUSO, C.J., FAGRE, D.B., 2008. Spatial Reconstructions and Comparisons of Historic Snow Avalanche Frequency and Extent Using Tree Rings in Glacier National Park, Montana, U.S.A. *Arct. Antarct. Alp. Res.* 40, 148–160. doi: 10.1657/1523-0430(06-069)[REARDON]2.0.CO;2

REID, P.C., HARI, R.E., BEAUGRAND, G., LIVINGSTONE, D.M., MARTY, C., STRAILE, D., BARICHIVICH, J., GOBERVILLE, E., ADRIAN, R., AONO, Y., BROWN, R., FOSTER, J., GROISMAN, P., HÉLAOUËT, P., HSU, H.-H., KIRBY, R., KNIGHT, J., KRABERG, A., LI, J., LO, T.-T., MYNENI, R.B., NORTH, R.P., POUNDS, J.A., SPARKS, T., STÜBI, R., TIAN, Y., WILTSHIRE, K.H., XIAO, D., ZHU, Z., 2016. Global impacts of the 1980s regime shift. *Glob. Change Biol.* 22, 682–703. doi: 10.1111/gcb.13106

ROMAN, J., 1887. *Les causes du déboisement des montagnes, d'après les documents historiques du XIIIe au XVIIIe siècle*. Imprimerie J.-C. Richaud, Gap.

ROUSSET, R., 1947. L'enneigement de printemps dans les Alpes du nord en 1946. *Rev. Géogr. Alp.* 119–121.

RUDOLF-MIKLAU, F., SAUERMOSER, S., MEARS, A.I., BOENSCH, M.M., 2015. *The technical avalanche protection handbook*. John Wiley & Sons, Berlin, Germany.

RUE, H., HELD, L., 2005. *Gaussian Markov Random Fields: Theory and Applications*. Chapman and Hall/CRC, New York, 280. doi: 10.1201/9780203492024

S

SALM, B., 1978. Snow forces on forest plants, in: In der Gand, H., Kronfeller, G., Ott, E., Salm, B. (Eds.), International Seminar on Mountain Forests and Avalanches. Presented at the IUFRO Working Party on Snow and Avalanches, Swiss Federal Institute for Snow and Avalanche Research, Davos, Switzerland, 156–181.

SALM, B., 1982. Mechanical properties of snow. *Rev. Geophys.* 20, 1–19. doi: 10.1029/RG020i001p00001

SALM, B., BURKARD, A., GUBLER, H., 1990. *Berechnung von Fliesslawinen: eine Anleitung für Praktiker mit Beispielen*. Mitteilung 47, Eidgenossichen Institut für Schnee- und Lawinenforschung SLF, Davos

SANSON, J., 1948. Les principales anomalies météorologiques de l'année 1947 en France. *Ann. Géogr.* 178–181.

SAULNIER, M., 2012. *Histoire et dynamique de la forêt subalpine dans les Alpes du Sud (Briançonnais, Queyras) : approches pédoanthracologique et dendrochronologique*. Aix-Marseille Université, Aix-en-Provence, 392 pp.

SAULNIER, M., EDOUARD, J.-L., CORONA, C., GUIBAL, F., 2011. Climate/growth relationships in a Pinus cembra high-elevation network in the Southern French Alps. *Ann. For. Sci.* 68, 189–200. doi: 10.1007/s13595-011-0020-3

SAULNIER, M., TALON, B., EDOUARD, J.-L., 2015. New pedoanthracological data for the long-term history of forest species at mid-high altitudes in the Queyras Valley

(Inner Alps). *Quat. Int.*, Charcoal: resource and ubiquitous proxy 366, 15–24. doi: 10.1016/j.quaint.2014.11.023

SAULNIER, M., ROQUES, A., GUIBAL, F., ROZENBERG, P., SARACCO, G., CORONA, C., EDOUARD, J.-L., 2017. Spatiotemporal heterogeneity of larch budmoth outbreaks in the French Alps over the last 500 years. *Can. J. For. Res.* 47, 667–680. doi: 10.1139/cjfr-2016-0211

SAULNIER, M., CORONA, C., STOFFEL, M., GUIBAL, F., EDOUARD, J.-L., 2019. Climate-growth relationships in a Larix decidua Mill. network in the French Alps. *Sci. Total Environ.* 664, 554–566. doi: 10.1016/j.scitotenv.2019.01.404

SCHAERER, P.A., 1972. Terrain and vegetation of snow avalanche sites at Rogers Pass, British Columbia in Mountain *Geomorphology*. In: SLAYMAKER, O., MCPHERSON, H.J. (EDS.), *Mountain Geomorphology: Geomorphological Processes in the Canadian Cordillera*, Vancouver B.C., 215–222

SCHLÄPPY, R., JOMELLI, V., GRANCHER, D., STOFFEL, M., CORONA, C., BRUNSTEIN, D., ECKERT, N., DESCHATRES, M., 2013. A New tree-ring-based, semi-quantitative approach for the determination of snow avalanche events: use of classification trees for validation. *Arct. Antarct. Alp. Res.* 45, 383–395. doi: 10.1657/1938-4246-45.3.383

SCHLÄPPY, R., ECKERT, N., JOMELLI, V., STOFFEL, M., GRANCHER, D., BRUNSTEIN, D., NAAIM, M., DESCHATRES, M., 2014. Validation of extreme snow avalanches and related return periods derived from a statistical-dynamical model using tree-ring techniques. *Cold Reg. Sci. Technol.* 99, 12–26. doi: 10.1016/j.coldregions.2013.12.001

SCHLÄPPY, R., JOMELLI, V., ECKERT, N., STOFFEL, M., GRANCHER, D., BRUNSTEIN, D., CORONA, C., DESCHATRES, M., 2016. Can we infer avalanche–climate relations using tree-ring data? Case studies in the French Alps. *Reg. Environ. Chang.* 16, 629–642. doi: 10.1007/s10113-015-0823-0

SCHNEEBELI, M., BEBI, P., 2004. Snow and avalanche control. In: BURLEY, J., EVANS, J., YOUNGQUIST, J.A. (EDS.), *Encyclopedia of Forest Sciences*, 397–402.

SCHNEEBELI, M., LATERNSER, M., WALTER, A., 1997. Destructive snow avalanches and climate change in the Swiss Alps. *Eclogae Geol. Helvetiae* 90, 457–461.

SCHNEUWLY, D.M., STOFFEL, M., BOLLSCHWEILER, M., 2009a. Formation and spread of callus tissue and tangential rows of resin ducts in Larix decidua and Picea abies following rockfall impacts. *Tree Physiol.* 29, 281–289. doi: 10.1093/treephys/tpn026

SCHNEUWLY, D.M., STOFFEL, M., DORREN, L.K.A., BERGER, F., 2009b. Three-dimensional analysis of the anatomical growth response of European conifers to mechanical disturbance. *Tree Physiol.* 29, 1247–1257. doi: 10.1093/treephys/tpp056

SCHNEUWLY-BOLLSCHWEILER, M., CORONA, C., STOFFEL, M., 2013. How to improve dating quality and reduce noise in tree-ring based debris-flow reconstructions. *Quat. Geochronol.* 18, 110–118. doi: 10.1016/j.quageo.2013.05.001

SCHÖNENBERGER, W., NOACK, A., THEE, P., 2005. Effect of timber removal from windthrow slopes on the risk of snow avalanches and rockfall. *For. Ecol. Manag.* 213, 197–208. doi: 10.1016/j.foreco.2005.03.062

SCHWEIZER, J., 2003. Snow avalanche formation. *Rev. Geophys.* 41. doi: 10.1029/2002RG000123

SCHWEIZER, J., KRONHOLM, K., JAMIESON, J.B., BIRKELAND, K.W., 2008. Review of spatial variability of snowpack properties and its importance for avalanche formation. *Cold Reg. Sci. Technol.* 51, 253–272. doi: 10.1016/j.coldregions.2007.04.009

SERQUET, G., MARTY, C., DULEX, J.-P., REBETEZ, M., 2011. Seasonal trends and temperature dependence of the snowfall/precipitation-day ratio in Switzerland. *Geophys. Res. Lett.* 38, L07703. doi: 10.1029/2011GL046976

SHRODER, J., 1978. Dendrogeomorphological analysis of mass movement on Table Cliffs Plateau, Utah. *Quat. Res.* 9, 168–185. doi: 10.1016/0033-5894(78)90065-0

SHRODER, J.F., 1980. Dendrogeomorphology: review and new techniques of tree-ring dating. *Prog. Phys. Geogr.* 4, 161–188. doi: 10.1177/030913338000400202

ŠILHÁN, K., STOFFEL, M., 2015. Impacts of age-dependent tree sensitivity and dating approaches on dendrogeomorphic time series of landslides. *Geomorphology* 236, 34–43. doi: 10.1016/j.geomorph.2015.02.003

ŠILHÁN, K., TICHAVSKÝ, R., 2017. Snow avalanche and debris flow activity in the High Tatras Mountains: New data from using dendrogeomorphic survey. *Cold Reg. Sci. Technol.* 134, 45–53. doi: 10.1016/j.coldregions.2016.12.002

ŠILHÁN, K., KLUZOVÁ, O., TICHAVSKÝ, R., 2019. The on field differentiation of snow avalanche- and debris flow-induced scars in trees as a fundament for improving dendrogeomorphic sampling strategy (case study from the Great Cold Valley in High Tatra Mountains). *Cold Reg. Sci. Technol.* 158, 1–9. doi: 10.1016/j.coldregions.2018.11.004

SLF, 1989. *Handbuch für Beobachter (Interner Bericht No. 637)*. Eidgenössisches Institut für Schnee- und Lawinenforschung, Weissfluhjoch-Davos.

SMITH, L., 1973. Indication of snow avalanche periodicity through interpretation of vegetation patterns in the North Cascades, Washington. In: BROWN, C.B., EVANS, R.J., FOX, T., LACHAPELLE, E.R., MCCLUNG, D.M., SMITH, L. (Eds.*), Methods of avalanche control on Washington mountain highways–Third annual report*. Washington State Highway Commission Department of Highways, 55–101.

SMITH, M.J., MCCLUNG, D.M., 1997. Avalanche frequency and terrain characteristics at Rogers' Pass, British Columbia, Canada. *J. Glaciol.* 43, 165–171.

SPECKMAN, P.L., SUN, D., 2003. Fully Bayesian spline smoothing and intrinsic autoregressive priors. *Biometrika* 90, 289–302. doi: 10.1093/biomet/90.2.289

SORG, A., BUGMANN, H., BOLLSCHWEILER, M., STOFFEL, M., 2010. Debris-flow activity along a torrent in the Swiss Alps: Minimum frequency of events and implications for forest dynamics. *Dendrochronologia* 28, 215–223. doi: 10.1016/j.dendro.2009.11.002

STOFFEL, M., BOLLSCHWEILER, M., 2008. Tree-ring analysis in natural hazards research – an overview. *Nat. Hazards Earth Syst. Sci.* 8, 187–202. doi: 10.5194/nhess-8-187-2008

STOFFEL, M., CORONA, C., 2014. Dendroecological dating of geomorphic disturbance in trees. *Tree-Ring Res.* 70, 3–20. doi: 10.3959/1536-1098-70.1.3

STOFFEL, M., CORONA, C., 2018. Future winters glimpsed in the Alps. *Nat. Geosci.* 11, 458–460. doi: 10.1038/s41561-018-0177-6

STOFFEL, M, PERRET, S., 2006. Reconstructing past rockfall activity with tree rings: Some methodological considerations. *Dendrochronologia* 24, 1–15. doi: 10.1016/j.dendro.2006.04.001

STOFFEL, M., HITZ, O.M., 2008. Rockfall and snow avalanche impacts leave different anatomical signatures in tree rings of juvenile Larix decidua. *Tree Physiol.* 28, 1713–1720. doi: 10.1093/treephys/28.11.1713

STOFFEL, M., BOLLSCHWEILER, M., HASSLER, G.-R., 2006. Differentiating past events on a cone influenced by debris-flow and snow avalanche activity – a dendrogeomorphological approach. *Earth Surf. Process. Landf.* 31, 1424–1437. doi: 10.1002/esp.1363

STOFFEL, M., LIEVRE, I., MONBARON, M., PERRET, S., 2005. Seasonal timing of rockfall activity on a forested slope at Täschgufer (Swiss Alps) – a dendrochronological approach. *Z. Für Geomorphol.* 49, 89–106.

STOFFEL, M., BOLLSCHWEILER, M., BUTLER, D.R., LUCKMAN, B.H., 2010. *Tree rings and natural hazards: A State-of-the-Art*. Springer, Dordrecht, New York.

STOFFEL, M., BUTLER, D.R., CORONA, C., 2013. Mass movements and tree rings: A guide to dendrogeomorphic field sampling and dating. *Geomorphology* 200, 106–120. doi: 10.1016/j.geomorph.2012.12.017

STOFFEL, M., CORONA, C., GUILLET, S., TRAPPMANN, D., 2015. *Räumlich-zeitliche Rekonstruktion der Lawinenaktivität am Standort Oberwald, Obergoms, Kanton Wallis, Schweiz (Technischer Bericht No. 1)*. Labor für Dendrogeomorphologie, Universität Bern, Bern, Schweiz.

STOFFEL, M., CORONA, C., TRAPPMANN, D., GUILLET, S., 2016. *Räumlich-zeitliche Rekonstruktion der Lawinenaktivität im Goms Münster–Geschinen,, Kanton Wallis, Schweiz (Technischer Bericht No. 2)*. Labor für Dendrogeomorphologie, Universität Bern, Bern, Schweiz.

STRAUB, D., GRÊT-REGAMEY, A., 2006. A Bayesian probabilistic framework for avalanche modelling based on observations. *Cold Reg. Sci. Technol.* 46, 192–203. doi: 10.1016/j.coldregions.2006.08.024

STUCKI, P., BRÖNNIMANN, S., MARTIUS, O., WELKER, C., IMHOF, M., VON WATTENWYL, N., PHILIPP, N., 2014. A catalog of high-impact windstorms in Switzerland since 1859. *Nat. Hazards Earth Syst. Sci.* 14, 2867–2882. doi: 10.5194/nhess-14-2867-2014

SZYMCZAK, S., BOLLSCHWEILER, M., STOFFEL, M., DIKAU, R., 2010. Debris-flow activity and snow avalanches in a steep watershed of the Valais Alps (Switzerland): Dendrogeomorphic event reconstruction and identification of triggers. *Geomorphology* 116, 107–114. doi: 10.1016/j.geomorph.2009.10.012

T

TANNER, M.A., 1992. *Tools for Statistical Inference: Observed Data and Data Augmentation Methods*. Springer-Verlag.

TECHEL, F., STUCKI, T., MARGRETH, S., MARTY, C., WINKLER, K., 2015. *Schnee und Lawinen in den Schweizer Alpen: Hydrologisches Jahr 2013/14 (No. 31)*. WSL-Insitut für Schnee- und Lawinenforschung, Birmensdorf

TECHEL, F., JARRY, F., KRONTHALER, G., MITTERER, S., NAIRZ, P., PAVŠEK, M., VALT, M., DARMS, G., 2016. Avalanche fatalities in the European Alps: long-term trends and statistics. *Geogr. Helvetica* 71, 147–159. doi: 10.5194/gh-71-147-2016

TEICH, M., BARTELT, P., GRÊT-REGAMEY, A., BEBI, P., 2012. Snow avalanches in forested terrain: influence of forest parameters, topography, and avalanche characteristics on runout distance. *Arct. Antarct. Alp. Res.* 44, 509–519. doi: 10.1657/1938-4246-44.4.509

TEICH, M., MARTY, C., GOLLUT, C., GRÊT-REGAMEY, A., BEBI, P., 2012. Snow and weather conditions associated with avalanche releases in forests: Rare situations with decreasing trends during the last 41years. *Cold Reg. Sci. Technol.* 83–84, 77–88. doi: 10.1016/j.coldregions.2012.06.007

TICHAVSKÝ, R., ŠILHÁN, K., 2016. The changing ability of Norway spruce (P. abies) to record hydro-geomorphic processes based on the age and diameter of the tree stem – A dendrogeomorphic approach. *CATENA* 147, 469–480. doi: 10.1016/j.catena.2016.07.052

TIMELL, T.E., 1986. *Compression wood in gymnosperms*. Springer, Berlin.

TORRENTE, A., 1888. *Les forêts et les avalanches de la vallée de Conches en Valais*. Jahrb. *Schweiz. Alpenclub* 23, 331–339.

TOUFLAN, P., TALON, B., WALSH, K., 2010. Soil charcoal analysis: a reliable tool for spatially precise studies of past forest dynamics: a case study in the French Southern Alps. *Holocene* 20, 45–52. doi: 10.1177/0959683609348900

TRAPPMANN, D., STOFFEL, M., 2013. Counting scars on tree stems to assess rockfall hazards: A low effort approach, but how reliable? *Geomorphology* 180–181, 180–186. doi: 10.1016/j.geomorph.2012.10.009

TRAPPMANN, D., CORONA, C., STOFFEL, M., 2013. Rolling stones and tree rings: A state of research on dendrogeomorphic reconstructions of rockfall. *Prog. Phys. Geogr.* 37, 701–716. doi: 10.1177/0309133313506451

TUMAJER, J., TREML, V., 2015. Reconstruction ability of dendrochronology in dating avalanche events in the Giant Mountains, Czech Republic. *Dendrochronologia* 34, 1–9. doi: 10.1016/j.dendro.2015.02.002

U

UHLMANN, B., GOYETTE, S., BENISTON, M., 2009. Sensitivity analysis of snow patterns in Swiss ski resorts to shifts in temperature, precipitation and humidity under conditions of climate change. *Int. J. Climatol.* 29, 1048–1055. doi: 10.1002/joc.1786

USBECK, T., WOHLGEMUTH, T., PFISTER, C., VOLZ, R., BENISTON, M., DOBBERTIN, M., 2009. Wind speed measurements and forest damage in Canton Zurich (Central Europe) from 1891 to winter 2007. *Int. J. Climatol.* 30, 347–358. doi: 10.1002/joc.1895

USTAOGLU, E., COLLIER, M.J., 2018. Farmland abandonment in Europe: an overview of drivers, consequences, and assessment of the sustainability implications. *Environ. Rev.* 26, 396–416. doi: 10.1139/er-2018-0001

V

VAN DER BURGHT, L., STOFFEL, M., BIGLER, C.J., 2012. Analysis and modelling of tree succession on a recent rockslide deposit. *Plant Ecol.* 213, 35–46. doi: 10.1007/s11258-011-0004-2

VASSKOG, K., NESJE, A., STOREN, E.N., WALDMANN, N., CHAPRON, E., ARIZTEGUI, D., 2011. A Holocene record of snow-avalanche and flood activity reconstructed from a lacustrine sedimentary sequence in Oldevatnet, western Norway. *The Holocene* 21, 597–614. doi: 10.1177/0959683610391316

VOELLMY, A., 1955. Uber die Zerstrungskraft von Lawinen. *Schweiz. Bauzig.* 73(12/15/17/19), 159–162, 212–217, 246–249, 280–285.

VOICULESCU, M., 2017. Snow Avalanche Activity in Southern Carpathians (Romanian Carpathians). In: RADOANE, M., VESPREMEANU-STROE, A. (EDS.), *Landform Dynamics and Evolution in Romania*. Springer International Publishing, Cham, 737–763. doi: 10.1007/978-3-319-32589-7_31

VOICULESCU, M., ONACA, A., 2013. Snow avalanche assessment in the Sinaia ski area (Bucegi Mountains, southern Carpathians) using the dendrogeomorphology method. *Area* 45, 109–122. doi: 10.1111/area.12003

VOICULESCU, M., ONACA, A., 2014. Spatio-temporal reconstruction of snow avalanche activity using dendrogeomorphological approach in Bucegi Mountains Romanian Carpathians. *Cold Reg. Sci. Technol.* 104–105, 63–75. doi: 10.1016/j.coldregions.2014.04.005

VOICULESCU, M., ONACA, A., CHIROIU, P., 2016. Dendrogeomorphic reconstruction of past snow avalanche events in Bâlea glacial valley–Făgăraş massif (Southern Carpathians), Romanian Carpathians. *Quat. Int.* 415, 286–302. doi: 10.1016/j.quaint.2015.11.115

W

WAHBA, G., 1978. Improper Priors, Spline Smoothing and the Problem of Guarding Against Model Errors in Regression. *J. Roy. Stat. Soc. B Met.* 40, 364–372. doi: 10.1111/j.2517-6161.1978.tb01050.x

WALTHER, G.-R., BERGER, S., SYKES, M.T., 2005. An ecological "footprint" of climate change. *Proc. R. Soc. B-Biol. Sci.* 272, 1427–1432. doi: 10.1098/rspb.2005.3119

WEBER, U.M., 1997. Dendroecological reconstruction and interpretation of larch budmoth (Zeiraphera diniana) outbreaks in two central alpine valleys of Switzerland from 1470 – 1990. *Trees* 11, 277–290. doi: 10.1007/PL00009674

WIKLE, C.K., 2003. Spatio-temporal models in climatology. In: *Encyclopedia of Life Support Systems (EOLSS)*, developed under the Auspices of the UNESCO. Eolss Publishers, Oxford, UK.

WIKLE, C.K., BERLINER, L.M., CRESSIE, N., 1998. Hierarchical Bayesian space-time models. *Environ. Ecol. Stat.* 5, 117–154. doi: 10.1023/A:1009662704779

Y

YANG, W., ZURBENKO, I., 2010. Kolmogorov-Zurbenko filters: Kolmogorov-Zurbenko Filters. *Wiley Interdiscip. Rev. Comput. Stat.* 2, 340–351. doi: 10.1002/wics.71

YOSHIDA, K., KIKUCHI, S., NAKAMURA, F., NODA, M., 1997. Dendrochronological analysis of debris flow disturbance on Rishiri Island. *Geomorphology* 20, 135–145. doi: 10.1016/S0169-555X(97)00010-X

TABLE DES ILLUSTRATIONS

Figure I.1 – Nombre d'avalanches de neige sèche (bleu) et de neige humide (rouge) observées entre les hivers 1952 et 2013. La ligne verticale grise indique l'hiver 2002 où le nouveau système de codification des observations et de la base de données a été mis en place. Cette date coïncide avec une baisse systématique de la quantité de données. Les lignes pointillées correspondent à la moyenne décennale, avant et après l'hiver 2001-2002. Adapté de Pielmeier et al. (2013).20

Figure I.2 – Variation interannuelle de l'altitude d'arrêt des avalanches dans les Alpes françaises, d'après l'EPA. Extrait de Eckert et al. (2010a). 21

Figure I.3 – Types de blessures observés dans les cernes de croissance après une avalanche, adapté de Corona et al. (2013). 25

Figure I.4 – Synthèse des chroniques d'avalanche reconstruites à partir de séries de cernes de croissance. **1**. Potter (1969) ; **2**. Schaerer (1972) ; **3**. Smith (1973) ; **4**. Ives et al. (1976) ; **5**. Butler (1979) ; **6**. Carrara (1979) ; **7**. Butler et Malanson (1985a) ; **8**. Bryant et al. (1989) ; **9**. Rayback (1998) ; **10**. Larocque et al. (2001) ; **11**. Boucher et al. (2003) ; **12.** Hebertson et Jenkins (2003) ; **13**. Dubé et al. (2004) ; **14**. Jenkins et Hebertson (2004) ; **15**. Kajimoto et al. (2004) ; **16**. Muntán et al. (2004) ; **17**. Germain et al. (2005) ; **18.** Pederson et al. (2006) ; **19**. Stoffel et al. (2006) ; **20**. Casteller et al. (2007) ; **21**. Mundo et al. (2007) ; **22**. Butler et Sawyer (2008) ; **23**. Casteller et al. (2008) ; **24**. Reardon et al. (2008) ; **25**. Germain et al. (2009) ; **26**. Laxton et Smith (2009) ; **27**. Muntán et al. (2009) ; **28**. Corona et al. (2010) ; **29**. Johnson et Smith (2010) ; **30**. Köse et al. (2010) ; **31**. Szymczak et al. (2010) ; **32**. Casteller et al. (2011) ; **33**. Garavaglia et Pelfini (2011); **34**. Kogelnig-Mayer et al. (2011) ; **35**. Corona et al. (2012) ; **36**. Decaulne et al. (2012) ; **37**. Püntener et al. (2012) ; **38**. Arbellay et al. (2013) ; **39**. Corona et al. (2013) ; **40**. Schläppy et al. (2013) ; **41**. Voiculescu et Onaca (2013); **42**. Decaulne et al. (2014) ; **43**. Schläppy et al. (2014) ; **44**. Voiculescu et Onaca (2014); **45**. Chiroiu et al. (2015) ; **46**. Tumajer et Treml (2015); **47**. Germain (2016); **48**. Lempa et al. (2016) ; **49**. Martin et Germain (2016a); **50**. Martin et Germain (2016b); **51**. Pop et al. (2016) ; **52**. Schläppy et al. (2016) ; **53**. Voiculescu et al. (2016) ; **54**. Favillier et al. (2017) – Chapitre 1 ; **55**. Gądek et al. (2017) ; **56**. Martin et Germain (2017); **57**. Pop et al. (2017) ; **58**. Šilhán et Tichavský (2017); **59**. Ballesteros-Cánovas et al. (2018) ; **60**. Bollati et al. (2018) ; **61**. Casteller et al. (2018) ; **62**. Favillier et al. (2018) – Chapitre 2 ; **63**. Krause et Křížek (2018); **64**. Meseșan et al. (2018a) ; **65**. Meseșan et al. (2018b) ; **66**. Šilhán et al. (2019) ; **Gv** Goms valley (Valais, Switzerland) ; **Qm** Queyras massif (Hautes-Alpes, France). 26

Figure I.5 – Localisation de (a) la haute vallée de Goms, Valais, Suisse, des versants étudiés de (b) Münster, (c) Geschinen et (d) d'Oberwald, et de leurs couloirs d'avalanches..... 30

Figure I.6 – Localisation (a) du Massif du Queyras, des versants étudiés (b) du Ravin de la Salce, (c) de Souliers et de leurs couloirs d'avalanches. 31

Figure 1.1 – Location of the study site in (a) Switzerland and (b) in the Goms Valley. (c) Spatial distribution of sampled trees. The colored areas represent the hazard map defined by the canton of Valais. Red indicates an area that is exposed to considerable danger with frequent avalanches (average return period of 30 years or less). In the blue colored area, avalanches are less frequent (30-100-year average return period) and have mean pressures of less than 30 kN/m². The yellow area is giving the extent of avalanches with return periods of 100–300 years, but also designates the runout zone of powder avalanches. 42

Figure 1.2 – Synoptic diagram of the 4-step approach used for the detection of avalanche events in tree-ring series. 46

Figure 1.3 – Mapping of the avalanche paths (OB1-OB5) at Oberwald based on field observations and digital terrain model (DTM) data derived from airborne Lidar data point clouds, as well as maximal extension of avalanche flows as derived from maximal pressure data from RAMMS numerical snow avalanche simulations. .. 49

Figure 1.4 – Age structure of the forest stand growing in and next to the Oberwald avalanche paths. 50

Figure 1.5 – Event-response histograms showing the total number of growth disturbances (GD, in red and orange) and the percentage of trees responding to an event (in green) at each of the five Oberwald paths (a-e). Orange bars show the total number of growth reductions which are possibly related to larch budmoth outbreaks or to climatic extremes. The dashed lines denote the GD and It thresholds used to reconstruct past avalanche events. The solid lines denote sample depth, i.e. the number of trees available for analysis for each year of the reconstruction. 51

Figure 1.6 – Radar chart showing the distributions of GD types and intensities for 50-year periods between 1800 and 2000. Panel (a) includes all GD detected in trees, except during LBM outbreaks; panel (b) only shows GDs attributed to snow avalanche events. 51

Figure 1.7 – Simplified synoptic diagram showing the characteristics (possible interference with climate or larch budmoth outbreaks, level of confidence, minimum slide extent) of the reconstructed events based on the 4-step procedure presented. 52

Figure 1.8 – Avalanche activity signals obtained with the weighted index factor (Wit) at (a) OB1, (b) OB2, (c) OB3 and (d) OB4. Light blue bars represent years rejected in step 1 and 2; dark blue bars denote avalanche years. 54

Figure 1.9 – Avalanche events reconstructed for the period 1780–2013 at the 5 avalanche paths. Symbol sizes are proportional to the level of confidence, whereas the color range denotes the minimum slide extent. Grey bands represent triplets of years associated to LBM outbreaks. Vertical lines show snow avalanche events documented in historical archives (black), as well as extremely dry (orange) and cold (blue) summers. 55

Figure 1.10 – Reconstructed minimum sliding extent for avalanches in (a) 1813, (b) 1966, (c) 1975, and (d) 2003; these events were reconstructed with high (HLC), medium (MLC) and low (LLC) level of confidence, respectively. Maps show all living trees and as well as those showing GDs related to the avalanche. Panels (e, f) are examples of events that were disregarded from the avalanche reconstruction due to the fact that geomorphic and LBM signals could not be disentangled in the tree-ring series. 56

Figure 1.11 – (a, b) Diachronic evolution of the forest at Oberwald between 1999 and 2005. (c), tree-ring-based reconstruction of the 2003 avalanche event. 61

Figure 2.1 – Synthesis of tree-ring based avalanche reconstructions. Colored dots represent dendrogeomorphic snow avalanche studies with (green) and without (yellow) an estimation of the spatial extent of reconstructed snow avalanche events. Red lozenges represent studies for which avalanche recurrence interval maps have been computed. The red star corresponds to the location of this study. **1.** Potter (1969); **2.** Schaerer (1972); **3.** Smith (1973); **4.** Ives et al. (1976); **5.** Butler (1979); **6.** Carrara (1979); **7.** Butler and Malanson (1985a); **8.** Bryant et al. (1989); **9.** Rayback (1998); **10.** Larocque et al. (2001); **11.** Boucher et al. (2003); **12.** Hebertson and Jenkins (2003); **13.** Dubé et al. (2004); **14.** Jenkins and Hebertson

(2004); **15.** Kajimoto et al. (2004); **16.** Muntán et al. (2004); **17.** Germain et al. (2005); **18.** Pederson et al. (2006); **19.** Stoffel et al. (2006); **20.** Casteller et al. (2007); **21.** Mundo et al. (2007); **22.** Butler and Sawyer (2008); **23.** Casteller et al. (2008); **24.** Reardon et al. (2008); **25.** Germain et al. (2009); **26.** Laxton and Smith (2009); **27.** Muntán et al. (2009); **28.** Corona et al. (2010); **29.** Köse et al. (2010); **30.** Szymczak et al. (2010); **31.** Casteller et al. (2011); **32.** Garavaglia and Pelfini (2011); **33.** Kogelnig-Mayer et al. (2011); **34.** Corona et al. (2012); **35.** Decaulne et al. (2012); **36.** Arbellay et al. (2013); **37.** Corona et al. (2013); **38.** Schläppy et al. (2013); **39.** Voiculescu and Onaca (2013); **40.** Decaulne et al. (2014); **41.** Schläppy et al. (2014); **42.** Voiculescu and Onaca (2014); **43.** Chiroiu et al. (2015); **44.** Tumajer and Treml (2015); **45.** Germain (2016); **46.** Lempa et al. (2016); **47.** Martin and Germain (2016a); **48.** Martin and Germain (2016b); **49.** Pop et al. (2016); **50.** Schläppy et al. (2016); **51.** Voiculescu et al. (2016); **52.** Favillier et al. (2017); **53.** Gądek et al. (2017); **54.** Krause and Krizek (2017); **55.** Pop et al. (2017); **56.** Šilhán and Tichavský (2017); **57.** Ballesteros-Cánovas et al. (2018); **58.** Casteller et al. (2018). 72

Figure 2.2 – Location of the study site: (a) the Zermatt valley in the canton of Valais, Switzerland, (b) Spatial distribution of the sampled trees within the three paths and their release areas. The green lines represent the avalanche dams built after major avalanche events. Map and aerial photography are reproduced by permission of swisstopo (BA18022). 74

Figure 2.3 – Synoptic diagram of the 4-step approach used for the detection of avalanche events in tree-ring series, adapted from Favillier et al. (2017). 77

Figure 2.4 – (a) Description of the avalanche of January 1920 in the Walliser Bote published 17th of January, 1920. English translation: "*Täsch: The new snow at the locality exceeded 2 meters. All avalanche couloirs produced events to rush down to the valley where they caused large damage, especially in the case of the large Täschwang avalanche. The avalanche did not follow its usual* trajectory but *left its couloir above the so-called "Metjen" from where it descended into a wonderful conifer forest to destroy it all the way down to the valley floor. Thousands of stems have been broken and are now accumulated in the valley. Eight stables and barns with plenty of hay reserves have been devastated and 18 sheep have been killed. Damage has to be estimated in the order of 30,000 francs*", (b) The snow avalanche (≈80,000 m^3) of March 4, 2014 buried the northern entrance of the avalanche protection tunnel and the road linking Täsch to Zermatt (Feistl et al., 2015), picture extracted from Techel et al. (2015). 81

Figure 2.5 – Age structure of the forest stand growing at the Täschwang sites and its avalanche paths. 82

Figure 2.6 – Diachronic evolution of the forest stand at Täschwang for the period 1909–2016: (a) 1909–1941, (b) 1941–1977, and (c) 2009–2016. 83

Figure 2.7 – Simplified synoptic diagram showing the characteristics (possible interference with climate or larch budmoth outbreaks, level of confidence, and minimum slide extent) of the reconstructed events. 84

Figure 2.8 – Avalanche events reconstructed for the period 1740–2015 in avalanche paths T1, T2, and T3. Symbol sizes are proportional to the level of confidence, whereas the colour range denotes the minimum slide extent. Grey bands represent triplets of years associated to LBM outbreaks. Vertical lines show snow avalanche events documented in historical archives (black), as well as extremely dry (orange) and cold (blue) summers. 85

Figure 2.9 – Reconstructed Minimum Sliding Extent (MSE) of avalanches that occurred (a) on January 16, 1920, at T1 (b) in 1986, at T1 and T2, and (c) in 2009, at T1, T2

and T3, as derived from the location of disturbed trees and interpretation of the aerial pictures taken in 1941, 1988 and 2009 (in the background, aerial photographs are reproduced by permission of swisstopo, BA18022)..... 86

Figure 2.10 – (a) Interpolation of individual tree recurrence intervals (Rim1) often assimilated to avalanche return periods in the tree ring literature. Recurrence intervals computed according to the spatial delineation of past events based on growth disturbances in trees for the period 1740–2015 (Rim2, b) and 1960–2015 (Rim3, c). Map on panel (d) (Rim4) was transformed in order to adjust recurrence interval values from Rim2 and to estimate recurrence intervals in the missing portions of Rim3. 88

Figure 3.1 – Location of the study site in the Guil valley (Queyras massif, French Alps) (a) and delineation of the four avalanche paths on the Ravin de la Salce slope (b). 101

Figure 3.2 – Synoptic diagram of the 4-step approach used for the detection of avalanche events in tree-ring series, adapted from Favillier et al. (2017)..... 105

Figure 3.3 – (a) Maximum velocities and (b) maximum pressures computed with the RAMMS snow avalanche model. Avalanche extensions obtained with RAMMS are used in this study to delineate avalanche paths E1-C2..... 108

Figure 3.4 – Age structure of the forest stand growing at the Ravin de la Salce slope.109

Figure 3.5 – Event-response histograms showing the total number of growth disturbances (GD, in red and orange) and the percentage of trees responding to an event (in green) at each of the four paths. Orange bars show the total number of growth reductions which are possibly related to larch budmoth outbreaks or to climatic extremes. The dashed lines denote the GD and It thresholds used to reconstruct past avalanche events. The solid lines denote sample depth, i.e. the number of trees available for analysis for each year of the reconstruction..... 110

Figure 3.6 – Results of the 4-step procedure. Reconstructed event characteristics consider possible interference with climate or larch budmoth outbreaks and include the level of confidence and the minimum slide extent..... 111

Figure 3.7 – Avalanche events reconstructed for the period 1720-2016 at the four avalanche paths. Symbol sizes are proportional to the level of confidence, whereas the color range denotes the minimum slide extent. Grey bands represent years associated to LBM outbreaks. Vertical lines show snow avalanche events documented in historical archives (black), as well as extremely dry (orange), cold (blue) summers and pointer years (green)..... 112

Figure 3.8 – Location of trees disturbed in 1961 and 2008 and presumably corresponding to avalanches that occurred (c) on February 7, 1961 and (f) on December 17, 2008 and diachronic comparisons of aerial photographs (IGN) highlighting the evolution of the forest stand between 1956 and 1962 (a, b) and between 1988 and 2009 (d,e)..... 114

Figure 4.1 – Location of the studied paths: (a) overview of the Queyras massif (French Alps), (b) detailed view of the Chateau-Ville-Vieille locality within the Queyras massif and the study site (c) detailed view of the six avalanche paths delineated on the Grand Bois de Souliers slope. 128

Figure 4.2 – Synoptic diagram of the 4-step approach used for the detection of avalanche events in tree-ring series, adapted from Favillier et al. (2017). Growth disturbance (GD) and intensity (It) thresholds vary according to the sample size: (a) <20 trees; (b) 20 to 49 trees; (c) 50 to 99 trees; and (d) >= 100 trees..... 131

Figure 4.3 – Age structure of the forest stand growing at Grand Bois de Souliers: (a) spatial distribution of individual tree and interpolated stand ages; (b) evolution of the sample size at the six avalanche paths. The black line represents the mean sample size evolution. 133

Figure 4.4 – Diachronic evolution of the forest stands at Grand Bois de Souliers between 1945 and 2015: (a) 1945-1971, (b) 1971-1981, (c) 1981-2003, and (d) 2003-2015. 134

Figure 4.5 – Evolution of the surfaces occupied by larch stands, computed for 100-m elevation bands, (a) at Grand Bois de Souliers; within (b) avalanche paths S1-S3; and (c) paths S4, A1 and A2 as delineated in Figure 4.1. 134

Figure 4.6 – Barplots showing the distributions of GD types and intensities between 1750 and 2000 for paths (a) S1-S3 and (b) S4-A1-A2. 136

Figure 4.7 – Synoptic diagram showing the characteristics of the reconstructed snow avalanche events and possible interferences with climate or larch budmoth outbreaks, level of confidence, and minimum slide extent. 138

Figure 4.8 – Avalanche events reconstructed for the period 1750–2015 in six paths at Grand Bois de Souliers. Symbol sizes are proportional to the level of confidence. The color range highlights the minimum slide extent determined from the position of impacted trees. Grey bands represent years associated to LBM outbreaks. Vertical lines show snow avalanches documented in chronicles (black), as well as extremely dry (orange) and cold (blue) summers. 139

Figure 4.9 – Diachronic comparison of topographical maps of (a) 1866, (b) 1896, (c) 1933, (d) 1971, and (e) 2015. Germination dates of sampled trees suggest that a devastating avalanche in the 1910s or 1920s would have cleared the forested surface in paths S1-A1-A2. This interpretation is supported by topographic maps showing the absence of forests (c) in 1933 and an almost complete (re)colonization (d) in 1971 and (e) in 2015. 142

Figure 5.1 – Synthesis of tree-ring based avalanche reconstructions. Small and white dots represent dendrogeomorphic snow avalanche studies that do not assess the linkage between snow avalanche activity and climate parameters. Colored lozenges represent dendrogeomorphic snow avalanche studies assessing the relation between snow avalanche activity and climatic parameters while triangles represent studies assessing relations between snow avalanche activity and meteorological parameters or avalanche-prone weathers. Colored dots represents other dendrogeomorphic snow avalanche studies. 154

Figure 5.2 – Location of the study sites: (a) the Goms Valley in the Canton of Valais, Switzerland, the (b) Münster, Geschinen (c) and Oberwald (d) avalanche paths. 157

Figure 5.3 – Age structure of the forest stands growing in the Goms valley: spatial distribution of individual tree and interpolated age at Münster (a) and Geschinen (b); (c) evolution of the sample size at the three avalanche slopes. The black dashed line represents the mean sample size evolution. Age structure maps and spatial distribution of sampled trees for Oberwald are given in Favillier et al. (2017). 164

Figure 5.4 – Evolution of the forest cover (1881-2015) at (a) Münster, (b) Geschinen and (c) Oberwald. 165

Figure 5.5 – Radar chart showing the distributions of GD types and intensities between 1800 and 2014. The figure only shows GDs attributed to snow avalanche events. 166

Figure 5.6 – Avalanche events reconstructed for the period 1720–2014 in studied avalanche paths based on the 4-step procedure developed by Favillier et al. (2017 – chapter 1). Symbol sizes are proportional to the level of confidence. The colour range highlights the minimum slide extent determined from the position of impacted trees. Grey bands represent triplets of years associated to LBM outbreaks. Vertical lines show snow avalanche events documented in site-specific historical chronicles (black), as well as extremely dry (orange) and cold (blue) summers. 168

Figure 5.7 – Comparison of raw snow avalanche activity at path scale for the period 1880–2014. Non-significant correlation coefficients are in gray. Significance levels are rated by a **.** (α=0,1), ***** (α=0,05), ****** (α=0,01), ******* (α=0,001). 169

Figure 5.8 – Comparison of the historical archives with the snow avalanche chronology derived from tree-ring series. Green bars represent the number of snow avalanches recorded in the historical database. Blue, orange and pink bars indicate the number of snow avalanche events reconstruted at Geschinen, Münster and Oberwald, respectively. 170

Figure 5.9 – (a) Regional snow avalanche activity computed from the dendrogeomorphological reconstruction using the hierarchical Bayesian approach. . The violet and green lines represent the annual and the decadal snow avalanche probability. Dashed lines indicate the 95% confidence level. The horizontal black lines represent the mean probability of snow avalanche computed form 30-yr periods. Reconstructed snow avalanche events are represented with blue, orange and purple bars for Geschinen, Münster and Oberwald slopes, respectively. .. 171

Figure 5.10 – Evolution of the dendrogeomorphic potential (POT) at (a) Oberwald, (b) Münster and Geschinen. The grey dashed line indicates the mean evolution of the dendrogeomorphic potential. 172

Figure 5.11 – Comparison of winter (a) mean temperatures and (b) precipitations fluctuations with (c) the standardized snow avalanche activity. The violet and green lines represent the annual and the decadal snow avalanche probability. Dashed lines indicate the 95% confidence level. The horizontal black lines represent the mean probability of snow avalanche computed form 30-yr periods. 173

Figure 5.12 – Comparison between (a) the regional avalanche activity and (b) the avalanche activity indicators for the Swiss (Laternser and Schneebeli, 2002; Pielmeier et al., 2013) (c) and French (Castebrunet et al., 2012; Eckert et al., 2010c) Alps. . The violet and green lines represent the annual and the decadal snow avalanche probability. Dashed lines indicate the 95% confidence level. The horizontal black lines represent the mean probability of snow avalanche computed form 30-yr periods. 175

Figure 6.1 – Localisation des versants de (b) la haute vallée du Guil et de (c) de la vallée de Souliers, dans (a) le massif du Queyras, Hautes-Alpes, France. 184

Figure 6.2 – Structure d'âge des populations forestières de (a) Souliers et du (b) Ravin de la Salce, Queyras, France. 187

Figure 6.3 – Avalanches reconstruites pour la période 1560-2017 dans les dix couloirs d'avalanches étudiés. La taille des symboles est proportionnelle au niveau de confiance, les couleurs indiquent l'extension minimale de chaque événement estimée à partir de la disposition spatiale des arbres blessés dans les couloirs. Les bandes grises représentent les années d'épidémies de tordeuse grise. Les lignes verticales indiquent les avalanches de neige documentées dans les archives historiques (noir), les étés extrêmement secs (orange) et froids (bleu) ainsi que les cernes étroits observés dans les chronologies de référence élaborées à partir d'arbres non impactés(vert). 189

Figure 6.4 – Comparaison de l'activité des avalanches par couloir pour la période 1790–2016. Les couloirs A1 et C1 ont été respectivement appariés avec A2 et C2 pour permettre leur comparaison avec les autres couloirs pour la même période. Les coefficients de régression non-significatifs apparaissent grisés. Les niveaux de significativité des p valeurs sont représentés par un **.** (α=0,1), ***** (α=0,05), ****** (α=0,01), ******* (α=0,001)..... 191

Figure 6.5 – Standardisation (a) de la reconstruction dendrogéomorphologique (b) au moyen de l'approche bayésienne hiérarchique. Sur le graphique supérieur (a), les lignes violettes et vertes pleines représentent les probabilités annuelles et décennales de déclenchement ; les lignes hachurées l'intervalle de confiance à 95% des deux chronologies standardisées. Les lignes horizontales noires indiquent les probabilités annuelles moyennes calculées pour des périodes de 50 ans. Sur le panneau du bas (b), les barres violettes, oranges et bleues représentent les avalanches reconstruites sur les versants du Ravin de la Salce, de Souliers et de l'Echalp. 192

Figure 6.6 – Comparaison des fluctuations (a) des températures et (b) des précipitations hivernales (DJFAM) et de des reconstructions avalancheuses standardisées. Les lignes violettes et vertes pleines représentent les probabilités annuelles et décennales de déclenchement ; les lignes hachurées l'intervalle de confiance à 95% des deux chronologies. Les lignes horizontales noires représentent les fréquences annuelles moyennes d'événement pour les périodes 1750–1800, 1801–1850, 1851–1900, 1901–1950 et 1951–2016..... 194

Figure 6.7 – Comparaison de (a) des moyennes à 5 ans, 10 ans et 30 ans de l'activité des avalanches dans le Queyras (rouge) avec (b) l'activité observée des avalanches (b) dans les Alpes françaises entre 1940 et 2016. L'activité des avalanches est représentée à l'échelle de l'ensemble du massif (rouge sombre), d'après Eckert et al.(2013), et à l'échelle des Alpes françaises du Sud (rouge clair), d'après Castebrunet et al. (2012)..... 197

Figure S.1 – Chronologies des événements d'avalanche de (a, c) la vallée de Goms et (b, d) du massif du Queyras et leur activité homogénéisée au moyen de l'approche bayésienne hiérarchique. Les lignes horizontales noires représentent les fréquences annuelles moyennes d'événement pour des périodes de (c) 30 ans et (d) de 50 ans. 205

Figure S.2 – Chronologie régionale de l'activité des avalanches pour 17 couloirs du massif des Făgăraş (Roumanie) pour la période 1884–2013. La taille des symboles est proportionnelle au niveau de confiance..... 213

TABLES ET TABLEAUX

Table 1.1 – Larch budmoth events (according to Esper et al., 2007 and Büntgen et al., 2009), as well as extremely cold and dry summers (Efthymiadis et al., 2006) in the Swiss Alps. All these years have been carefully analyzed due to probable interferences between snow avalanche damage in trees, as well as LBM and climatic signals. 48

Table 1.2 – Intensity of reactions and types of growth disturbances (GD) assessed in the 564 larch trees selected for analysis. 50

Table 1.3 – Characteristics of reconstructed events coinciding with LBM outbreak episodes or extreme climatic events. The above events were retained in the final reconstruction due to their high proportion of strong GDs (i.e. callus tissue, injury, tangential rows and traumatic resin ducts, compression wood) which cannot be attributed to LBM outbreaks or climatic signatures. Nonetheless, events were rated

with a low level of confidence due to probable interferences between the avalanche signals with growth suppressions induced by larch budmoth outbreaks and/or climatic extremes. 53

Table 1.4 – Synthesis of dendrogeomorphic studies using growth disturbances in tree-ring series to reconstruct past snow avalanche activity. Almost one-fourth (22.9%) of the studies published after the year 2000 utilized European larch (Larix decidua Mill.). 59

Table 2.1 – Larch budmoth events (according to Esper et al., 2007 and Büntgen et al., 2009), as well as extremely cold and dry summers (Battipaglia et al., 2010; Efthymiadis et al., 2006) in the Swiss Alps. All these years have been carefully analyzed due to probable interferences between snow avalanche damage in trees, as well as LBM and climatic signals that may induce comparable growth reduction in tree-ring series. 78

Table 2.2 – Intensity of reactions and types of growth disturbances (GD) assessed in the 307 larch trees selected for analysis. 83

Table 3.1 – Larch budmoth events and pointer years (according to Saulnier et al., 2017), as well as extremely cold and dry summers (Efthymiadis et al., 2006) in the French Alps. All these years have been carefully analyzed due to probable interferences between snow avalanche damage in trees, as well as LBM and climatic signals that may induce growth reductions comparable to those observed after snow avalanches in the tree-ring series. 106

Table 3.2 – Geomorphic characteristics and soil occupation of the studied avalanche paths and their release zones. 107

Table 3.3 – Intensity of reactions and types of growth disturbances (GD) assessed in the 306 larch trees selected for analysis. 111

Table 4.1 – Main characteristics of the studied avalanche paths. Numerical values correspond to the areas delineated in Figure 4.1c and derived from crossed a 5-m DEM. 128

Table 4.2 – Larch budmoth events and pointer years (according to Saulnier et al., 2017), as well as extremely cold and dry summers (Efthymiadis et al., 2006; Saulnier et al., 2011) in the French Alps. All these years have been carefully analyzed due to probable interferences between snow avalanche damage in trees with LBM and/or climatic signals that may induce growth reductions comparable to those observed after snow avalanches in the tree-ring series. 132

Table 4.3 – Intensities of reactions and types of growth disturbances (GD) assessed in the 825 larch trees selected for analysis. 137

Table 5.1 – Main characteristics of the studied avalanche paths 157

Table 5.2 – Intensity and types of growth disturbances (GD) identified in the 1014 sampled trees. 166

Tableau 6.1 – Principales caractéristiques morphologiques des couloirs d'avalanches étudiés 185

Tableau 6.2 – Caractéristiques des peuplements forestiers échantillonnés 187

Tableau 6.3 – Type et intensité des perturbations de croissance (GD) détectées dans les 1131 mélèzes d'Europe échantillonnés pour chaque couloir des deux versants étudiés, pour la période 1560–2016. Les données non-précisées sont notées n.p. 188

Tableau 6.4 – Niveau de confiance et nombre d'événements d'avalanche détectés dans les séries de perturbations de croissance, par couloir. 190

TABLE DES MATIERES

SOMMAIRE **13**

INTRODUCTION GENERALE **15**

1. Contexte **16**

1.1. Les avalanches, un aléa majeur en région de montagne 16
1.2. Réchauffement climatique et réduction du manteau neigeux dans les Alpes 18
1.3. Réchauffement climatique et évolution de l'activité avalancheuse . 18

1.3.1. Évolutions pluriséculaires de la dynamique avalancheuse : l'apport des études paléo-environnementales et des archives historiques *18*
1.3.2. Évolutions de la dynamique avalancheuse au cours des dernières décennies : l'apport des observations systématiques *19*
1.3.3. Évolutions de l'activité avalancheuse dans un climat futur *22*

1.4. Déprise agro-sylvo-pastorale et évolution de l'activité avalancheuse 23
1.5. Dendrogéomorphologie et reconstruction pluriséculaire de l'activité des avalanches 24

2. Objectifs et structure de la recherche **30**

CHAPITRE 1 **37**
Disentangling the impacts of exogenous disturbances on forest stands to assess multi-centennial tree-ring reconstructions of avalanche activity

1. Introduction **41**
2. Study site **43**
3. Material and methods **43**

3.1. Compilation of historical archives 43
3.2. Delineation of avalanche path 44
3.3. Sampling strategy, identification, dating and classification of growth disturbances 44
3.4. Detection of past avalanche events in growth disturbance series .. 45

4. Results **48**

4.1. Mapping of avalanche path at Oberwald 48
4.2. Snow avalanches recorded in historical archives 49
4.3. Age structure of the stand 49
4.4. Distribution of growth disturbances 50
4.5. Chronology of avalanche events 52
4.6. Spatial extent of avalanche events 55

5. Discussion **57**

5.1. Isolation of the avalanche signal in tree-ring series 57
5.2. Robustness of the reconstruction 58
5.3. Increase in avalanche frequency over the last decades 62

6. Conclusion **63**

CHAPITRE 2 **65**
Spatio-temporal maps of past avalanche events derived from tree-ring analysis

1. Introduction **69**
2. Study site **73**
3. Material and methods **75**
3.1. Compilation of historical archives 75
3.2. Sampling strategy, identification, dating and classification of growth disturbances 75
3.3. Detection of past avalanche events in growth disturbance series 76
3.4. Computation of avalanche events recurrence interval maps 80
4. Results **81**
4.1. Snow avalanches recorded in historical archives 81
4.2. Age structure of the stand 82
4.3. Distribution of growth disturbances and chronology of avalanche events 84
4.4. Spatial extent of avalanche events and recurrence interval maps 86
5. Discussion **89**
5.1. Spatio-temporal accuracy of the reconstruction 89
5.2. From events to return period mapping 90
6. Conclusion **92**

CHAPITRE 3 **95**
Tree-ring reconstruction of snow avalanche activity: Does avalanche path selection matter?

1. Introduction **99**
2. Study site **101**
3. Material and methods **102**
3.1. Archival data on past events 102
3.2. Delineation of avalanche paths 102
3.3. Sampling strategy, identification, dating, and classification of growth disturbances 103
3.4. Detection of past avalanche events in growth disturbance series 104
4. Results **107**
4.1. Delineation of avalanche paths at Ravin de la Salce 107
4.2. Snow avalanches recorded in historical archives 107
4.3. Age structure of the stands 108
4.4. Distribution of growth disturbances and chronology of avalanche events 109
4.5. Spatial extent of reconstructed events 113
5. Discussion **113**
5.1. Accuracy of the reconstructions 113
5.2. Two different avalanche dynamics 116
6. Conclusions **118**

CHAPITRE 4 **121**
Non-stationarities induced by land-cover changes in dendrogeomorphic reconstructions of snow avalanche activity

1. Introduction **125**
2. Study site **127**
3. Material and methods **129**
3.1. Sampling strategy, dating and classification of growth disturbances 129
3.2. Detection of past avalanche events in growth disturbance series 130
3.3. Documentation of forest dynamics 132
4. Results **133**
4.1. Evolution of the forest cover 133
4.2. Past snow avalanche activity 136
5. Discussion **139**
5.1. Non-stationarity of the dendrogeomorphic reconstruction potential in paths A1, A2 and S4 140
5.2. Non-stationarity of the snow avalanche activity related to slope afforestation 141
6. Conclusion **144**

CHAPITRE 5 **147**
Complex signals in regional tree-ring reconstructions of snow avalanches

1. Introduction **151**
2. Regional settings **155**
3. Methods **156**
3.1. Sampling strategy and detection of past avalanche events in tree-ring series 156
3.2. Estimation of the regional snow avalanche activity since 1880 using a hierarchical Bayesian modelling approach 158
3.2.1. Principle *158*
3.2.2. Hierarchical Bayesian model specification *159*
3.2.3. Variance decomposition *161*
3.2.4. Model inference and posterior estimates *162*
3.3. Compilation of historical archives 163
3.4. Documentation of land cover changes and climatic fluctuations .. 163
4. Results **163**
4.1. Age structure and land cover changes 163
4.2. Growth disturbances and snow avalanche activity 167
4.3. Comparison with historical chronicles 169
4.4. Hierarchical modelling of snow avalanche activity at the regional scale 171
4.5. Impacts of climatic fluctuations on the regional avalanche activity 173
5. Discussion **174**
6. Conclusion **177**

CHAPITRE 6 **147**
Impacts des fluctuations climatiques sur l'activité des avalanches dans le Queyras

1. Introduction **181**
2. Sites d'étude **183**
2.1. Vallée du Haut Guil 183
2.2. Vallée de Souliers 183
3. Matériel et méthodes **185**
3.1. Estimation de l'activité régionale des avalanches 185
3.2. Influence des fluctuations du climat sur l'activité avalancheuse 186
4. Résultats **186**
4.1. Structure d'âge des peuplements 186
4.2. Reconstruction de la chronologie des avalanches dans le Queyras 188
4.3. Standardisation de la chronologie régionale au moyen de la modélisation bayésienne hiérarchique 192
4.4. Relations avalanche–climat. 193
5. Discussion et conclusion **195**
5.1. Robustesse de la reconstruction 195
5.2. Modélisation de l'activité régionale des avalanches 196
5.3. Fluctuations du climat et activité des avalanches 197

SYNTHESE GENERALE **201**
1. Principaux résultats **203**
1.1. Elaboration de deux chronologies régionales inédites 203
1.2. Amélioration de la détection des événements passés 204
1.3. Dendrogéomorphologie et cartographie de l'aléa avalancheux 204
1.4. Mise en évidence de non-stationnarités dans les reconstructions 207
1.5. Reconstruction régionale de l'activité des avalanches 208
1.6. Variations de l'activité avalancheuse *vs.* fluctuations du climat 209
2. Perspectives de recherches **211**
2.1. Ajustement des seuils de détection des événements 211
2.2. Densification de l'échantillonnage à l'échelle régionale 211
2.3. Meilleure intégration des non-stationnarités liées à l'approche dendrogéomorphologique et des impacts des changements socio-économiques 212
2.4. Améliorations des chronologies régionales par convergence avec d'autres sources d'informations 212
2.5. Utilisation de l'approche dans d'autres contextes bioclimatiques . 214

BIBLIOGRAPHIE **217**

TABLE DES ILLUSTRATIONS **247**

TABLES ET TABLEAUX **253**

TABLE DES MATIERES **255**

Au 20ème siècle, les massifs montagneux, dont les Alpes, ont connu un réchauffement significatif avec une augmentation des températures deux fois plus importante que la moyenne mondiale. Un tel réchauffement altère les composantes de la cryosphère. Elle induit, par exemple, un passage des précipitations solides aux précipitations liquides, des phases de fonte des neiges plus fréquentes et plus intenses, ainsi qu'une forte diminution de la quantité de neige et une réduction de la durée de la couverture neigeuse. Aux horizons 2050–2100, les modèles climatiques prévoient que l'épaisseur du manteau neigeux sera considérablement réduite et que les propriétés de la neige, et notamment la stabilité du manteau neigeux, seront modifiées. Ces changements devraient entraîner des modifications importantes dans l'activité des avalanches. Parallèlement, l'afforestation induite par la déprise agro-sylvo-pastorale, la démocratisation des sports d'hiver et l'urbanisation des versants ont profondément modifié les paysages de montagne depuis le milieu du 18ème siècle, de même que l'exposition des individus.

Dans ce contexte, une documentation précise de l'activité passée des avalanches est cruciale pour mettre en évidence et comprendre les impacts du réchauffement climatique sur l'activité avalancheuse. Jusqu'à présent, cette documentation s'appuyait sur des chroniques historiques ou des observations systématiques. Cependant, les premières sont souvent discontinues et axées sur des événements catastrophiques, tandis que les secondes se limitent à la seconde moitié du 20ème siècle, excluant toute comparaison avec des périodes climatiques distinctes – tel que les phases froides du Petit Âge Glaciaire, par exemple. Sur les versants forestiers, l'approche dendrogéomorphique apparaît être un complément fiable aux archives historiques et aux séries d'observations systématiques, car elle permet de reconstruire l'activité passée des avalanches, en continu, à l'échelle des plusieurs siècles, avec une résolution annuelle. Pourtant, jusqu'à présent, même si de nombreuses reconstructions locales ont été proposées, la fiabilité de l'approche a été peu souvent analysée et aucune chronologie régionale – cruciale pour distinguer les interférences potentielles entre l'activité des avalanches, les fluctuations climatiques et les changements socio-économiques – n'a été développée dans les Alpes.

Dans cette thèse de doctorat, des avancées méthodologiques significatives ont été réalisées afin (1) d'améliorer la détection des avalanches dans les cernes de croissance, (2) d'éliminer les non-stationnarités liées à la diminution du nombre d'arbres au cours du temps dans les reconstructions et (3) d'agréger les reconstructions locales en chronologies régionales. Sur la base de ces développements, des chronologies régionales pluriséculaires homogénéisées ont été développées (4) pour 10 couloirs d'avalanche de la vallée de Goms (Valais, Alpes suisses, 1880-2014) et (5) 11 couloirs du massif du Queyras (Alpes françaises, 1560-2016). Ces dernières ont été confrontées aux fluctuations climatiques et aux changements d'occupation du sol. À Goms, l'absence de signal climatique clair dans la chronologie régionale souligne les interférences induites par les non-stationnarités locales et démontre qu'une stratégie d'échantillonnage à l'échelle régionale devra nécessairement constituer un préalable au développement d'une chronologie robuste. Dans le massif du Queyras, la forte diminution de l'activité avalancheuse observée au cours du 20ème siècle est attribuée au réchauffement climatique et au processus d'afforestation des versants.

Mots-clefs : dendrogéomorphologie ; avalanches ; changement climatique ; Alpes suisses ; Alpes françaises.